Mechanistic determination of 6-hydroxymethyl-7, 8 -dihydropterin pyrophosphokinase (HPPK)

by

Simon Richard Foster B.Sc. (Leicester)

A Thesis submitted for the Degree of
Doctor of Philosophy
in the
Faculty of Science
of the
Department of Chemistry
at the
University of Leicester

JANUARY 2003

ProQuest LLC
789 East Eisenhower Parkway
P.O. Box 1346
Ann Arbor, MI 48106-1346

Dedicated to my mum and dad

STATEMENT

The accompanying thesis submitted for the degree of Doctor of Philosophy entitled "Mechanistic determination of 6-hydroxymethyl-7, 8-dihydropterin pyrophosphokinase (HPPK)" is based on work conducted by the author in the Department of Chemistry of the University of Leicester between the period September 1999 and December 2002.

All the work recorded in this thesis is original unless otherwise acknowledged in the text or by references. None of the work has been submitted for another degree in this or any other University.

Signed: Simon Foster ..... Date: 19/03/03

ACKNOWLEDGEMENTS

I would like to thank my supervisor Professor Paul Cullis, for his guidance and helpful discussion during the period of my research.

I am grateful to Steve Baker who has provided help and support whenever needed. Many thanks to Professor Paul Cullis and Mondane Carden for their help in proof reading the manuscript. Thanks are also due to Mick Lee for technical assistance, Dr. Graham Eaton for the kinetic study, Dr. Gerry Griffiths for the NMR study and to Ann Crane for design assistance.

I am also grateful to my fellow students, especially Raul and Mel, and staff of the department for providing an enjoyable working and social atmosphere.

I would like to thank my family who have shown understanding, and given encouragement and moral support throughout my studies and at other times. I am grateful to Sarah and Andrew for the kind donation of their flat, my parents Sue and Don for providing financial support well in advance of my eighteenth year and Natalie and John for help and encouragement.

ABBREVIATIONS AND SYMBOLS

A	Adenine
Ac	Acetyl
Ad	Adenosine
Ar	Aryl
ADP	Adenosine-5′-diphosphate
AMP	Adenosine-5′-monophosphate
AMPCPP	2'(3')-O-(N-methyleneadenosine triphosphate
ATP	Adenosine-5′-triphosphate
β_{lg}	Brønsted coefficient for the leaving group
β_{nuc}	Brønsted coefficient for the nucleophile
b.p.	boiling point
br	broad
Bu^t	tertiary-Butyl
Bz	Benzyl
C	Carbon
cm	centimetre
cm^{-1}	wavenumber
cm^3	cubic centimetre
d	doublet
dd	doublet of doublets
DEAE	Diethylaminoethyl
DMF	N,N-dimethylformamide
DMSO	Dimethyl sulphoxide
DNA	Deoxyribonucleic acid
dq	doublet of quartets
dqn	doublet of quintets
DTT	dithiothreitol
E	Enzyme
EDTA	Ethylenediaminetetraacetic acid
eq	equivalent
Et	Ethyl

Et_3N	Triethylamine
EtOH	Ethanol
g	gram
H	Hydrogen
HEPES	*N*-2-Hydroxyethylpiperazine-*N*'-2-ethanesulphonic acid
HMDP	6-Hydroxymethyl-7,8-dihydropterin pyrophosphate
HPPK	6-Hydroxymethyl-7,8-dihydropterin pyrophosphokinase
Hz	Hertz
Hg	Mercury
^1H NMR (or δ_H)	Proton nuclear magnetic resonance spectroscopy
H.P.L.C.	High performance liquid chromatography
IR	Infra-Red
J	coupling constant
k	rate constant
k_{cat}	catalytic constant
K_M	overall dissociation constant
KHz	Kilohertz
LFER	linear free energy relationship
m	multiplet
M	Molar
M^+	Molecular ion
Me	Methyl
MeOH	Methanol
mg	milligram
ml	millilitre
mm	millimetre
mM	millimolar
mol	mole
mmol	millimole
m.p.	melting point
m/z	mass to charge ratio (Mass spectrometry)
N	Nitrogen
Na	Sodium

NAD^+	nicotinamide adenine dinucleotide (oxidised form)
NADH	nicotinamide adenine dinucleotide (reduced form)
nm	nanometre
NMR	nuclear magnetic resonance spectroscopy
Nu	Nucleophile
O	Oxygen
P	Phosphorus
Pa	Pascal
Pd	Palladium
PEP	Phosphoenolpyruvate
Ph	Phenyl
P_i	Inorganic phosphate
^{31}P NMR	Phosphorus nuclear magnetic resonance spectroscopy
PP_i	Inorganic pyrophosphate
p.p.m.	parts per million
P_iS	Inorganic thiophosphate
q	quartet
R_f	Retention factor
Rp	R configuration at phosphorus
rt	room temperature
s	singlet
S	Sulphur
S_N1	Unimolecular nucleophilic substitution
S_N2	Bimolecular nucleophilic substitution
Sp	S configuration at phosphorus
st	strong
t	triplet
tbp	trigonal bipyramid
TEAB	Triethylammonium bicarbonate
THF	Tetrahydrofuran
t.b.p.	trigonal bipyramidal
t.l.c.	thin layer chromatography
TMSiI	Trimethylsilyl iodide
Tris	Tris (hydroxymethyl) methyl amine

UV	Ultra-Violet
vol	volume
v/v	volume per volume
w.r.t.	with respect to
λ_{max}	Ultra-Violet wavelength
μmol	micromole
ν_{max}	Infra-Red wavenumber

In the diagrams throughout this thesis the following notations for oxygen isotopes are used:

^{16}O = O
^{17}O = ⊖
^{18}O = ●

R and S configurational assignments are made in accordance with the Cahn-Ingold-Prelog rules* on the basis that peripheral oxygen atoms are always singly bonded to phosphorus.

* R. S. Cahn, C. K. Ingold and V. Prelog, *Angew. Chem., Int. Ed. Engl.*, **1966**, *5*, 385.

ABSTRACT

The development of widespread, high level resistance to antibiotics has made the quest for the discovery or design of new antibacterial agents a matter of some urgency. Tetrahydrofolate is synthesised *de novo* in micro-organisms and plants *via* the folic acid biosynthetic pathway whereas mammals acquire this crucial cofactor in their diets. The individual enzymes involved in this pathway are attractive potential targets for the development of new antibacterial agents.

6-Hydroxymethyl-7,8-dihydropterin pyrophosphokinase (HPPK) an enzyme of the folic acid biosynthetic pathway catalyses the magnesium-dependent pyrophosphorylation of 6-hydroxymethyl-7,8-dihydropterin, utilising ATP to form 6-hydroxymethyl-7,8-dihydropterin pyrophosphate. This substitution reaction occurs *via* a nucleophilic displacement reaction at the β-phosphoryl centre of ATP.

The stereochemical course of the HPPK catalysed reaction has been investigated by substituting ATP for an analogue that is chiral at the β-phosphoryl centre by virtue of sulphur and ^{18}O substitution. The determination of whether the configuration at this centre is inverted or retained as a result of nucleophilic substitution required the development of a new configurational analysis based on ^{18}O isotopic shifts seen in ^{31}P NMR spectroscopy. This method has allowed us to determine that the configuration at the chiral β-phosphoryl centre has been inverted as a result of pyrophosphoryl transfer. This suggests a mechanism that proceeds *via* a single in-line associative nucleophilic displacement reaction. The alternative mechanism resulting in retention of configuration at the chiral β-phosphoryl centre would require a double displacement (*via* two consecutive inversions of configuration) involving a covalent phosphoenzyme intermediate.

The observation that HPPK facilitates the pyrophosphorylation of 6-hydroxymethyl-7,8-dihydropterin *via* a single in-line associative nucleophilic displacement reaction on the Pβ of ATP using the 6-hydroxy group of the pterin as a nucleophile will be of use in the design of inhibitors with a potential therapeutic value.

Furthermore a kinetic investigation into the diastereoselectivity of HPPK toward the diastereoisomers of ATPβS [(Rp) and (Sp)] has required the development of a new assay to measure the rate of reaction utilizing HPLC-mass spectrometry. This study has provided evidence that the chemical pyrophosphoryl transfer step is not rate-limiting in the HPPK catalysed reaction.

CONTENTS

CHAPTER 1 INTRODUCTION

CHAPTER 2 SYNTHESIS OF ISOTOPICALLY LABELLED CHIRAL ALKYL AND NUCLEOTIDE THIOPHOSPHATE ESTERS

CHAPTER 3 CONFIGURATIONAL ANALYSIS OF ISOTOPICALLY LABELLED CHIRAL THIOPHOSPHATE MONOESTERS

CHAPTER 4 STEREOCHEMICAL COURSE OF THE HPPK CATALYSED PYROPHOSPHORYLATION OF 6-HYDROXYMETHYL-7,8-DIHYDROPTERIN

CHAPTER 5 KINETICS

CHAPTER 6 EXPERIMENTAL

CHAPTER 1
General Introduction

1.1 Displacement reactions at the phosphoryl centres of phosphate esters and anhydrides.

1.1.1 Biological importance of displacement reactions at the phosphoryl centres of phosphate esters.

The mechanisms of nucleophilic substitution in tetrahedral phosphorus (V) compounds, such as phosphate esters, Figure 1.1, have been extensively studied as they represent models for enzyme-catalysed processes.[1]

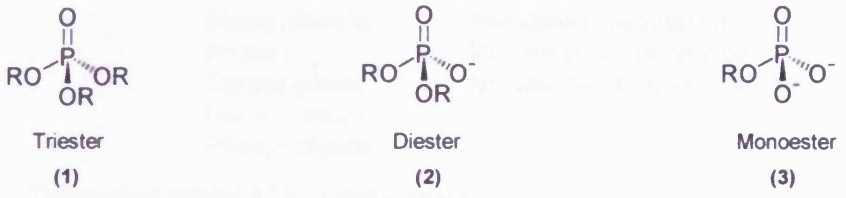

Fig. 1.1 Phosphate esters.

Phosphate esters play a central role in biochemistry; the genetic information of all living organisms is stored in the phosphodiester polymers DNA and RNA. Adenosine triphosphate (ATP) contains a monosubstituted and two disubstituted phosphoryl groups. Displacement reactions at the phosphoryl centres of ATP play a central role in the bioenergetics of cells, Figure 1.2.[2,3] The formation of ATP from ADP and P_i is coupled with energy-producing reactions such as oxidation through the electron-transport system, photophosphorylation, and glycolysis.[2] Conversely, its exergonic conversion to ADP and P_i, or to AMP and PP_i, is coupled to a large number of endergonic reactions and processes.[2] These include: the maintenance of a transmembrane chemical potential; provision of chemical free energy for mechanical, electrical, or photochemical events[2] and the synthesis of metabolic intermediates and macromolecules from smaller precursors.

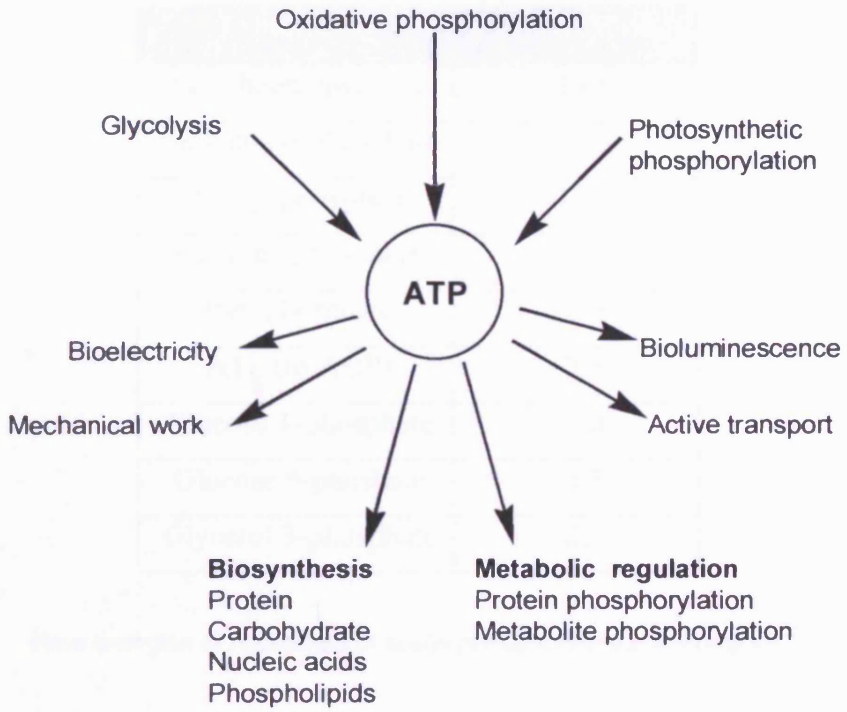

Fig. 1.2 The central role of ATP in metabolism.[3]

Various other compounds in biological systems have a high phosphoryl transfer potential. Some of them, in fact, have a higher transfer potential than ATP. These include: phosphoenolpyruvate, acetyl phosphate and creatine phosphate.[2] Consequently phosphoenolpyruvate can transfer its phosphoryl group to ADP to form ATP. This is one of the ways in which ATP is generated in the breakdown of sugars. It is significant that ATP has a phosphoryl transfer potential that is intermediate among the biologically important phosphorylated molecules, Table 1.1. This intermediate position enables ATP to function efficiently as a carrier of phosphoryl groups.[2]

Compound	ΔG (Kcal mol)
Phosphoenolpyruvate	-14.8
Carbamoyl phosphate	-12.3
Acetyl phosphate	-10.3
Creatine phosphate	-10.3
Pyrophosphate	-8.0
ATP (to ADP)	-7.3
Glucose 1-phosphate	-5.0
Glucose 6-phoshate	-3.3
Glycerol 3-phosphate	-2.2

Table 1.1 Free energies of hydrolysis of some phosphorylated compounds.[2]

The reversible phosphorylation of proteins by the ATP-dependent protein kinases is a universal mechanism for cellular control and adaptation.[4] Protein kinases can regulate a wide range of processes including carbohydrate and lipid metabolism, neurotransmitter biosynthesis, DNA transcription and replication, smooth muscle contraction, and cell differentiation. Phosphorylation of metabolites is often required to increase their solubility or prevent their passage across membranes.[4]

1.1.2 Fundamental mechanisms for phosphoryl transfer reactions.

There are four fundamental mechanisms for nucleophilic substitution reactions of phosphate esters, of which one is dissociative and three are associative, Scheme 1.1. The rate-limiting step (r.l.s.) in the dissociative $S_N1(P)$ mechanism (A) is the loss of the leaving group, resulting in the formation of a planar metaphosphate intermediate **(5)**. Subsequent nucleophilic attack on the planar metaphosphate leads to the substitution products. Exploitation of isotopically labelled chiral phosphate esters has shown this process to occur with racemisation as expected.

Dissociative reaction via a monomeric metaphosphate **(A)**

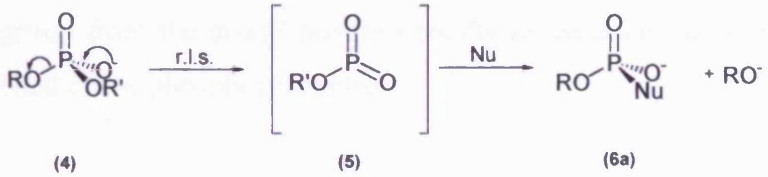

(4) (5) (6a)

Associative reaction via a penta-co-ordinate transition state **(B)**

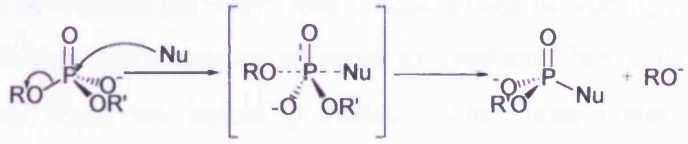

(4) (7) (6b)

In-line addition-elimination mechanism via a penta-co-ordinate intermediate **(C)**

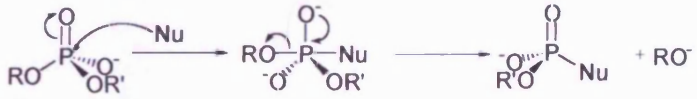

(4) (8a) (6b)

Adjacent addition-elimination mechanism involving a Pseudorotation **(D)**

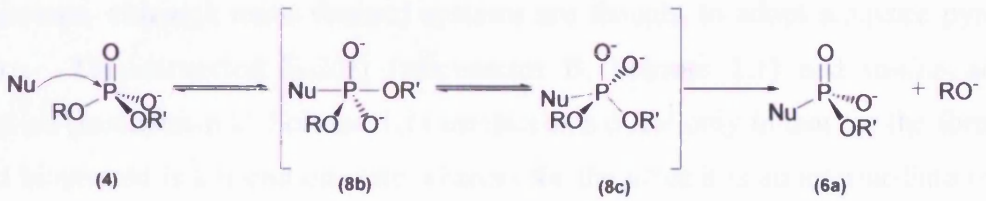

(4) (8b) (8c) (6a)

Scheme 1.1 Fundamental mechanisms for nucleophilic displacement reactions at phosphorus of disubstituted phosphate esters.

The first of the three associative mechanisms, (B), is a concerted $S_N2(P)$ process, which proceeds *via* a penta-coordinate transition state (**7**). Studies with isotopically labelled chiral phosphate esters show this process to result in inversion of configuration.

For mechanism (C) the nucleophile attacks opposite the leaving group to form a penta-coordinate trigonal bipyramidal intermediate **(8a)**. The leaving group and the nucleophile are in apical positions with the other three substituents in the equatorial plane. Elimination of the leaving group from the apical position results in inversion of configuration at an isotopically labelled chiral phosphoryl centre.

For mechanism (D) the nucleophile attacks adjacent to the leaving group. The nucleophile therefore, will occupy an apical position and the leaving group an equatorial position, in the first trigonal bipyramidal intermediate **(8b)**. The principle of microscopic reversibility states that the most favourable pathway from products back to starting material is the same as the reaction pathway from starting material to products; hence the leaving group is expected to depart from an apical position. This necessitates a pseudorotatory rearrangement which results in a second intermediate **(8c)** in which the two apical groups are exchanged with two equatorial ligands. The leaving group then departs from the apical position. Exploitation of isotopically labelled chiral phosphate esters has shown this process to occur with overall retention of configuration.

1.1.3 Penta-coordinate intermediates.

The associative addition-elimination mechanism for nucleophilic substitution at tetrahedral phosphorus leads to a penta-coordinate intermediate of trigonal bipyramidal geometry (t.b.p.). The trigonal bipyramidal geometry is the lowest energy for simple 5-coordinate phosphoranes, although more strained systems are thought to adopt a square pyramidal structure. The concerted $S_N2(P)$ (mechanism B, Scheme 1.1) and in-line addition elimination (mechanism C, Scheme 1.1) mechanisms differ only in that for the former the trigonal bipyramid is a transition state whereas for the latter it is an intermediate of finite lifetime. When the trigonal bipyramid species **(11)** is sufficiently long-lived to be considered an intermediate along the reaction pathway, it may be considered as analogous to the mechanism of reaction at the sp^2-hybridised carbon (for example nucleophilic attack at carbonyl groups) which are usually assumed to go *via* a tetrahedral intermediate **(10)**, Scheme 1.2.

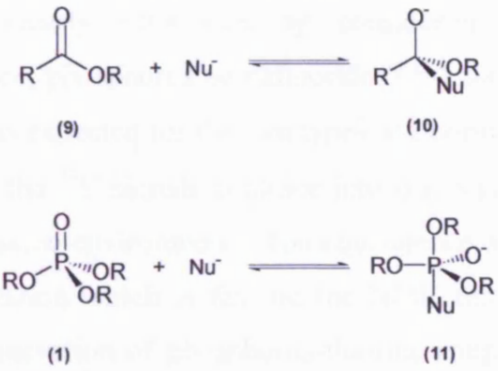

Scheme 1.2 Comparison of tetrahedral **(10)** and penta-coordinate **(11)** intermediates.

However, greater mechanistic diversity is observed in the substitution reactions of phosphate esters (mechanisms B, C and D, Scheme 1.1) relative to carboxylic acid derivatives, since the dynamics of the penta-coordinate intermediate are far more complex.

Two types of position exist in the trigonal bipyramid intermediate **(12)**, Figure 1.3, three equatorial and two apical positions.

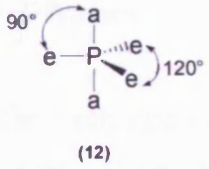

Fig. 1.3 Equatorial (e) and apical (a) positions in a trigonal bipyramid intermediate **(12)**.

The ligands are therefore non-equivalent; the apical bonds are longer and weaker than the equatorial bonds because an equatorial bonding electron pair experiences bonding pair ↔ bonding pair repulsion from only two other electron pairs at 90° (i.e. the apical pairs) whereas the apical bonding pairs experience repulsion from three electron-pairs at 90° (i.e. the equatorial trio).

In addition, ligand reorganization[5] (alternatively termed polytopal or permutational isomerization) may occur, rearranging the position of the ligands about phosphorus in the t.b.p. intermediate and as a result several isomeric t.b.p. intermediates may be involved in a single mechanistic pathway.

These points can be clearly illustrated by considering stable penta-coordinate phosphoranes. For instance, phosphorus pentafluoride (PF_5) shows two ^{19}F NMR signals at -85°C in a ratio of 3:2 as expected for the two types of fluorine atoms. However, as the temperature is increased, the ^{19}F signals coalesce into one signal indicating that all the fluorine atoms are in the same environment. The equivalence of atoms comes about as a result of ligand reorganization which is fast on the NMR timescale leading to a time-averaged signal. The observation of phosphorus-fluorine coupling in PF_5 indicates that this process must be occurring intramolecularly. Ligand reorganization is believed to follow the Berry pseudorotation mechanism,[6] illustrated in Figure 1.4.

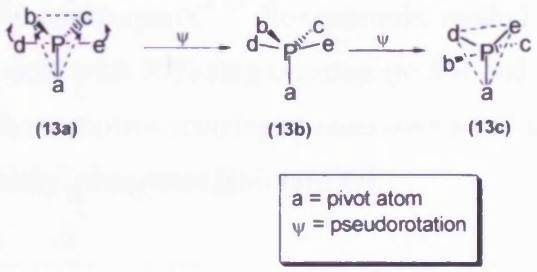

Fig. 1.4 The Berry pseudorotation mechanism.

The pseudorotation process involves the exchange of two equatorial ligands with two apical ligands by a non-dissociative process. The apical atoms become equivalent to two of the equatorial atoms by deforming the trigonal bipyramid **(13a)** to the intermediate square pyramidal structure **(13b)**. Further deformation produces a new trigonal bipyramid **(13c)** in which the new apical groups are derived from two original equatorial ligands. After the pseudorotation, the axis of the trigonal bipyramid **(13c)** is 90° to the original axis found in **(13a)**; throughout the operations one of the equatorial ligands acts as a pivot and remains equatorial in the isomeric trigonal bipyramid.

Much work can be cited which supports the importance of penta-coordinate phosphoranes and pseudorotation in the displacement reactions of phosphate esters:

[1] *Stable penta-coordinate phosphoranes.* Some stable penta-alkoxyphosphoranes have been prepared and characterized, for example pentaethoxyphosphorane **(14)**, Figure 1.5.[7]

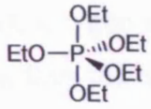

(14)

Fig. 1.5 Pentaethoxyphosphorane.

[2] *Rate acceleration and isotope exchange in the hydrolysis of five-membered cyclic phosphates.* Westheimer and workers discovered that the hydrolyses in acid or base of five-membered cyclic esters of phosphoric acid proceed millions of times faster than the hydrolyses of their acyclic counterparts.[8-10] For example, methyl ethylene phosphate **(15)** undergoes hydrolyses in acid with 70% ring opening (to **16)** and 30% exocyclic cleavage (to **17)**, Scheme 1.3, both reactions occurring at rates over a million times faster than that for the hydrolysis of trimethyl phosphate [$(MeO)_3PO$].

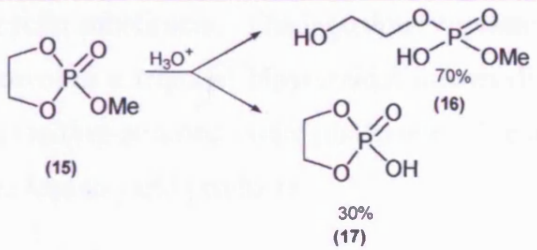

(15) (16) (17) 70% 30%

Scheme 1.3 Hydrolyses of methyl ethylene phosphate.

On the other hand, the rates of hydrolysis of six and seven-membered cyclic phosphates **(18 and 19)**, Figure 1.6, are comparable with those of acyclic analogues.[11]

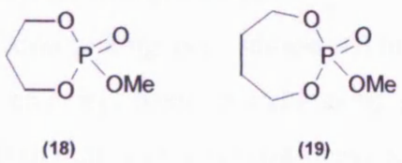

(18) (19)

Fig. 1.6 Six and seven-membered cyclic phosphates.

A striking and key observation is that the hydrolysis of the diester **(20)** in acid or base is not only 10^8 times faster than the hydrolysis of the acyclic analogue, dimethyl phosphate

$[(MeO)_2P(O)OH]$, but that it is accompanied by rapid oxygen isotope exchange into the starting material, Scheme 1.4.[12] In fact, oxygen exchange occurs at approximately one-fifth the rate of ring opening hydrolysis, thus the exchange is *ca.* 2×10^7 times faster than the hydrolysis of dimethyl phosphate; this acyclic compound shows no detectable incorporation of ^{18}O.

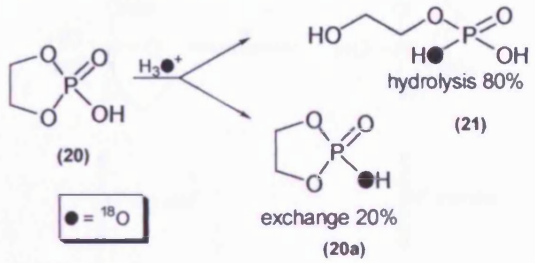

Scheme 1.4 Oxygen isotope exchange.

Although one might be tempted to argue that the relief of ring strain can account for the accelerated opening of the ring in cyclic phosphates, it cannot explain the increased rate of displacement of the exocyclic substituent. The ingenious explanation of these effects, due largely to Westheimer, invokes a trigonal bipyramidal intermediate that is formed in an accelerated process from the ring-strained cyclic phosphate. The intermediate can undergo pseudorotation and ligand loss to yield products.

Westheimer rationalized the rate acceleration of cyclic esters by making four assumptions about the penta-coordinate intermediate.[13,14]

i) The more electronegative ligand prefers to occupy the apical positions.

ii) The five-membered ring will be more stable bridging apical-equatorial positions with an O-P-O bond angle of 90°, rather than bridging equatorial-equatorial positions with an angle of 120°.

iii) Pseudorotation is facile as long as conditions (i) and (ii) are preserved.

iv) Nucleophiles enter an apical position and leaving groups ultimately depart from an apical position (principle of microscopic reversibility).

On this basis, the hydrolysis (endo- and exocyclic cleavage) of **(15)** can be visualised as shown in Scheme 1.5.

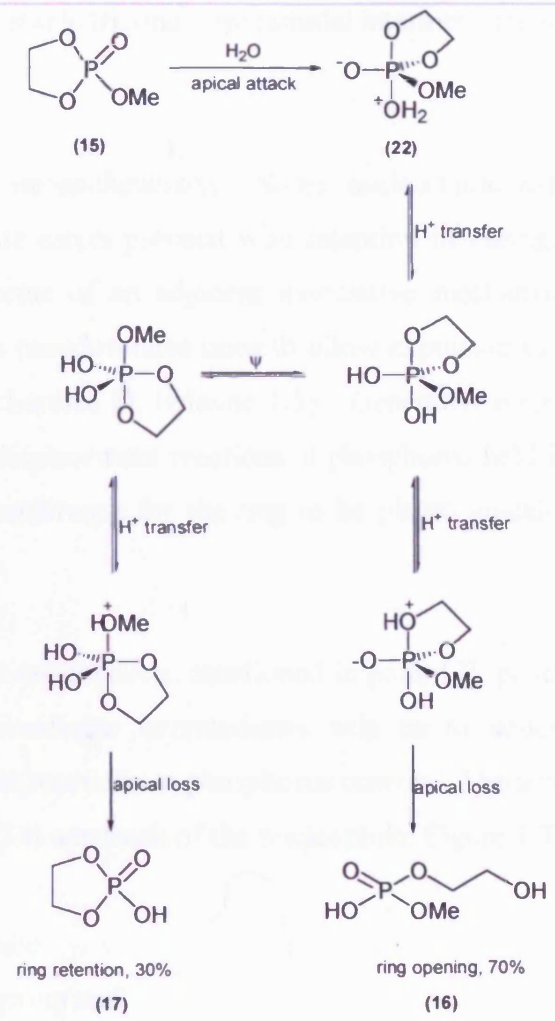

Scheme 1.5 The hydrolysis of methyl ethylene phosphate **(15)** *via* penta-coordinate intermediates.

From this scheme, it can be seen that the enhanced rate of exocyclic hydrolysis also arises from the relief of strain in the ring on going from the tetra-coordinate **(15)** to the penta-coordinate configuration **(22)** with the ring spanning apical-equatorial positions. Pseudorotation then allows the methoxy group to leave from the apical position.

Pseudorotation, as mentioned, was originally proposed to explain the behaviour of stable phosphoranes and has now been extended to trigonal-bipyramidal intermediates. However, in order for pseudorotation to occur, the intermediate must be sufficiently long-lived. In reactions of acyclic compounds this may not be the case. Only when the intermediate is especially stabilized (e.g. by relief of ring strain in five-membered rings) is

there clear evidence for stable trigonal bipyramidal intermediates involving pseudorotatory processes.

[3] *Implications from stereochemistry.* Some nucleophilic displacement reactions at phosphorus in phosphate esters proceed with retention of configuration.[15] This is most simply explained in terms of an adjacent associative mechanism in which the penta-coordinate intermediate pseudorotates once to allow expulsion of the leaving group from an apical position (mechanism D, Scheme 1.1). Generally, retention of configuration is observed in exocyclic displacement reactions at phosphorus held in a five-membered ring because of the strong preference for the ring to be placed apical-equatorial in the penta-coordinate intermediate.

The empirical rules and assumptions, mentioned in point [2], governing the formation and breakdown of penta-coordinate intermediates help us to understand much about the associative displacement reactions at phosphorus centres. The actual balance between in-line **(23)** and adjacent **(24)** approach of the nucleophile, Figure 1.7, very much depends on the nature of:

i) the nucleophile

ii) the leaving group and

iii) other substituents around the phosphorane.

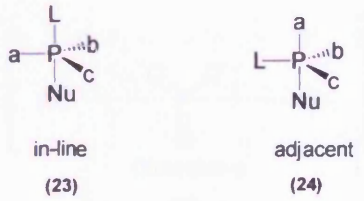

Fig. 1.7 In-line **(23)** and adjacent **(24)** approach of the nucleophile with respect to the leaving group L.

The idea of apicophilicity (preference for the apical position in a trigonal bipyramid) helps to rationalize the preference for an observed displacement mechanism by predicting the relative energies of the alternative phosphoranes. A quantitative scale of relative apicophilicities was developed by Trippett[16] (Figure 1.8) and is derived from NMR studies on the dynamic interconversion of stable phosphoranes.

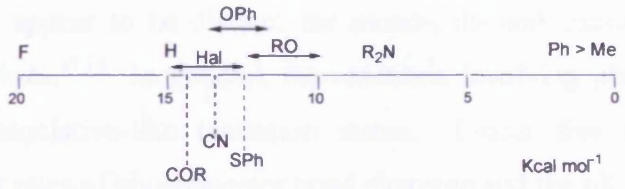

Fig. 1.8 Trippett's relative apicophilicity scale (Kcal mol^{-1}) for ligands attached to trigonal bipyramid penta-coordinate phosphorus.

1.1.4 Model solution studies of phosphoryl transfer reactions (associative *vs.* dissociative mechanisms).

The transition states for nucleophilic attack on phosphate mono-, di- and triesters have been characterized as either dissociative or associative.[17,18] In the dissociative transition state, bond breaking between the phosphorus centre and the leaving group atom is more advanced than bond making between the phosphorus centre and the incoming nucleophile, Scheme 1.6.[4] In the most extreme case, a dissociative mechanism would require the formation of a metaphosphate intermediate. This contrasts with an associative transition state where bond formation between the nucleophile and phosphorus centre is advanced, Scheme 1.6.

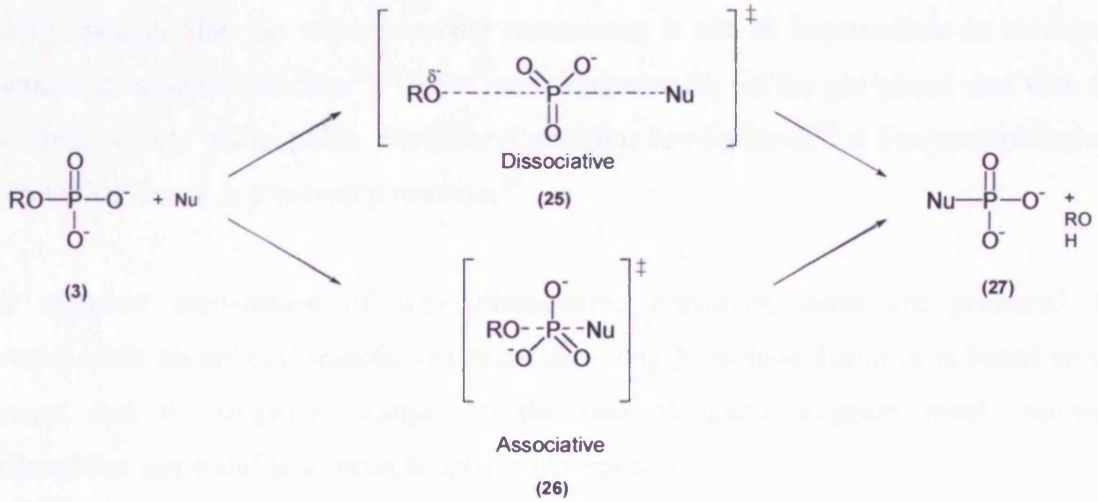

Scheme 1.6 Associative and dissociative reaction transition states.[4]

The degree of dissociative **(25)** and associative **(26)** character in the transition states of transfer mechanisms appear to be distinct for mono-, di- and triesters of phosphates in model solution reactions,[17,19] In general, the reactions involving phosphoryl monoesters proceed through dissociative-like transition states. Linear free energy relationships (LFERs) between the rates of phosphoester bond cleavage and the pK_a values of a series of nucleophile (nuc) and leaving group (lg) have been used in the analysis of these reaction mechanisms.[20] The Brønsted coefficients (β_{nuc} and β_{lg}) determined from these plots provide information concerning the transition state of the reaction.

For example, model studies of nucleophilic attack on aryl phosphate dianions are accompanied by low values for β_{nuc} and large negative values of β_{lg}.[21-23] A large negative β_{lg} denotes a strong dependence between reaction rates and the pK_a's of the leaving group and implies that a large amount of bond breaking between the phosphorus centre and the leaving group atom occurs in the transition state.[4] The large value of this coefficient also implies a large charge development on the leaving group. The low β_{nuc} denotes insensitivity between the reaction rates and the pK_a's of the attacking nucleophiles. This is consistent with little bond formation between the nucleophile and the phosphorus atom in the transition state.[4] These two coefficients (β_{nuc} and β_{lg}) are complementary and consistent with a concerted mechanism with a very loose transition state that has a dissociative character in which the phosphoryl group resembles a metaphosphate ion.[1]

LFERs indicate that the metaphosphate monoanion is not an intermediate in solvolysis reactions in aqueous solution.[24] Under rare circumstances (in the gas phase, and with the hindered, weakly nucleophilic phosphoryl acceptor *tert*-butanol),[25] a free metaphosphate intermediate forms in a two-step reaction.[26]

The simplest explanation of why dissociative transition states are preferred for nonenzymatic phosphoryl transfer reactions involving phosphate dianions, is based on the concept that the negative charges on the two phosphate oxygens repel incoming nucleophiles and stabilize a metaphosphate-like species.[27]

As the degree of esterification or of protonation of the monoester dianion increases, the negative charge on the phosphate ester is reduced. This results in a reduction of

electrostatic repulsion between the nucleophile and the phosphate anions. This leads to a reduction in the driving force for the dissociative reaction pathway. As a consequence an increase in the associative characteristics of the nucleophilic displacement reaction is seen.

An increase in β_{nuc} is observed for phosphate diesters (2,4-dinitrophenyl phosphate monoanion, or for methyl-2,4-dinitrophenyl phosphate), implying the transition state is developing more associative characteristics.[28] For triesters having poor leaving groups, LFERs show that the reaction rates are equally sensitive to the pK_a's of the nucleophile and the leaving group. This suggests an addition-elimination mechanism that involves nucleophilic attack in the first step to form a penta-coordinate phosphorane intermediate.

Primary and secondary oxygen kinetic isotope effects in phosphoryl transfer reactions can give information on the change in P-O bonding between the transition and ground states. If a certain P-O bond order decreases in the transition state then the ratio between the ^{16}O and ^{18}O isotope reaction rates $^{16}k/^{18}k > 1$ and a normal isotope effect is observed. Conversely, if the bond order increases we get an inverse isotope effect ($^{16}k/^{18}k < 1$) if that particular oxygen is isotopically substituted.[20]

These measurements can distinguish between associative, dissociative and S_N2-like mechanisms. An associative mechanism, such as that which occurs with cyclic phosphotriesters where a phosphorane intermediate is formed, results in decreased bond order to the nonbridge oxygen atoms in the transition state, giving a normal isotope effect. In a dissociative mechanism, like that for monoester hydrolysis, bonding to the nonbridge oxygen atoms is increased in the transition state and an inverse isotope effect is observed.[29]

1.1.5 Enzyme catalysed phosphoryl transfer (associative *vs.* dissociative mechanisms).

At the active site of an enzyme, where we have a fixed disposition of attacking, leaving, and charge-stabilizing groups, we may assume that the reaction will have a defined stereochemical course. Consequently, determination of the stereochemical outcome of an

enzyme catalysed phosphoryl transfer allows for a direct analogy with the nonenzymatic mechanism to be made.

It has been suggested that enzymatic and nonenzymatic phosphoryl transfer reactions occur through similar transition states that differ only in the extent of stabilization.[30-32] If the active site of the enzyme alters the energy without affecting the nature of the transition state, then it is expected that enzymes utilizing phosphate monoesters such as protein kinases and phosphatases, will adopt dissociative-like transition states akin to the solution reactions on phosphate monoesters.[33]

It can also be speculated that stabilizing the transition state for a phosphoryl transfer involving a phosphate monoester may lead to a more associative mechanism. In extreme cases a change to a two-step associative mechanism with an intermediate, may be anticipated.[34,35]

Phosphatases utilize different catalytic strategies and functional groups, and comparisons of the structures show that the only similarity is the presence of a positive charge at the active site, in the form of an arginine residue and/or a binuclear metal centre.[25] It is reasonable to suggest that these metal ions and/or cationic residues might change the normally dissociative phosphoryl transfer into a more associative one *via* electron withdrawal from the phosphorus atom, thus promoting nucleophilic attack.

A direct in-line associative reaction (illustrated chemically in Scheme 1.1, B and C) between two enzyme bound substrates (*via* a pentacoordinate transition state or intermediate **(29)**) leads to inversion of configuration to give **(30a)**, Scheme 1.7a. A dissociative mechanism, Scheme 1.7b, may result in racemisation, as demonstrated for dissociative reactions in solution,[28] or to inversion of configuration to give **(30a)**, as a consequence of the fixed arrangements of substrates in an ordered enzyme active site.

An enzyme catalysed adjacent associative mechanism would result in retention of configuration to give **(30b)**, Scheme 1.7c. It is arguable that an adjacent displacement which involves pseudorotation is unlikely on two grounds: (i) a pseudorotation pathway will need a multi-step mechanism and (ii) the molecular movement involved in pseudorotation may demand a conformational change of the enzyme active site to

accommodate this motion. In most cases where overall retention of configuration is observed, there is either presumptive or compelling evidence for a phosphoenzyme intermediate **(34)** (see section 1.2.3) which would accord with a mechanism involving two in-line displacements,[36] Scheme 1.7d.

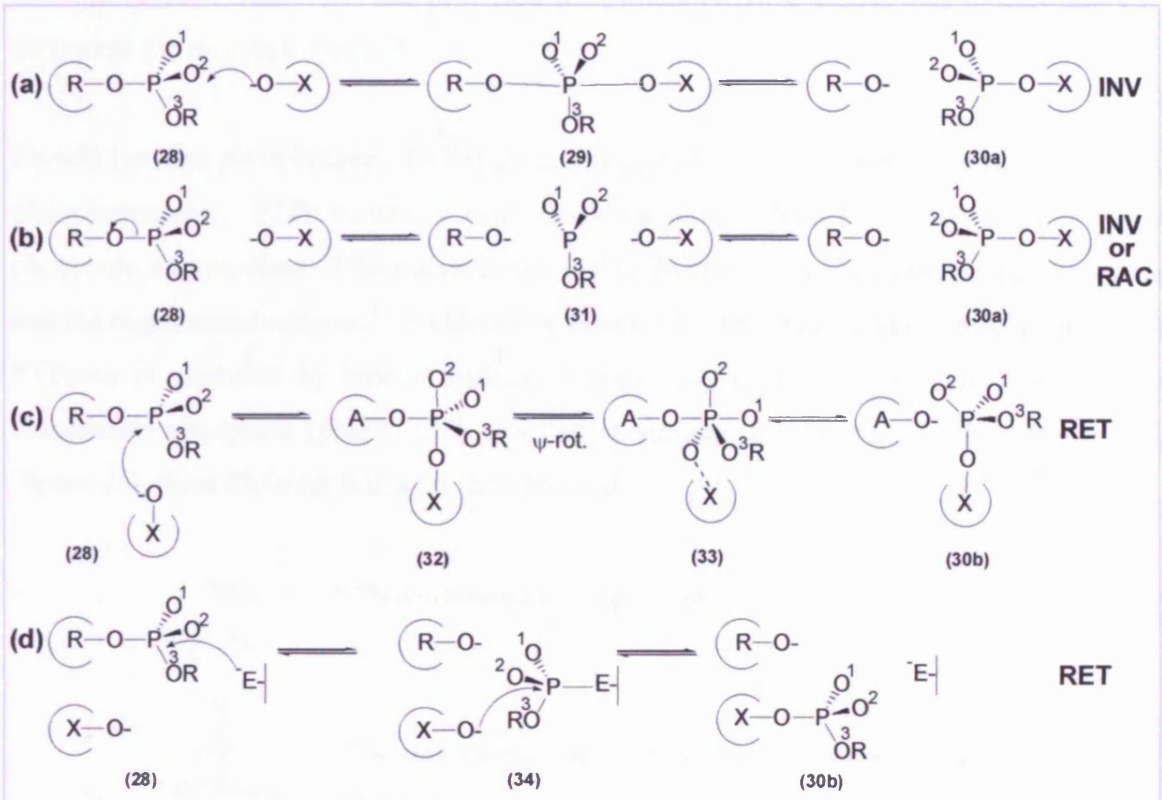

Scheme 1.7 The four mechanisms of enzyme catalysed phosphoryl transfer. The three peripheral oxygen atoms of the phosphoryl group are each labelled to illustrate the stereochemical consequences of the mechanisms.[37]

Details concerning the transition state structures in enzyme catalysed phosphoryl transfer reactions have been investigated by linear free energy relationships (LFERs),[38] kinetic isotope effects (KIEs),[25,34,39] positional isotope exchange studies, NMR and crystal structure analysis.

The Brønsted nucleophilic coefficient (β_{nuc}) has been determined for the ATP-dependant protein tyrosine kinase csk catalysed phosphorylation of a peptide substrate family.[38] This enzyme can phosphorylate fluorotyrosine peptides so that the acidity of the nucleophile can be altered and detailed LFERs can be derived. The Brønsted plots of k_{cat} and k_{cat}/K_m

versus the pK_a's of various fluorotyrosine peptides have very low values for β_{nuc}.[38] This is consistent with a transition state for phosphoryl transfer that possesses a high degree of dissociative character akin to the solution reactions on phosphate monoesters. The catalytic cores of protein serine/threonine and tyrosine kinases are extremely conserved.[40] The dissociative transition state proposed for protein tyrosine kinase Csk is thus likely to be typical for protein kinases.[38]

Protein tyrosine phosphatases (PTPs) are a subclass of protein phosphatases that hydrolyse phosphotyrosine. PTPs contain a cysteine nucleophile, which forms an initial enzyme-phosphate intermediate. This intermediate is then hydrolysed to form inorganic phosphate and the regenerated enzyme.[41] Evidence in favour of a dissociative-like mechanism for the PTPases is provided by kinetic isotope studies. By using the substrate analogue, *p*-nitrophenyl phosphate (*p*NPP) **(35)**, labelled at various positions with either ^{18}O or ^{15}N, Figure 1.9, three different KIEs can be observed.

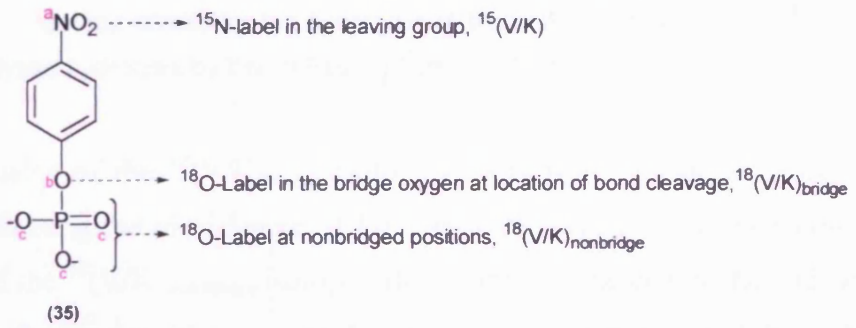

(35)

Fig. 1.9 p-Nitrophenyl phosphate **(35)** used for kinetic isotope studies, indicating the location and type of label used for measurements.

Primary ^{18}O isotope effects ($^{18}k_{bridge}$) provide a reliable indication of the degree of transition-state bond cleavage of the bridged oxygen atom. Secondary ^{18}O isotope effects ($^{18}k_{nonbridge}$) are observed in the non-bridged oxygen atoms and probe the changes in bond order that occur in the phosphoryl group. The magnitude of $^{18}k_{nonbridge}$ reveals whether the transition state goes through a dissociative-like or associative-like mechanism (illustrated in Section 1.1.4, Scheme 1.6). By placing ^{15}N in the nitro group of *p*NPP, the ^{15}N isotope effect (^{15}k) measures the extent of charge delocalisation in the phenyl ring of the leaving group. The primary, secondary and ^{15}N isotope effects for the nonenzymatic hydrolysis of both the monoanion and dianion of *p*NPP in solution have been reported and are consistent

with a dissociative transition state for the nonenzymatic hydrolysis of phosphate monoesters.[34]

Kinetic isotope studies on the enzymatic hydrolysis of *p*NPP by the PTPases, *Yersinia* PTP and PTP1, have allowed direct comparison with the solution reactions,[39] Table 1.2. For these enzymatic reactions, isotope effects are manifested in k_{cat}/K_M (customarily referred to as *V/K*) and provide information on the chemical step of phosphoryl transfer from substrate to nucleophilic cysteine residue.

Enzyme reaction	^{15}**(V/K)**	^{18}**(V/K)$_{bridge}$**	^{18}**(V/K)$_{non\text{-}bridge}$**
Native Yersinia PTP	0.9999	1.0152	0.9998
Native rat PTP1	1.0001	1.0142	0.9981
Solution reaction	^{15}k	$^{18}k_{bridge}$	$^{18}k_{non\text{-}bridge}$
Dianion in water	1.0034	1.0230	0.9993

Table 1.2 Isotope effects for the hydrolysis of the *p*NPP dianion in water[34] compared to the enzyme catalysed hydrolysis by the PTPases, *Yersina* PTP and PTP1.[42]

The magnitudes of the $^{18}(V/K)_{bridge}$ isotope effects were similar to those measured in solution, reflecting the high degree of P-O bond cleavage in both transition states. The similarity of the $^{18}(V/K)_{non\text{-}bridge}$ isotope effects between the enzymatic and nonenzymatic reaction for the dianion (that are small and inverse in both cases), Table 1.2, suggests a loose transition state in which the phosphorus atom adopts a metaphosphate-like structure. This is in contrast to the phosphorane-like transition states of phosphate diesters and triesters, where a normal isotope effect is seen.[25]

The uncatalysed system has a near maximal value for ^{15}K, reflecting the high amount of negative charge developed on the nitrophenyl leaving group. The catalysed system has a zero value for $^{15}(V/K)$, suggesting that the leaving group is fully neutralised in the transition state. Crystal structures show a conserved aspartate residue that may act as a general acid and neutralize the charge on the leaving group.[42] These kinetic isotope studies suggest that the PTPase catalysed and uncatalysed solution reactions have transition states with very similar amounts of dissociative character, Figure 1.10.

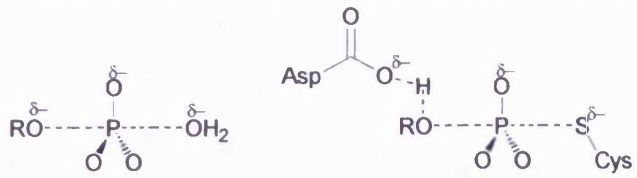

(36) (37)

Fig. 1.10 **(36)**: A schematic diagram of the loose transition state for phosphoryl transfer from the dianion of a phosphate monoester to water. The phosphoryl group resembles metaphosphate, the leaving group bears substantial negative charge and there is little bond formation with the nucleophile. **(37)**: The transition state implied by the KIE data for the reaction catalysed by the PTPases utilizing the *p*NPP dianion as the substrate. The phosphoryl group also resembles metaphosphate, and the leaving group is neutralized by a conserved aspartate general acid.

Experimentally, the existence of a truly dissociative mechanism may be probed by positional isotope exchange experiments, illustrated by the reactions of ATP, Scheme 1.8. The dissociative mechanism is stepwise with prior formation of the metaphosphate intermediate. Thus a kinase that catalyses the transfer of the terminal phosphoryl group of ATP to an acceptor may, in the absence of acceptor molecule, generate a metaphosphate ion and ADP in a rapid reversible reaction. If the β, γ-bridge oxygen is tagged, as in Scheme 1.8, then due to the torsional symmetry of the phosphate group, the bridge oxygen may become scrambled.[43] This scrambling implies a dissociative mechanism and the existence of a metaphosphate intermediate.

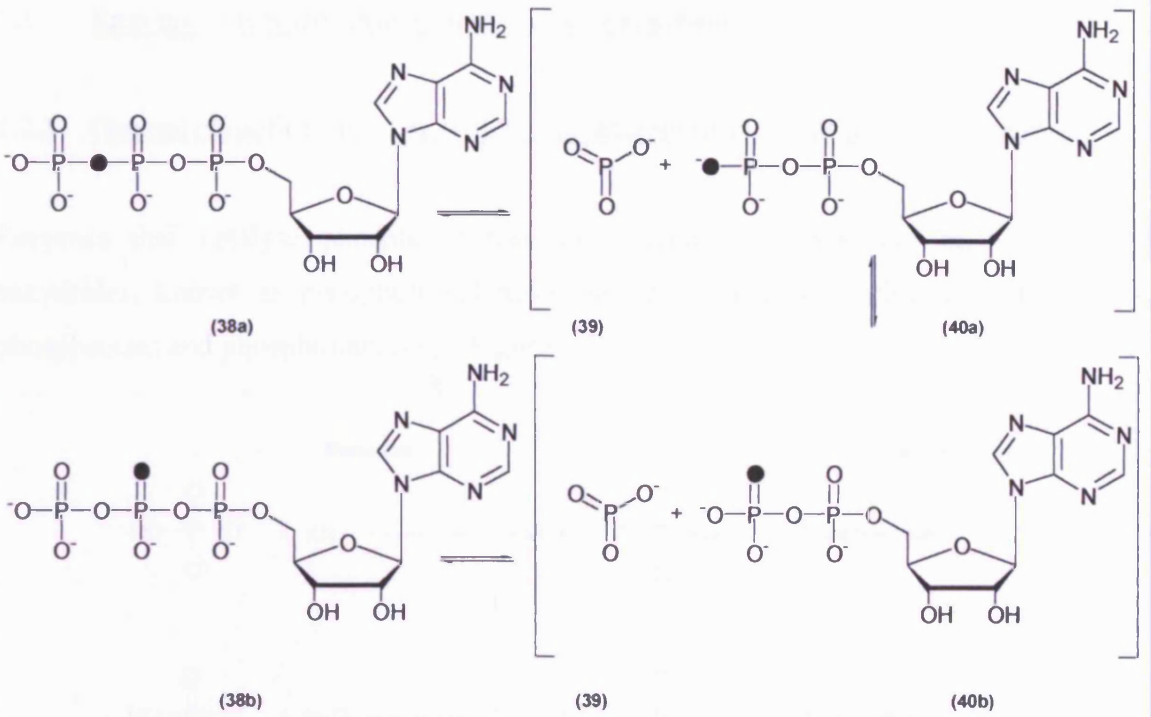

Scheme 1.8 Positional isotope exchange.

Positional isotope exchange experiments and stereochemical studies conducted on creatine kinase,[44] hexokinase,[45] and pyruvate kinase[35] have provided no firm evidence in favour of a dissociative mechanism involving a metaphosphate ion intermediate. In each case, the data are consistent with a straightforward nucleophilic attack on phosphorus to generate a trigonal bipyramidal transition state or intermediate.

KIE studies on enzymatic reactions[46] and of alkaline hydrolysis of phosphodiesters[47] show that these reactions are concerted with slightly associative character. In general it can be expected that phosphotransferase enzymes that catalyse nucleophilic substitution on phosphate diesters, such as nucleotidyl transferases, have transition states that have increased associative character compared to enzyme catalysed substitutions at phosphate monoesters.

This general trend is confirmed by the characterisation of the transition state structure involved in the kanamycin nucleotidyl transferase reaction.[46] This enzyme catalyses the transfer of an AMP moiety from ATP to the 4' hydroxyl group of kanamycin A. As expected, the primary and secondary isotope effects are consistent with a concerted mechanism with a slightly associative transition-state.

1.2 Enzyme-catalysed phosphoryl transfer reactions.

1.2.1 General classification of enzymes that catalyse reactions at phosphoryl centres.

Enzymes that catalyse phosphoryl transfer reactions of phosphate monoesters and anhydrides, known as phosphotransferases, fall into three categories: phosphokinases, phosphatases and phosphomutases,[36] Figure 1.11.

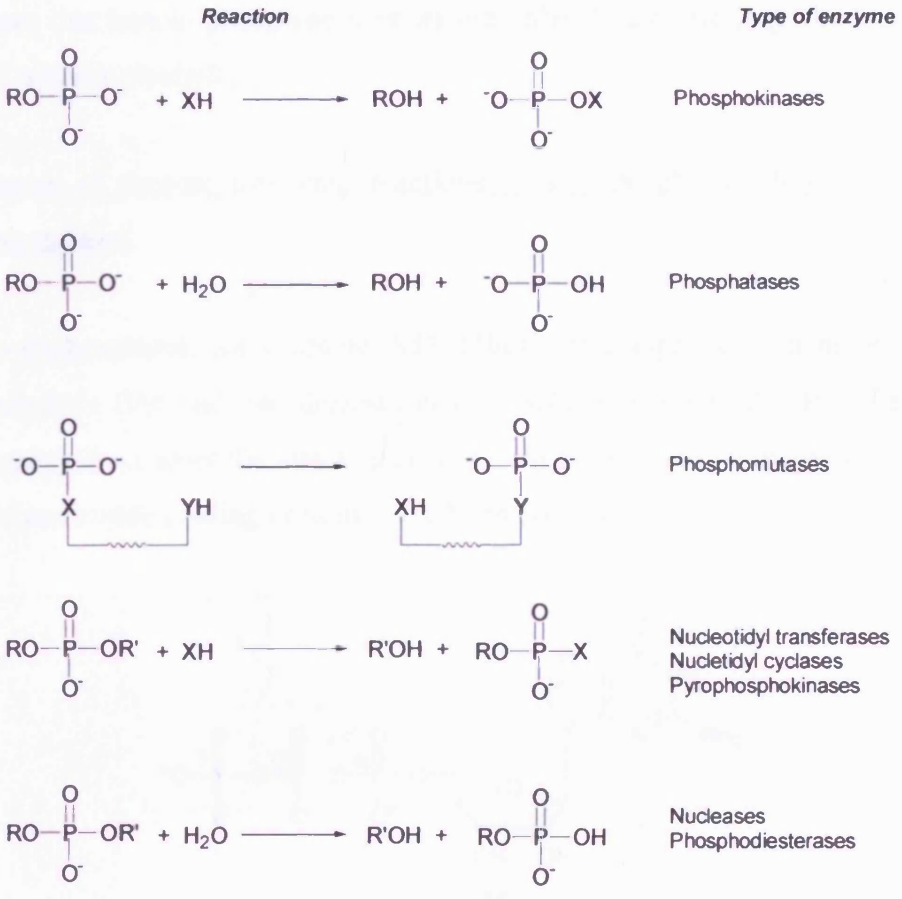

Fig. 1.11 Classes of enzymes that catalyse reactions at phosphoryl centres.[36]

Phosphokinases catalyse phosphoryl transfer of the terminal (γ) phosphoryl group of a nucleotide triphosphate, e.g. ATP, to an acceptor nucleophile which can be a hydroxyl group, e.g. protein kinase, hexokinase; a nitrogen group, e.g. creatine kinase, arginine kinase; a carboxyl group, e.g. acetate kinase; or a phosphate group, e.g. adenylate kinase, nucleoside diphosphate kinase.

Phosphatases are enzymes that catalyse phosphoryl transfer to water which acts as the acceptor nucleophile (hydrolysis), e.g. ATPases catalyse transfer of the terminal phosphoryl group of ATP to H_2O.

Phosphomutases catalyse phosphoryl transfer to an acceptor which is another functional group on the donor molecule, i.e. an intramolecular reaction, e.g. phosphoglycerate mutase, phosphoglucomutase, etc.

The enzymes that handle phosphate diesters are either hydrolytic (e.g. the nucleases) or nucleotidyl transfer catalysts.

1.2.2 Classes of enzyme involving reactions at the phosphorus atoms of nucleotide triphosphates.

Nucleotide triphosphates, for example ATP **(38c)**, are comprised of a monosubstituted phosphoanhydride (Pγ) and two disubstituted phosphoanhydrides (Pα, Pβ), Figure 1.12. Enzyme catalysed nucleophilic attack occurs at each phosphorus atom and on this basis a selection of nucleotide binding proteins have been classified.

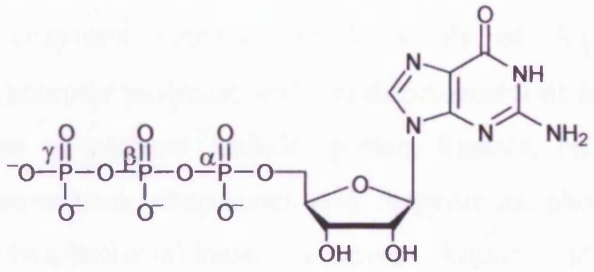

(38c)

Fig. 1.12 Enzyme catalysed attack at ATP **(38c)**.

Attack at the α-phosphate

Nucleotidyl transfer enzymes produce an adenylated intermediate during their reaction or directly cleave the α-β-anhydride bond *via* nucleophilic attack at Pα of ATP. The reaction results in the adenylation of an acceptor molecule with the displacement of pyrophosphate. Enzymes that catalyse nucleophilic substitution at the α-phosphate are very abundant and

include: nucleotidyl transferases, nucleotidyl cyclases, DNA-ligases, mRNA capping enzymes, class II aminoacyl tRNA synthetases, biotin synthetases, luciferases, nucleic acid, dUPase and pyrases.

Attack at the β-phosphate

Mut T, a pyrophosphoryl transfer enzyme, catalyses the hydrolysis of all eight nucleotide triphosphates by nucleophilic substitution at the rarely attacked β-phosphorus. Substitution at the α- and γ-phosphate are quite common.[48] In contrast, substitution at the β-phosphate is rare, and it has been speculated that this might be due to the higher electron density at this position.[49] The only other known enzymes that catalyse such a reaction are six synthetases, namely: phosphoribosyl-pyrophosphate synthetase,[50] thiamine pyrophosphokinase,[51] HPPK[52], 3-pyrophosphorylguanosine-5'-diphosphate synthetase, phosphoenolpyruvate synthetase[53.54] and pyruvate-orthophosphate dikinase.[54] Their action results in the pyrophosphorylation of an acceptor molecule with the displacement of adenosine monophosphate.

Attack at the γ-phosphate

Phosphoryl transfer enzymes, catalyse attack at Pγ of ATP, resulting in the phosphorylation of an acceptor molecule with the displacement of adenosine diphosphate. Examples of this type of enzyme include: protein kinases, NDP kinases, transport ATPases, DNA topoisomerases, chaperones and chaperonins, phosphoglycerate kinase, pyruvate kinase, phosphofructokinase, creatine kinase, glutamine synthetase, phosphokinase and ATPase. Phosphorylation, as with adenylation and pyrophosphorylation, activates molecules for further nucleophilic attack.

Nucleotide triphosphate-binding proteins can also be classified on the basis of common structural similarities based on investigations into conserved sequence motifs.[55] Alternatively, enzymes can be grouped according to their mechanistic relationship, Table 1.3, with division criteria based on fundamental mechanistic data such as: involvement of intermediates, nature and selection of P—O cleavage and type of phosphate group acceptor.

Mechanistic details	Enzymes
Transfer of γ-phosphate, no intermediate	PEP-carboxykinases, all kinases except NDP kinase
Transfer/Release of γ-phosphate	G-proteins, motor proteins, RecA family, nitrogenase, tubulin, chaperones, actin, topoisomerases, adenylosuccinate synthetase*, dethiobiotin-synthetase*, glutamine synthetase*, glutathione synthetase*, carbamoyl phosphate synthetase*
Transfer/Release of γ-phosphate *via* a Phosphate-enzyme intermediate	NDP kinase, E1-E2 ATPases, succinyl-CoA-synthetase
Release of β,γ-pyrophosphate	MutT, apyrases, dUTPase
Transfer/Release of β,γ-pyrophosphate *via* a pyrophosphate-enzyme intermediate	Pyruvate phosphate dikinase
Release of α,β,γ triphosphate	SAM synthetase
Transfer of AMP to acceptor	Aminoacyl-tRNA synthetases, polymerases
AMP-substrate intermediate	GMP/NAD synthetase*, luciferase*

* With covalent non-enzyme intermediate.

Table 1.3 Classification of nucleotide binding enzymes on the basis of reaction mechanisms.[55]

1.2.3 Phosphoenzyme reaction intermediates.

There is no convincing evidence that phosphoryl transfer enzymes, such as the protein kinases utilize a phosphoenzyme intermediate to facilitate protein phosphorylation. Examples of phosphotransferases that do utilize a phosphoenzyme intermediate include: alkaline phosphatase, protein tyrosine phosphatases, nucleotide diphosphate kinase and P-ATPases. In these two-stage reactions, a nucleophilic group at the enzyme active site attacks the phosphoryl group, displaces the leaving group and forms a stable intermediate.

This intermediate is then attacked by an incoming nucleophile, in the case of alkaline phosphatase a water molecule, which regenerates the free enzyme and final product.[27]

Crystal structures of many protein kinases reveal that there are no suitable nucleophiles, such as a cysteine residue positioned close enough to the terminal phosphate of ATP to form a phosphoenzyme intermediate. In contrast, some protein phosphatases (enzymes that catalyse phosphoryl transfer to water, which acts as an acceptor nucleophile), such as the tyrosine protein phosphatases utilize phosphoenzyme intermediates. Crystal structures reveal that there is a cysteine residue positioned close enough to the phosphoryl group to transiently form the thiophosphoryl enzyme adduct.

Along with the thiol of a cysteine residue (used as a nucleophilic amino acid residue by protein tyrosine phosphatases), phosphotransferases use a variety of enzyme nucleophiles to facilitate turnover, including: the carboxylate group of aspartate (P-ATPases),[56] the hydroxyl group of serine (alkaline phosphatase),[57] and the imidazole of histidine (nucleoside diphosphate kinase).

The assumption that most protein kinases utilize a single step, in-line mechanism is supported by the high levels of sequence similarity within their superfamily. By comparison, not all protein phosphatases involve a phosphoenzyme intermediate, but this family is composed of three unique gene families with distinctive three-dimensional structures and active site configurations.[58,59]

A key consideration when examining crystal structure data is that it represents a static structure that may or may not resemble the active species involved in enzyme turn over. When protein crystal structures show nucleophilic amino acid residues that are correctly positioned to be involved in the generation of a phosphoenzyme intermediate; these findings are very often complementary with stereochemical studies that indicate a mechanism involving a double displacement mechanism which is indicative of the involvement of a phosphoenzyme intermediate. The importance and findings of a number of stereochemical studies is the topic of discussion in Section 1.3.

1.3 Stereochemical studies of enzyme catalysed reactions at phosphorus.

This section will discuss how chirality can be built into the phosphate groups of ATP and how this chirality can be used to determine the stereochemical course of an enzyme catalysed reaction. A knowledge of the stereochemical course of an enzymatic reaction can be used to identify the presence of a covalent phosphoenzyme intermediate.

1.3.1 Introduction of stereochemistry into ATP.

The stereochemical course of a multitude of enzyme catalysed nucleophilic substitution on the phosphorus atoms of ATP **(38c)** have been studied. None of the three phosphorus centres in ATP are chiral hence the stereochemical consequences of nucleophilic displacement reaction are normally cryptic. Pα and Pβ are pro-chiral centres, with two identical substituents, and Pγ is a pro,pro-chiral centre with three equivalent oxygens. Chirality at phosphorus in ATP must be built into the molecules by synthesis using sulphur (chiral thiophosphates) and/or heavy isotopes of oxygen (isotopic chirality), Figure 1.13.

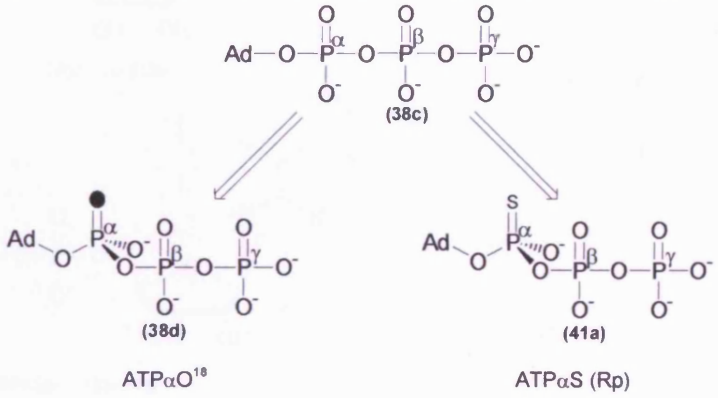

Fig. 1.13 The introduction of chirality into ATP **(38c)** using sulphur (chiral thiophosphates) and heavy isotopes of oxygen (isotopic chirality).

The two non-bridging oxygens at Pα and Pβ are diastereotopic since these are pro-chiral centres. Substitution of one of them by S, ^{17}O, or ^{18}O will lead to a chiral centre at that phosphorus.

The two possible isomers resulting from such substitution are not enantiomers but diastereoisomers, since there are other centres of asymmetry in adenosine. More

specifically, they are epimers since the configurations about the four asymmetric carbons in ribose are fixed in adenosine. To create a chiral centre at Pγ (which is pro-pro-chiral), two oxygens must be substituted by S, ^{17}O, or ^{18}O, and the two substituents must be different. It is possible to synthesise almost any nucleoside phosphate with any desired pattern of S or/and ^{17}O or/and ^{18}O substitution. These can reside, for example on either the α, β, or γ-phosphate of a nucleoside triphosphate or at an internucleotidic phosphate linkage, Figure 1.14.

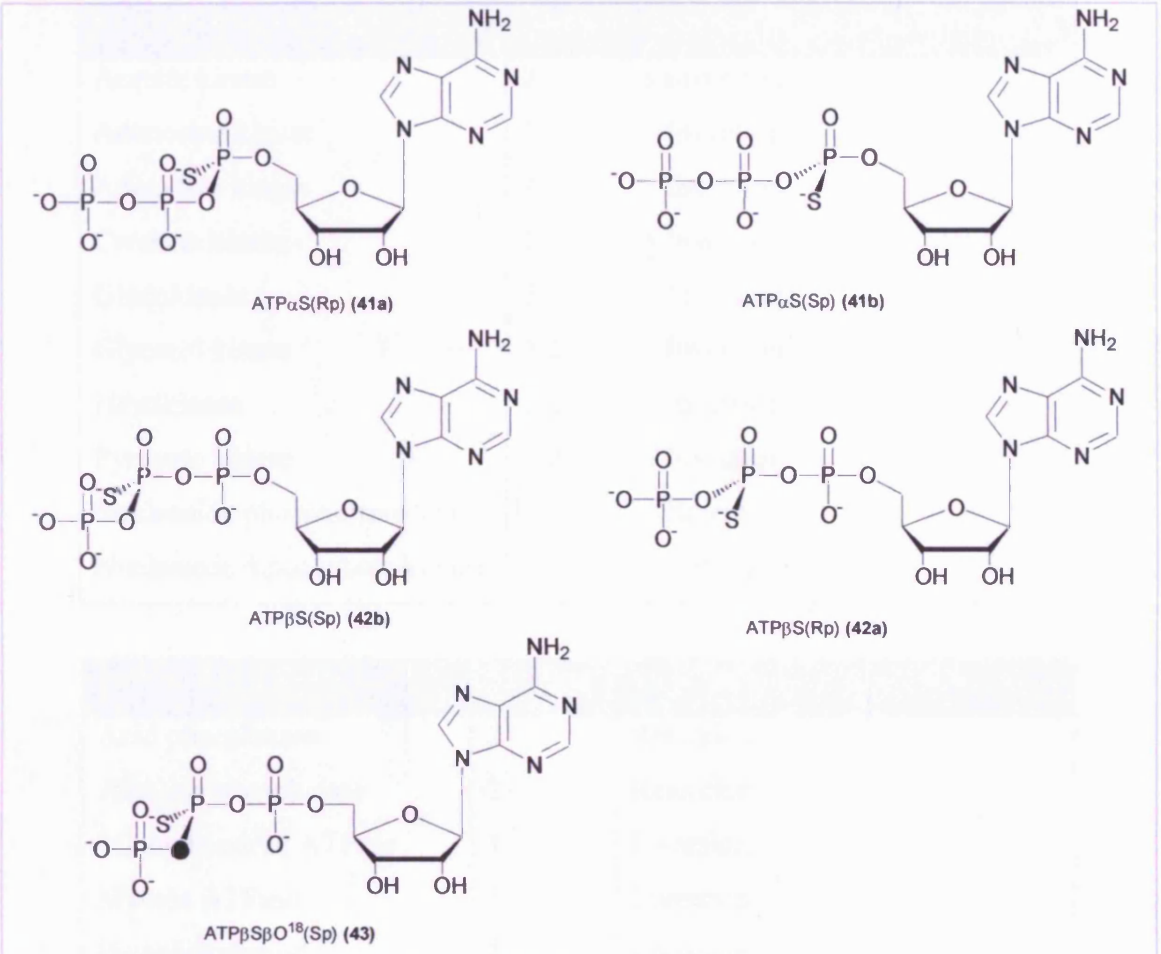

Fig. 1.14 Structural formulae for various adenosine 5′-phosphorothioates and the equivalent isotopically labelled chiral analogues.

Thiophosphate analogues of ATP are satisfactory substrates for many enzymes hence allowing the stereochemical courses of these enzymatic processes to be determined. These studies address the question of whether a reaction proceeds with inversion or retention of configuration at the phosphorous. The simplest interpretation of inversion of configuration is that the phosphoryl transfer proceeds by a single associative in-line phosphoryl transfer between two substrates in a ternary complex. However, it must be appreciated that overall inversion of configuration would also be consistent with a pathway involving an odd

number of phosphoryl transfers or even a double displacement entailing an in-line displacement followed by an adjacent displacement (see mechanism C, Scheme 1.1). However, there is no firm evidence which supports multiple (>2) phosphoryl transfer reactions or other composite pathways for simple phosphokinases. Where retention of configuration is found, it is considered that a double displacement (*via* two consecutive inversions of configuration) occurs, suggesting that a covalent phosphoenzyme intermediate is utilized by the enzyme

PHOSPHOKINASES	Method	Stereochemical Consequence
Acetate kinase	2	Inversion
Adenosine kinase	1	Inversion
Adenylate kinase	1	Inversion
Creatine kinase	2	Inversion
Glucokinase	2	Inversion
Glycerol kinase	1,2	Inversion
Hexokinase	1,2	Inversion
Pyruvate kinase	1,2	Inversion
Nucleoside phosphotransferase	1	Retention
Nucleoside diphosphate kinase	1	Retention

PHOSPHATASES	Method	Stereochemical Consequence
Acid phosphatase	2	Retention
Alkaline phosphatase	2	Retention
Mictochondrial ATPase	1	Inversion
Myosin ATPase	1	Inversion
Pyrophosphatase	1	Inversion
Glucose-6-phosphatase	2	Retention

PHOSPHOMUTASES	Method	Stereochemical Consequence
Phosphoglucomutase	2	Retention
Phosphoglycerate mutase	2	Retention

Method 1 : [^{16}O, ^{18}O] thiophosphate

Method 2 : [^{16}O, ^{17}O, ^{18}O] phosphate

Table 1.4 Stereochemical course of a number of phosphoryl and nucleotidyl transfer reactions.[36]

The results of experiments that have used the ^{16}O, ^{17}O, ^{18}O methodology to investigate the stereochemical course of phosphoryl transfer reactions catalysed by phosphokinases, phosphatases and phosphomutases are listed in Table 1.4.[36] Also shown in this table are results from experiments in which the stereochemical course of the corresponding thiophosphoryl transfers have been assessed.

The majority of the enzymes catalyse transfer of the phosphoryl group with inversion of configuration at phosphorus except for nucleoside diphosphate kinase. Some of the phosphatases and all of the phosphomutases catalyse the transfer with retention of configuration.

1.3.2 Structural aspects of nucleoside phosphorothioates.

Nucleoside phosphorothioates and their application to investigate the mechanisms of many enzyme catalysed reactions at phosphorus centres, have been the subject of many reviews.[28,60-63] They are in general, poor substrates for phosphotransferases and are processed very slowly in comparison to their all-oxygen counterparts; in some extreme cases, thiophosphates are not substrates at all, e.g. phosphoglycerate mutase.[64] The use of the ^{16}O, ^{17}O, ^{18}O methodology to investigate the stereochemical course of phosphoryl transfer reactions, allowed the reliability of the thiophosphate method to be determined. Subsequent comparisons between isotopically labelled chiral phosphates and thiophosphates as stereochemical probes, Table 1.4, have revealed no contradiction, and thiophosphates are accepted as reliable alternative substrates.

Phosphorothioate anions are probably best represented with the negative charge localised on the sulphur and the P-S bond order of 1.[65,66] The arguments in favour of this were based on data from a variety of solution techniques including ^{18}O-induced upfield shifts in ^{31}P NMR, ^{17}O NMR chemical shifts, ^{31}P-^{17}O coupling constants, and vibrational spectroscopy.[66] It is recognised however that some delocalisation of charge from sulphur may be significant in thiophosphate diesters such as ATPαS and ATPβS.

Thiophosphoric acids and esters are more acidic than the corresponding phosphoric acids and esters. For example the pK_a values of thiophosphoric acid are 1.67, 5.40, and 10.14, compared to 2.1, 7.2, and 12.3 for phosphoric acid.[66] This reflects the greater stability of

negative charges on sulphur than on oxygen and is probably due to the larger size and greater polarisability of the sulphur which gives lower charge densities than in oxyanions.

The substitution of oxygen by sulphur may be expected to alter several of the key substrate properties, (intrinsic reactivity in the uncatalysed reaction, steric properties, pK_a, metal ion coordination or hydrogen bonding) any one of which may be responsible for the general slower reactivity with respect to the corresponding oxy substrates.

1.4 6-Hydroxymethyl-7,8-dihydropterin pyrophosphokinase (HPPK).

1.4.1 Folic acid biosynthetic pathway.

Dihydroneopterin aldolase (DHNA) converts dihydroneopterin **(44)** into 6-hydroxymethyl-7,8-dihydropterin **(46)** by removal of glycolaldehyde **(45)**, a reaction that constitutes the first step in the biosynthesis of folic acid, Scheme 1.9. 6-Hydroxymethyl-7,8-dihydropterin pyrophosphokinase (HPPK) catalyses the transfer of pyrophosphate from ATP to 6-hydroxymethyl-7,8-dihydropterin **(46)**, to give 6-hydroxymethyl-7,8-dihydropterin pyrophosphate **(47a)**.

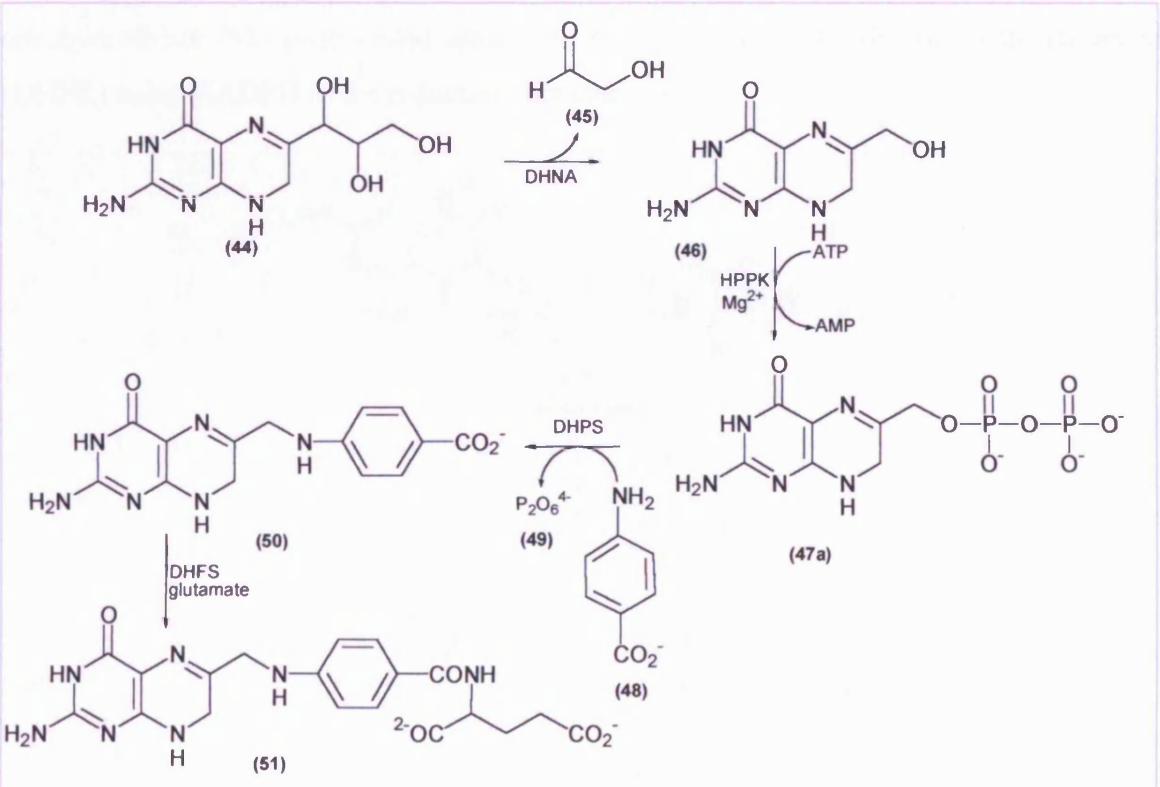

Scheme 1.9 The biosynthesis of folic acid.

6-Hydroxymethyl-7,8-dihydropterin pyrophosphate **(47a)** is linked to *para*-aminobenzoate **(48)** to give 7,8-dihydropteroate **(50)** and pyrophosphate **(49)** in a condensation reaction catalysed by dihydropteroate synthase (DHPS). Finally, the dihydrofolate synthase (DHFS) catalysed addition of glutamate to 7,8-dihydropteroate **(50)** gives dihydrofolate **(51)**.[67]

Bacteria, fungi and protozoa must synthesise folates *de novo* since they lack the carrier-mediated active transport system of mammalian cells that allows the use of pre-formed folates obtained from their diets or from micro-organisms in their intestinal tracts.[68] Mammals can synthesise a pteridine ring, but they are unable to conjugate it to the other two units of dihydrofolate since they lack the enzymes: HPPK, DHPS and DHFS. For this reason, these enzymes are important targets for developing new antimicrobial agents.

1.4.2 Biosynthesis of tetrahydrofolate and its derivatives.

Dihydrofolate **(51)**, the product of the folic acid biosynthetic pathway, is converted to tetrahydrofolate **(52)** (also called tetrahydropteroylglutamate) by dihydrofolate reductase (DHFR) using NADPH as the reductant, Scheme 1.10.

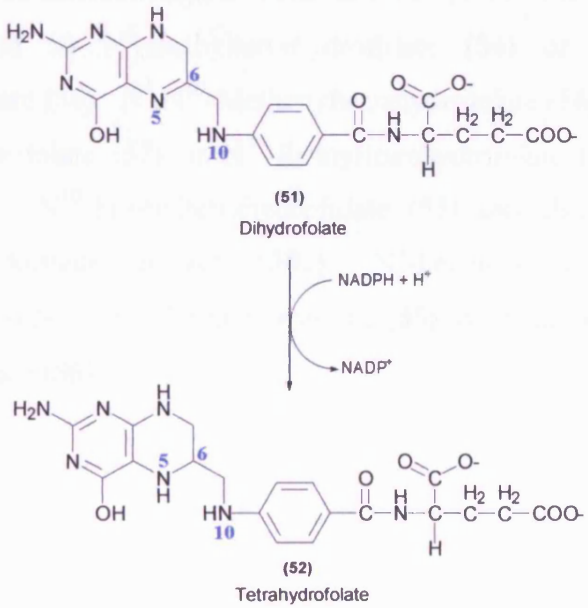

Scheme 1.10 Biosynthesis of tetrahydrofolate.

Tetrahydrofolate **(52)** is a highly versatile carrier of activated one-carbon units, which are bonded to its N-5 or N-10 nitrogen atom or both. This unit can exist in three oxidation states, Table 1.5. The most reduced form carries a methyl group, whereas the intermediate form carries a methylene group. More oxidised forms carry a formyl, formimino, or methenyl group.[2]

Oxidation States		Group
Most reduced (= methanol)	$-CH_3$	Methyl
Intermediate (= formaldehyde)	$-CH_2-$	Methylene
Most oxidized (= formic acid)	-CHO -CHNH -CH=	Formyl Formimino Methenyl

Table 1.5 One-carbon groups carried by tetrahydrofolate.[2]

The one-carbon units are interconvertible, Scheme 1.11. N^5,N^{10}-Methylenetetrahydrofolate **(53)** can be reduced to N^5-methyltetrahydrofolate **(54)** or oxidised to N^5,N^{10}-methenyltetrahydrofolate **(56)**. N^5,N^{10}-Methenyltetrahydrofolate **(56)** can be converted into N^5-formiminotetrahydrofolate **(57)** or N^{10}-formyltetrahydrofolate **(55)**, which are at the same oxidation level. N^{10}-Formyltetrahydrofolate **(55)** can also be synthesised from tetrahydrofolate **(52)**, formate, and ATP **(38c)**.[2] N^5-Formyltetrahydrofolate **(58)** can be reversibly isomerised to N^{10}-formyltetrahydrofolate **(55)** or it can be converted to N^5,N^{10}-methenyltetrahydrofolate **(56).**

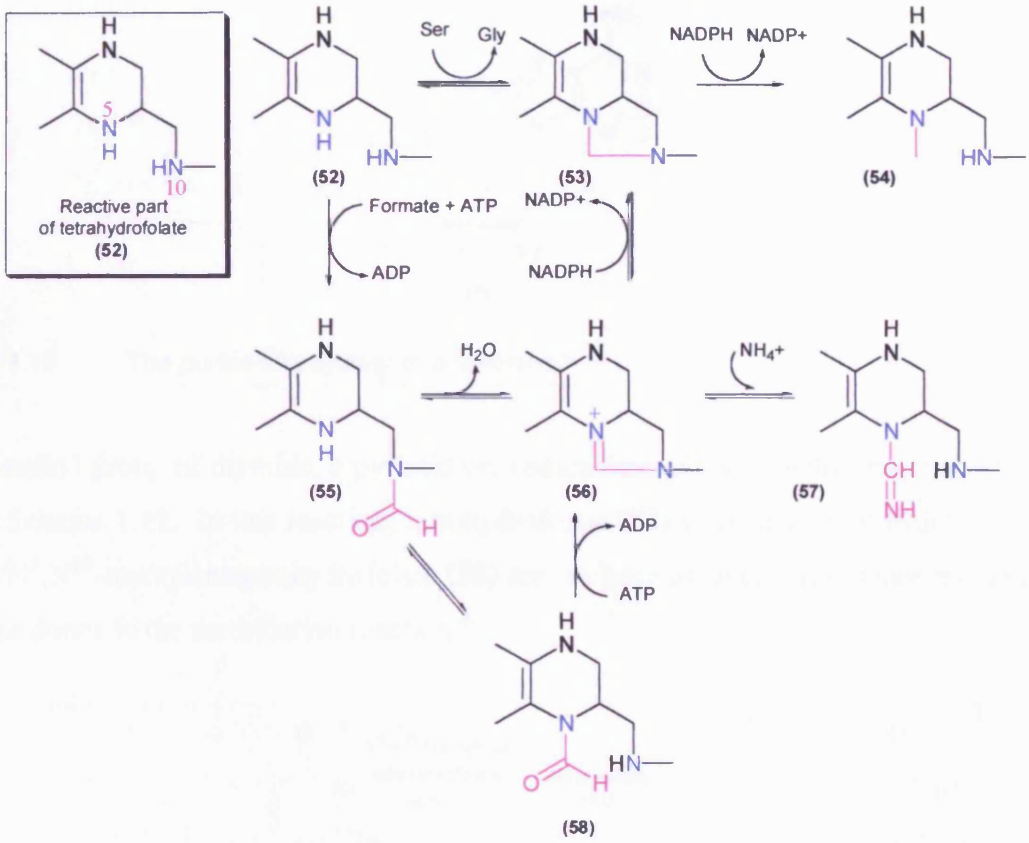

Scheme 1.11 Conversion of one-carbon units attached to tetrahydrofolate.[2]

1.4.3 Biological role of tetrahydrofolate derivatives.

Tetrahydrofolate derivatives serve as donors of one carbon units in a variety of biosyntheses including the synthesis of purines, thymidylate, glycine, methionine, pantothenic acid and N-formylmethionyl-tRNA in all cells.[2]

Methionine is regenerated from homocysteine by transfer of the methyl group of N^5-methyltetrahydrofolate **(54)**. The carbon atoms C2 and C8 of purines, such as the purine ring system of adenosine **(59)**, are derived from N^{10}-formyl derivatives of tetrahydrofolate, Figure 1.15.[2]

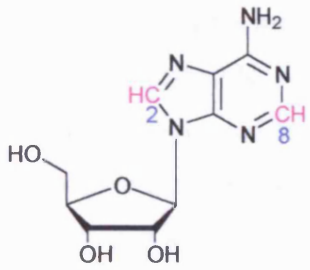

(59)

Fig. 1.15 The purine ring system of adenosine.[2]

The methyl group of thymine, a pyrimidine, comes from N^5,N^{10}-methylenetetrahydrofolate **(53)**, Scheme 1.12. In this reaction, tetrahydrofolate **(52)** is oxidised to dihydrofolate **(51)**. Thus N^5,N^{10}-methylenetetrahydrofolate **(53)** serves both as an electron donor and as a one-carbon donor in the methylation reaction.[2]

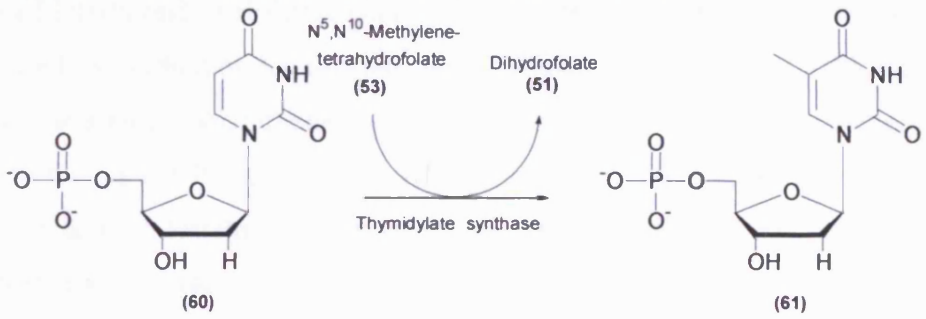

Scheme 1.12 Thymidylate synthase catalyses the methylation of dUMP to dTMP.[2]

N^5,N^{10}-Methylenetetrahydrofolate **(53)** donates a one-carbon unit in the synthesis of glycine from CO_2 and NH_4^+, a reaction catalysed by glycine synthase (called the glycine cleavage enzyme when it operates in the reverse reaction), Scheme 1.13.[2]

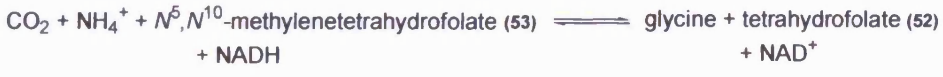

Scheme 1.13 Synthesis of glycine.[2]

Thus, one-carbon units at each of the three oxidation levels are utilised in many biosynthetic pathways. Furthermore, tetrahydrofolate **(52)** serves as an acceptor of one-

carbon units in degradative reactions. The major source of one-carbon units is the facile conversion of serine into glycine, which yields N^5,N^{10}-methylenetetrahydrofolate **(53)**. Serine can be derived from 3-phosphoglycerate, and so this pathway enables one-carbon units to be formed *de novo* from carbohydrate. The breakdown of glycine by the glycine cleavage enzyme yields CO_2 and NH_4^+, and a one carbon fragment that becomes part of N^5,N^{10}-methylenetetrahydrofolate **(53)**. Likewise, one-carbon units from betaine and choline funnel into tetrahydrofolate to form the N^5,N^{10}-methylene derivative. The breakdown of histidine yields N-formiminoglutamate, which transfers its formimino group to tetrahydrofolate to give the N^5 derivative.[2]

1.4.4 Folic acid biosynthetic pathway enzymes as targets for antimicrobial chemotherapy.

Inhibitors of DHPS and DHFR, the second and fourth enzymes in the folate pathway, are currently used as antibiotics for treating many infectious diseases.[69] DHPS represents an ideal target for antimicrobial chemotherapy; since it has no mammalian counterparts high-level selectivity should be achievable. DHFR, an enzyme that catalyses the reduction of dihydrofolate to form tetrahydrofolate in bacteria and mammalian cells, has also proved to be an important drug target.

Trimethoprim (TMP) and sulphonamides (SULs) are synthetic antibacterial agents, with a wide antibacterial spectrum including common urinary tract pathogens (*Escherichia coli*), respiratory tract pathogens (*Streptococcus pneumoniae, Haemophilus influenzae*) and skin pathogens (*Staphylococcus aureus*) as well as certain enteric pathogens (*Shigella*). Both compounds are relatively inexpensive, allowing them to be used outside of developed countries.[70]

DHFRs from different organisms do not have identical structures and a survey of a wide range of compounds have resulted in the identification of drugs that inhibit the enzyme in protozoa and bacteria but not in higher organisms.[71] Trimethoprim is a pteridine analogue that acts as a competitive inhibitor of DHFR, due to its structural analogy to the substrate of this enzyme, dihydrofolate. The human DHFR is resistant to trimethoprim, which is the basis for its selectivity and its clinical use.[70]

DHPS catalyses the condensation of p-aminobenzoic acid (Abz) and 6-hydroxymethyl-7,8-dihydropterin to form dihydropteroate in microorganisms, but is not present in mammalian cells. SUL drugs act as competitive inhibitors of DHPS, thereby blocking folate biosynthesis in bacterial cells. SULs are structural analogues of the normal substrate *para*-aminobenzoic acid and can indeed work as alternative substrates to produce sulphur containing pteroate adducts.[70]

As a consequence of the development of bacterial resistance to TMP and SULs, studies have been conducted to determine the spread and mechanisms of TMP and SULs resistance at the molecular level. This work is complemented with studies on the mechanism of the enzymes and their mode of inhibition in order to identify better drug targets.

Resistance to sulphonamides is caused by either specific mutations in the DHPS gene (*dhps*) on the bacterial chromosome, or by drug-resistant variants of the DHPS enzyme carried on plasmids.

Chromosomal sulphonamide resistance occurs naturally by mutational changes such as point mutations and recombination in the gene that codes for DHPS. Point mutations have been detected in the nucleotide sequence of the *dhps* gene from *Escherichia coli* C, in which two identical mutants differed from the wild-type strain by a single base pair. This change alters the phenylalanine residue at position 28 in the wild type to an isoleucine residue in the mutant,[72] conferring high levels of sulphonamide resistance. Resistance introduced by recombination has been detected in *N. meningitidis* were the *dhps* gene was found to be 10% different from the SUL-susceptible isolates.[70]

Sulphonamide resistance in gram-negative enteric bacteria is largely plasmid borne. Plasmids are mobile genetic elements (Episome) that can exist as a separate piece of DNA or become integrated into the bacterial genome. These circular duplex DNA molecules may carry genes such as alternative drug-resistant variants of the DHPS enzymes that can be replicated autonomously. Two such plasmid-encoded enzymes that have been characterised are *sulI* and *sulII*. Both have substantial sequence divergence compared with the chromosomal *dhps* genes from *Escherichia coli* and other bacteria. The sulI gene is normally found linked to other resistance genes on R factor plasmids and is located on the transposons of the Tn21 family.[70]

R factor (resistance factor) plasmids are highly mobile transposons that link together genes conferring resistance to multiple antibiotics.[2] These plasmids contain a resistance transfer factor (RTF) in addition to several r-genes. The RTF region enables the plasmid to be transmitted to other bacteria by conjugation and the r-genes, such as *sulI,* code for enzymes that inactivate specific antibiotics. Multiple drug-resistance is extremely infectious as R factor plasmids can be transmitted in mixed cultures and between bacterial species.[2]

Chromosomal TMP resistance has also been detected in *Escherichia coli.* These highly resistant strains combine a several hundred-fold overproduction of the chromosomal DHFR with an increase in the K_i for the drug.[73] A mutational substitution of a glycine for a tryptophan at position 30 was thought to relate to the observed threefold increase in the K_i for TMP. The number of plasmid-encoded, drug-resistant DHFRs appearing in pathogenic bacteria is constantly increasing, with many variations of the *dhfr* gene detected.[70]

1.4.5 Rational drug design based on structural and kinetic data concerning DHPS and HPPK.

Studies have been conducted to allow the development of new variations of sulphonamides that are more target specific. For example, equilibrium binding assays and kinetic measurements have highlighted that the target for sulphonamide inhibition in *Streptococcus pneumoniae* DHPS is the enzyme-substrate binary complex, rather than the apoprotein form of the enzyme.[74]

The crystal structure of *Mycobacterium tuberculosis* DHPS in complex with 6-hydroxymethylpterin monophosphate has provided structural insights for the design of novel inhibitors.[75] Analysis of crystallographic data has highlighted a highly conserved pterin-binding pocket. Sulphur containing drugs, such as the sulphonamides **(62)** and sulphones **(63)**, that are generally substituted on the sulphonamide position, Figure 1.16, can be modified in a position opposite to where substitutions are traditionally made, resulting in their extension into the pterin pocket. This may result in a new set of

chemically diverse molecules that may serve as lead compounds for antimycobacterial drug design.

(62)

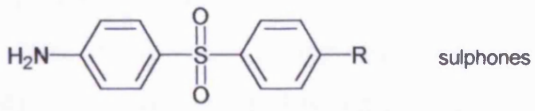

(63)

Fig. 1.16 Chemical formulas of sulphur containing drugs, competitive antagonists of *para*-aminobenzoic acid.[75]

HPPK represents a new target in a biosynthetic pathway that has proven effective for the development of novel antimicrobial agents. Crystal structures have been published by several authors[52,69,76,77] providing a framework, (for example, the identification of hydrophobic areas, conserved amino acid residues and active site structure) for structural based design of new antimicrobial agents.

Bisubstrate analogues, mimicking the HPPK catalysed reaction have been developed consisting of a pterin, an adenosine moiety, and a link composed of 2-4 phosphoryl groups **(64)**, Figure 1.17.

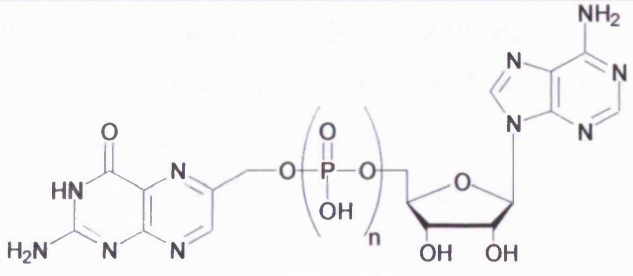

n = 2,3,4

(64)

Fig. 1.17 Structure of bisubstrate analogues.[78]

Inhibition and binding studies of the bisubstrate analogues have shown that P^1-(6-hydroxymethylpterin)-P^4-(5'-adenosyl)tetraphosphate **(64)** (n = 4) is the most potent inhibitor of HPPK (Kd = 0.47 μM in the presence of Mg^{2+} and IC_{50} = 0.44 μM). Crystal structures have indicated that this compound occupies both the pterin and adenosine binding sites and induces significant conformational changes. Although such compounds would not be useful as drug candidates, they do indicate that the bisubstrate inhibitor approach can produce potent inhibitors for HPPK and demonstrate that the minimum length of the link for these compounds is approximately 7 Å.[78] It is significant that although compound **(64)** is the most potent bisubstrate inhibitor, it does not appear to be the closest analogue of the direct pyrophosphoryl transfer. The transition state for this type of reaction, Figure 1.18, more closely resembles a bisubstrate analogue containing a link composed of two phosphate groups.

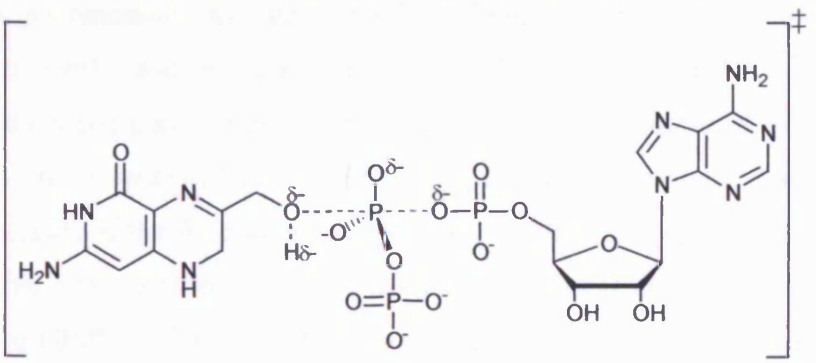

Fig. 1.18 The transition state for an S_N2 displacement reaction at the β-phosphorus centre.

The usual reason for additional phosphate groups in the link segment of a bisubstrate inhibitor is to compensate for the penta coordinate phosphate in the transition state, which contains partially formed bonds which are longer than those of the tetrahedral phosphate groups in the link. It can be imagined though that one additional phosphate group would be sufficient to make the linker segment the appropriate length to mimic the transition state illustrated in Figure 1.18. It may be that the additional two phosphate groups in the linker allow additional hydrogen bonding with constituents of the active site (i.e. amino acid residues and magnesium metal ions). This additional binding may explain why the bisubstrate analogue with four phosphate groups in the linker is the most potent inhibitor of HPPK.

Equilibrium and kinetic studies of substrate binding to HPPK from *Escherichia coli*[68] provide evidence for a compulsory order of addition of the two substrates to HPPK, with ATP binding first with high affinity in a slower step to form a binary complex followed by the more rapid addition of 6-hydroxymethyldihydropterin. Experiments were performed using the nonhydrolysable ATP analogue 2'(3')-O-(N-methyleneadenosine triphosphate (AMPCPP). The very high binding affinity of the ATP-HPPK complex for 6-hydroxymethyldihydropterin suggests that the design of antimicrobial inhibitors that target the 6-hydroxymethyldihydropterin binding site, should be based on the ATP-HPPK binary complex, rather than the apo-enzyme.

1.4.6 Discovery and purification of HPPK.

HPPK was first identified in *Escherichia coli* in 1964[79] and its DNA sequence from *Streptococcus pneumoniae* was determined in 1990.[80] The enzyme was purified to homogeneity in 1991[81] and the gene encoding HPPK was cloned in 1992.[82] Most of the bacterial genes encode a monofunctional protein with a molecular mass of approximately 18 kDa. In *Escherichia coli*, DHNA, HPPK and DHPS, the enzymes that catalyse three sequential reactions in the folic acid biosynthetic pathway, are separate proteins encoded by chromosomal genes located on the same operon.[52] This is in contrast to all eukaryotic proteins, where HPPK activity is either associated with DHPS, as observed for protozoa *Plasmodium falciparum* and *Toxoplasma,* or is part of a trifunctional protein composed of DHNA, HPPK, and DHPS, as in *Pneumocystis carinnii.* A putative multifunctional folic acid synthesis gene from the eukaryote *Pneumocystis carinii*, encodes a protein with an apparent molecular mass of 69 kDa.

Most recently, HPPK was purified from the mitochondria of pea leaves and was shown to be part of a bifunctional protein consisting of HPPK and DHPS.[83,84] In a recent publication,[52] it was reported that the *fol*K gene from *Haemophilus influenzae* had been cloned and expressed in *Escherichia coli.* The purified HiHPPK protein was a monomer.

The elucidation of amino acid sequences from many HPPKs through genome sequencing projects have revealed 13 strictly conserved residues.[76] The *Escherichia coli* enzyme is highly homologous to HPPKs from many pathogenic microbial organisms. For example, it shares a 56% identity with *Haemophilus influenzae* HPPK, 40% identity with

Pneumocystis carinnii HPPK/DHPS and a 33% identity with *Mycobacterium tuberculosis* HPPK.[76,77] Consequently, the structural information derived from the *Escherichia coli* HPPK could be used in the design of novel broad-spectrum antimicrobial agents.[76]

Considerable variation in gene evolution is suggested by the differences observed among the HPPKs and DHPSs from various species.[83] Multifunctional enzymes are thought to have evolved by the fusion of smaller monofunctional proteins, each functional domain being connected by protease-sensitive linker regions.[85] In connection with this, it has been shown that the HPPK domain of the multifunctional protein of *Pneumocystis carinnii* can be over expressed as an independent enzyme in *Escherichia Coli*[86], and refolding of the recombinant protein yielded enzymatically active HPPK in its monomeric form. Although the function of such an evolution is not clearly understood, a possible advantage of the bifunctional nature of HPPK/DHPS could be to bring the two catalytic sites closer. As these two activities are sequential in folate synthesis, such a situation would reduce the diffusional pathway in the mitochondrial matrix space.[83]

1.4.7 HPPK crystal structures.

As a small (158 residues, 18 kDa), stable, monomeric protein, *Escherichia coli* HPPK is not only a new target for development of antimicrobial agents but also an excellent model system for studying the mechanisms of pyrophosphoryl transfer.[76] The crystal structure of *Escherichia coli*[69,76,77,87,88] and the *Haemophilus influenzae*[52] HPPK have been solved providing a structural framework for elucidating structure/function relationships of HPPK and the mechanism of pyrophosphoryl transfer.[52]

Recently a 1.25 Å crystal structure of the *Escherichia coli* HPPK in complex with 6-hydroxymethyldihydropterin, two Mg^{2+} ions and an ATP analogue, AMPCPP **(65)** was published by Yan *et al.*[76] AMPCPP **(65)**, Figure 1.19 does not have an ester bond between the α- and β-phosphate groups. Consequently HPPK-HP-MgAMPCPP is a dead-end complex that closely mimics the ternary complex HPPK-HP-MgATP.[76]

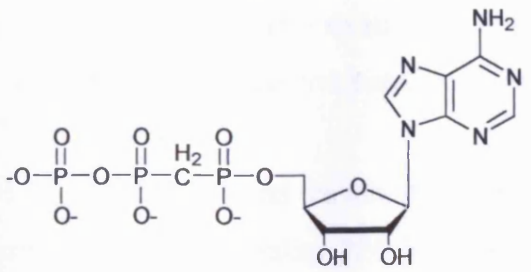

(65)

Fig. 1.19 AMPCPP.

The functional monomer consists of a three-layered αβα fold formed by six β strands and four α helices in the sequence β1-α1-β2-β3-α2-β4-β5-β6-α3-α4, Figure 1.20.

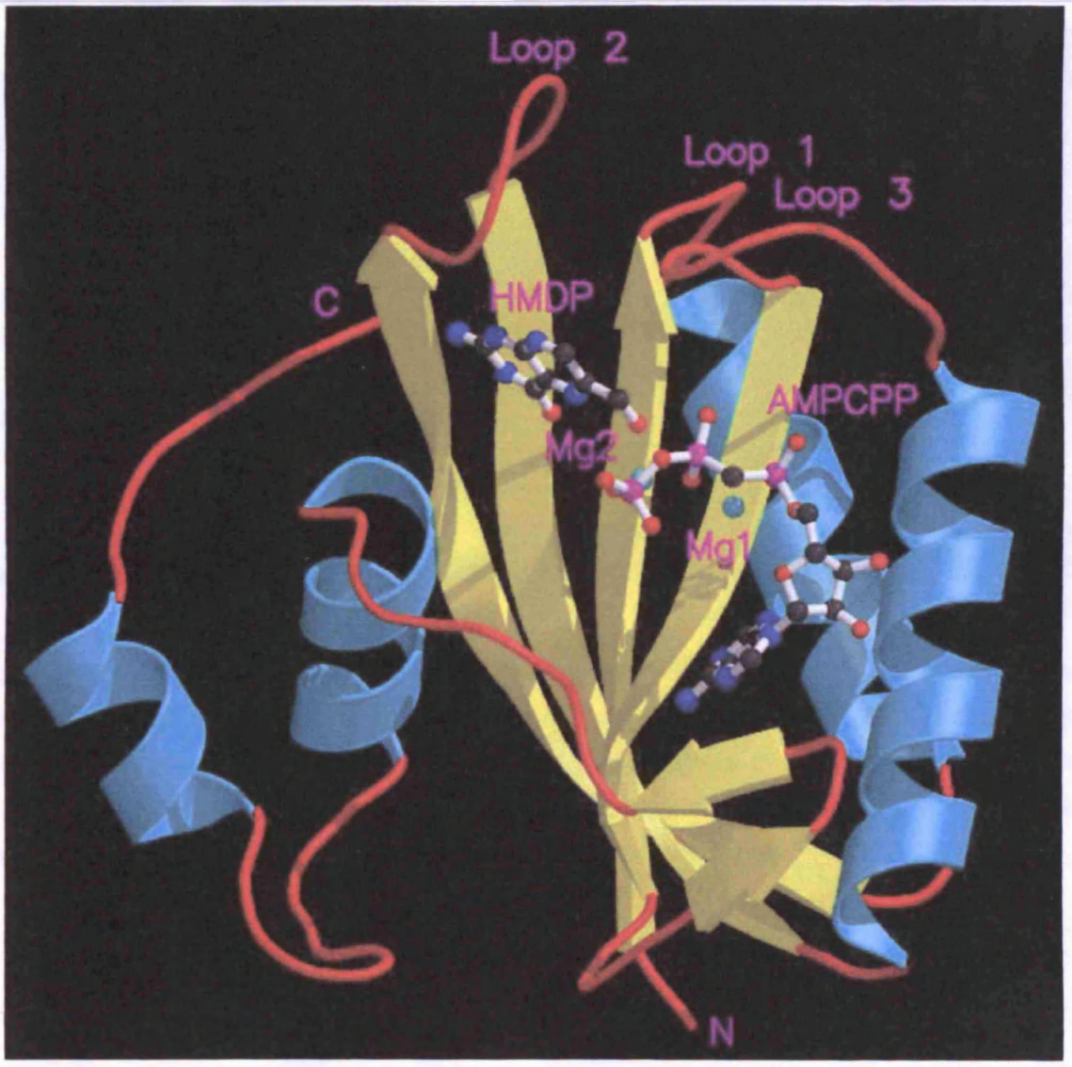

Fig. 1.20 Crystal structure of HPPK in complex with 6-hydroxymethyl-7,8-dihydropterin, AMPCPP and Mg^{2+} showing the secondary structure elements (α helices as spirals, β strands as arrows, and loops as tubes), substrate molecules and Mg^{2+} ions (ball-and-stick models with atomic colour scheme: carbon in black, nitrogen in blue, oxygen in red, phosphorus in pink and magnesium in grey).[89]

In the centre, the six β strands are organized into an antiparallel β sheet (β2,β3,β1,β4) and a β hairpin (β5 and β6). On each side of the central β structure there are two α-helices.[76]

The surface illustration of the apo-HPPK[77] and the ternary complex[76] is depicted in Figure 1.21. The three-layered αβα fold creates a valley 25Å long, 10Å wide and 10Å deep that has both ends and the front open to the solvent when the protein is not bound to the substrates, Figure 1.21a. In HPPK-HP-MgAMPCPP, one end and the front of the valley are sealed, leaving only one end open. Figure 1.21b.

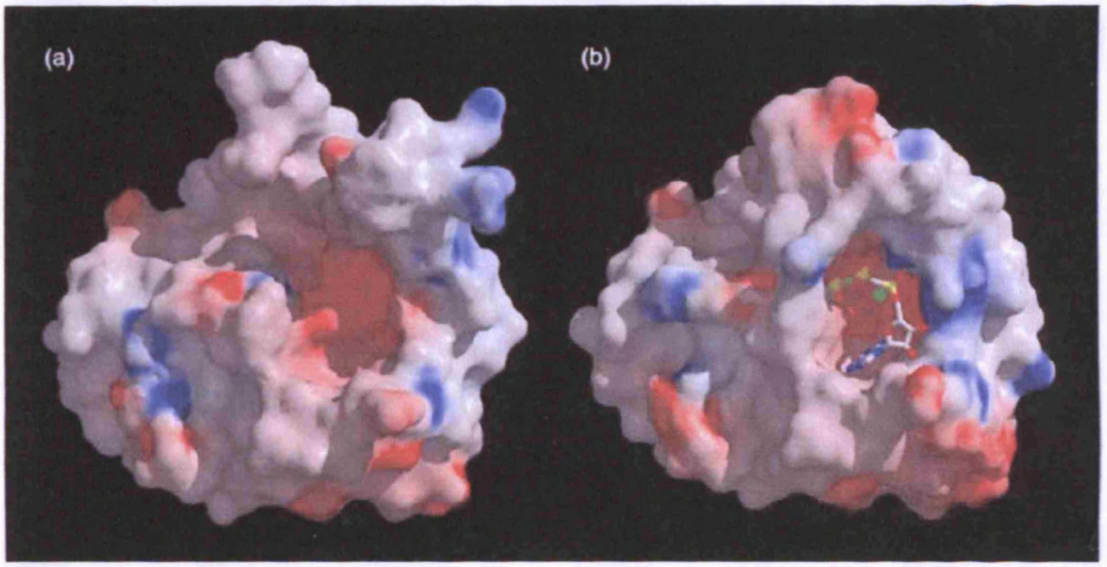

Fig. 1.21 (a) Apo-HPPK,[77] (b) HPPK-HP-MgAMPCPP[76] illustrating the conformational differences between the two structures. The surface is coloured according to electrostatic potential: blue for positive and red for negative. The substrate molecules and cofactors are represented as ball-and-stick models with the atomic colour scheme (carbon in white, nitrogen in blue, oxygen in red, phosphorus in yellow and magnesium in green).[89]

Ligand binding induces a conformational change in three flexible loops, Figure 1.22. In the apo-HPPK, loop-1 assumes two conformations with almost equal probabilities,[77] whereas in the ternary complex it has one well-defined conformation. Loops 2 and 3 appear to close in towards the valley and cover up the catalytic centre when the Mg^{2+} ions and both substrates are bound.[76]

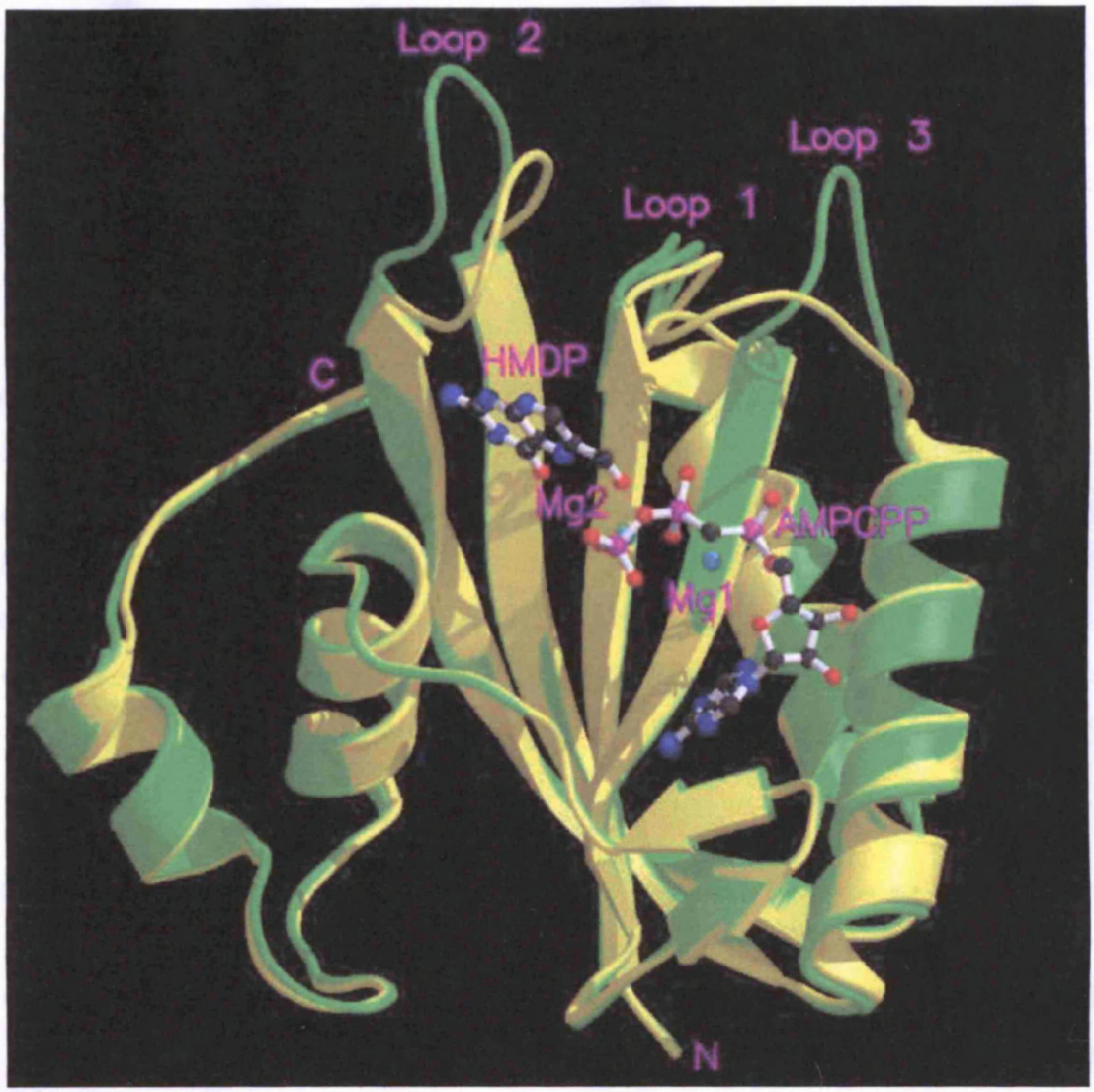

Fig. 1.22 The overall fold of HPPK. The Apo-HPPK (green,[77]) superimposed with the ternary complex HPPK-HP-Mg-AMPCPP (yellow,[76]) showing the secondary structure elements (α helices as spirals, β strands as arrows, and loops as tubes), substrate molecules and Mg^{2+} ions (ball-and-stick models with atomic colour scheme: carbon in black, nitrogen in blue, oxygen in red, phosphorus in pink and magnesium in grey).[89]

1.5 AIMS.

This general introduction has explained how displacement reactions at the phosphoryl centres of phosphate esters are a biologically important and a much studied reaction type. The chemistry and kinetics of this reaction have been evaluated, concentrating primarily

on stereochemical, crystallographic and NMR methods. These have been used to determine details concerning the fundamental mechanism of enzyme catalysed and uncatalysed processes. HPPK, a pyrophosphoryl transfer enzyme, has been described as an important member of the folic acid biosynthetic pathway and a potential drug target. This stable monomeric protein can be used to study the poorly understood mechanism of pyrophosphoryl transfer.

The exploitation of isotopically labelled chiral phosphorothioate analogues of ATP, coupled to the measurement of ^{18}O isotopic shifts in the ^{31}P NMR of isotopically labelled chiral phosphate monoesters has been used to provide a new method to determine the stereochemical course of HPPK. The methodology for our technique required the introduction of chirality at the prochiral β-phosphorus centre of ATP of known absolute configuration. This has involved the stereospecific synthesis and configurational analysis of chiral and isotopically labelled chiral phosphorothioate analogues of ATP (Chapters 2 and 3).

The absolute stereochemistry of isotopically labelled chiral phosphate and thiophosphate monoesters can be determined by ^{18}O isotopic shifts in ^{31}P NMR. We intend to generate an isotopically labelled chiral phosphate monoester of unknown configuration utilizing the catalytic action of HPPK on ATPβSβγ^{18}O (Sp), and subsequent chemical modification (Chapter 5). The absolute stereochemistry at this centre will be determined by comparison of ^{18}O isotopic shifts in ^{31}P NMR with a structurally identical isotopically labelled chiral phosphate monoester of known absolute configuration, synthesised by an independent, stereospecific and unambiguous method (Chapters 2 and 3).

The study will distinguish between a single-step pyrophosphoryl transfer *via* a penta-co-ordinate transition state and a two-step transfer believed to involve an enzyme bound intermediate. A detailed understanding of the mechanism of the reaction will facilitate the design and synthesis of new therapeutic agents with enhanced potency.

A kinetic investigation into the diastereoselectivity of HPPK toward the diastereoisomers of ATPβS [(Rp) and (Sp)] has required the development of a new assay to measure the rate of reaction utilizing HPLC-mass spectrometry (Chapter 4).

CHAPTER 2
Synthesis of Isotopically Labelled Chiral Alkyl and Nucleotide Thiophosphate Esters

2.1 Introduction.

In order to study the stereochemical course of enzyme catalysed phosphoryl, pyrophosphoryl and nucleotidyl transfer reactions, methods for the stereospecific synthesis of isotopically labelled chiral phosphate **(66a)** and thiophosphate **(67a)** esters have been developed [R = alkyl, aryl, nucleoside/nucleotide], Figure 2.1.[63,64,90-95]

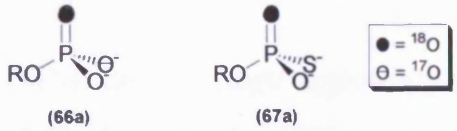

(66a) (67a)

Fig. 2.1 Isotopically labelled chiral phosphate **(66a)** and thiophosphate **(67a)** esters.

2.2 Literature synthesis of isotopically labelled chiral phosphates.

Many stereospecific syntheses described in this chapter begin with either 1,3,2-oxazaphospholidin-2-ones or 2-thiones (P=O = P=S) as the chiral precursor. An indisputable assignment of the absolute configuration of the phosphorus centre in these compounds was achieved by a combination of ^{1}H NMR, ^{31}P NMR, crystal structure and optical rotatory evidence.

The cis **(68a)** and trans **(68b)** cyclic compounds adopt an ^{1}E ring conformation, Figure 2.2, resulting in a Karplus-type relation between the P-O-C-H and the P-N-C-H vicinal (^{3}J) couplings and the corresponding dihedral angles.

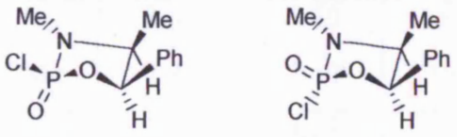

(68a) (68b)

Fig. 2.2 The ^{1}E ring conformation for *cis* **(68a)** and *trans* **(68b)** 1,3,2-oxazaphospholidin-2-one.

NMR data presented in Table 2.1 for the phosphoramidic chlorides **(68-74a)** and **(68-74b)** and several esters derived from alcoholysis of these chlorides, Figure 2.3, is consistent

with a ^1E ring conformation in which the oxygen is out of the plane of the other four atoms.

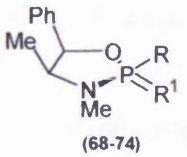

(68-74)

Fig. 2.3 Phosphoramidic esters.

In this conformation the P-O-C-H dihedral angle approaches 90°, consistent with a small $J_{P,H-5}$ value, and the P-N-C-H dihedral angle is >120°, consistent with a large $J_{P,H-4}$ value. The coupling constant data for compounds (68-74b) are consistent with similar but less puckered conformations than those for (68-74a), Table 2.1.

Compound	R	R'	δ H-4	δ H-5	J P, H-4	J P, H-5	$[\alpha]_D$
(68a)	Cl	O	3.85	5.84	26	1	-64
(68b)	O	Cl	3.70	5.54	14	7	-26
(69a)	OMe	O	3.70	5.63	20	1.9	-110
(69b)	O	OMe	3.64	5.52	14	3.6	-37
(70a)	OPh	O	3.61	5.65	14	1	-102
(70b)	O	OPh	3.51	5.28	10	4	-34
(71a)	Me	O	3.69	5.74	12.2	1-2	-81
(71b)	O	Me	3.55	5.43	14	4.5	-65
(72a)	Me	S	3.18	4.89	1.2	1	-128
(72b)	S	Me	3.11	4.87	<1	1.1	-25
(73a)	OMe	S	3.65	5.60	16.25	4.4	-140
(73b)	S	OMe	3.73	5.60	14.5	2.7	+2
(74a)	OEt	S	3.66	4.25	16	4.2	-122
(74b)	S	OEt	3.77	4.20	14	2.8	-5

Table 2.1 ^1H NMR and optical rotation data for a variety of Phosphoramidic esters.

The configurations at phosphorus in compounds **(68-74)** were assigned on the basis that in the phosphorus containing heterocycles those protons in a 1,3-cis relationship to a P=O

group are deshielded. Thus, since H-4 and H-5 resonate at a lower field in compounds **(68-74a)** than in compounds **(68-74b)** the P=O group must be cis to H-4 and H-5 in the 'a' series, Table 2.1. The deshielding effect is greater for H-5 than for H-4, a result which is to be expected in a ^{1}E conformation in which P=O is closer to H-5 than to H-4.[96]

The configurational analysis of the 1,3,2-oxazaphospholidin-2-thiones are complicated by the fact that the observed deshielding effect of sulphur is only very small compared to that of oxygen. This problem was solved on the basis that P=S is oxidised to P=O by *m*-chloroperbenzoic acid with retention of configuration.[97] For example **(73a)** was converted to **(69a)**, Scheme 2.1, allowing the absolute configuration to be assigned on the basis of deshielding effect of the P=O group.

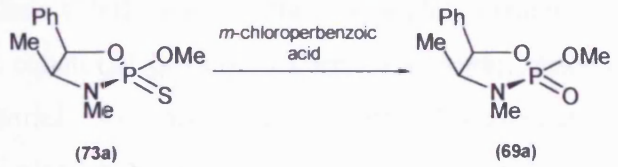

(73a) (69a)

Scheme 2.1 P=S is oxidation.

Additional comparative evidence for the structures of thiones comes from optical rotations. For P=O derivatives all the compounds in the 'b' series have higher rotations (i.e. less negative) than those in the 'a' series, a trend that is followed by the P=S compounds, Table 2.1.

The stereochemical course of many nucleophilic displacements of the exocyclic substituent in five-membered ring phosphoryl compounds such as 1,3,2-oxazaphospholidin-2-one **(68a** and **68b)** and -2-thione have been established. The absolute configurations of the phosphoramidic esters follows from the configuration of the chloride since there is a good precedent (Table 2.1) for assuming that the displacement reaction occurs with retention of configuration.[8,96]

The most simple explanation for the experimental evidence that retention of configuration is observed in exocyclic displacement reactions at phosphorus held in a five-membered

ring is in terms of an adjacent associative mechanism, Scheme 2.2. For a more detailed explanation of this mechanism see Chapter 1, Section 1.1.

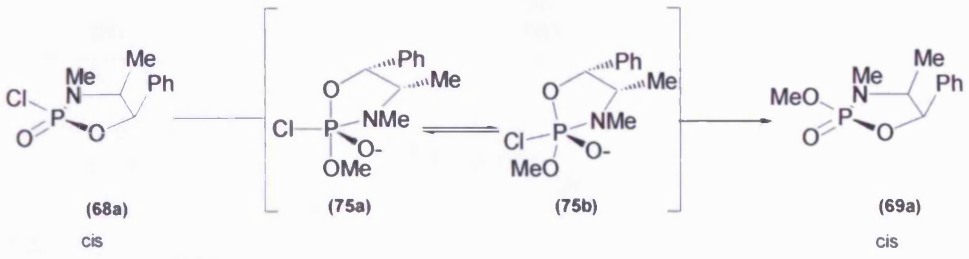

Scheme 2.2 The adjacent associative mechanism.

The nucleophile (-OMe) attacks adjacent to the leaving group (Cl) to form the trigonal-bipyramidal-intermediate **(75a)** in which the nucleophile occupies an apical position and the leaving group an equatorial position. There is a strong preference for the ring to be placed apical-equatorial in accordance with Westheimers preference rules.[8] Pseudorotation takes place between the two bracketed intermediates **(75a)** and **(75b)**, about the phosphoryl oxygen atom as a pivot; this atom remains equatorial, while the substituents that were equatorial in the first intermediate move (relative to the viewer) forward to become apical, and the substituents that were apical move backwards to become equatorial. This process generates trigonal-bipyramidal-intermediate **(75b)** and allows expulsion of the leaving group (Cl) from an apical position in accordance with the principle of microscopic reversibility to give a product **(69a)** in which the absolute configuration at phosphorus has been retained.

The incorporation of oxygen isotopes (^{17}O, ^{18}O) *via* strategic synthesis can be used to generate chiral phosphate esters. In 1978 two basic strategies were reported for the synthesis of chiral [^{16}O, ^{17}O, ^{18}O] phosphate monoesters, by Knowles[90] and Lowe.[98] Both syntheses rely on the stereocontrolled exocyclic displacement reactions at phosphorus held in five-membered rings.[8]

The Knowles synthesis is illustrated in Scheme 2.3 and is based on the studies of Inch.[96] The reaction of (-)ephedrine **(76)** with [^{17}O] phosphorus oxychloride in the presence of triethylamine gave an epimeric mixture of five membered ring phosphoramidic chlorides **(68c)** and **(68d)**.

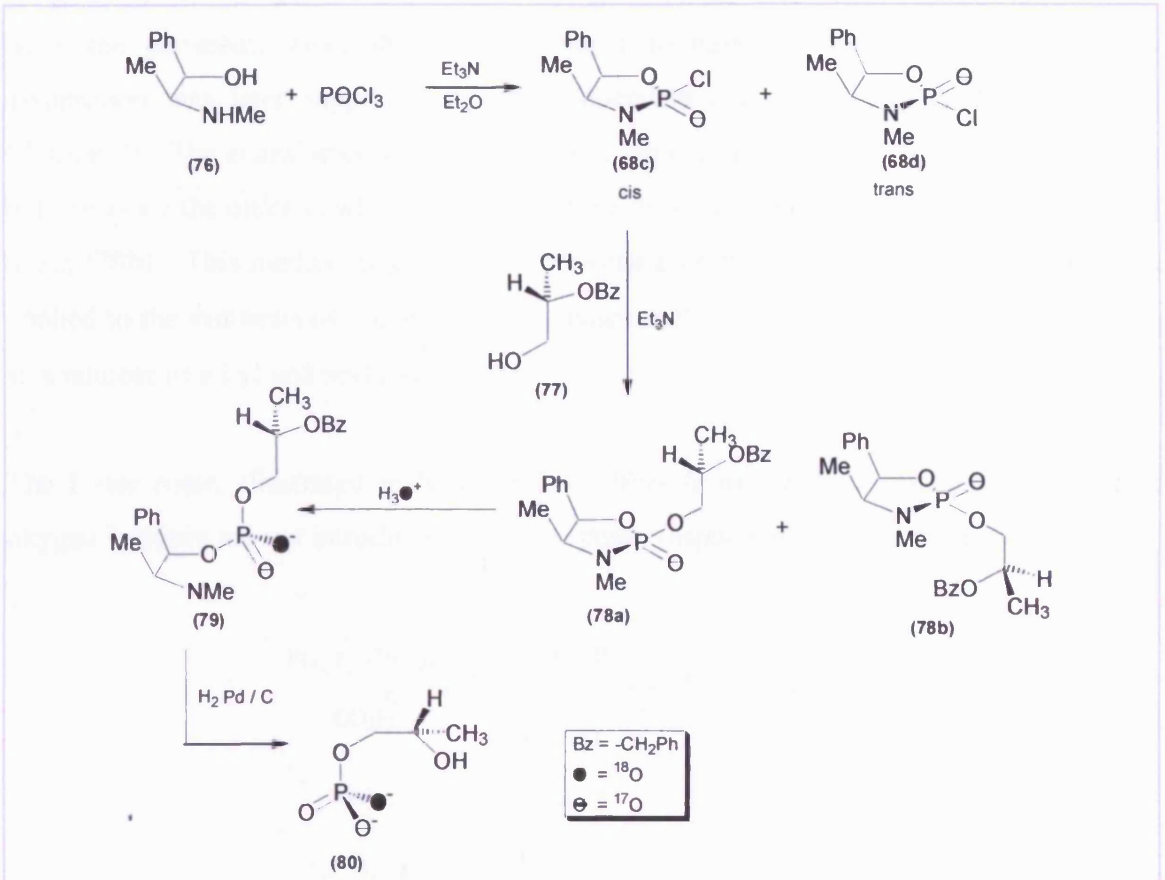

Scheme 2.3 Synthesis of the Rp diastereoisomer of 1-[^{16}O, ^{17}O, ^{18}O]phospho-(S)-1,2-propanediol **(80)** devised by Knowles *et al.*[90]

The mixture of diastereoisomers was reacted directly with a variety of nucleophiles (in this illustration 2-benzyl-(S)-propane-1,2-diol **(77)** is used), to afford a mixture of cyclic phosphoramidic esters **(78a)** and **(78b)** which can be separated by column chromatography. The configurations of the phosphoramidic chlorides **(68c)** and **(68d)** and several esters derived from alcoholysis of these chlorides have been assigned.[96]

The next step involves the introduction of ^{18}O by hydrolysing the P—N bond of the major phosphoramide ester **(78a)**, under acidic conditions in $H_3{}^{18}O^+$, Scheme 2.3. The stereochemical course of P—N ring opening is known to proceed with inversion of configuration at the phosphorus.[96]

Catalytic hydrogenolysis of the acyclic ^{17}O, ^{18}O chiral diester **(79)** removes the benzyl group as well as the ephedrine moiety by C— O cleavage resulting in the formation of 1-[^{16}O, ^{17}O, ^{18}O]-phospho-1,2-(S)-propane diol **(80)**. The absolute configuration can be

assigned by knowledge of the stereochemistry of the key steps in the synthesis. On this basis the phosphate ester **(80)** was predicted to have the Rp configuration. This assumption was later supported by an independent analytical method (full details in Chapter 3). The enantiomer with Sp configuration can be produced using the same route but reversing the order in which ^{17}O and ^{18}O are introduced in the synthetic pathway or by using **(78b)**. This method is general for phosphate esters and anhydrides[99] and has been applied to the synthesis of nucleoside phosphates such as [γ-^{16}O, ^{17}O, ^{18}O]ATP,[99] as well as a number of alkyl and aryl monoesters.[100]

The Lowe route, illustrated in Scheme 2.4 differs from the Knowles' method[90] in that oxygen isotopes are not introduced by nucleophilic displacement reactions at phosphorus.

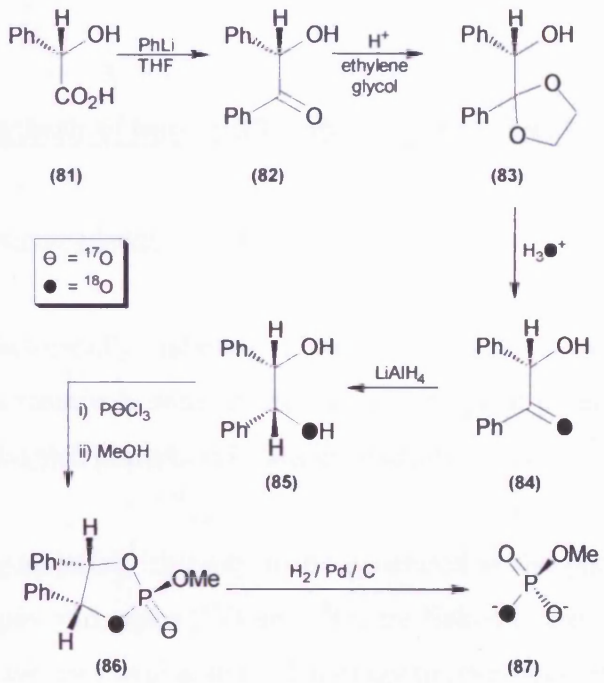

Scheme 2.4 Synthesis of the Sp enantiomer of methyl [^{16}O, ^{17}O, ^{18}O] phosphate monoester **(87)** reported by Lowe *et al.*

The synthesis started from (S)-mandelic acid **(81)** which is reacted with phenyl lithium to form (S)-benzoin **(82)**. Acid catalysed hydrolysis of the corresponding ethylene ketal **(83)** in $H_3{}^{18}O^+$ introduces the isotope in the carbonyl oxygen **(84)**. Reduction of this ketone gives the stereospecifically labelled [^{18}O]-hydrobenzoin **(85)** which is chiral by virtue of the isotopic substitution. The second isotope is introduced by reacting ^{17}O-enriched phosphorus oxychloride with the isotopically labelled [^{18}O]-hydrobenzoin **(85)**. The

chloride is treated with methanol to give the corresponding cyclic methyl phosphotriester **(86)**. Catalytic hydrogenolysis releases the [^{16}O, ^{17}O, ^{18}O] methyl ester **(87)** of the Sp configuration.

The Rp configuration can be formed by reversing the introduction of the isotopes or preparing the compound from (R)-mandelic acid. This is also a general route for phosphate esters and anhydrides.

Both synthetic routes use a five-membered ring to introduce chirality at phosphorus. Many displacement reactions involving such five-membered cyclic phosphoryl compounds have been shown to proceed stereospecifically, thus providing a good precedent for the stereocontrolled introduction of isotopes.

2.3 Literature synthesis of isotopically labelled chiral thiophosphates.

2.3.1 Nucleoside thiophosphates.

The synthesis of isotopically labelled chiral thiophosphate analogues of adenine nucleotides has been extensively studied because of their great potential as stereochemical probes for enzyme catalysed phosphoryl transfer reactions in nature.

Thiophosphate analogues allow chirality to be generated at the phosphorus centre when only two stable isotopes of oxygen (^{16}O and ^{18}O) are linked to the thiophosphoryl group. Thiophosphates offer the only available methodology to investigate stereochemical aspects of some enzymatic reactions, most notably phosphatases.

In 1968 Eckstein[101] reported the synthesis of the first thiophosphate, uridine-2',3'-cyclic diester **(88)**, Figure 2.4, which was used to determine the stereochemical course of the reaction catalysed by ribonuclease A.[102] Since that initial experiment, stereochemical studies on a number of phosphoryl and nucleotidyl transfer reactions have resulted in the synthesis of thiophosphate analogues of almost all the common diastereoisomers of adenine nucleotides.

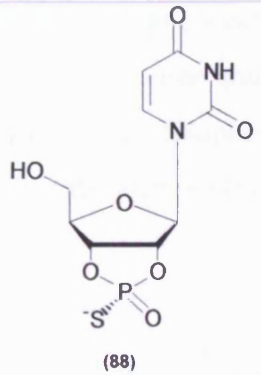

(88)

Fig. 2.4 Uridine-2',3'-cyclic diester **(88)**.

Stereochemical studies using isotopically labelled chiral analogues of adenine nucleotides are usually more demanding than those utilizing chiral thiophosphate analogues of adenine nucleotides. This is because in the preparation of isotopically labelled chiral thiophosphates it is often possible to separate diastereoisomers that are epimeric at the chiral phosphorus atom by normal anion-exchange chromatography. Also, some enzymes have the ability to distinguish the prochiral phosphoryl oxygen atoms of a thiophosphoryl group. The analogous distinction of prochiral oxygen atoms is not possible.

2.3.2 Terminal thiophosphoryl group.

Phosphoryl transfer enzymes such as protein kinases, DNA topoisomerases, pyruvate kinase, phosphofructokinase, creatine kinase and ATPase catalyse attack at Pγ of ATP. In order to study these types of enzyme-catalysed phosphoryl transfer reactions it is necessary to use adenine nucleotides with terminal thiophosphoryl groups, e.g. adenosine-5'-[γ-^{18}O,thio] triphosphate (ATPγS^{18}O). The synthesis of [^{16}O, ^{18}O]-chiral samples of AMPαS, ADPβS and ATPγS, Schemes. 2.5, 2.6 and 2.7 has been accomplished.[103]

The Rp **(93a)** and Sp **(93b)** diastereoisomers of [^{16}O, ^{18}O]AMPαS were prepared by a method that combined chemical and enzymatic synthesis as shown in Scheme 2.5. The key reactant, AMPαS$^{18}O_2$ **(89)**, was prepared by treating adenosine with $P(S)Cl_3$, followed by hydrolysis with $H_2{}^{18}O$. This was activated with diphenyl phosphorochloridate **(91)** and coupled with AMP **(90)** to produce **(92a)** and **(92b)** as an epimeric mixture. After separation by chromatography, hydrolyses of these diastereoisomeric mixed anhydrides in

parallel using nucleotide pyrophosphatases gave diastereoisomerically pure samples of [^{16}O,^{18}O]AMPαS **(93a)** and **(93b)** along with some unlabelled AMP **(90)**. This enzymatic reaction does not alter the configuration of the thiophosphoryl group when the AMP **(90)** group is removed. Although the enzymatic step is efficient, the overall yield of **(93a)** and **(93b)** was 39%.

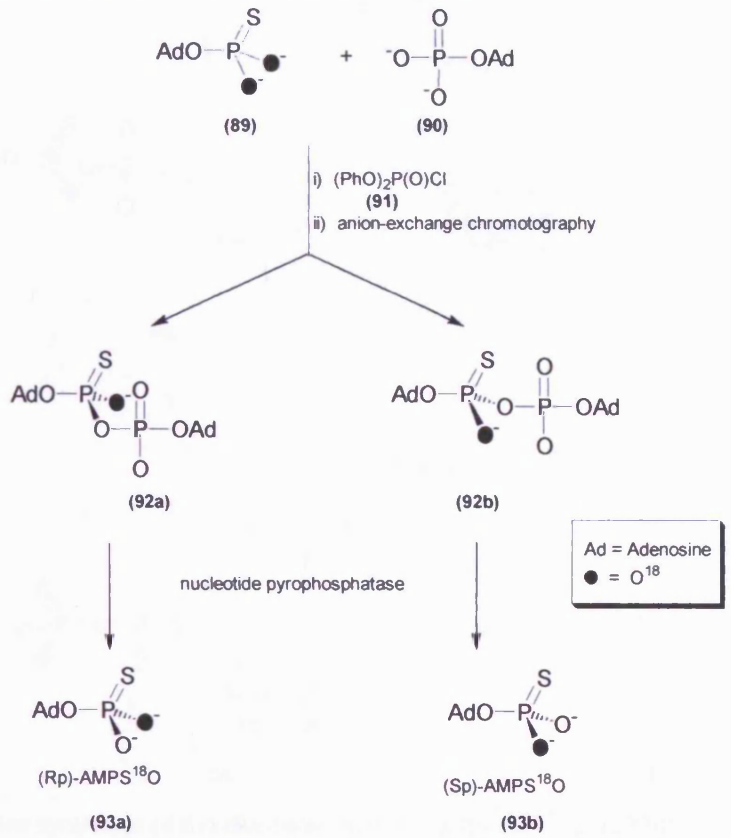

Scheme 2.5 The synthesis of the diastereoisomers of [^{16}O, ^{18}O] AMPS **(93a)** and **(93b)**.

The Rp and Sp diastereoisomers of [β-^{16}O,^{18}O]ADPβS were synthesised by the methodology illustrated in Scheme 2.6. Again, the important steps in the synthesis are the separation of the diastereomeric mixed anhydrides **(95a)** and **(95b)** (formed by the reaction of 2',3'-methoxymethylidene AMP **(94)** with AMPαS^{18}O$_2$ **(89)** *via* activation with diphenyl phosphorochloridate **(91)**) and the use of the adenosine moiety associated with the AMPαS^{18}O$_2$, as a blocking group which was removed by periodate cleavage to yield (Rp) and (Sp)-ADPβSβ^{18}O, **(96a)** and **(96b)**.

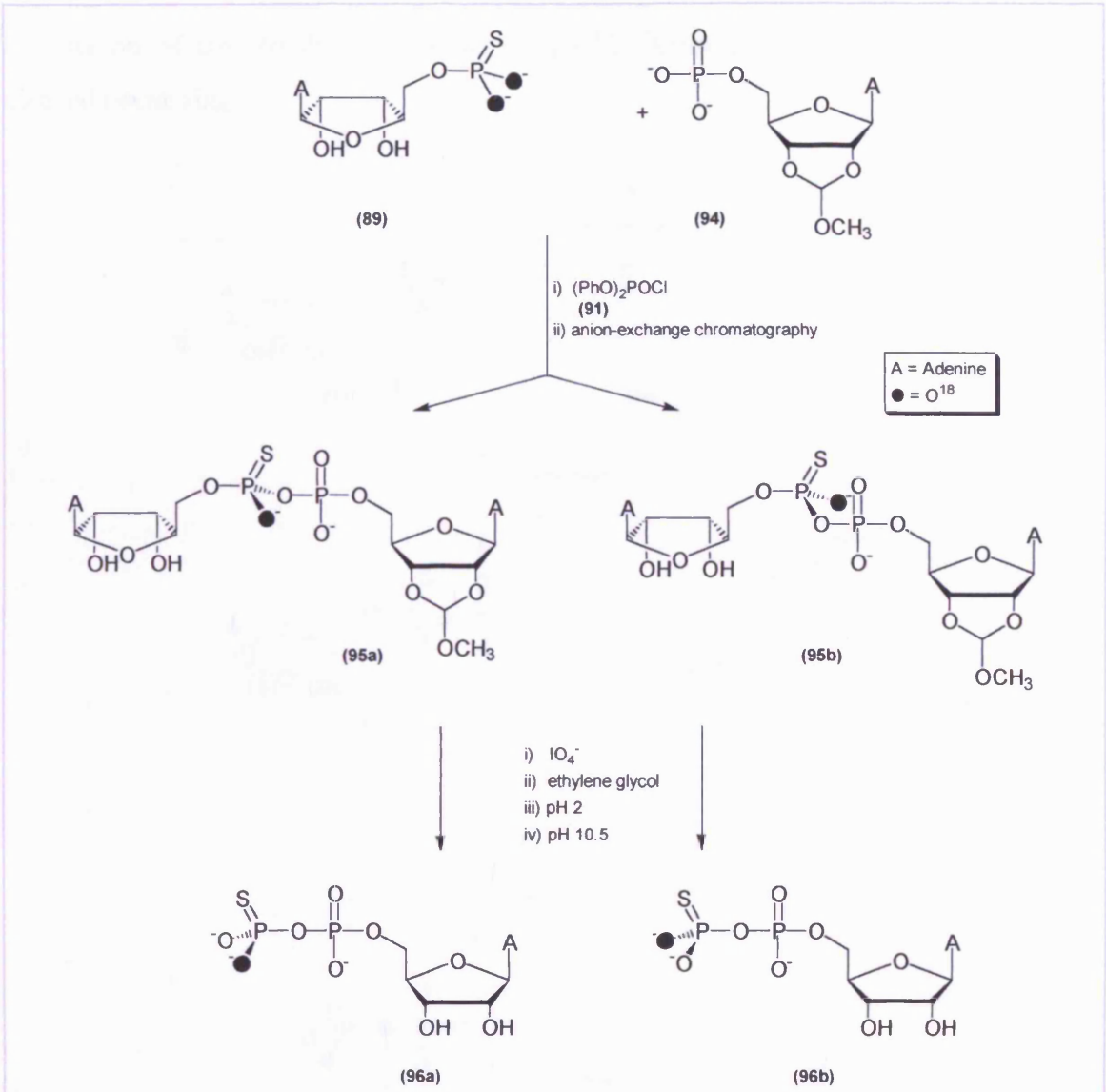

Scheme 2.6 The synthesis of the diastereoisomers of [β-^{16}O, ^{18}O] ADPβS.

A similar strategy was employed in the synthesis of the Rp diastereoisomer of [γ-^{16}O,^{18}O,thio]ATP **(99)**, Scheme 2.7. The key reactant in this synthesis, Sp-ADPαSα$^{18}O_2$ **(97)** is prepared from AMPαS$^{18}O_2$ by stereospecific phosphorylation to Sp-ATPαS$^{18}O_2$ with phosphoenolpyruvate in the presence of adenylate kinase and pyruvate kinase followed by dephosphorylation to **(97)** with glucose and hexokinase.

2',3'-(Methoxymethylidene)-AMP **(94)** is activated with diphenyl phosphorochloridate and coupled to Sp-ADPαSα$^{18}O_2$ **(97)** by the Michelson procedure to give **(98)**. The unprotected ribose is cleaved with IO_4^- and the methoxymethylidene protecting group is removed under mildly acidic conditions. Finally, mild alkaline conditions result in β

elimination of the Rp diastereoisomer of [γ-^{16}O,^{18}O,thio]ATP **(99)** from C-5' of the cleaved ribose ring.

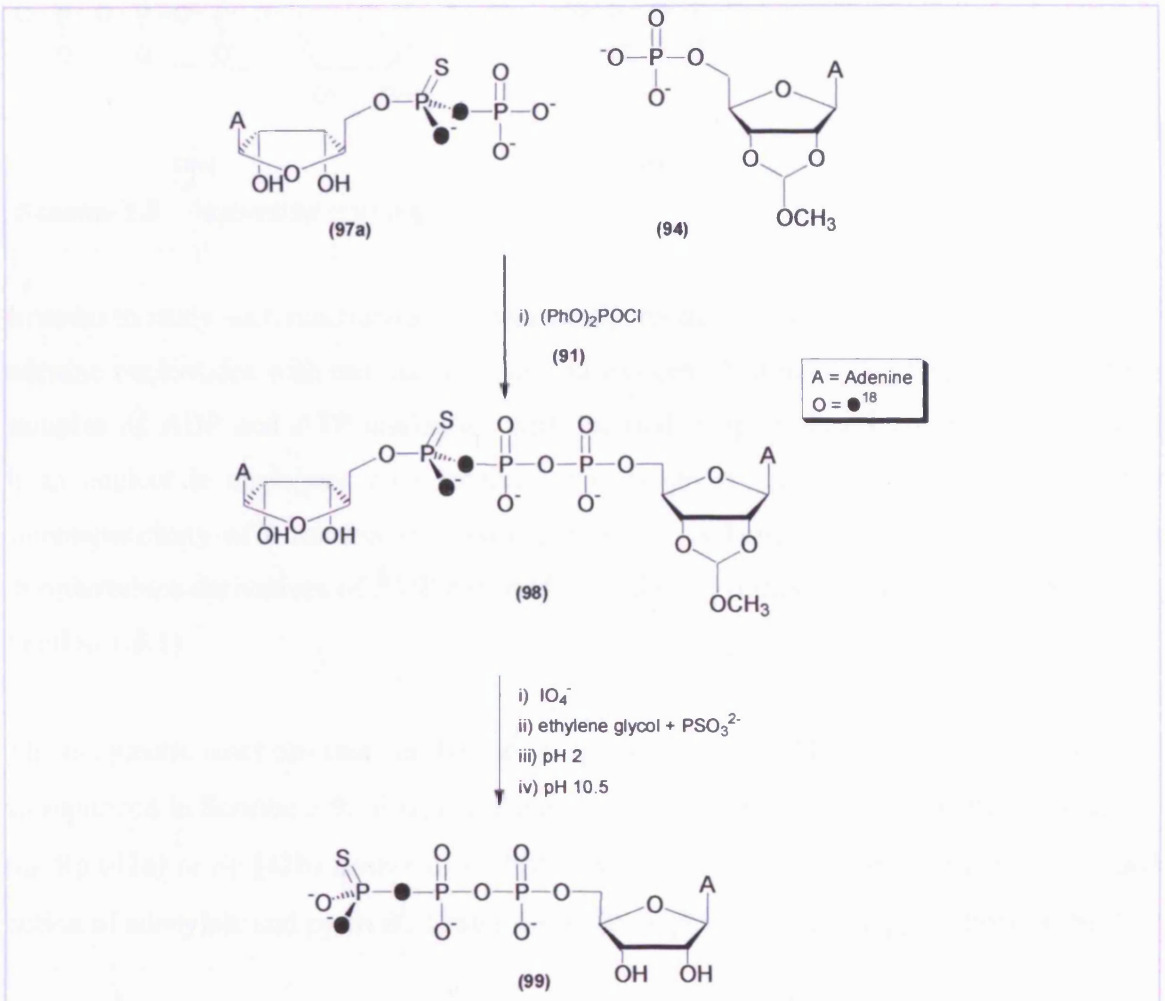

Scheme 2.7 The synthesis of the Rp diastereoisomer of [γ-^{16}O, ^{18}O]ATPγS **(99)**.

2.3.3 Internal thiophosphoryl group.

Nucleotidyl transfer reactions involve nucleophilic substitution at internal phosphorus atoms of nucleotides, such as ATP **(38c)**, with the displacement of pyrophosphate **(49)** and formation of an AMP derivative **(100)**, Scheme 2.8.

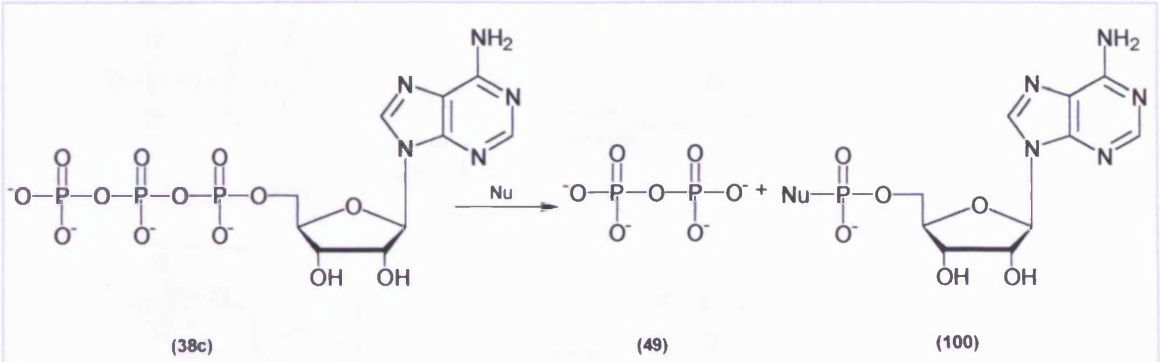

(38c) (49) (100)

Scheme 2.8 Nucleotidyl transfer.

In order to study such reactions stereochemically, methods have been devised to synthesise adenine nucleotides with internal sulphur and oxygen-18 atoms. Diastereomerically pure samples of ADP and ATP analogues with internal thiophosphoryl groups can be made from nucleotide analogues with terminal thiophosphoryl groups by making use of the stereospecificity of a number of kinase reactions. A large number of oxygen labelled thiophosphate derivatives of ADP and ATP have been synthesised in this way (Chapter 2, Section 1.3.1).

The enzymatic reactions that can be used to prepare various ADP and ATP analogues are summarized in Scheme 2.9. Enzymatic reactions that can convert ADPβS **(96c)** into either the Rp **(42a)** or Sp **(42b)** isomer of ATPβS have been reported.[104] In addition the coupled action of adenylate and pyruvate kinase on AMPαS **(93c)** can give (Sp)-ATPαS **(41b)**.[105]

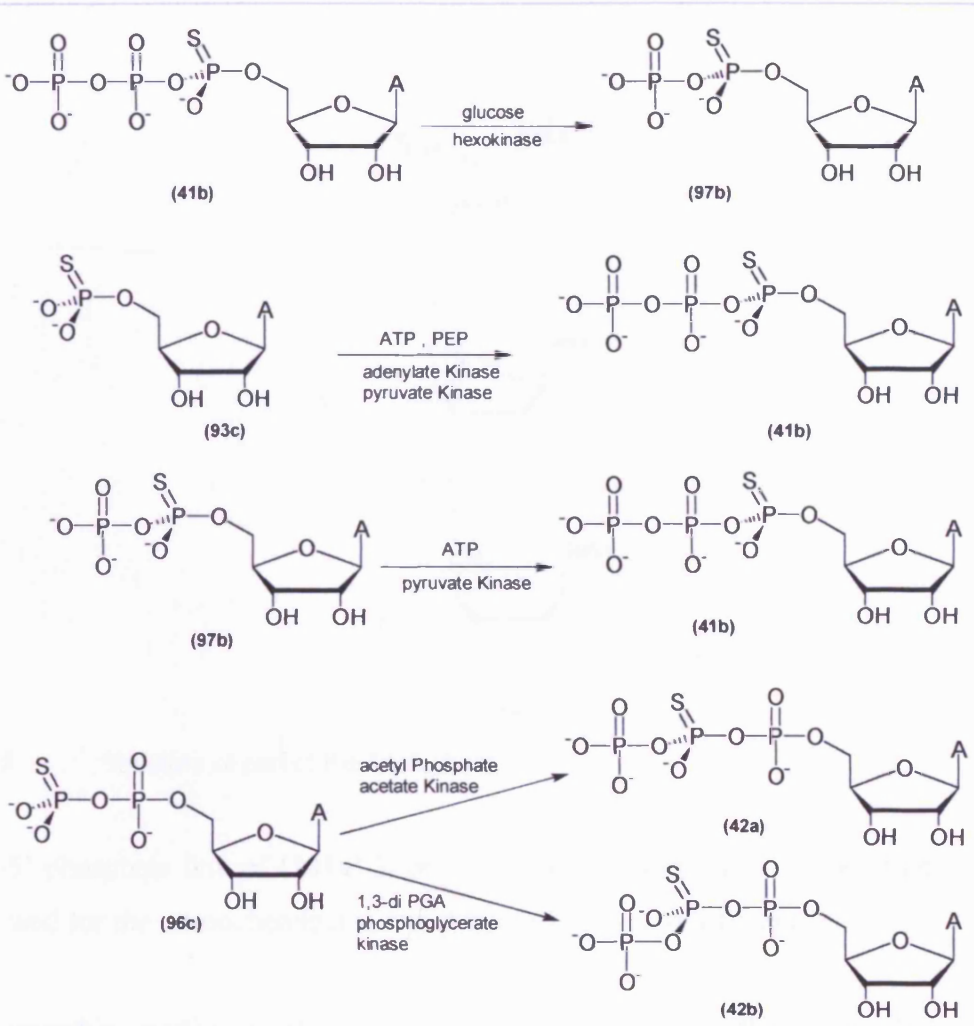

Scheme 2.9 Methods for the synthesis of the diastereoisomers of ADPαS, ATPαS and ATPβS.

2.4 Chiral phosphorus internucleotide bonds.

The nucleic acid, DNA **(101a)**, is a polymer of deoxyribonucleotide units linked by phosphate groups, Figure 2.5. Specifically, the 3'-hydroxyl of the sugar moiety of one deoxyribonucleotide is joined to the 5'-hydroxyl of the adjacent sugar by a phosphodiester bridge.[2]

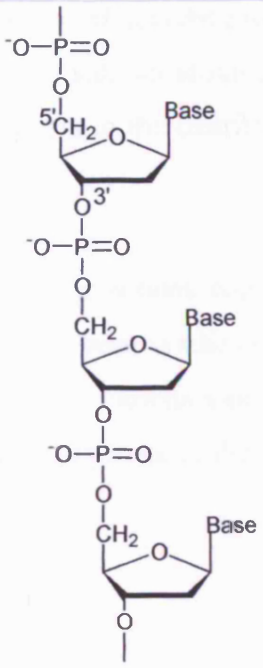

(101a)

Fig. 2.5 Structure of part of the DNA chain.

The 3'-5' phosphate link of **(101a)** is prochiral and conversion to a chiral thiophosphate has allowed for the stereochemical study of the metabolism of oligonucleotides.[63]

The enzymatic synthesis of stereodefined (Sp or Rp) oligo(deoxyribonucleoside phosphorothioate)s (PS-Oligos) is limited to the preparation of (all-Rp)-oligomers because of the stereoselectivity of available DNA and RNA polymerases, unlike stereocontrolled chemical synthesis of PS-Oligos that can provide either Sp or Rp absolute configuration,[106-110] Figure 2.6.

Stereodefined PS-Oligos have been utilised to study the mode of action of several bacterial and human enzymes. Examples include; the role of metal ions in the *Escherichia coli* DNA polymerase I exonuclease mechanism,[111] the effect of phosphorus chirality (Sp *vs* Rp stereodifferentiation) of oligo(nucleoside phosphorothioates) on the activity of bacterial RNase H,[112] the mechanism of the phosphoryl transfer steps catalysed by DNA transposases[113] and the determination of the stereochemistry of DNA cleavage reactions mediated by SfiI and HpaII restriction endonucleases and the MuA transposase.[114]

The presence of a sulphur atom however, affects the properties of internucleotide bonds,[106] mostly due to the steric requirements of sulphur atoms (P-S *vs* P-O bond length), different affinity towards metal ions, and changes in the distribution of the negative charge in the phosphorothioate anion.[66]

To avoid these inconveniences, oligonucleotides containing a single P-chiral [^{16}O,^{18}O] internucleotide bond (P^{18}O-Oligos) have been synthesised,[106,115] Figure 2.6. Stereodefined P^{18}O-Oligos have been used to investigate various aspects of nucleic acid metabolism such as probing the palindromic recognition sequence of the restriction endonuclease, Eco RI[115]

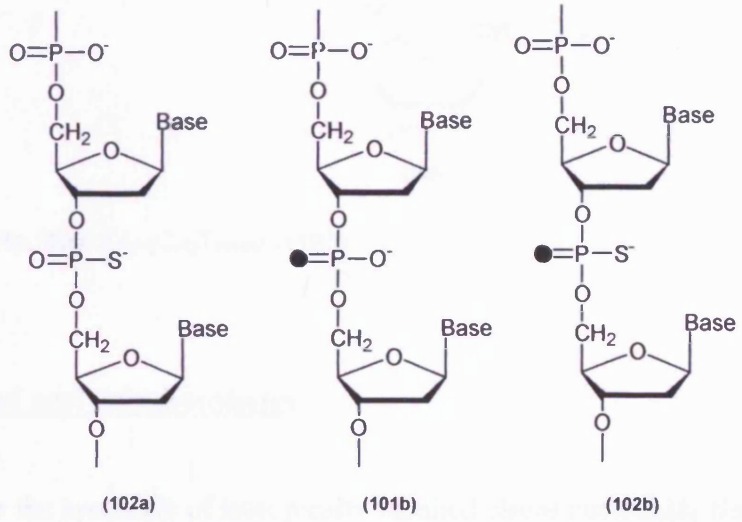

Fig. 2.6 Stereodefined (Sp or Rp) oligo(deoxyribonucleoside phosphorothioate)s (PS-Oligos) **(102a)**, oligo(deoxyribonucleoside [^{18}O]phosphate)s (P^{18}O-Oligos) **(101b)** and oligo(deoxyribonucleoside [^{18}O]phosphorothioate)s (PS^{18}O-Oligos) **(102b).**

Medium sized oligonucleotides can be synthesized with any combination of internucleotide bond with respect to its type (P-S *vs* P-O) or absolute configuration (Rp *vs* Sp), as well as to the position and the number of isotope labels along the chain. This flexibility is exemplified by the solid-phase synthesis of (Rp,Mix)-d($A_{PS}C_{PO}T_{PS}{}^{18}C$)[106] **(103)**, Figure 2.7.

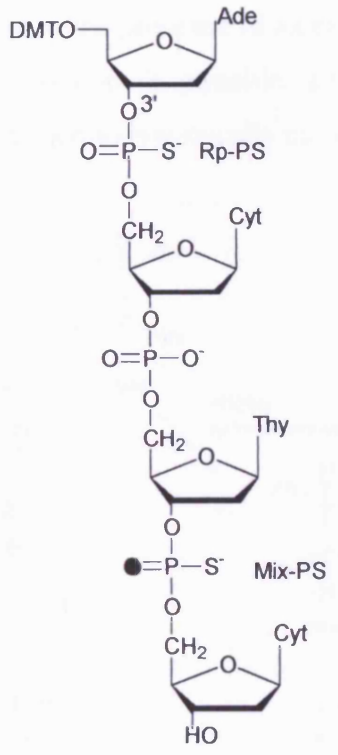

(103)

Fig. 2.7 (Rp,Mix)-d($A_{PS}C_{PO}T_{PS18C}$) **(103).**

2.5 Alkyl and aryl thiophosphates.

The methods for the synthesis of isotopically labelled chiral nucleoside thiophosphates are not, in general, applicable to the synthesis of simple thiophosphate monoesters **(67b)**; R = alkyl or aryl), Figure 2.8

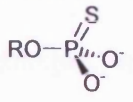

(67b)

Fig. 2.8 Thiophosphate monoester **(67b).**

Synthesis of these thiophosphates based on the *meso*-hydrobenzoin route to isotopically labelled chiral phosphate monoesters however, has been reported by Jarvest and Lowe.[116] Again, the key step is the synthesis of the [^{18}O]-labelled *meso*-hydrobenzoin **(85)** (Scheme 2.10) which was treated with thiophosphoryl tribromide with varying amounts of pyridine. When two equivalents of pyridine are used, the diastereoisomer **(104a)** (kinetic product) is

the predominant product; however in the presence of an excess of pyridine, reversible ring opening of the cyclic phosphobromidate is possible, allowing the kinetically favoured product to be transformed into the thermodynamically more stable one **(104b)**.

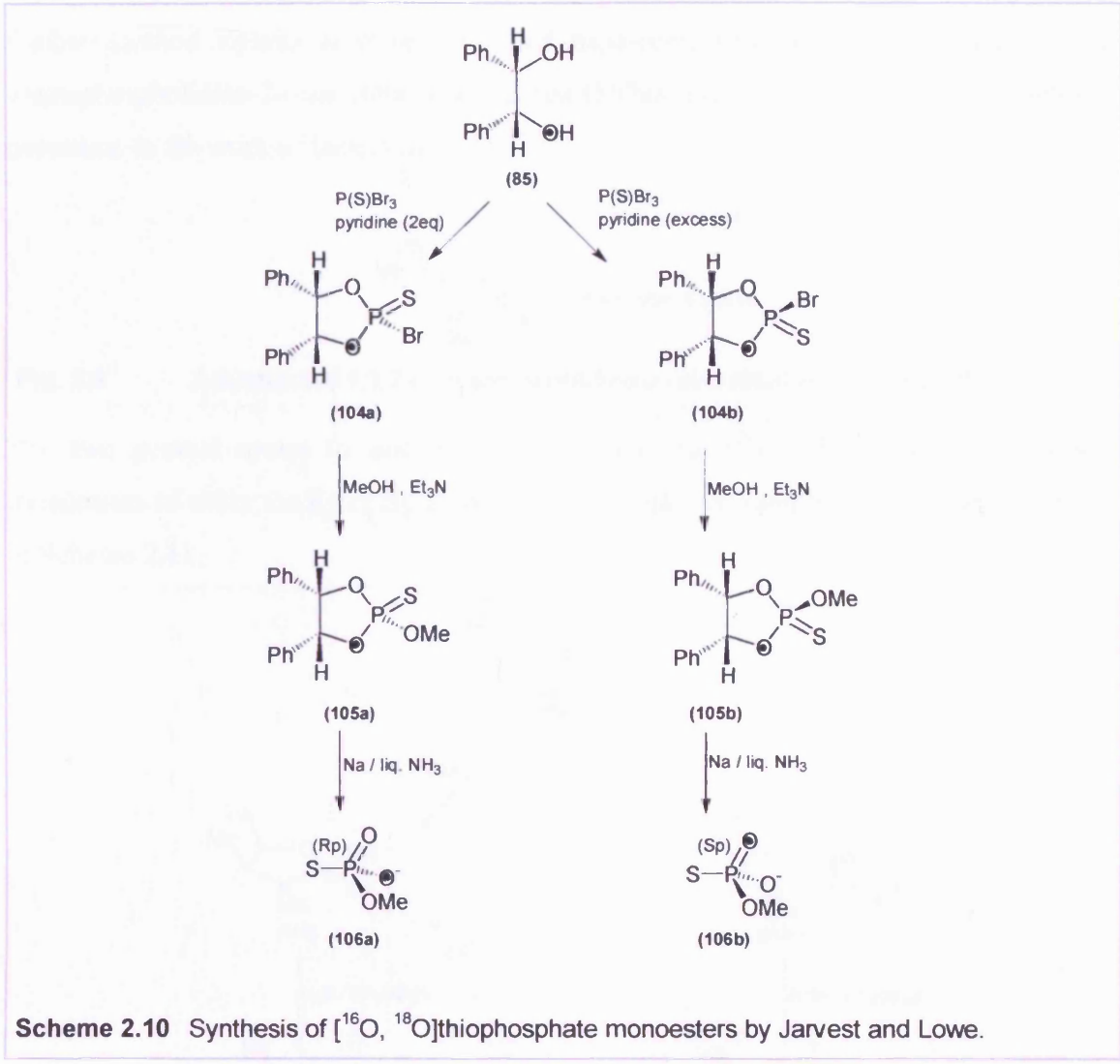

Scheme 2.10 Synthesis of [^{16}O, ^{18}O]thiophosphate monoesters by Jarvest and Lowe.

Reaction of these bromidates with, for example, methanol gave the corresponding triesters **(105a)** and **(105b)**. Reduction of the hydrobenzoin framework with sodium in liquid ammonia gave the enantiomerically pure methyl [^{16}O,^{18}O] thiophosphates **(106a)** and **(106b)** which were purified by anion-exchange chromatography. The yield of the product was quite low due to competing aminolysis of the five-membered ring and difficulty in removing the hydrobenzoin framework. This and the fact that the ^{18}O *meso*-hydrobenzoin **(85)** is difficult to prepare in large amounts means this route is not widely used.

An alternative method has been reported by Cullis *et al.*[117,118] who used simple thiophosphate monoesters to study thiophosphoryl transfer reactions. This method is analogous to the previously published route to [^{16}O,^{17}O,^{18}O]phosphate monoesters by Knowles *et al.*[90,119] mentioned at the beginning of the chapter. Like Knowles's syntheses, Cullis's method exploits the stereocontrolled displacement reactions of 2-substituted 1,3,2-oxazaphospholidine-2-ones **(68a)** and thiones **(107a)**, Figure 2.9, which have established precedent in the work of Inch *et al.*[96]

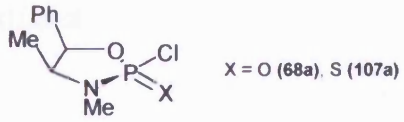

Fig. 2.9 2-Substituted 1,3,2-oxazaphospholidine-2-ones **(68a)** and thiones **(107a)**.

The two general routes to isotopically labelled chiral [^{16}O,^{18}O,(or ^{17}O)]thiophosphate monoesters of either the Rp or Sp absolute configuration devised by Cullis *et al.* are shown in Scheme 2.11.

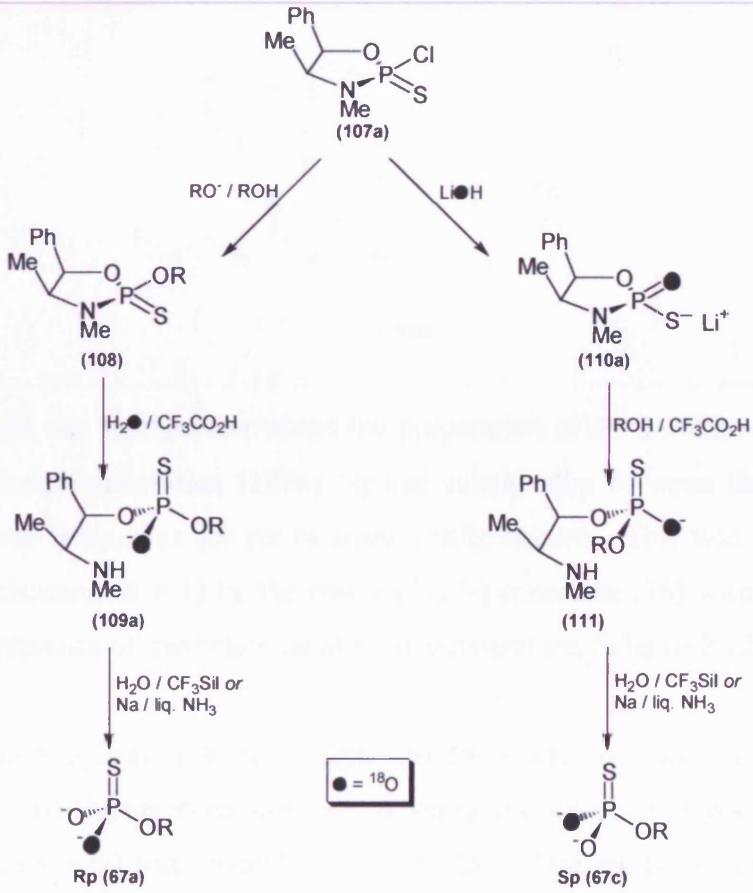

Scheme 2.11 Two general syntheses of isotopically labelled chiral [^{16}O, ^{18}O]thiophosphate monoesters.

This synthetic route is potentially general; 4-nitrophenyl [^{16}O,^{18}O]thiophosphate and ethyl [^{16}O,^{18}O]thiophosphate monoesters are examples that have been prepared this way. However, the extension of the published route to isotopically labelled chiral phosphate monoesters to the synthesis of thiophosphate monoesters is non-trivial. The thiophosphorochloridate **(107a)** is less reactive than its oxy counterpart **(68a)**, as expected from the known difference in reactivity of trisubstituted thiophosphates as compared to phosphates in associative nucleophilic substitution reactions.[120] Furthermore, removal of the ephedrine framework is difficult.

2.6 Synthesis of Rp-[^{16}O,^{18}O]thiophosphoric acid O-[3-benzyl-2-(dimethylamino-methinimino)-4-oxo-3,4-dihydro-pteridin-6-ylmethyl] ester S-(6,6-dimethyl-bicyclo[3.1.1]hept-2-en-2-ylmethyl) ester (112a).

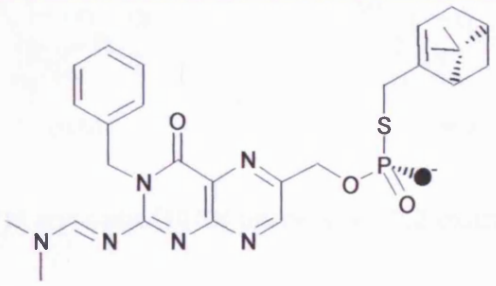

(112a)

The initial step in our synthesis involved the preparation of *cis* 2-chloro-3,4-dimethyl-5-phenyl-1,3,2-oxazaphospholidine **(107a)** (spatial relationship between the phenyl group and chloro group designates the *cis* or *trans* configuration). This was prepared as the major epimer (cis:trans ca. 8:1) by the reaction of (-) ephedrine **(76)** with thiophosphoryl chloride in the presence of triethylamine at room temperature, Scheme 2.12.[96]

The major chloro epimer **(107a)** (kinetic product) was isolated in pure form by chromatography and then recrystallisation. A small amount of the trans material **(107b)** (thermodynamic product) was isolated by concentration of the mother liquor.

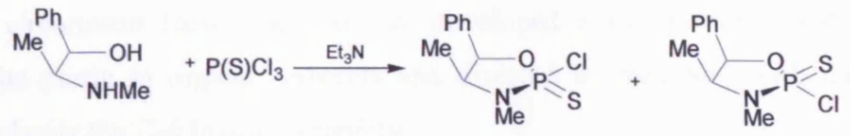

(76) (107a) (107b)

Scheme 2.12 Preparation of *cis* 2-chloro-3,4-dimethyl-5-phenyl-1,3,2-oxazaphospholidine-2-thione **(107a)**.

Assignments of the configuration in the 1,3,2-oxazaphospholidines, Figure 2.10, can be made on the basis of observed chemical shifts.[96] Protons in a 1,3 *cis* relationship to a P=X group (X = O or S) are deshielded, therefore H-4 and H-5 resonate at a lower field in compound **(107a)** than in **(107b)**. The deshielding effect is greater for H-5 than for H-4, a result which is expected in a puckered ring in which P=S is closer to H-5 than H-4. The epimers **(107a)** and **(107b)** also have different ^{31}P NMR resonances which differ by 5 p.p.m. (*cis* +75.2 p.p.m.; *trans* +80.3 p.p.m.).

(107a) (107b)

Figure 2.10 The cis **(107a)** and trans **(107b)** epimers of 1,3,2-oxazaphospholidines.

Reaction of the *cis*-chloro adduct **(107a)** with the hydroxyl moiety at the C-6 position of 2-amino-6-hydroxymethyl-3H-pteridin-4-one **(113)**, Scheme 2.13, was impossible due to the multiple reaction sites and poor solubility of the pterin in both organic and aqueous media.

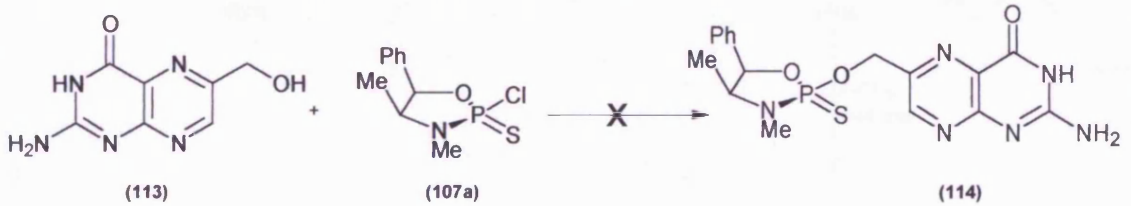

(113) (107a) (114)

Scheme 2.13 Proposed synthesis of 2-Amino-6-(3,4-dimethyl-5-phenyl-2-thioxo-2λ^5-[1,3,2]oxazaphospholidin-2-thio-yloxymethyl)-3H-pteridin-4-one **(114)**.

In order to circumvent these obstacles we developed a methodology that sufficiently solubilised the pterin in organic solvents and directed its reactivity with the *cis*-chloro adduct toward only the C-6 hydroxyl moiety.

The elaboration of the side chains at C-6 in pterins and their close relatives has been largely restricted to N-alkylation of 4-aminobenzoate analogues using 6-bromomethylpterins,[121] to palladium-mediated couplings of 6-iodo analogues with alkynes,[122] and to their inclusion directly by ring synthesis.[123]

A deterrent to the development of more complex derivatives has been the well-known poor solubility of pterins in organic media. This problem has been overcome by protection of the 2-amino group of 2-amino-6-hydroxymethyl-3H-pteridin-4-one **(113)**, with groups that have solubilising properties.

We initially investigated the selective protection of the 2-amino group of 2-amino-6-hydroxymethyl-3H-pteridin-4-one **(113)**, using pivaloylation, Scheme 2.14.[124] In this case the 2,6-dipivaloyl derivative **(115)** was obtained in good yield, but in our hands the selective deprotection of the 6-pivalate ester gave poor yields of the 2-pivaloyl amide, N-(6-hydroxymethyl-4-oxo-3,4-dihydro-pteridin-2-yl)-2,2-dimethyl-propionamide **(116)**, which in any case was inadequately soluble.

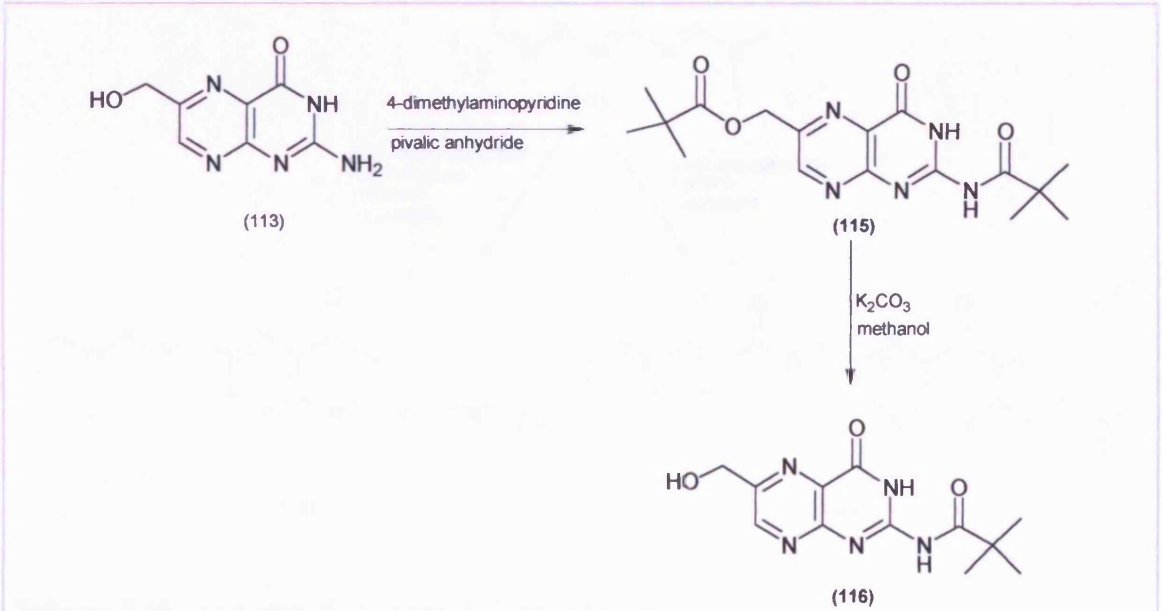

Scheme 2.14 Synthesis of N-(6-Hydroxymethyl-4-oxo-3,4-dihydro-pteridin-2-yl)-2,2-dimethyl-propionamide **(116)**.

The most promising protecting group was dimethylaminomethylene, introduced using DMF dimethyl acetal, Scheme 2.15.[125] N'-(6-Hydroxymethyl-4-oxo-3,4-dihydro-pteridin-2-yl)-N,N-dimethyl-formamidine **(117)** had satisfactory solubility and was obtained in good yield.

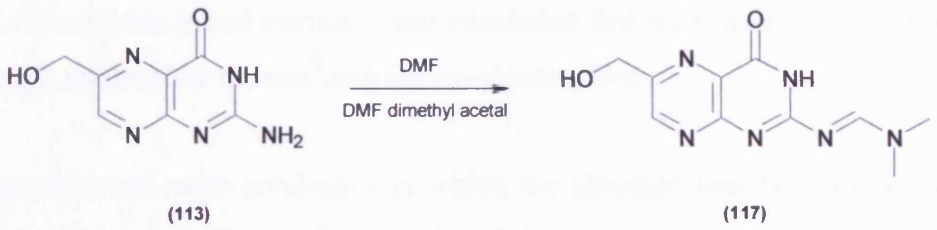

Scheme 2.15 Synthesis of N'-(6-Hydroxymethyl-4-oxo-3,4-dihydro-pteridin-2-yl)-N,N-dimethyl-formamidine **(117)**.

A brief investigation into the nucleophilic properties of the 6-hydroxyl group was conducted. Previously,[126] it had been established that **(117)** reacts smoothly with ethyl chloroformate and 2-(4-nitrophenyl)ethyl chloroformate, respectively, to give the corresponding carbonates **(118)** and **(119)**, Scheme 2.16.

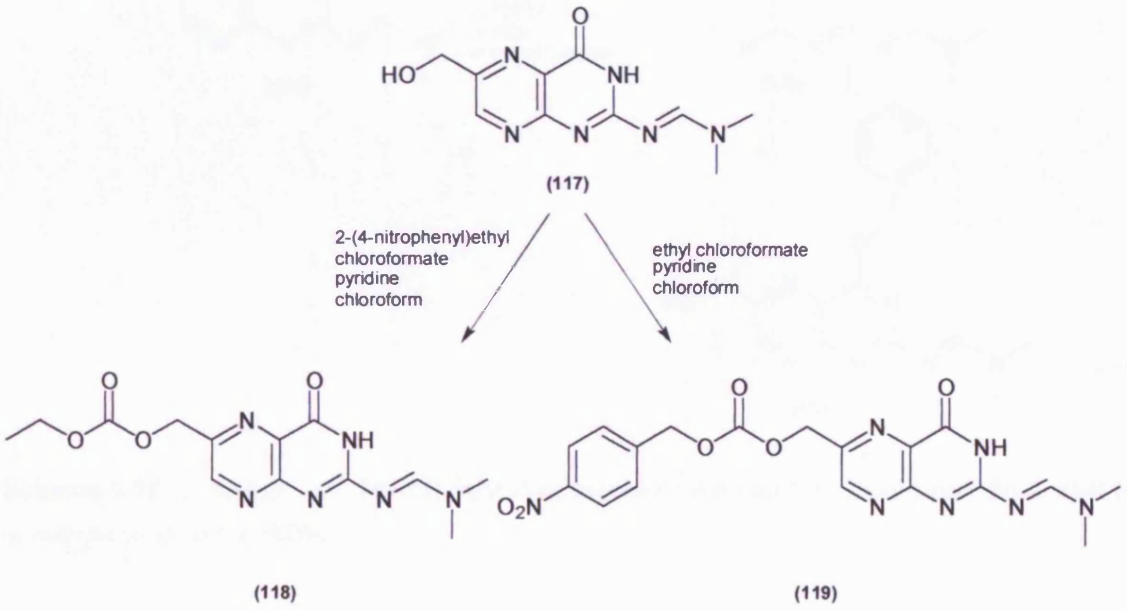

Scheme 2.16 Synthesis of carbonates **(118)** and **(119)**.

No reaction was found to occur between *cis* 2-chloro-3,4-dimethyl-5-phenyl-1,3,2-oxazaphospholidine-2-thione **(107a)** and 6-hydroxy group of the pterin **(113)** under identical conditions to those used in the model studies above involving ethyl chloroformate and 2-(4-nitrophenyl)ethyl chloroformate. The option of exploiting a nucleophilic catalyst such as pyridine or 4-(N,N-dimethylamino)pyridine (DMAP) to drive the reaction was unsuitable as these would have unpredictable effects on the stereospecificity of the reaction. From these initial studies it was concluded that the 6-hydroxy group was not a good enough nucleophile to react with the *cis*-chloro adduct.

Further experiments were conducted in which the alkoxide was first formed at the 6-hydroxy position using either NaH, or ^{t}BuLi. Subsequent reaction with one equivalent of *cis*-2-chloro-3,4-dimethyl-5-phenyl-1,3,2-oxazaphospholidine-2-thione **(107a)** established that reaction occurred at the undesired 3-amide position. In order to direct nucleophilic attack from the 6-hydroxyl group it was necessary to selectively protect the 3-amide position. Initial trials focused on bromide displacement from simple haloalkanes such as benzyl bromide in the presence of KOH, Scheme 2.17.

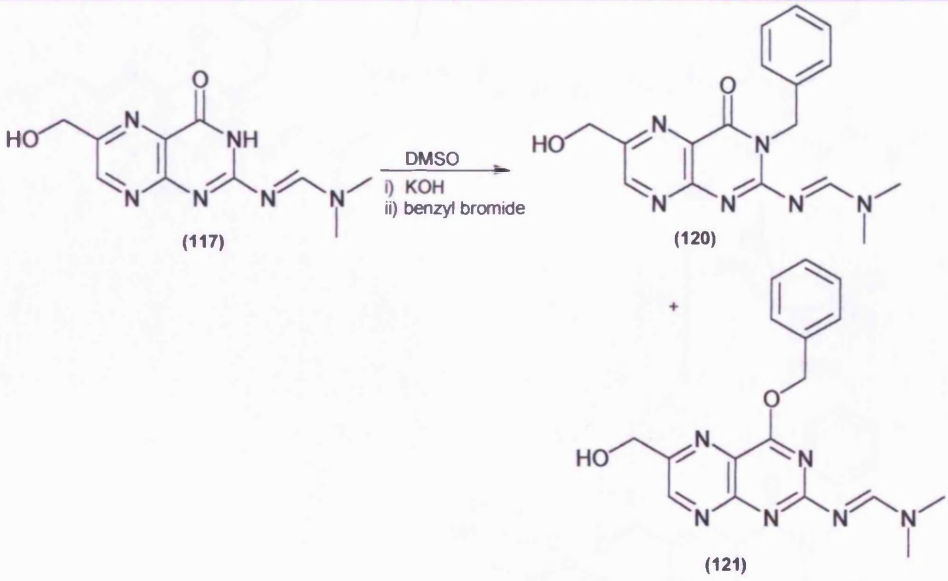

Scheme 2.17 Synthesis of N'-(3-Benzyl-6-hydroxymethyl-4-oxo-3,4-dihydro-pteridin-2-yl)-N,N-dimethyl-formamidine **(120).**

The chemistry proceeded selectively at the 3-amide position and in high yield to give a 9:1 mixture of regioisomers **(120)** and **(121)** which were separable by silica gel column chromatography allowing isolation of N'-(3-benzyl-6-hydroxymethyl-4-oxo-3,4-dihydro-

pteridin-2-yl)-N,N-dimethyl-formamidine **(120)** as the regioisomer produced in the highest yield. Regioisomers were identified on the basis of heteronuclear multiple bond correlation (HMBC) NMR spectroscopy. It was found that a benzyl protecting group solubilised the pterin sufficiently for subsequent synthetic steps.

Alkoxide formation of the protected pterin **(120)** using ^{t}BuLi at room temperature provided a suitably nucleophilic oxygen **(122)** to react with the *cis*-chloro adduct **(107a)** at the desired 6-hydroxy position. This gave essentially a single diastereoisomer of N'-[3-benzyl-6-(3,4-dimethyl-5-phenyl-2-thio-2λ^5-[1,3,2]oxazaphospholidin-2-yloxymethyl)-4-oxo-3,4-dihydro-pteridin-2-yl]-N,N-dimethyl-formamidine **(123)**, Scheme 2.18, as judged by ^{31}P NMR spectroscopy. As has frequently been observed, exocyclic displacement reactions at phosphorus held in a five-membered ring of this kind proceed with retention of configuration[8,96] therefore the product **(123)** can be assumed to have an Sp configuration at phosphorus.

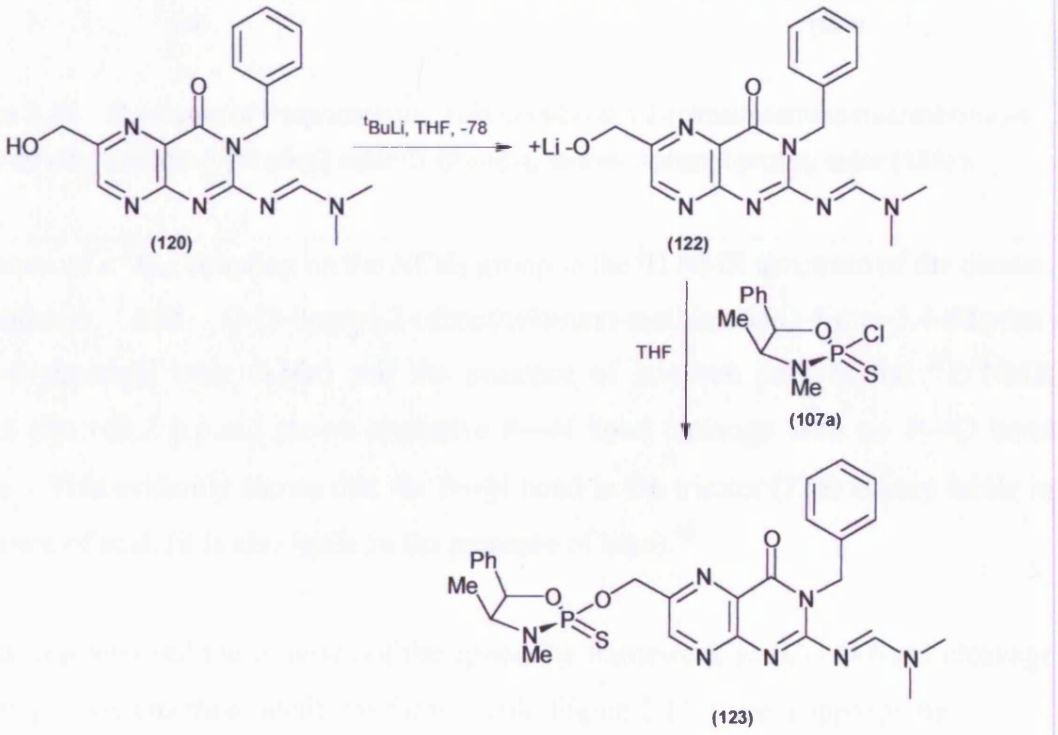

Scheme 2.18 Synthesis of N'-[3-Benzyl-6-(3,4-dimethyl-5-phenyl-2-thio-2λ^5-[1,3,2]oxazaphospholidin-2-yloxymethyl)-4-oxo-3,4-dihydro-pteridin-2-yl]-N,N-dimethyl-formamidine **(123)**.

The next stage in the synthesis involved endocyclic cleavage of the P—N bond in **(123)** leading to the incorporation of an ^{18}O atom by the use of labelled water ($H_2{}^{18}O$) and trifluoroacetic acid, Scheme 2.19. Therefore the initial step involves protonation of the nitrogen followed by direct S_N2 displacement of the now good leaving group ($-^{+}NH_2Me$) by $H_2{}^{18}O$.

This acid-catalysed ring opening occurs essentially stereospecifically with inversion of configuration at phosphorus.[96] Other related studies have demonstrated that acid-catalysed cleavage of P—N bonds in acyclic phosphinates[127] and acyclic alkylmethyl phosphonamidothioates occur with inversion of configuration.

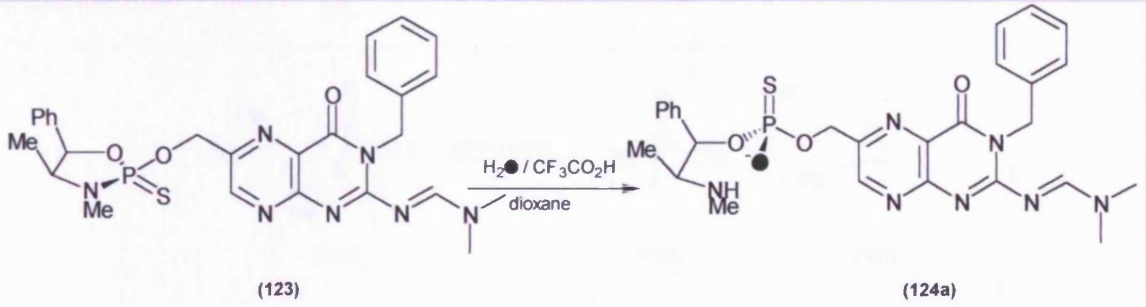

(123) (124a)

Scheme 2.19 Synthesis of thiophosphoric acid O-[3-benzyl-2-(dimethylamino-methinimino)-4-oxo-3,4-dihydro-pteridin-6-ylmethyl] ester O'-(2-methylamino-1-phenyl-propyl) ester **(124a)**.

The absence of a $^{3}J_{P\text{-}H}$ coupling on the NCH_3 group in the ^{1}H NMR spectrum of the diester, thiophosphoric acid O-[3-benzyl-2-(dimethylamino-methinimino)-4-oxo-3,4-dihydro-pteridin-6-ylmethyl] ester **(124a)** and the presence of just one peak in the ^{31}P NMR spectrum (δp +60.2 p.p.m.) shows exclusive P—N bond cleavage with no P—O bond cleavage. This evidently shows that the P—N bond in the triester **(123)** is very labile in the presence of acid, (it is also labile in the presence of base).[96]

The next step involved the removal of the ephedrine framework *via* C—O bond cleavage. However, previous methods available for this task, Figure 2.11, were inappropriate.

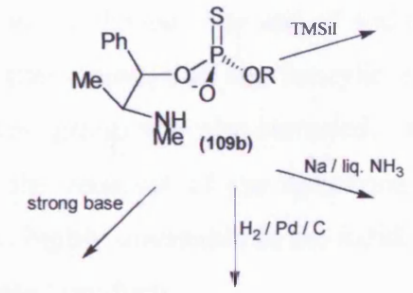

Fig. 2.11 Methods for removal of the ephedrine framework *via* C—O bond cleavage.

Inch *et al.*[15] removed the ephedrine moiety from a variety of thiophosphorus acid derivatives **(125)** by treatment with strong base which led to elimination of the thiophosphoryl component **(126)** with concomitant aziridine **(127)** formation, Scheme 2.20.

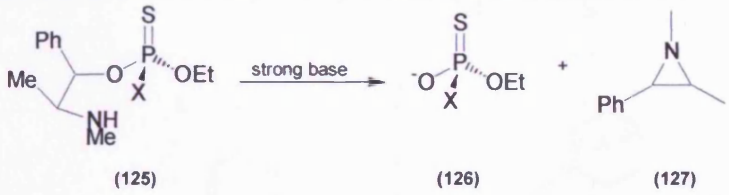

Scheme 2.20 C-O bond cleavage by treatment with strong base.

When this method was used on **(124a)** however, it resulted in only the formation of 2-oxy-oxazaphospholidine **(128)**, Scheme 2.21.

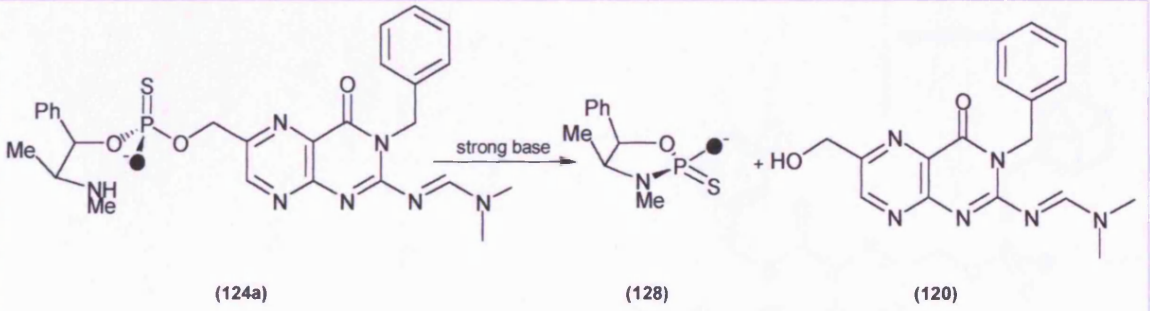

Scheme 2.21 Treatment of **(124a)** with strong base.

The presence of sulphur in **(124a)** prevents the use of hydrogenolysis to effect C-O bond cleavage as divalent sulphur deactivates metal catalysts.

Removal of the ephedrine moiety through the use of sodium metal in liquid ammonia proved unsuccessful. Reductive cleavage of the benzylic ephedrine group was detected but it was found that the pterin group was also removed. Trimethylsilyl iodide (TMSiI) has been used to facilitate the removal of the ephedrine group in O-aryl containing compounds.[36] This method is highly unsuitable as the iodide would also cleave off the O-pterin group leading to unwanted products.

A new method was employed to facilitate the elimination of the ephedrine group. On addition of myrtenyl bromide in the presence of triethylamine to **(124a)** it was found that the ephedrine moiety was lost spontaneously to form thiophosphoric acid O-[3-benzyl-2-(dimethylamino-methinimino)-4-oxo-3,4-dihydro-pteridin-6-ylmethyl] ester S-(6,6-dimethyl-bicyclo[3.1.1]hept-2-en-2-ylmethyl) ester **(112a)**, Scheme 2.22.

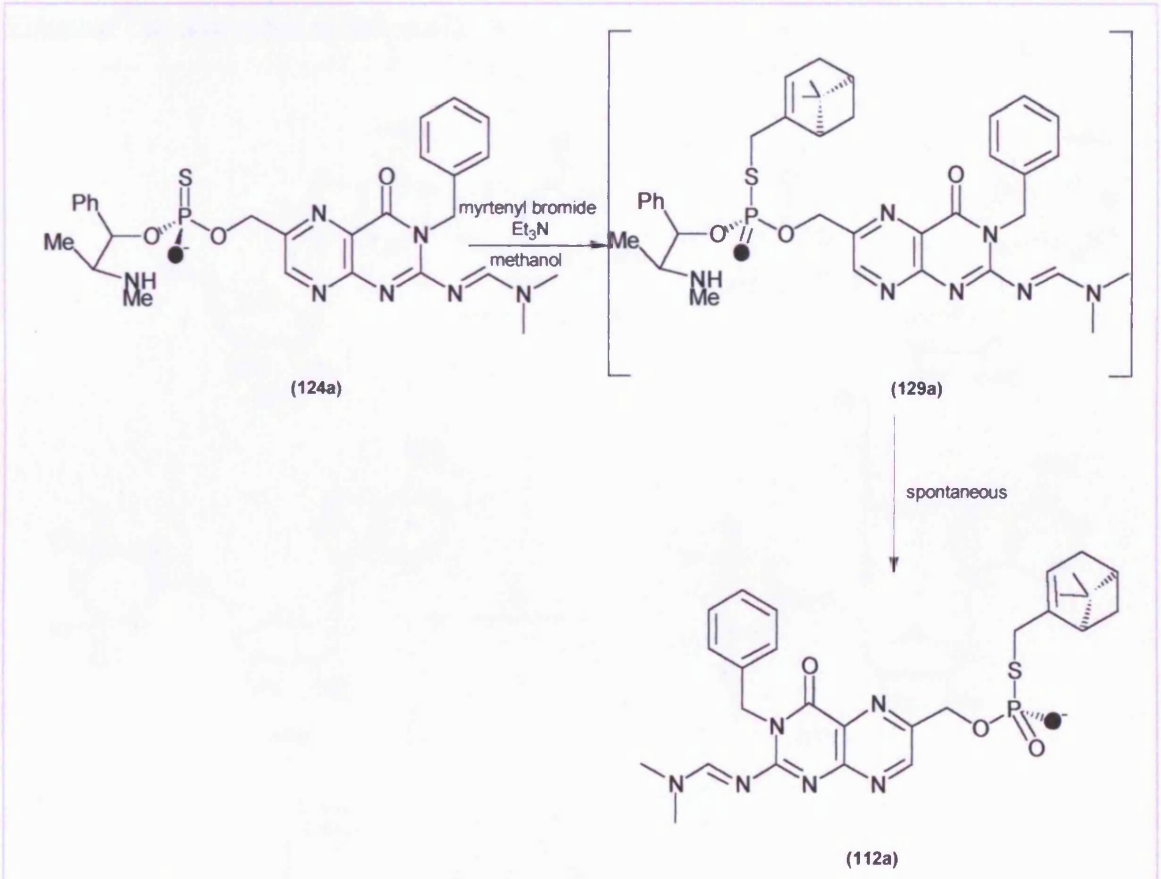

Scheme 2.22 Synthesis of thiophosphoric acid O-[3-benzyl-2-(dimethylamino-methinimino)-4-oxo-3,4-dihydro-pteridin-6-ylmethyl] ester S-(6,6-dimethyl-bicyclo[3.1.1]hept-2-en-2-ylmethyl) ester **(112a)**.

S-Alkylation was confirmed by the large upfield shift of the ^{31}P NMR signal. Spontaneous elimination of the ephedrine moiety was presumably due to the predicted drop in the pK_a value of the oxygen atom the ephedrine is bonded to from 7 to 2 on binding of myrtenyl to the sulphur atom. This change would greatly enhance the tendency of the phosphorus compound to be a leaving group, allowing for aziridine formation.

2.7 Synthesis of chiral nucleoside phosphorothioates.

2.7.1 Synthesis and characterisation of the diastereoisomers of adenosine 5′-[α-thio] triphosphate (ATPαS)(41).

ATPαS **(41)** was synthesised as a racemic mixture by the methods of Ludwig and Eckstein[93] as illustrated in Scheme 2.23.

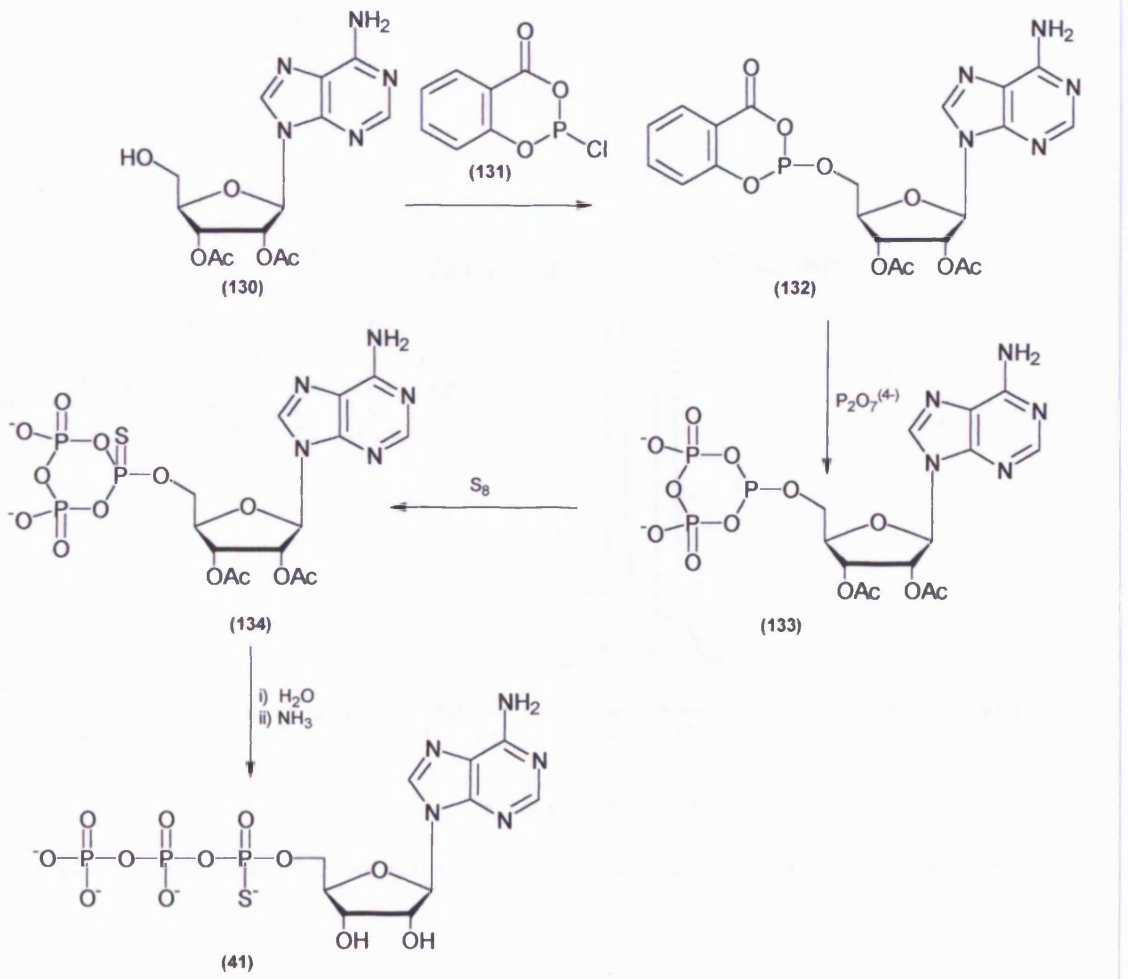

Scheme 2.23 Synthesis of racemic ATPαS **(41)**.

2',3'-Di-O-acetyl adenosine **(130)** was phosphitylated with 2-chloro-4H-1,3,2-benzodioxaphosphorin-4-one (Salicyl phosphorochloridite) **(131)** to give the intermediate 2-(2',3'-di-O-acetyladenosyl)-4H-1,3,2-benzodioxaphosphorin-4-one **(132)** which was converted to the mixed phosphate-phosphite species P^1-(2',3'-di-o-acetyladenosyl)-P^2,P^3-dioxo-cyclotriphosphite **(133)** in two consecutive displacement reactions with pyrophosphate. Oxidation with a suspension of sulphur to give 2',3'-di-acetyladenosine 5'-thiocyclotriphosphate **(134)** followed by deprotection of the ribose hydroxyl groups gave ATPαS **(41)** in 69% yield (lit. yield = 65%-75%).[93]

Preparative reverse phase HPLC was used to obtain the pure Rp and Sp diastereoisomers of ATPαS **(41)**. A typical separation is shown in Figure 2.12. Previously the assignment of a particular diastereoisomer of ATPαS (i.e. Sp or Rp at Pα) to a HPLC peak was achieved using crystal structure data.[93]

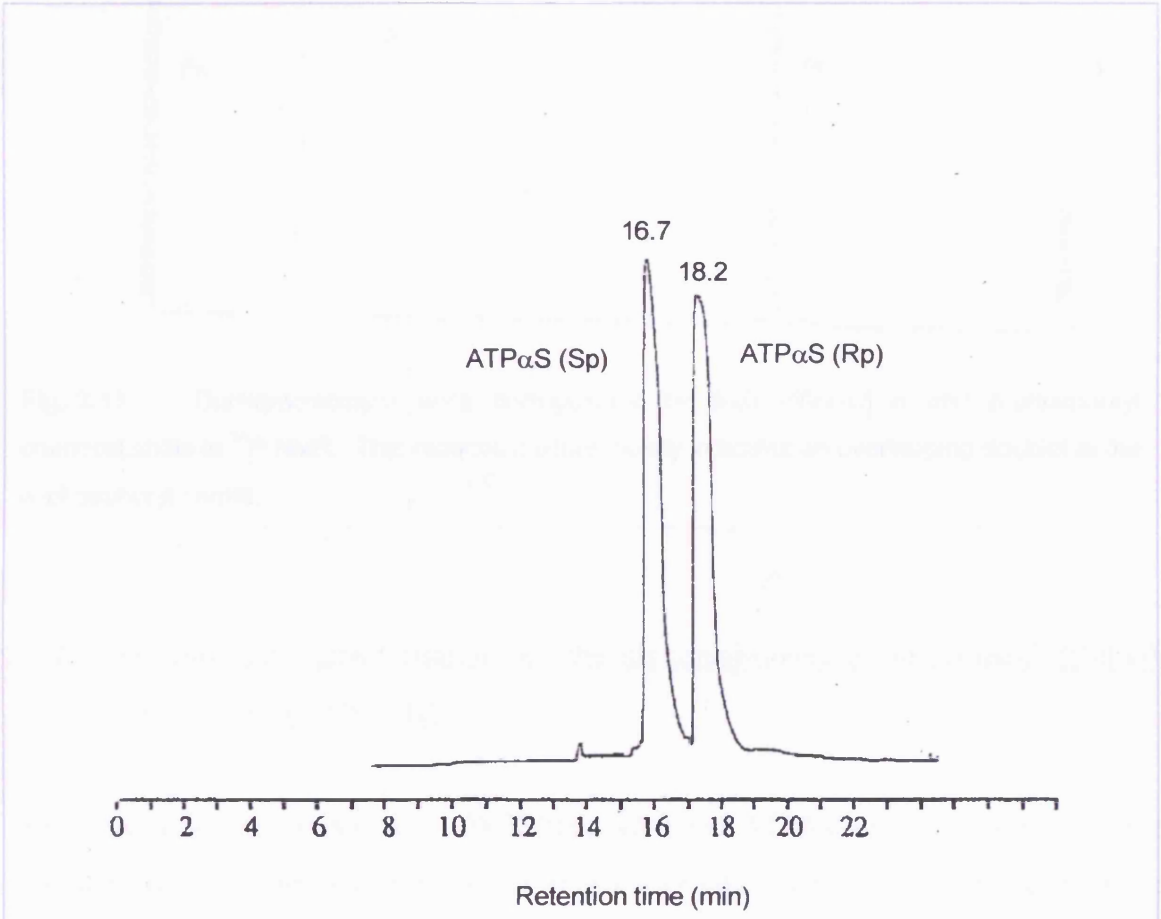

Fig. 2.12 A typical HPLC separation of Rp **(41a)** and Sp **(41b)** diastereoisomers of ATPαS.

After passage through the column, peak fractions were pooled and freed of triethylammonium bicarbonate. Further HPLC analysis of these concentrated samples on an analytical reverse phase column showed, in all cases, a single peak with no trace of the other isomer. In addition, as a racemic mixture two sets of peaks (i.e. overlapping doublets) are clearly seen at the α-phosphoryl centre in ^{31}P NMR, Figure 2.13. On separation only a doublet is visible at the α-phosphoryl centre, suggesting a complete separation.

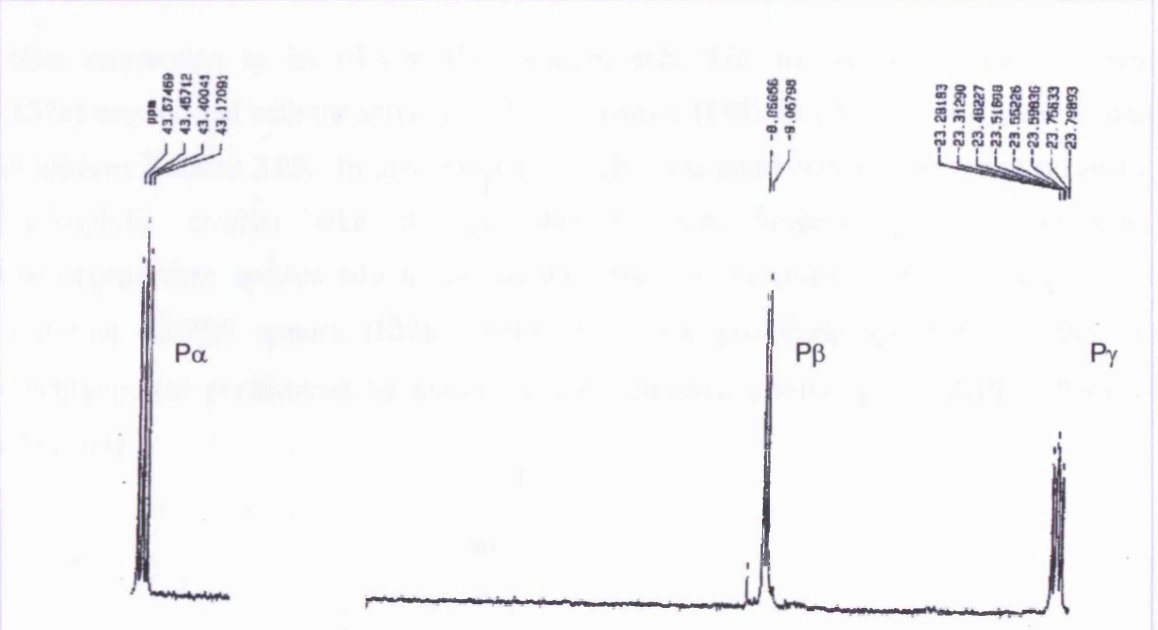

Fig. 2.13 Diastereoisomers were distinguished by their different α and β-phosphoryl chemical shifts in ^{31}P NMR. This racemic mixture clearly indicates an overlapping doublet at the α-phosphoryl centre.

2.7.2 Synthesis and characterisation of the diastereoisomers of adenosine-5′-[β-thio] triphosphate (ATPβS) (42).

The diastereoisomers of ATPβS; ATPβS(Rp) **(42a)** and ATPβS(Sp) **(42b)** were prepared following the procedures reported by Eckstein and Goody.[93] The first step in the synthesis involved the coupling of the thiophosphate **(135)** with 3-chloropropionamide **(136)** to produce the protected thiophosphate derivative, S-2-carbamoylethyl thiophosphate **(137a)** shown in Scheme 2.24.

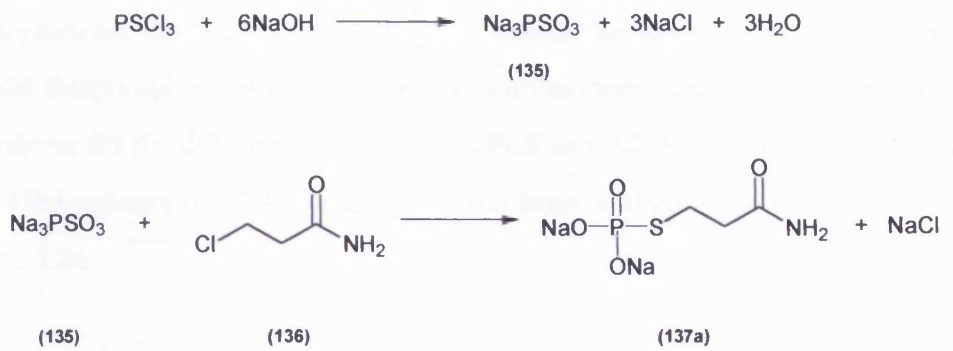

Scheme 2.24 The synthesis of S-2-carbamoylethyl thiophosphate **(137a)**.

After conversion to its tri-*n*-butylammonium salt, S-2-carbamoylethyl thiophosphate **(137a)** was reacted with the activated AMP derivative **(138)**, in a Michelson-type coupling procedure, Scheme 2.25. In this reaction pyridine was employed as both a solvent and a nucleophilic catalyst with the probable transient formation of a pyridinium phosphoramidate species which reacted with the thiophosphate derivative to give the protected ADPβS species **(139)**. Removal of the protecting group under alkaline conditions and purification by anion-exchange chromatography, gave ADPβS **(96c)** in 20% yield.

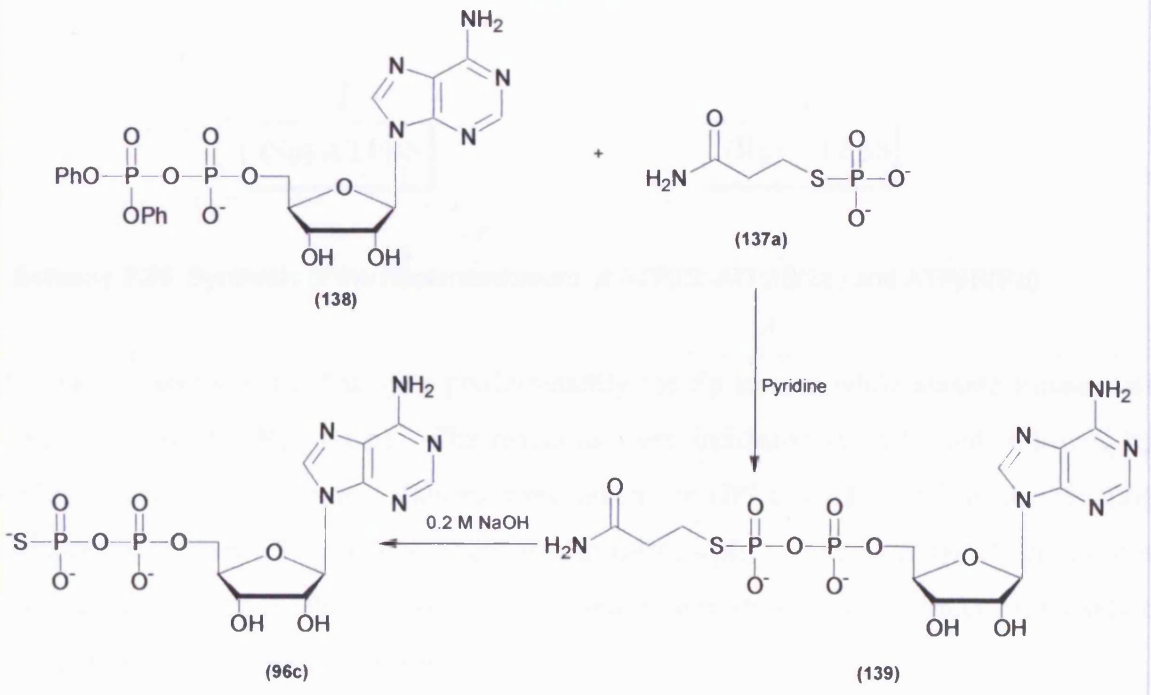

Scheme 2.25 Synthesis of the racemic ADPβS **(96c)**.

Since enzymes are themselves chiral they can exhibit stereospecificity at prochiral centres such as the thiophosphoryl group of ADPβS. Furthermore many kinases have been shown to be selective for the different epimers of ATPαS and ATPβS. In this work the Rp **(42a)** and Sp **(42b)** epimers of ATPβS were prepared from ADPβS enzymatically, as illustrated in Scheme 2.26.

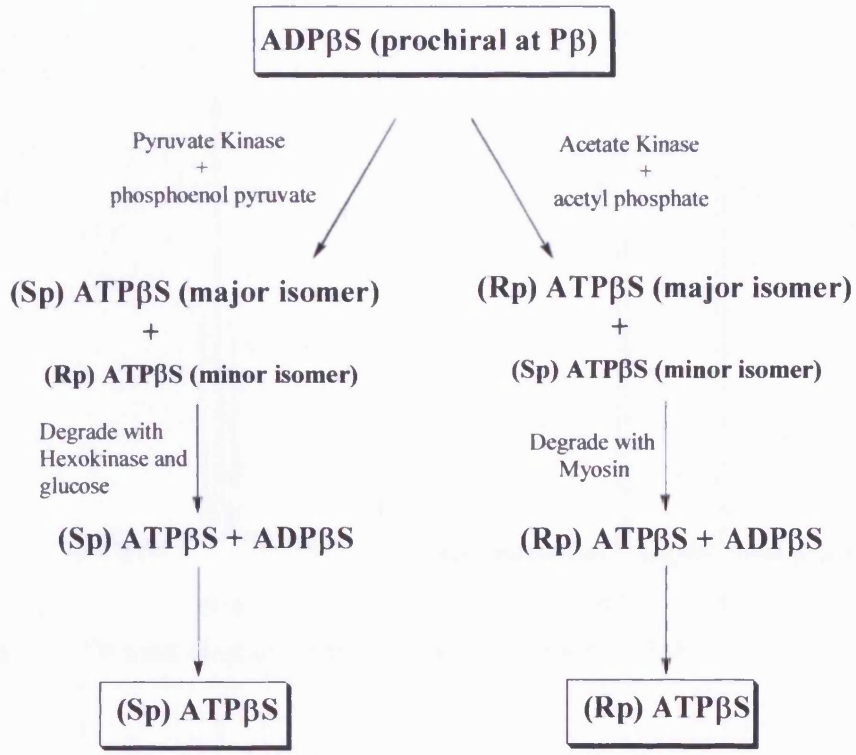

Scheme 2.26 Synthesis of the diastereoisomers of ATPβS; ATPβS(Sp) and ATPβS(Rp).

Pyruvate kinase was used to give predominantly the Sp isomer while acetate kinase was used to furnish the Rp isomer. The reactions were incubated at 25°C and followed by HPLC. After 4 hours small aliquots were taken for HPLC analysis while the reaction mixtures were purified by anion-exchange chromatography. Under the HPLC conditions used, the epimers of ATPβS had different retention times thus allowing direct visualisation of the stereoselectivities of the reaction.

After anion-exchange chromatography ATPβS (Sp) was freed of the contaminating Rp diastereoisomer by degradation with hexokinase. This reaction was followed by HPLC.

After 30 minutes incubation with hexokinase the contaminating minor diastereoisomer had been completely degraded to ADPβS. The reaction was continued for 90 minutes and then applied to DEAE-Sephadex columns for purification to yield the pure Sp diastereoisomer of ATPβS. The diastereomeric purity was estimated to be >99.5% and gave the expected ^{31}P NMR spectra, Figure 2.14. ATPβS (Rp) was judged sufficiently pure by HPLC analysis not to require degradation with myosin. The diastereomeric purity was estimated to be >99.5% and gave the expected ^{31}P NMR spectra, Figure 2.14.

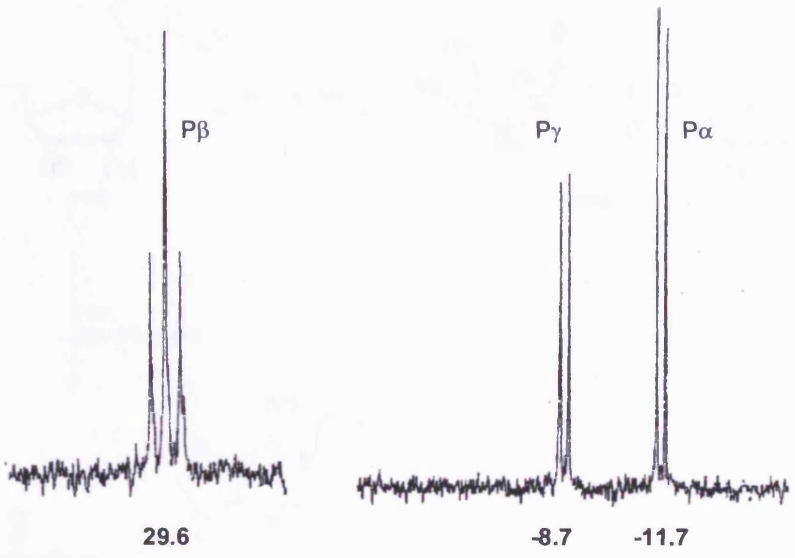

Fig. 2.14 ^{31}P NMR spectrum of the Sp diastereoisomer of ATPβS.

2.7.3 Synthesis of (Sp)-adenosine-5'-[β-^{18}O, β-thio]triphosphate [(Sp)-ATPβSβ^{18}O] (42c).[36]

Thio analogues of adenine nucleotides have been used extensively to study the stereochemical course of enzyme catalysed thiophosphoryl transfer reactions,[128,129] since they are substrates common to many of the phosphoryl transferase enzymes in nature. The synthesis of an isotopically labelled chiral thiophosphate analogue of ATP was synthesised using a combination of chemical and enzymatic methods, Scheme 2.27.

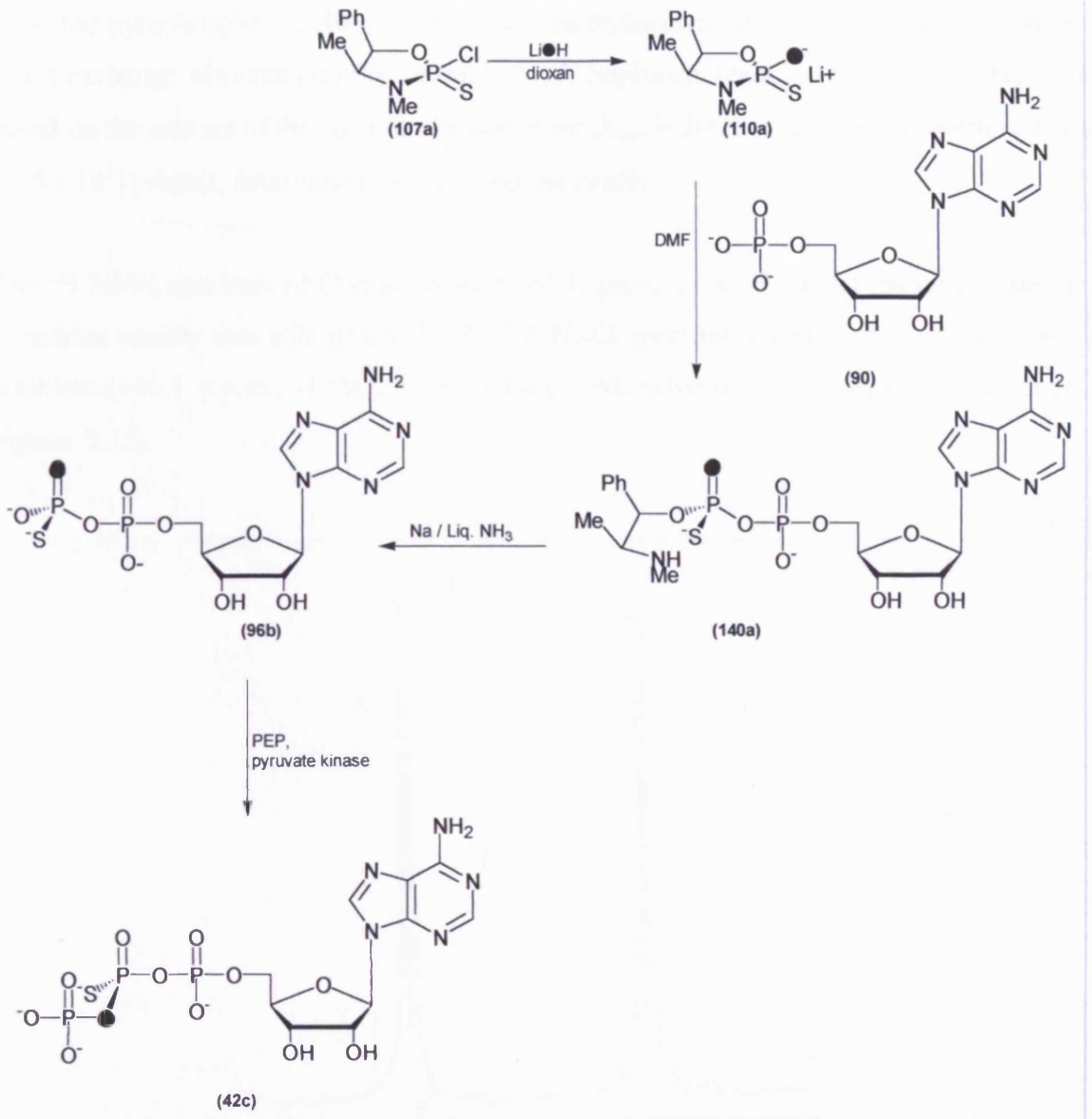

Scheme 2.27 Synthesis of ATPβSβ^{18}O (Sp) **(42c)** *via* the ephedrine route.

Our preparation began with the hydrolysis of the chloro adduct **(107a)** with ^{18}O-labelled lithium hydroxide, made from lithium metal in $H_2{}^{18}O$ (96 atom %) to give the product **(110a)**.

The freeze-dried lithium salt **(110a)** then underwent P-N bond cleavage in acidic conditions with adenosine-5'-monophosphoric acid (AMP free acid) **(90)** in DMF. Despite the limited solubility of AMP free acid in DMF, the heterogeneous reaction mixture was stirred rapidly at 60°C for 8 hours and gave a reasonable amount of the

expected pyrophosphate **(140a)** as its mono-triethylammonium salt after purification by anion-exchange chromatography through A-25 Sephadex resin. The yield (67%) was based on the amount of the adenine chromophore (λ_{max} = 260 nm, extinction coefficient (ε) = 15 x 10^3) present, determined spectrophotometrically.

The ^{1}H NMR spectrum of **(140a)** showed NCH_3 group as a 3H singlet indicated that the ephedrine moiety was still attached; the ^{31}P NMR spectrum showed two well separated doublets (+46.1 p.p.m., -10.9, J = 35.6 Hz), indicative of a pyrophosphate structure, Figure. 2.15.

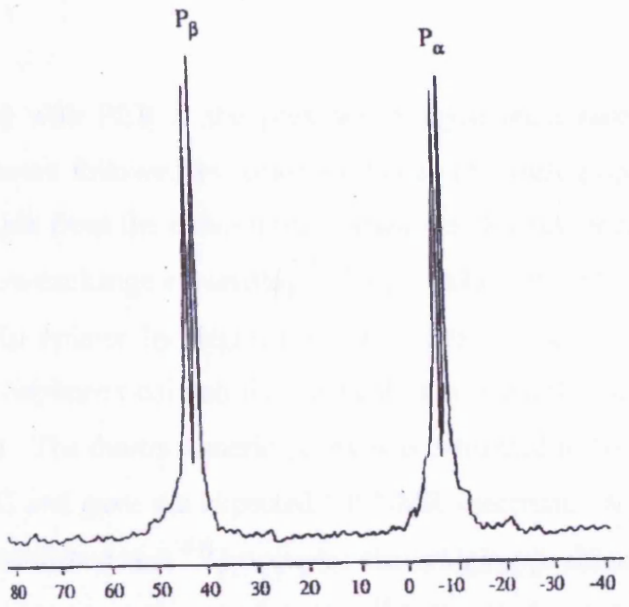

Fig. 2.15 ^{31}P NMR spectrum of pyrophosphate **(140a).**

The doublet at 46.1 p.p.m. is assigned to the β-phosphorus atom, as phosphorus atoms attached to sulphur resonate at a lower field in comparison with oxygen equivalents.

The presence of sulphur in the thiophosphoryl moiety of **(140a)** prevented hydrogenolysis of the benzylic ester (C-O bond cleavage) and the presence of the adenosine group prevented the use of trimethylsilyl iodide. Reductive cleavage of the ephedrine group with sodium (15 eq) in liquid ammonia however, proved effective to give ADPβSβ^{18}O **(96b)**

which was purified by anion-exchange chromatography; its position of elution from the column suggested a molecule with three negative charges. The ^{31}P NMR spectrum of **(96b)** again showed the presence of a pyrophosphate, indicated by the P-P coupling. Removal of the ephedrine framework resulted in the ^{31}P NMR chemical shift of the β-phosphorus of **(96b)** appearing more upfield than that of **(140a)**, as removal of the ephedrine moiety changes the bond order to sulphur.

Since the conversion of **(107a)** to **(110a)** is known to proceed with retention of configuration at phosphorus,[96] the ring opening of **(110a)** to **(140a)** involves inversion of configuration and C-O bond cleavage of **(140a)** to **(196b)** has no stereochemical consequences at phosphorus, the product will have an Sp configuration at the β-phosphorus.

Incubation of **(96b)** with PEP in the presence of pyruvate kinase under typical assay conditions for 25 hours followed by anion-exchange chromatography gave a compound whose elution position from the column was indicative of a compound with four negative charges. After anion-exchange chromatography the ATPβSβγ^{18}O (Sp) sample was freed of contaminating Rp epimer by degradation with hexokinase. The reaction was then applied to a DEAE-Sephadex column for purification to yield the pure Sp diastereoisomer of ATPβSβ^{18}O **(19)**. The diastereomeric purity was estimated to be >99.5% by analytical reverse phase HPLC and gave the expected ^{31}P NMR spectrum. A previous synthesis of this compound[36] established that ^{18}O occupies the bridging position between Pβ and Pγ. This conclusion was based on the principle that ^{18}O directly bonded to phosphorus causes an upfield (isotopic) shift on the ^{31}P NMR resonance of the phosphorus[130-132] by an amount that increases with increasing bond order[116,133] (see Chapter 3 for a detailed discussion). The phosphorus resonances that suffer isotopic shifts were shown to be the Pβ and Pγ by ^{31}P NMR of a 1:1 mixture of labelled and unlabelled material (prepared in the same way), the size of these isotopic shifts (2.7 Hz in each case) being proof that the ^{18}O is in the βγ-bridge, while the Pα remains a doublet, Figure 2.16.

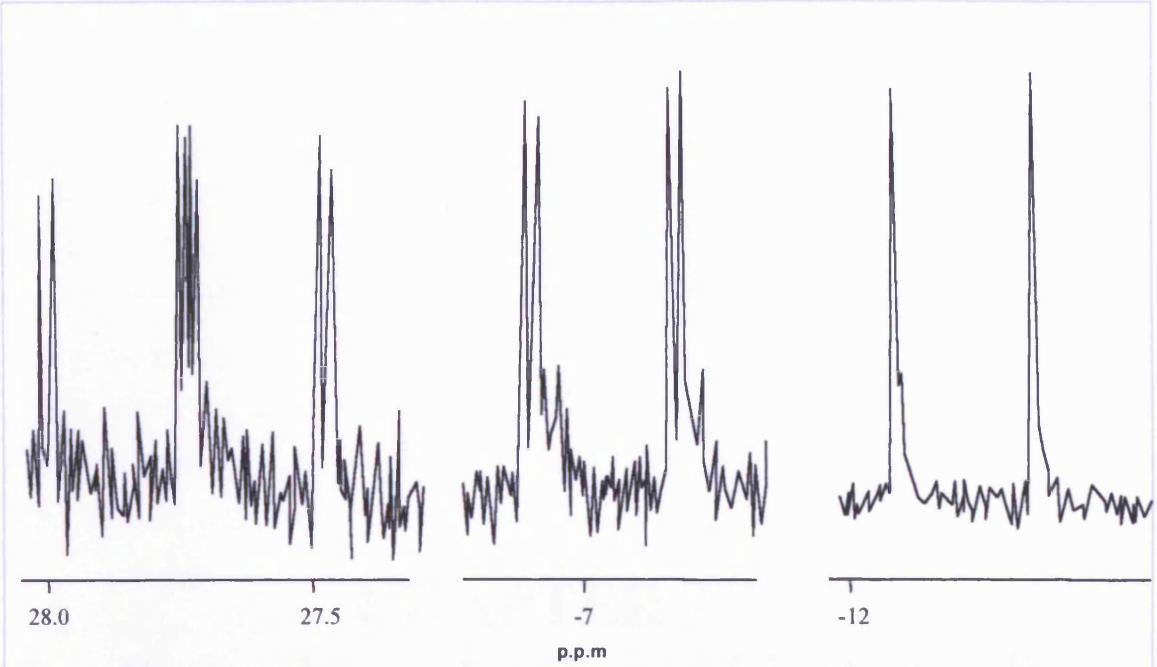

Fig 2.16 Expanded ^{31}P NMR spectrum of ATPβSβγ^{18}O mixed with authentic ATPβS.

2.8 Conclusion.

Isotopically labelled chiral Rp-[^{16}O,^{18}O]thiophosphoric acid O-[3-benzyl-2-(dimethylamino-methinimino)-4-oxo-3,4-dihydro-pteridin-6-ylmethyl] ester S-(6,6-dimethyl-bicyclo[3.1.1]hept-2-en-2-ylmethyl) ester **(112a)** has been synthesised *via* the ephedrine route. The Rp **(41a)** and Sp **(41b)** diastereoisomers of ATPαS and the Rp **(42a)** and Sp **(42b)** diastereoisomers ATPβS have been synthesised. The Sp diastereoisomer of ATPβSβγ^{18}O **(42c)** has been synthesised *via* the ephedrine route.

CHAPTER 3
Configurational Analysis of Isotopically Labelled Chiral Thiophosphate Monoesters

3.1 Introduction.

In Chapter 2 the synthesis of several isotopically labelled chiral thiophosphate esters was described. This work was put in context by an historical account of the syntheses of isotopically labelled chiral phosphate and thiophosphate monoesters. This account highlighted the pioneering work of Westheimer[8] who in 1968 developed the idea that the hydrolysis of cyclic five-membered phosphate esters proceeds *via* a pseudo-rotation mechanism and concludes with the most recent attempts to study thiophosphoryl transfer reactions using isotopically labelled chiral thiophosphate monoesters.

In order to investigate the stereochemical course of the (thio)phosphoryl transfer reaction (enzyme catalysed or chemical) that these chiral materials may undergo, an independent method for determining the absolute configuration of [^{16}O, ^{18}O] thiophosphate monoesters and [^{16}O, ^{17}O, ^{18}O] phosphate monoesters is required. Coupled to this a quantitative assessment of the enantiomeric excess at phosphorus is required. The development of techniques for configurational analysis is described in this Chapter. The account concludes with the configurational analysis of the isotopically labelled chiral thiophosphates synthesised in Chapter 2.

3.2 Literature configurational analyses of [^{16}O, ^{17}O, ^{18}O] phosphate esters.

Mass spectrometry and ^{31}P NMR spectroscopy techniques are the powerful analytical tools that have been employed to analyse the absolute chirality of [^{16}O, ^{17}O, ^{18}O] phosphate monoesters. The advantages and limitations of these methods will be reviewed here.

3.2.1 Mass spectrometry method.

Metastable ion mass spectrometry[119] has provided a reliable method for the configurational analysis of isotopically labelled chiral phosphate esters.

This strategy is based on the conversion of a pro-prochiral phosphate monoester to a prochiral phosphate diester so that the isotopic identity of the resulting diastereotopic oxygens can be established by virtue of their chemical non-equivalence. To generate a

phosphate diester that is diastereoisomeric at phosphorus demands the presence of a second conventional chiral centre in the phosphate monoester. The introduction of this chiral centre has been accomplished as illustrated in Scheme 3.1.

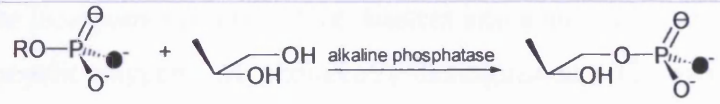

(66a) (141) (142a)

Scheme 3.1 Generation of the Rp phosphate monoester **(142)** attached to (S)-propane-1,2-diol.

Alkaline phosphatase in the presence of (S)-propane-1,2-diol **(141)** catalyses the transfer of a phosphoryl group from any phosphate monoester to the diol. It has been shown that this transfer proceeds with overall retention of configuration at phosphorus.[134] This process has been used to generate both the Rp **(142a)** and Sp **(142b)** phosphate monoesters attached to the conventional chiral centre (S)-propane-1,2-diol **(141)**.

The oxygen atoms of the Rp monoester **(142a)** and the Sp monoester **(142b)** are now diastereotopic and are randomly activated for ring closure by reaction with diphenylphosphorylimidazole to give, in each case, a mixture of three isotopomeric five-membered ring cyclic phosphates, i.e. $^{16}O,^{17}O$-, $^{17}O,^{18}O$- and $^{16}O,^{18}O$- diastereoisomers **(143a,b,c)** and **(143d,e,f)**, Scheme 3.2.

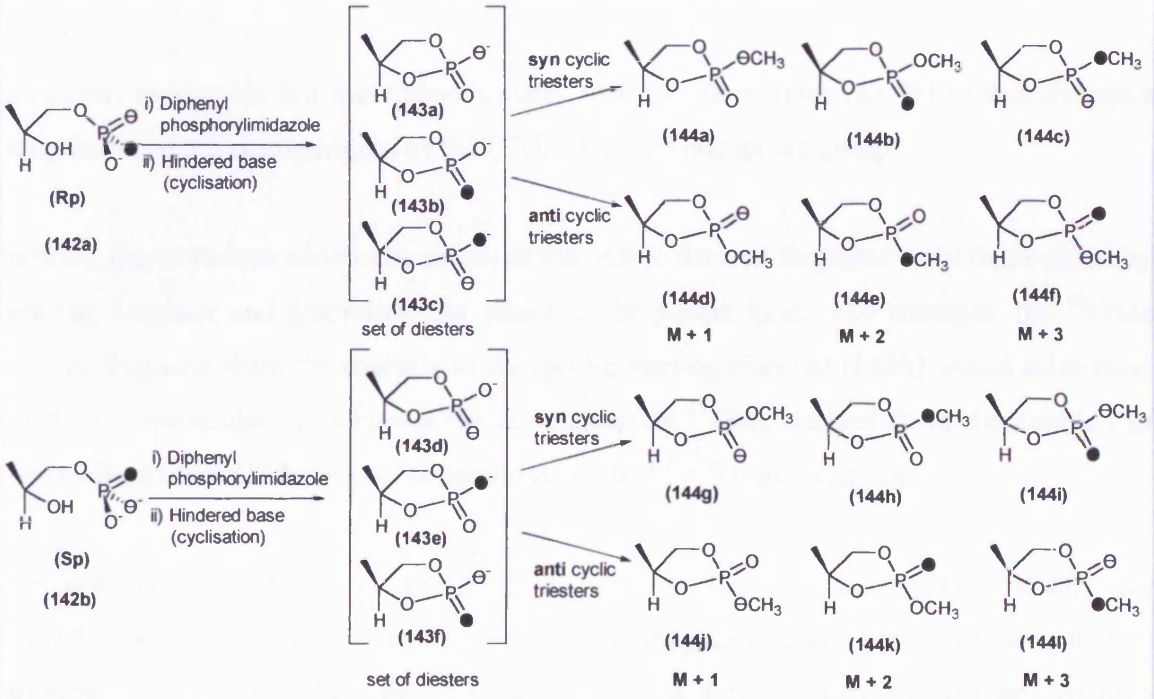

Scheme 3.2 Mass spectral analysis of isotopically labelled chiral [^{16}O, ^{17}O, ^{18}O] phosphate monoesters.

The ring closure leads to loss of one of the three isotopic sites. The stereochemical course of this reaction has been shown to proceed with inversion of configuration.[90,119]

Methylation of the isotopomers converts the diesters into a mixture of *syn* and *anti* triesters in which the exocyclic oxygens are chemically distinguished. The *syn* and *anti* isomers are diastereoisomeric and are separated chromatographically. The isomers that would arise from either the Rp or Sp [^{16}O, ^{17}O, ^{18}O] phosphate ester, **(144a-f)** and **(144g-l)** respectively, are shown in scheme 3.2.

The stereochemical information is contained in the identity of the oxygen that is methylated as well as the isotope in the other site, e.g. in the ^{16}O, ^{18}O labelled cyclic methyl ester, the ester is methylated on ^{16}O from the Rp(*syn*) monoester **(144b)** and on ^{18}O from the Sp(*syn*) monoester **(144h)**. This alone is not sufficient however, to distinguish the Rp and Sp configurations in the parent molecule.

Normal mass spectral techniques cannot be used to determine directly the distribution of oxygen isotopes, because each mixture contains equal amounts of species that are methylated on each isotope of oxygen.

However, metastable ion mass spectrometry of these derivatives has led to unambiguous assignment of the configuration of the [^{16}O, ^{17}O, ^{18}O] phosphate group.

In brief, the technique allows the origin of the –OMe derived fragment to be determined by relating daughter and granddaughter peaks to the parent ions. For example, the ^{18}OMe derived fragment from the analysis of the *syn* Sp starting material **(144h)** would arise from the M + 2 molecular ion whereas the corresponding ^{18}OMe derived from the analysis of the *syn* Rp isomer **(144c)** would originate from the M + 3 molecular ion.

The analysis is technically quite difficult in that the five-ring cyclic triesters are hydrolytically labile and the method requires handling and separation of the *syn* and *anti* isomers. Furthermore, this method is not general as it is restricted to systems that give suitable metastable peaks. For this reason, the mass spectral technique has now been superseded by a ^{31}P NMR method discussed in Section 3.2.2.

3.2.2 ^{31}P NMR spectroscopy method.

^{31}P NMR spectroscopy has become the most important and reliable method for the configurational analysis of chiral [^{16}O, ^{17}O, ^{18}O] phosphate esters. This method is based on observations that have been made about the effect of oxygen isotopes directly bonded to phosphorus on the ^{31}P NMR resonances.

The configurational analysis, described by Lowe[135] and Knowles and Buchwald,[136] is conceptually related to the mass spectral method in that it requires the phosphate monoester to be cyclised onto an appropriate functionality to provide a conformationally locked system as shown in Scheme 3.3.

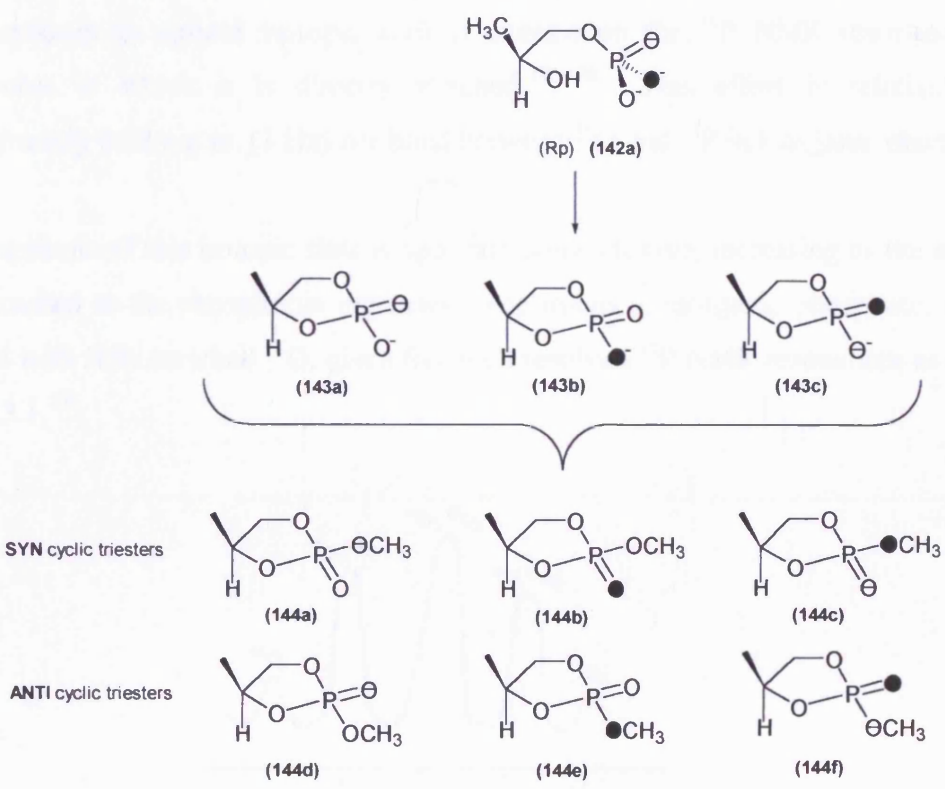

Scheme 3.3 ^{31}P NMR configurational analysis of isotopically chiral [^{16}O, ^{17}O, ^{18}O] phosphate monoester.

The analysis of Knowles *et al.*[136] requires the general [^{16}O, ^{17}O, ^{18}O] PO_3 unit to be attached to propane-1,2-diol. Analysis of a range of simple phosphate monoesters and pyrophosphates can be achieved using alkaline phosphatase to catalyse

transphosphorylation reactions in which the propanediol serves as the acceptor of the phosphoryl group from a phosphate monoester. This has been shown to occur with retention of configuration.[119,134] The diastereoisomeric monoesters, for example **(142a)**, are converted into the corresponding phosphodiesters **(143a-c)** as with the mass spectrometry method.

As with the mass spectral method the phosphate esters are cyclised and methylated to give the *syn* **(144a-c)** and *anti* **(144d-f)** isotopomers of the cyclic phosphate diester. In contrast to the analysis based on the metastable ion mass spectroscopy, the ^{31}P NMR spectral analysis does not require the separation of the *syn* and *anti* isomers since these are well separated in terms of ^{31}P NMR resonances.

The configurational analysis relies upon the observation that when ^{18}O is directly bonded to phosphorus an upfield isotopic shift is exerted on the ^{31}P NMR resonance of the phosphorus to which it is directly attached.[130-132] This effect is relatively small, approximately 0.02 p.p.m. (3 Hz) per bond between ^{18}O and ^{31}P in inorganic phosphate.

The magnitude of this isotopic shift is approximately additive, increasing as the number of ^{18}Os attached to the phosphorus increases. For instance, inorganic phosphate, randomly labelled with 50% enriched ^{18}O, gives five well resolved ^{31}P NMR resonances as shown in Figure 3.1.[131]

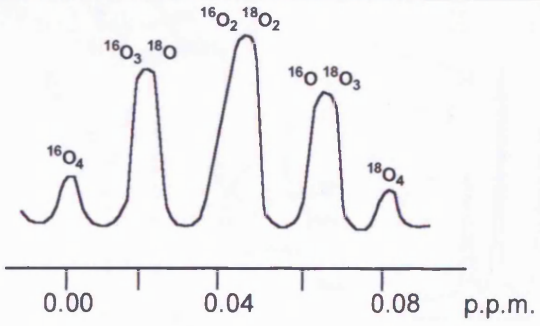

Fig. 3.1 The ^{31}P NMR spectrum (145.7 MHz) of randomly ^{18}O-labelled inorganic phosphate.[131]

The size of this isotopic perturbation on the chemical shift is dependent on the order of the bond between ^{18}O and ^{31}P, with increasing bond order resulting in a larger isotopic perturbation.[116,133] For example, in the series inorganic phosphate, monomethyl phosphate, dimethyl phosphate and trimethyl phosphate, the ^{18}O isotopic shift resulting from the labelling of one phosphoryl oxygen were 0.02, 0.024, 0.029 and 0.035 p.p.m. respectively.[133]

^{17}O has a nuclear spin of $^{5}/_{2}$ and therefore would be expected to couple to phosphorus. However, due to the permanent quadrupole moment, in practice the ^{31}P NMR resonances of phosphorus centres are broadened to such an extent that they are undetectable.[133]

These two effects have been elaborated into a semi quantitative configurational analysis. The ^{31}P NMR spectra for the analysis of Sp and Rp [^{16}O, ^{17}O, ^{18}O] phosphate monoesters are shown in Figure 3.2.

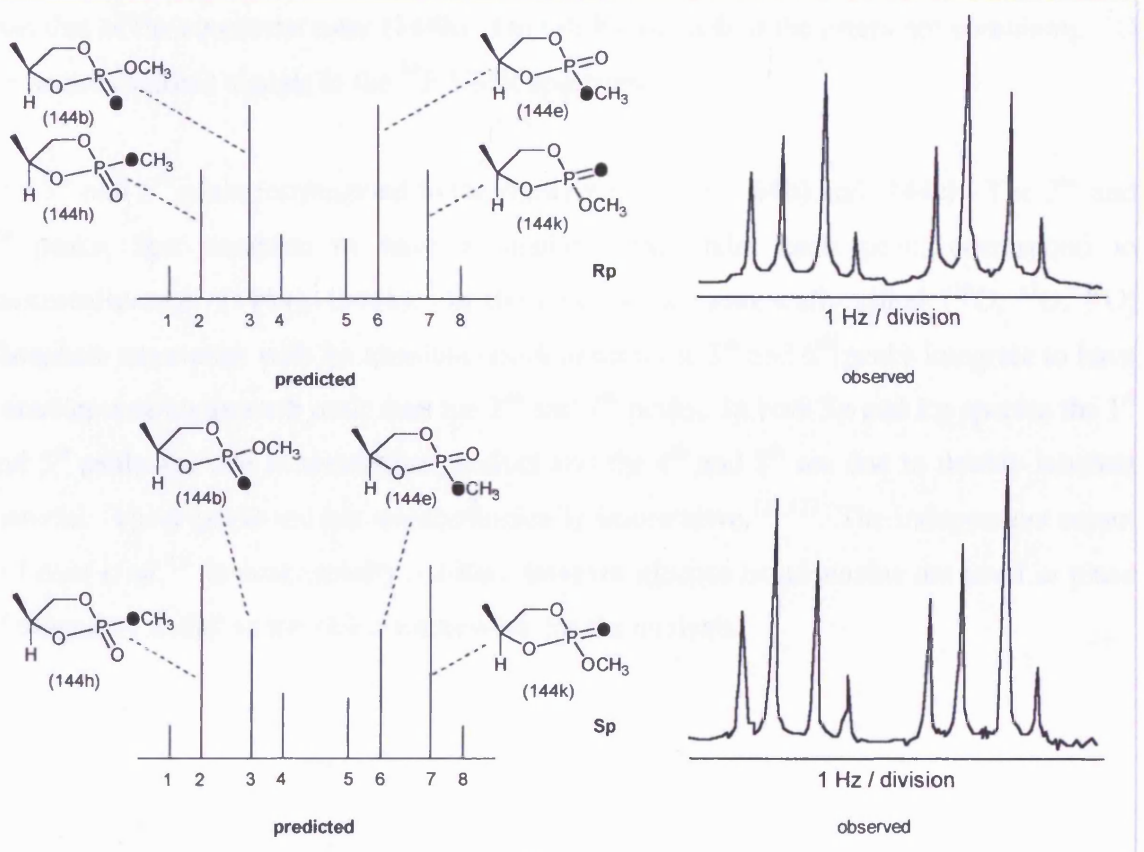

Fig. 3.2 The predicted and observed ^{31}P NMR spectra of the mixture of methyl esters prepared from the diastereoisomers of [^{16}O, ^{17}O, ^{18}O] phospho-(S)-1,2-propandiol (1:2:1 for ^{16}O, ^{17}O, ^{18}O).

Interpretation of these spectra requires us to apply several concepts that we have already encountered in this chapter. In Scheme 3.3 we identified the cyclic phosphate esters **(144a-f)** that would result from cyclisation and methylation of the isotopically chiral [^{16}O, ^{17}O, ^{18}O] phosphate monoester with Rp absolute configuration. Four of these compounds, **(144a)**, **(144d)**, **(144c)** and **(144f)**, contain a ^{17}O atom. As ^{17}O bonded to phosphorus virtually obliterates the ^{31}P NMR signal owing to its nuclear electric quadrupole moment these signals should not be observed. However, in these experiments although the ^{18}O enrichment is in excess of 99 atom% the ^{17}O is only 50% enriched. As a result peaks representing compounds **(144a)**, **(144d)**, **(144c)** and **(144f)** are observed in the ^{31}P NMR spectrum but at a lesser intensity than the signals corresponding to **(144b)** and **(144e)** that contain only ^{16}O and ^{18}O atoms. Furthermore, ^{18}O when singly bonded to a phosphorus atom causes a smaller isotope shift than when doubly bonded to phosphorus atom, so that the isotope shift on the ^{31}P resonance in the axial ester **(144h)** is smaller than for axial ester **(144b)**. Similarly, the isotope shift on the ^{31}P resonance of the equatorial **(144e)** is smaller than that of the equatorial ester **(144k)**. On this basis, each of the esters not containing ^{17}O are seen as distinct signals in the ^{31}P NMR spectrum.

The 3rd and 6th peaks, correspond to the diastereoisomers **(144b)** and **(144e)**. The 2nd and 7th peaks, that integrate to have a smaller area under each peak, correspond to diastereoisomers **(144h)**, **(144k)**. In the case of the isotopically chiral [^{16}O, ^{17}O, ^{18}O] phosphate monoester with Sp absolute configuration the 3rd and 6th peaks integrate to have a smaller area under each peak than the 2nd and 7th peaks. In both Sp and Rp spectra the 1st and 5th peaks are due to unlabelled product and the 4th and 8th are due to doubly labelled material. These peaks are not stereochemically informative.[131,132] The independent report of Lowe *et al.*[135] is conceptually similar, however glucose or adenosine are used in place of propane-1,2-diol as the chiral framework for the analysis.

3.3 Literature configurational analyses of [^{16}O, ^{18}O] thiophosphate esters.

3.3.1 Stereoselectivity of enzymes.

Enzyme catalysed stereospecific reactions have been utilised to allow the configurational analysis of nucleotides such as [^{16}O, ^{18}O] adenosine-5'-thiophosphate, Scheme 3.4.

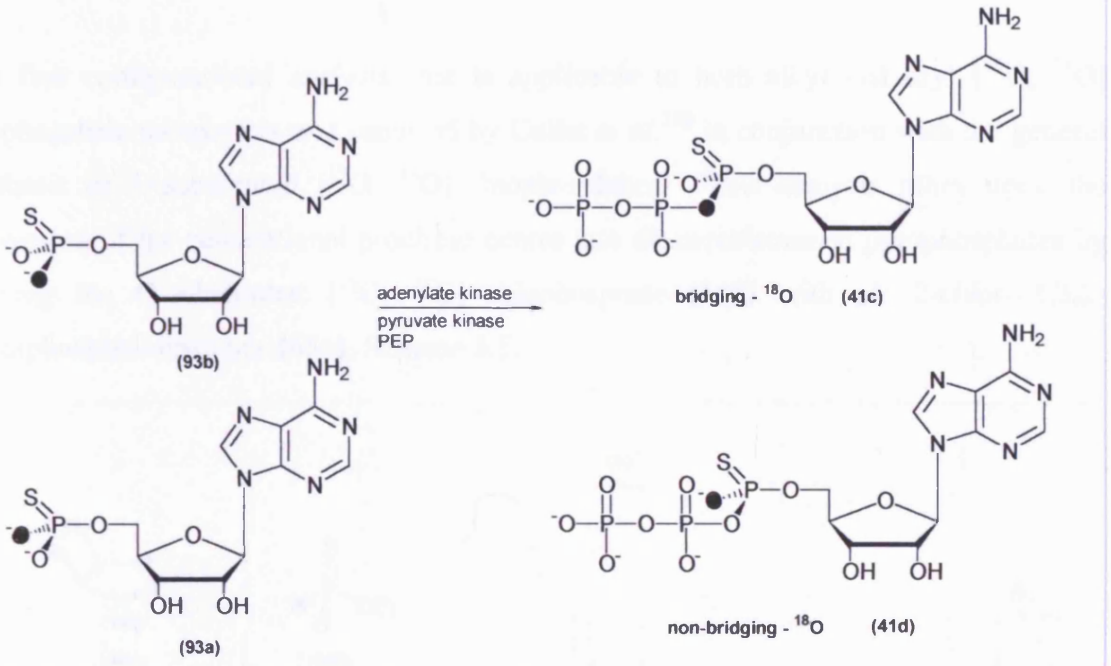

Scheme 3.4 Enzymatic analysis of [^{16}O, ^{18}O] adenosine-5'-thiophosphate.

Frey[105] has shown that myokinase (≡ adenylate kinase) catalyses the phosphorylation of AMPαS on oxygen to give the Sp isomer of ADPαS[104] which was established by snake venom phosphodiesterase digestion.[137] By the action of pyruvate kinase and phosphoenol pyruvate this is converted to the corresponding Sp ATPαS triphosphate. Applying this sequence of reactions to Rp [^{16}O, ^{18}O] AMPαS **(93b)** leads to ^{18}O exclusively in the bridging position **(41c)**. Applying this same sequence of reactions to Sp [^{16}O, ^{18}O] AMPS **(93a)** leads to ^{18}O exclusively in the non-bridging position **(41d)**. These two can be distinguished by mass spectrometry following degradation or directly on the Sp ATPαS by ^{31}P NMR spectroscopy.

3.3.2 General configurational analysis.

In order to study the stereochemical course of thiophosphoryl transfer reactions of [^{16}O, ^{18}O] thiophosphate monoesters, a general method that allows the assignment of the absolute configuration of both starting material and products of the reaction is required. We have seen (Chapter 2) that [^{16}O, ^{18}O] thiophosphate monoesters can be synthesised stereospecifically with known absolute configurations.

The first configurational analysis that is applicable to both alkyl and aryl [^{16}O, ^{18}O] thiophosphate monoesters was reported by Cullis *et al.*[118] in conjunction with the general synthesis of O-substituted [^{16}O, ^{18}O] thiophosphates. This analysis relies upon the conversion of the conventional prochiral centre into diastereoisomeric pyrophosphates by reacting the O-substituted [^{16}O, ^{18}O] thiophosphate **(145)** with *cis* 2-chloro-1,3,2-oxazaphospholidin-2-one **(68a)**, Scheme 3.5.

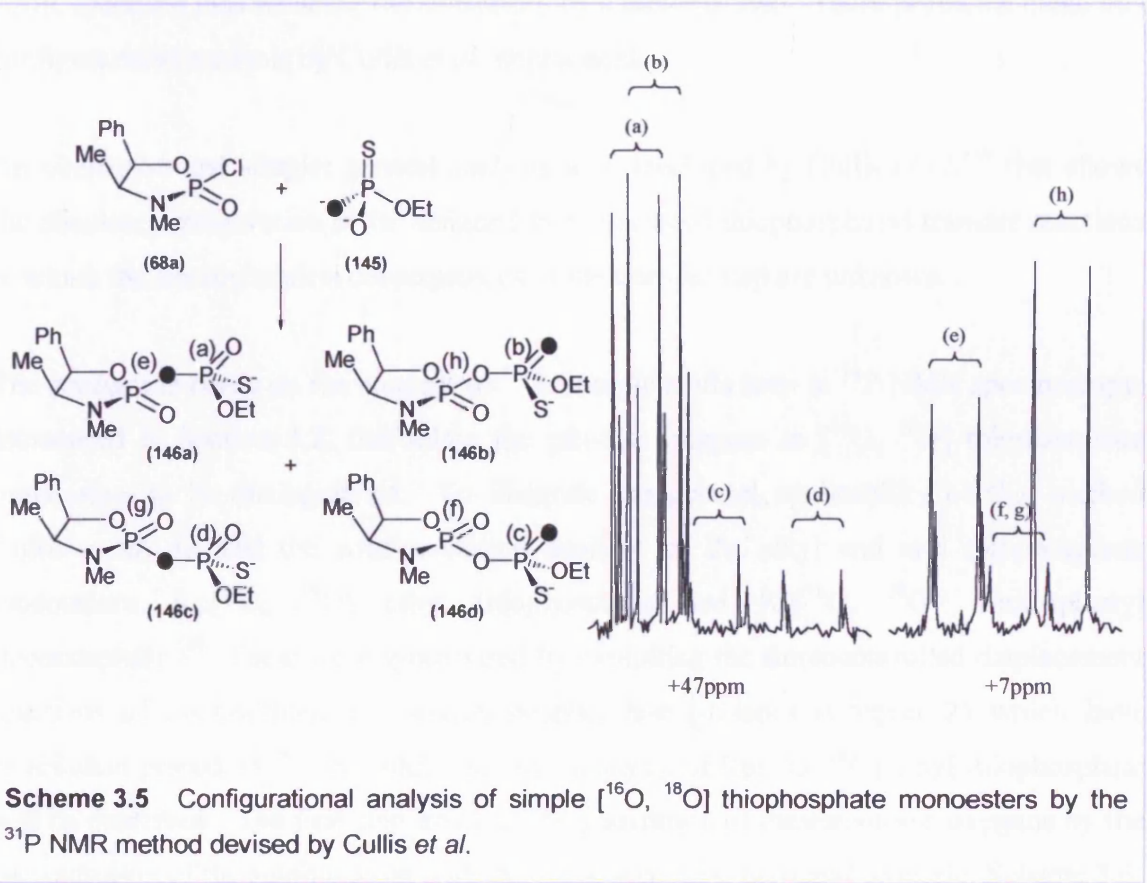

Scheme 3.5 Configurational analysis of simple [^{16}O, ^{18}O] thiophosphate monoesters by the ^{31}P NMR method devised by Cullis *et al.*

The location of the ^{18}O within the two epimers was established by the size of the ^{18}O isotopic shift induced on the ^{31}P NMR resonances thus assigning the absolute

configuration of the initial O-substituted [^{16}O, ^{18}O] thiophosphate monoester **(145)**. Two main problems are apparent with this analysis. Firstly, there is some loss of stereochemical control in the derivatisation reaction leading to four epimers instead of two. Normally exocyclic displacement reactions of these oxazaphospholidine-2-ones **(68a)** proceed stereospecifically with retention of configuration.[96] However, in the presence of nucleophilic catalysts such as pyridine, *N*-methylimidazole and *N*,*N*-dimethylaniline, epimerisation of the chloro compound **(68a)** occurs prior to its reaction with the thiophosphate **(145)**[138] thus giving four epimers **(146a, 146b, 146c, 146d)**. This problem has been eliminated by using tertiary amines like tributylamine under anhydrous conditions. In this case, the product was shown to be principally the two diastereoisomers **(146a** and **146b)**.

The second problem encountered with the analysis concerns the chiral auxiliary **(68a)**. As this is a phosphorus centre, this introduces a phosphorus-phosphorus coupling in the ^{31}P NMR spectrum thus reducing the sensitivity by a factor of two. These problems make this configurational analysis by Cullis *et al.* impractical.

An alternative and simpler general analysis was developed by Cullis *et al.*[139] that allows the absolute configuration to be assigned to products of thiophosphoryl transfer reactions in which the stereochemical consequences of the transfer step are unknown.

The analysis is based on the concept of ^{18}O isotopic shifts seen in ^{31}P NMR spectroscopy, introduced in Section 3.2, that allow the pro-R/S oxygens in [^{16}O, ^{18}O] thiophosphate monoesters to be distinguished. To illustrate the general applicability of this method Cullis *et al.* devised the configurational analysis of the alkyl and aryl thiophosphate monoesters: Rp[^{16}O, ^{18}O] ethyl thiophosphate and Rp[^{16}O, ^{18}O] 4-nitrophenyl thiophosphate.[139] These were synthesised by exploiting the stereocontrolled displacement reactions of 2-substituted 1,3,2-oxazaphospholidine-2-thiones (Chapter 2) which have established precedent.[96] The configurational analysis of Rp[^{16}O, ^{18}O] ethyl thiophosphate will be described. The first step involves the generation of diastereotopic oxygens by the derivatisation of the sulphur atom with the chiral auxiliary, myrtenyl bromide, Scheme 3.6.

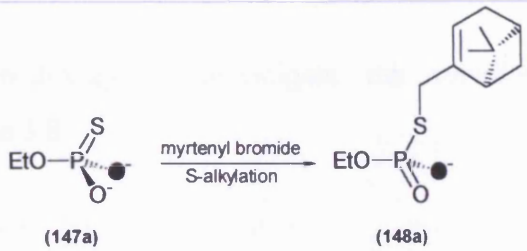

(147a) (148a)

Scheme 3.6 Derivatisation of sulphur by myrtenyl bromide.

Derivatising the diastereotopic oxygen atoms of the diester **(148a)** gave a pair of diastereoisomers **(149a)** and **(149b),** Scheme 3.7.

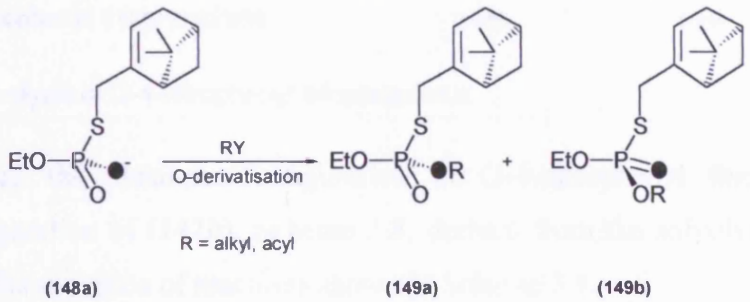

(148a) (149a) (149b)

Scheme 3.7 O-Derivatisation.

The incorporation of the unlabelled triesters **(149c)** and **(149d)** allows the diastereoisomers **(149a)** and **(149b)** to be distinguished on the basis of ^{18}O isotopic shifts seen in their ^{31}P NMR spectrum. In one diastereoisomer **(149a)** the ^{18}O appears in the bridging position while in the other diastereoisomer **(149b)** it appears in the non-bridging position, Figure 3.3. The isotopic shift patterns represent diastereoisomers synthesised from Rp [^{16}O, ^{18}O] ethyl thiophosphate.

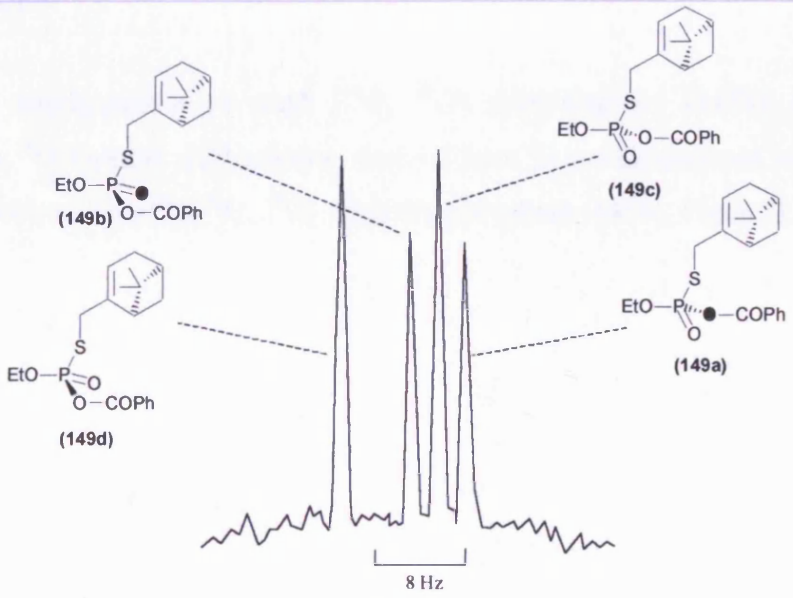

Fig. 3.3 Isotopic shifts seen in the ^{31}P NMR of diastereoisomers **(149a)** and **(149b)** synthesised from Rp [^{16}O, ^{18}O] ethyl thiophosphate.

Cullis used this methodology to investigate the solvolysis of O-4-nitrophenyl thiophosphate,[139] Scheme 3.8.

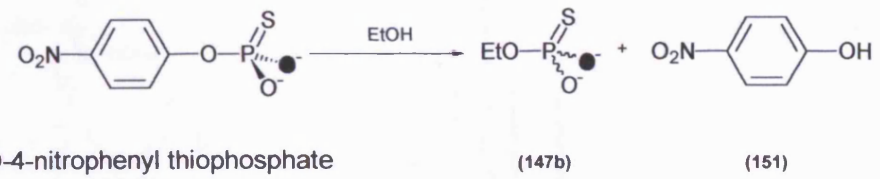

O-4-nitrophenyl thiophosphate (147b) (151)

Scheme 3.8 Solvolysis of O-4-nitrophenyl thiophosphate.

Having assigned the absolute configuration of O-4-nitrophenyl thiophosphate, the unknown configuration of **(147b)**, Scheme 3.8, derived from the solvolysis reaction was determined by the sequence of reactions shown in Scheme 3.9.

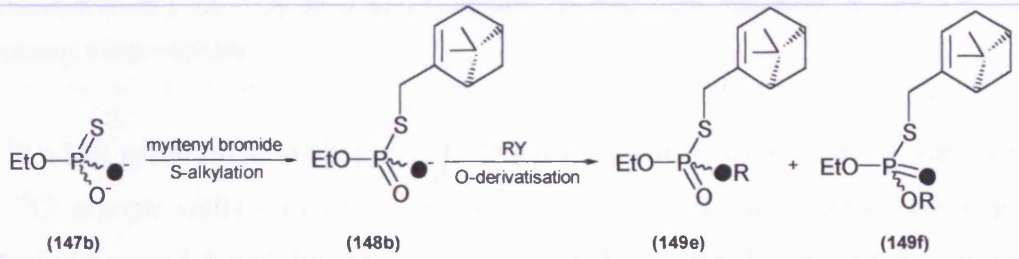

(147b) (148b) (149e) (149f)

Scheme. 3.9 Configurational analysis of [^{16}O, ^{18}O] ethyl thiophosphate derived from the solvolysis reaction.

The absolute configuration of ethyl [^{16}O, ^{18}O] thiophosphate **(147b)** is derived by comparing the ^{18}O isotopic shift patterns derived from its configurational analysis, Figure 3.4, to those derived from Rp[^{16}O, ^{18}O] ethyl thiophosphate **(147a)**, Figure 3.3.

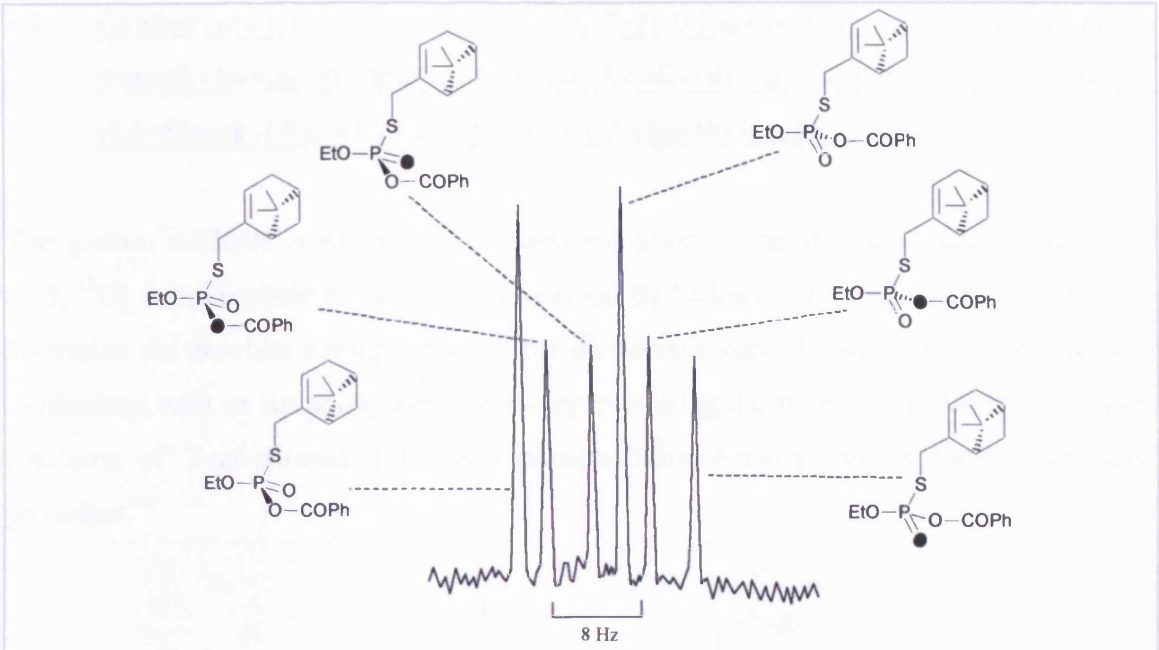

Fig. 3.4 Isotopic shifts seen in the ^{31}P NMR of diastereoisomers **(149e)** and **(149f)** synthesised from [^{16}O, ^{18}O] ethyl thiophosphate derived from solvolysis of Rp[^{16}O, ^{18}O] 4-nitrophenyl thiophosphate.

The ^{31}P NMR spectrum of **(147b)**, after configurational analysis, Figure 3.4, shows double bond ^{18}O isotopic shifts on both downfield and the upfield unlabelled diastereoisomers. Comparing Figure 3.4 with Figure 3.3, it can be deduced that the product was essentially completely racemic. As the configurational analysis does not depend on the absolute intensities of the peaks but on the relative intensities, the enantiomeric excess in the product can be quantified directly from these relative intensities of the resonances. It can be seen from Figure 3.4 that the intensities of the peaks of the four labelled triesters are virtually the same, therefore, it can conclude that the [^{16}O, ^{18}O] ethyl thiophosphate obtained from the solvolysis reaction was 100% racemic. This means that (Rp) and (Sp)-ethyl [^{16}O, ^{18}O] thiophosphate were produced in equal amounts during the solvolysis reaction.

3.4 Configurational analysis of Rp[^{16}O, ^{18}O] thiophosphoric acid O-[3-benzyl-2-(dimethylamino-methinimino)-4-oxo-3,4-dihydro-pteridin-6-ylmethyl] ester S-(6,6-dimethyl-bicyclo[3.1.1]hept-2-en-2-ylmethyl) ester (112a).

The general methods employed for the determination of the absolute stereochemistry of [^{16}O, ^{18}O] thiophosphate monoesters, developed by Cullis *et al.*, are used in this study to determine the absolute configuration of the diastereoisomer **(112a)**. This compound was synthesised with an Rp phosphorus centre by exploiting the stereocontrolled displacement reactions of 2-substituted 1,3,2-oxazaphospholidine-2-thione which have established precedent.[96]

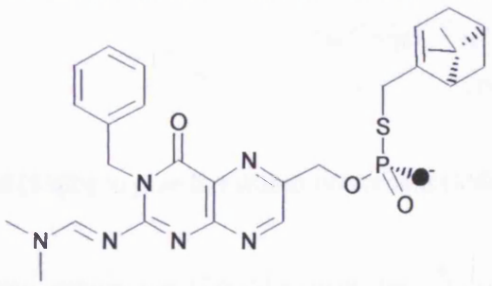

(112a)

A detailed discussion of the synthesis of diastereoisomer **(112a)** is presented in Chapter 2, Section 2.6. The incorporation of the myrtenyl group in this synthesis provides an ideal chiral auxiliary for configurational analysis of the thiophosphates in our study.

The unlabelled thiophosphate diester of **(112a)** was also synthesised as the ^{18}O isotopic shifts in the ^{31}P NMR can only be visualised when a mixture of labelled and unlabelled material is used. The thiophosphate diester **(112a)** has diastereotopic oxygen atoms due to the presence of the two asymmetric centres in the chiral auxiliary.

3.4.1 O-Derivatisation.

Acetylation of the unlabelled diester of **(112a)** with acetyl chloride shifted the ^{31}P NMR resonances downfield. This acetylation gave a pair of diastereoisomers **(150a)** and **(150b)**, Scheme 3.10, which are only distinguishable by ^{31}P NMR (162 MHz), with a diastereoisomeric separation of 4.3 Hz.

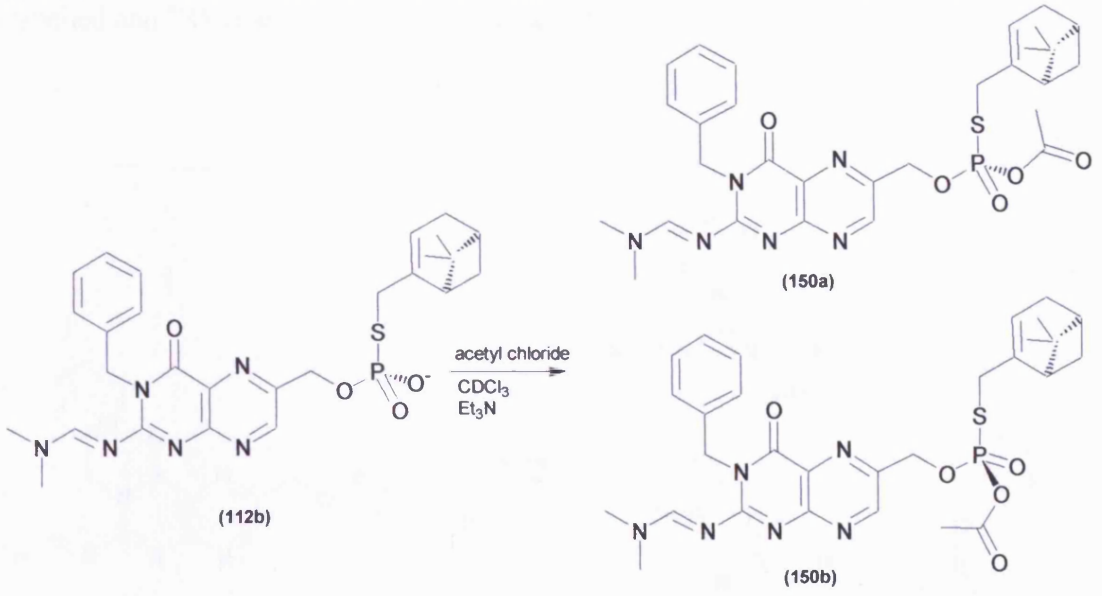

Scheme 3.10 Acetylation of **(112b)** to give the diastereoisomers **(150a)** and **(150b)**.

Ideally, the diastereoisomeric separation should exceed the ^{18}O double bond isotopic shift, (ca. 7.8 Hz at 162 MHz for phosphates of this type) in order to make NMR interpretation straightforward and unambiguous when labelled thiophosphates are taken through the analysis sequence.

Various O-derivatising compounds were used, Table 3.1, in order to find the system that gave the greatest separation of diastereoisomers.

O-Derivatising group	Diastereoisomeric separation (Hz)
Isobutyryl	6
Acetyl	4
Benzoyl	3
Diphenylmethyl	3

Table 3.1

At this stage it is impossible to assign the absolute configurations of **(150a)** and **(150b)**. Having established the conditions for the configurational analysis of unlabelled

diastereoisomers **(150a)** and **(150b)**, the next step was to apply it to a 3:2 mixture of unlabelled and ^{18}O-labelled material, Scheme 3.11.

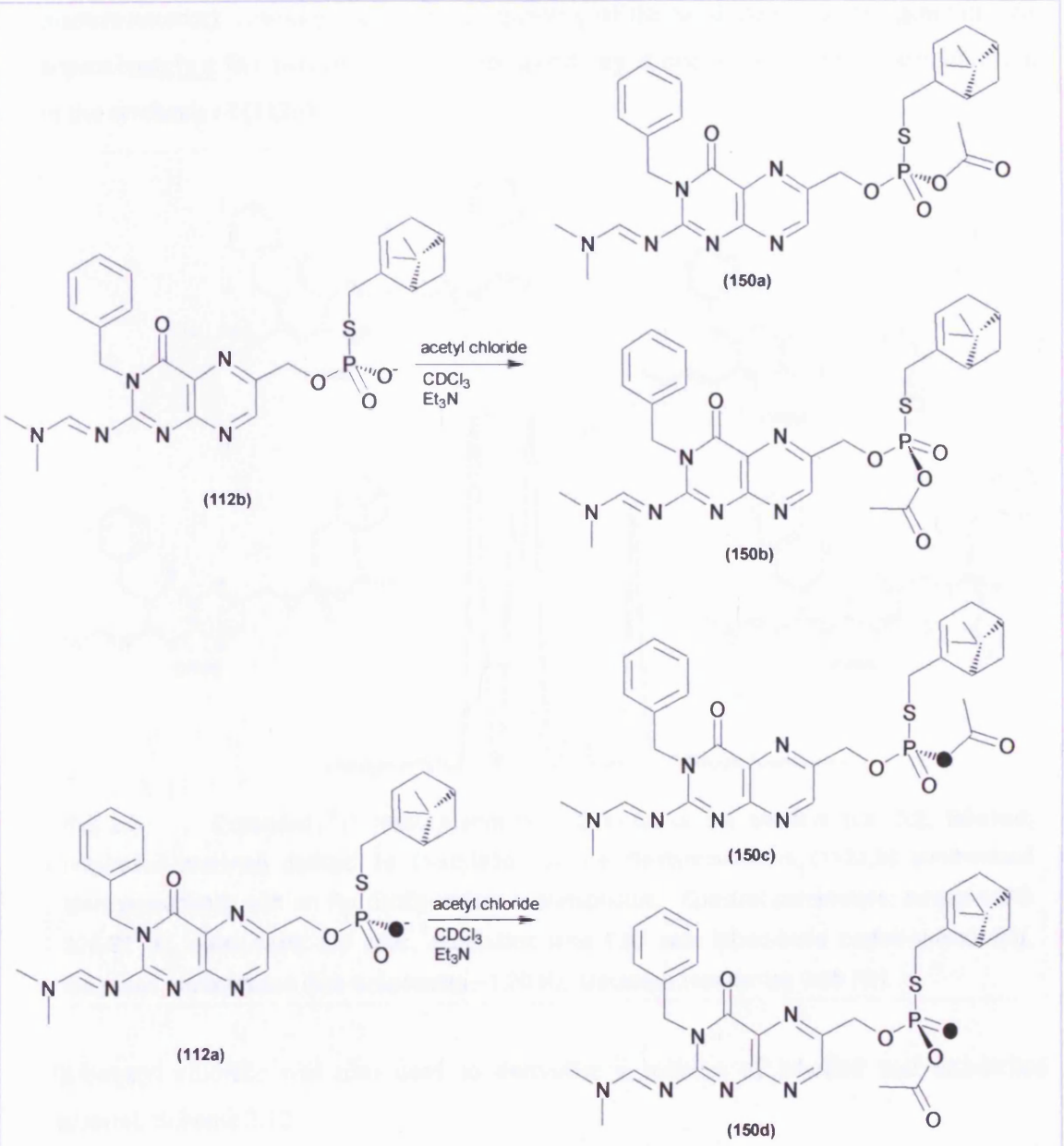

Scheme 3.11 Acetylation of **(112a,b)** to give a 3:2 mixture of triesters **(150a,b)** and **(150c,d)**.

The ^{31}P NMR spectrum shown in Figure 3.5 illustrates the configurational analysis of **(112a)** using an acetyl O-derivatising group. Since the absolute configuration follows from synthesis, the absolute configurations of **(150a)** and **(150b)** can be assigned on the basis of the observation of a single bond ^{18}O isotopic shift on the downfield diastereoisomer and a double bond ^{18}O isotopic shift on the upfield diastereoisomer. Therefore the downfield isomer has the Sp configuration and the upfield isomer has the Rp

configuration. The assignments are shown in Figure 3.5. The unassigned peak is most reasonably attributed to ^{18}O isotopic shifts (i.e. a double bond isotopic shift from the downfield diastereoisomer and a single bond isotopic shift from the upfield diastereoisomer) resulting from a small quantity of the Sp diastereoisomer generated by approximately a five percent loss of stereospecificity at one or more of the steps involved in the synthesis of **(112a)**.

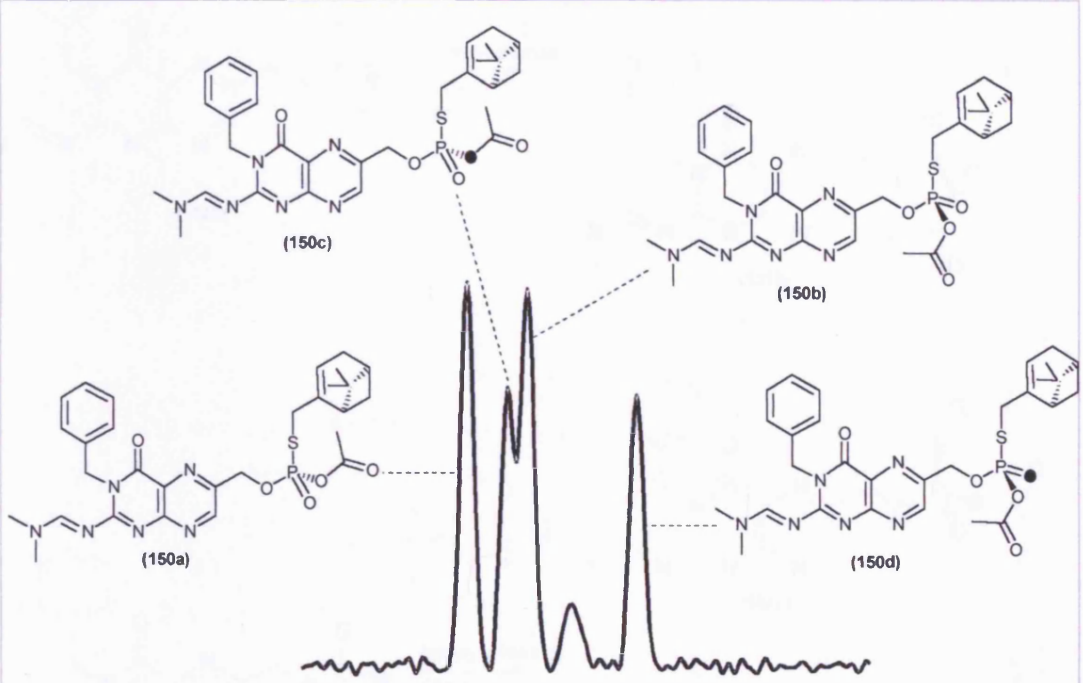

Fig. 3.5 Expanded ^{31}P NMR spectrum (162 MHz) of the triesters (ca. 3:2, labelled; unlabelled material) derived by O-acylation of the diastereoisomers **(112a,b)** synthesised stereospecifically with an Rp configuration at phosphorus. Spectral parameters: sweep width 325.52 Hz, pulse width 6.0 μsec, acquisition time 1.57 sec, broad-band proton decoupling, Gaussian multiplication (line-broadening –1.20 Hz, Gaussian broadening 0.55 Hz).

Isobutyryl chloride was also used to derivatise a mixture of labelled and unlabelled material, Scheme 3.12.

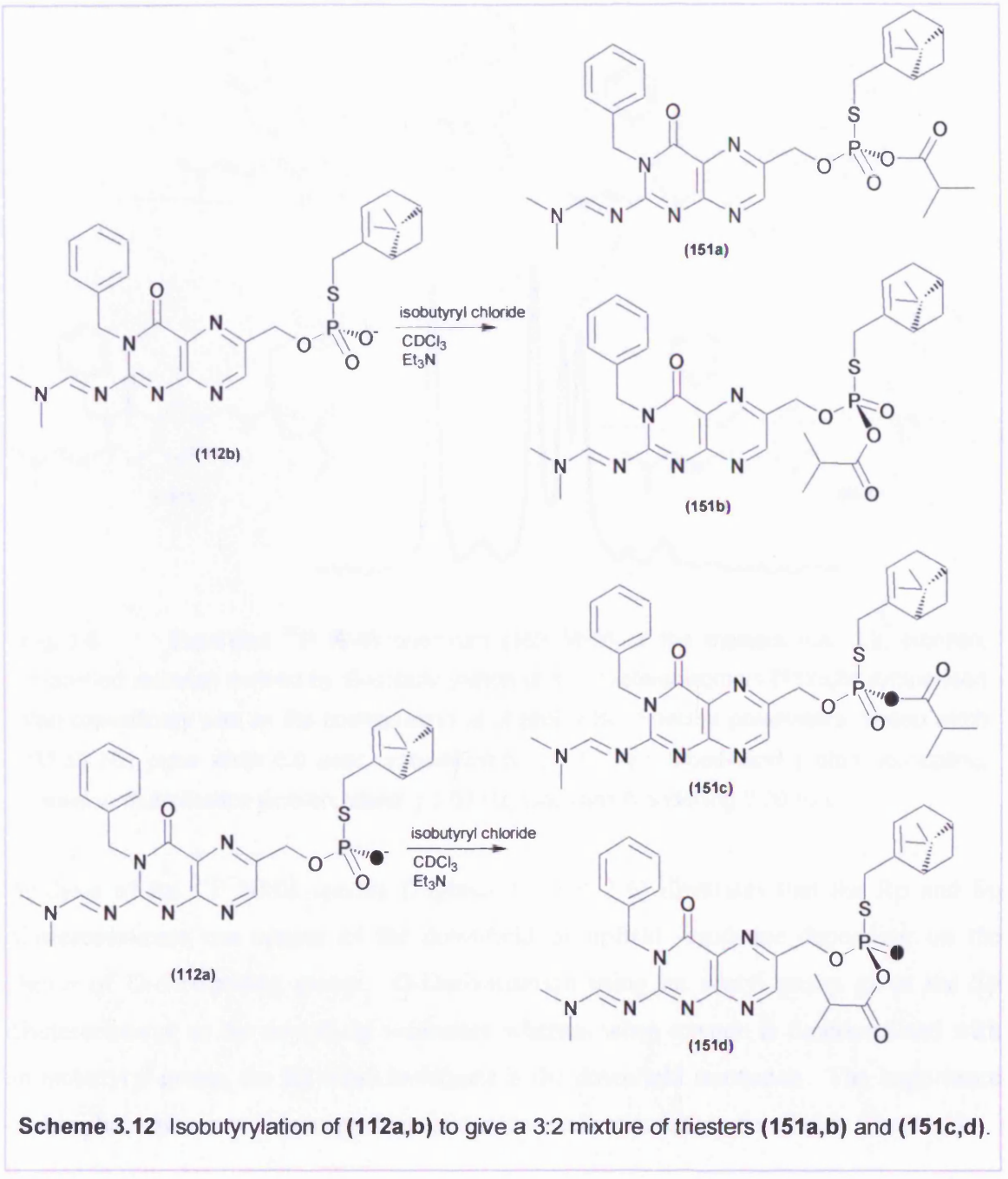

Scheme 3.12 Isobutyrylation of **(112a,b)** to give a 3:2 mixture of triesters **(151a,b)** and **(151c,d)**.

The ^{31}P NMR spectrum shown in Figure 3.6 illustrates the configurational analysis of **(112a)** using an isobutyryl O-derivatising group. Since the absolute configuration follows from synthesis, the absolute configurations of **(151a)** and **(151b)** can be assigned on the basis of the observation of a double bond ^{18}O isotopic shift on the downfield diastereoisomer and a single bond ^{18}O shift on the upfield diastereoisomer. Therefore, the downfield isomer has the Rp configuration and the upfield isomer has the Sp configuration. The assignments are shown in Figure 3.6.

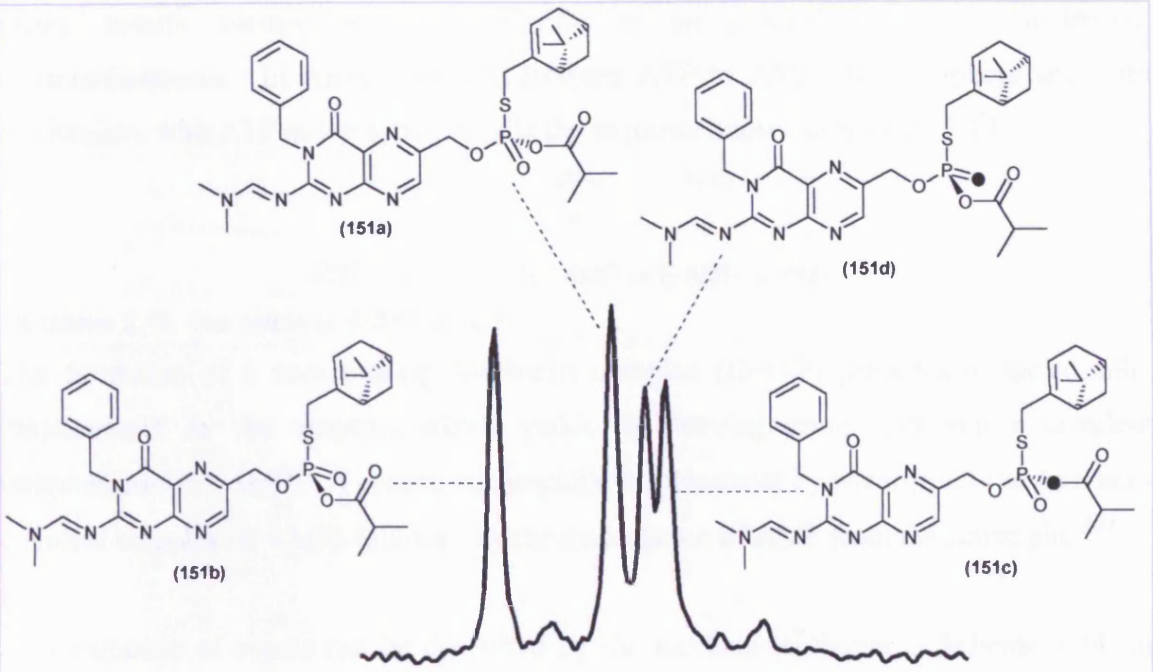

Fig. 3.6 Expanded ^{31}P NMR spectrum (162 MHz) of the triesters (ca. 3:2, labelled; unlabelled material) derived by O-isobutyrylation of the diastereoisomers **(112a,b)** synthesised stereospecifically with an Rp configuration at phosphorus. Spectral parameters: sweep width 325.52 Hz, pulse width 6.0 μsec, acquisition time 1.57 sec, broad-band proton decoupling, Gaussian multiplication (line-broadening 0.00 Hz, Gaussian broadening 0.00 Hz).

Analysis of the ^{31}P NMR spectra (Figures 3.5 and 3.6) illustrates that the Rp and Sp diastereoisomers can appear as the downfield or upfield resonance depending on the choice of O-derivatising group. O-Derivatisation using an acetyl group gives the Sp diastereoisomer as the downfield resonance whereas when oxygen is functionalised with an isobutyryl group, the Rp diastereoisomer is the downfield resonance. The importance of this phenomenon will become clear in our stereochemical study detailed in Chapter 4.

3.5 Configurational analysis of the diastereoisomers of ADPαS using snake venom phosphodiesterase.

3.5.1 Introduction.

5'-Nucleotide phosphodiesterases, catalyse the hydrolysis of 5'-nucleotide-containing phosphodiesters or phosphoanhydrides and yield a 5'-nucleotide as one of the products.[140]

Snake venom phosphodiesterase (SVPD) is an example of a 5'-nucleotide phosphodiesterase. In water SVPD hydrolyses ATP to AMP and pyrophosphate. Its mechanism, with ATP as the substrate, fits the sequence shown in Scheme 3.13.

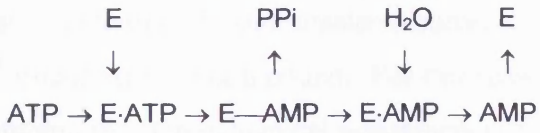

Scheme 3.13 The action of SVPD on ATP.

The formation of a non-covalent Michaelis complex (E·ATP) precedes a nucleophilic displacement by the enzyme, which yields the leaving group PPi and a covalent intermediate (E—AMP). A second nucleophilic displacement by water gives rise to a non-covalent complex (E·AMP) followed by the dissociation of AMP from the active site.[140]

This sequence of events can be described by the mechanism shown in Scheme 3.14, in which a threonine residue in the active centre has been identified as the site of 5'-nucleotide attachment.

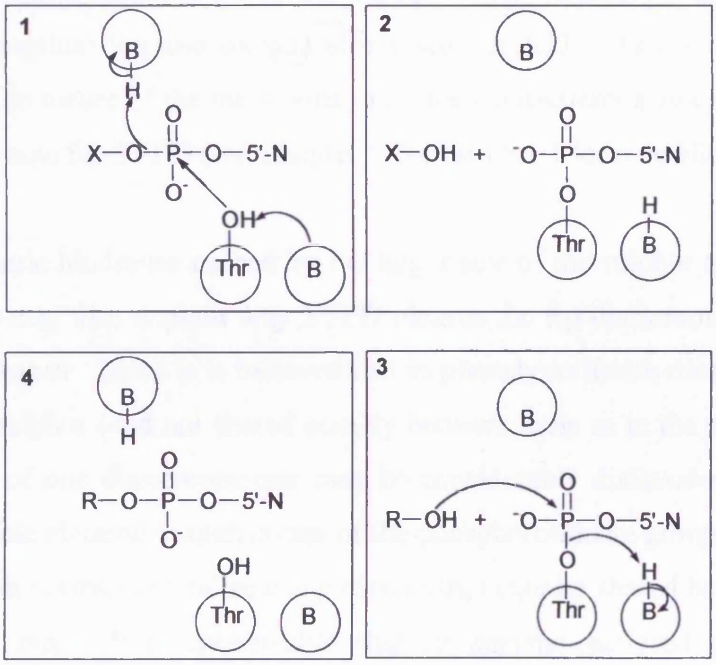

Scheme 3.14 Mechanism for the solvolysis of substrates by SVPD. Reaction of a nucleophilic solvent (R-OH) with a general type substrate (X-O-PO_2-O-5'-N). R-OH may be an alcohol or water, X-O- and alkyl or (oligo)phosphoryl group, and 5'-N is adenosine. Thr-OH is the threonine lateral chain with which the covalent intermediate is formed.[141] B/B-H are acid-base groups that facilitate the leaving of X-O- and the nucleophilic attack by R-OH; their number, disposition and mode of participation are hypothetical.[140]

3.5.2 Diastereoselectivity of SVPD for phosphorothioate esters and anhydrides.

SVPD is known to cleave preferentially one diastereoisomer of phosphorothioate esters and anhydrides,[140,142-144] usually the Rp compound. For this reason it has been used as an analytical tool for determining the stereochemical assignments of these compounds at their chiral phosphoryl centres.

The usual method for the detection of digestion products produced by the selective hydrolysis of the Rp diastereoisomer of a phosphorothioate ester or anhydride is by HPLC analysis. It is usual that the Sp diastereoisomer is not hydrolysed, so there are no detectable digestion products, and the distinction between Sp and Rp diastereoisomers is clear.

Crystal structure data suggests that the Sp diastereoisomer is subject to a forced magnesium ion-sulphur interaction whereas the Rp diastereoisomer retains the interactions between the magnesium ion and oxygen atoms seen in ATP. As a consequence of the oxophilic/thiophilic nature of the metal ions, only the Rp diastereoisomer will be expected to be a good substrate for SVPD (see Chapter 5, Section 5.1.1 for a detailed explanation).

In addition the steric hindrance caused by the larger size of the sulphur atom compared to the oxygen atom may also explain why SVPD cleaves the Rp diastereoisomer faster than the Sp diastereoisomer. Since it is believed that in phosphorothioate diesters the charge is localised on the sulphur (and not shared equally between them as in the case of phosphate diester), binding of one diastereoisomer may be considerably disfavoured over the other due to unfavourable electronic interactions of the phosphorothioate group in the active site with groups which normally stabilise a negative charge equally shared between two atoms at a prochiral centre. It is conceivable that an enzyme-catalysed protonation of a phosphate oxygen necessary for catalysis of the cleavage reaction (see Scheme 3.14) may not be able to occur for one diastereoisomer.

3.5.3 Aims and predictions.

For the HPPK catalysed pyrophosphorylation of 6-hydroxymethyl-7,8-dihydropterin utilising a single epimer ATPβS to form a specific enantiomer of 6-hydroxymethyl-7,8-dihydropterin pyrophosphorothioate, there was the potential application of SVPD to determine the identity of the reaction products. As with other 5'-nucleotide-containing phosphoanhydrides it was expected that the Rp isomer of 6-hydroxymethyl-7,8-dihydropterin pyrophosphorothioate would be a substrate for the SVPD and give digestion products identifiable by HPLC, but the Sp isomer of 6-hydroxymethyl-7,8-dihydropterin pyrophosphorothioate would not.

To confirm the diastereoselectivity of SVPD, it was necessary to perform a model study using racemic ADPαS **(97)** (which closely resembles 6-hydroxymethyl-7,8-dihydropterin pyrophosphorothioate), as a substrate for the enzyme. Analysis of this competitive study by HPLC was expected to show that the rate of hydrolysis of the Rp isomer of ADPαS was significantly faster than for the Sp isomer. The expected hydrolysis products were AMPαS **(93)** and, after slow desulphurisation, AMP **(90)**, Scheme 3.15.

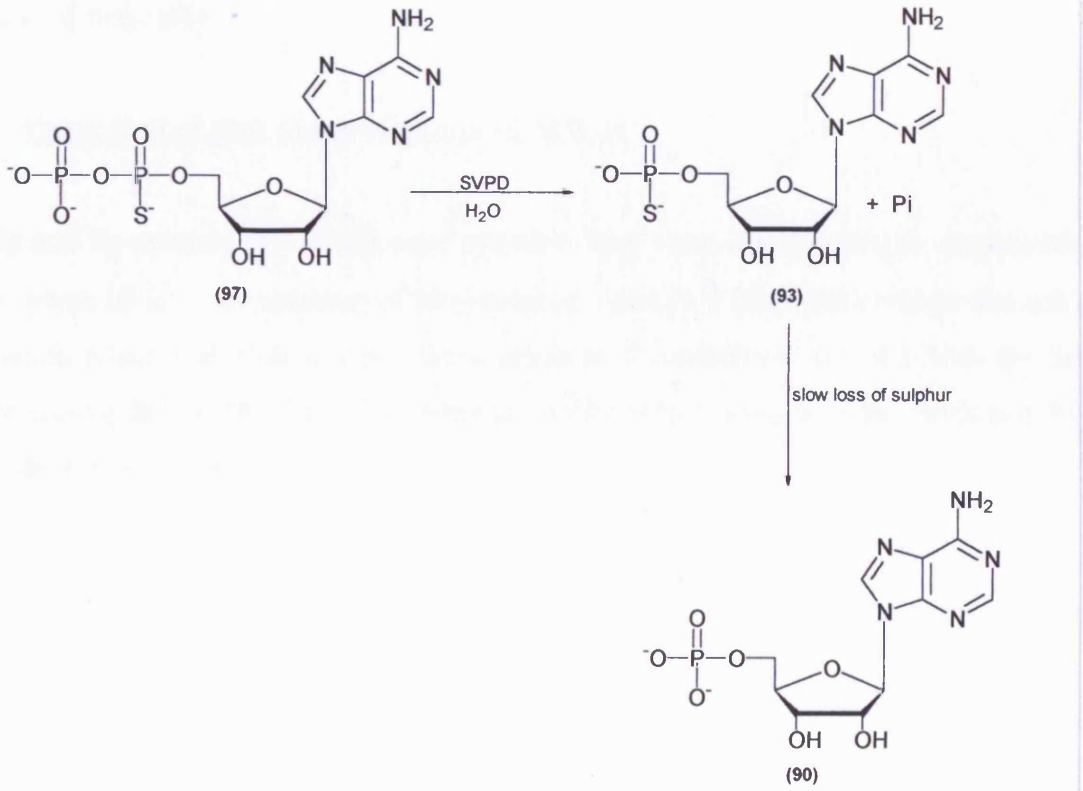

Scheme 3.15 Proposed hydrolysis of ADPβS by SVPD.

3.5.4 Preparation of racemic adenosine 5`-O-(-1-thiodiphosphate), (ADPαS) (97).

Hexokinase was used to degrade a racemic mixture of ATPαS **(41)** to racemic ADPαS **(97)**, Scheme 3.16. Standard reaction conditions for the hexokinase catalysed reaction were used and aliquots were removed at intervals for analysis by HPLC to monitor the reaction.

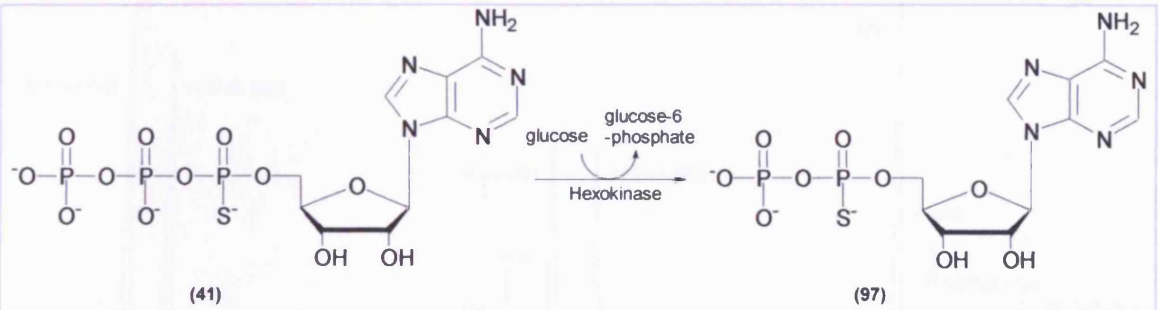

Scheme 3.16 Hexokinase catalysed degradation of ATPαS to ADPαS.

After 4 hours ADPαS **(97)** was purified by anion-exchange chromatography, eluting from the column in a position that was indicative of a compound with three negative charges in a 56% yield from **(41)**.

3.5.5 Preparation of pure diastereoisomers of ADPαS.

The Rp and Sp epimers of ADPαS were prepared from a racemic mixture by preparative reverse phase HPLC. A maximum of 60 μmoles of racemic ADPαS **(41)** was loaded onto the column which was eluted with a linear gradient of acetonitrile in water with the Sp epimer eluting before the Rp. The isomeric purity of the samples was confirmed by analytical reverse phase HPLC.

3.5.6 Snake venom phosphodiesterase hydrolysis of a racemic mixture of ADPαS.

The diastereoisomers of ADPαS were hydrolysed with snake venom phosphodiesterase. Standard reaction conditions were used for the snake venom catalysed reaction. The reaction was incubated at 37°C for 15 hours. Aliquots were removed every 1 hour for analysis by HPLC, Figure 3.7.

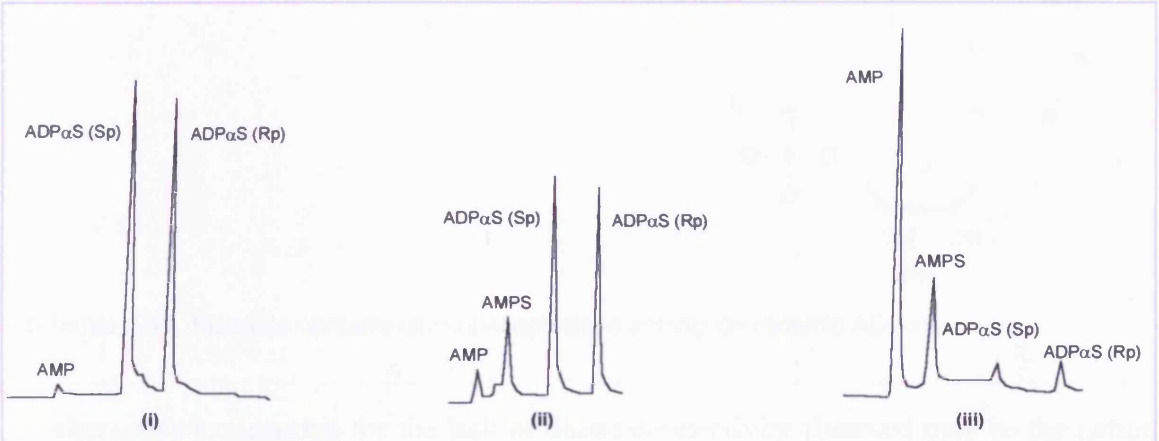

Fig. 3.7 Time course of the SVPD hydrolysis of a racemic mixture of ADPαS monitored by HPLC. After 0 minutes (i) both diastereoisomers are present in approximate equal amounts. After 20 hours (ii) a significant amount of the hydrolysis product, AMPS is present, with both diastereoisomers being hydrolysed at equal rates. After 50 hours (iii) both diastereoisomers have been almost completely hydrolysed.

The identity of peaks on the HPLC traces were confirmed by co-elution with pure samples of AMP, AMPαS, ADPαS (Sp) and ADPαS (Rp). The large amount of AMP detected is due to the slow desulphurisation of AMPαS as illustrated in Scheme 3.15.

It is apparent that the Rp and Sp diastereoisomers of ADPαS are hydrolysed by SVPD at the same rate. This result was unexpected and contrary to the diastereoselectivity observed in many literature studies. A possible explanation for these findings is the presence of phosphatase enzyme contaminating the SVPD sample. The action of phosphatase on racemic ADPαS, Scheme 3.17, is without diastereoselectivity and would result in the hydrolysis of both isomers at the same rate.

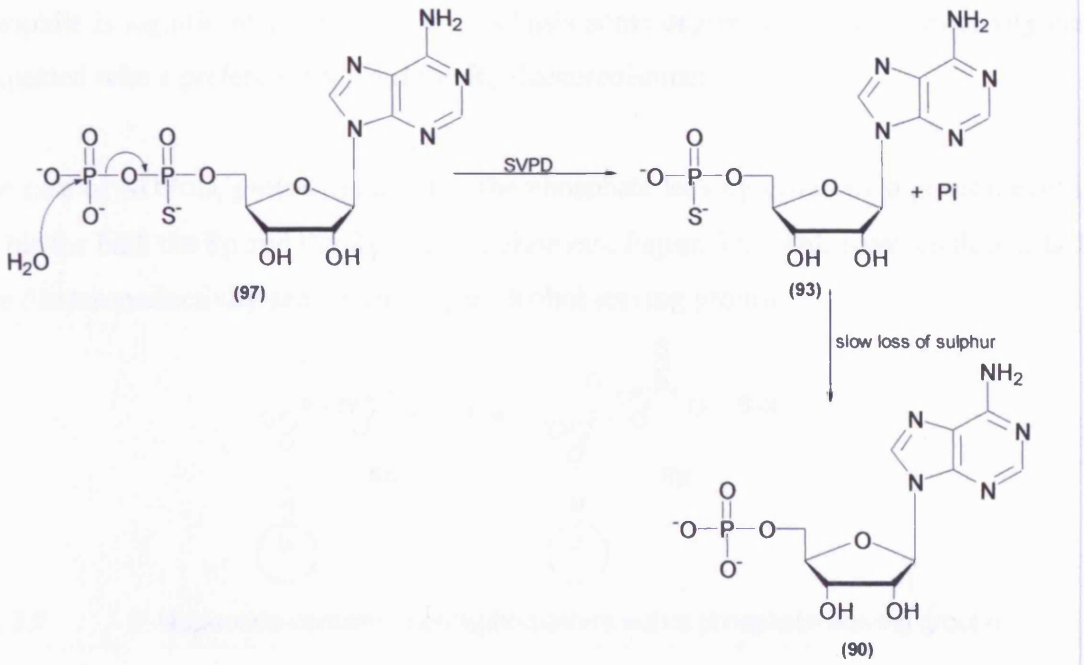

Scheme 3.17 Possible contaminating phosphatase activity on racemic ADPαS.

An alternative explanation for the lack of diastereoselectivity observed may be the nature of the leaving group. Previous stereochemical studies using SVPD hydrolysis and esterification (where an alcohol is the acceptor for enzyme-bound AMP instead of water) reactions,[142,144] to determine stereochemistry at a phosphoryl centre have used 5'-nucleotide-containing phosphodiesters or phosphoanhydrides substrates with simple alcohols as leaving groups, Figure 3.8.

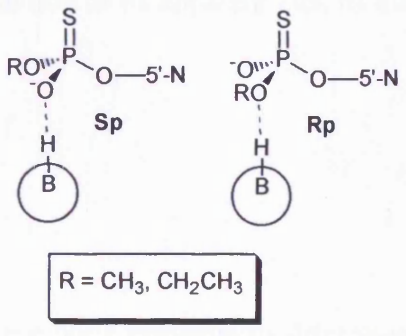

Fig. 3.8 5'-Nucleotide-containing phosphodiesters with simple alcohols as leaving groups.

The simple alcohol leaving group of the Rp diastereoisomer is orientated to coordinate with a proton donated by an acidic amino acid residue at the enzyme active site. This proton donation facilitates the leaving of RO^- and the attack of a nucleophile. As a consequence of the spatial arrangement of the Sp diastereoisomer at the enzyme active site the leaving group is not protonated, and as a result, its displacement by an attacking

nucleophile is significantly slower. On this basis some degree of diastereoselectivity can be expected with a preference toward the Rp diastereoisomer.

In the case of ADPαS, proton donation to the phosphate leaving group by a general acid is possible for both the Sp and the Rp diastereoisomers, Figure 3.9. This may result in a lack of the diastereoselectivity seen with simple alcohol leaving groups.

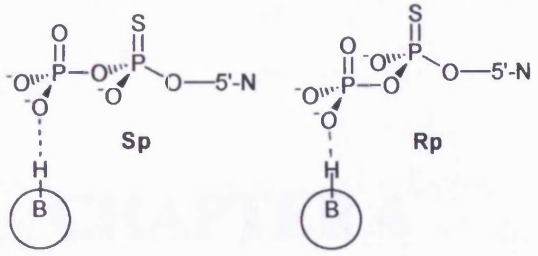

Fig. 3.9 5'-Nucleotide-containing phosphodiesters with a phosphate leaving groups.

The lack of diastereoselectivity observed can also be rationalised by considering that the rate-limiting step for the SVPD reaction is not the chemical step. Although the constraints imposed by the active site that determine diastereoselectivity would still occur, they would only have a nominal affect on the overall rate of reaction resulting in no observable difference in reaction rate between ADPαS (Rp) or ADPαS (Sp).

The application of SVPD to determine the stereochemical course of the HPPK catalysed reaction was judged unsuitable due to its apparent lack of diastereoselectivity towards our model ADPαS system.

3.6 Conclusion.

We have seen the variety of methods available to determine the absolute stereochemical configuration of [^{16}O, ^{18}O] phosphate monoesters and [^{16}O, ^{18}O] thiophosphate monoesters by combining the use of chiral auxiliaries with powerful spectroscopic techniques. The configurational analysis of **(112a)** by a previously established route and an investigation into the diastereospecificity of SVPD has been achieved.

CHAPTER 4
Stereochemical Course of the HPPK Catalysed Pyrophosphorylation of 6-Hydroxymethyl-7,8-Dihydropterin

4.1 Introduction.

The results of the many stereochemical studies of enzyme-catalysed phosphoryl[28,145] and thiophosphoryl[128,129] transfer reactions, have shown that these reactions are stereospecific. The majority proceed with inversion and a few with retention of configuration of the transferred phosphoryl (or thiophosphoryl) moiety (Chapter 1, Table 1.4).

The simplest interpretation of inversion of configuration is that the displacement reaction proceeds by a single associative in-line phosphoryl transfer between two substrates in a ternary complex. However, overall inversion of configuration would also be consistent with a pathway involving an odd number of phosphoryl transfers or even a double displacement entailing an in-line displacement followed by an adjacent displacement (see Chapter 1, Section 1.1). However, there is no firm evidence that supports multiple (>2) phosphoryl transfer reactions or other composite pathways for simple phosphokinases. Where retention of configuration is found, it is considered that a double displacement (*via* two consecutive inversions of configuration) occurs, suggesting that the enzyme utilizes a covalent phosphoenzyme intermediate.

This evidence would not rigorously prove the involvement of a phosphoryl-enzyme intermediate, since adjacent attack by a nucleophile followed by a pseudorotation and elimination of the leaving group from the apical position would also give retention of configuration at phosphorus, (see Chapter 1, Section 1.1). There is also the remote possibility that the reaction may involve more than one phosphoryl-enzyme intermediate.

There are no precedents for enzyme-catalysed phosphoryl transfer reactions occurring *via* a mechanism involving pseudorotation. Furthermore, it is not clear what catalytic advantage would be gained from multiple phosphoryl transfer steps. When thiophosphates are used as P-chiral substitutes of ATP there is also the possibility that they may react *via* an alternative mechanism. This would seem unlikely as previous studies, (Chapter 1, Table 1.4), have demonstrated that thiophosphates react *via* an analogous mechanism to their natural substrate counterparts in a wide range of enzymes.[99,146]

4.2 Aims.

HPPK catalyses the magnesium-dependent pyrophosphorylation of 6-hydroxymethyl-7,8-dihydropterin **(46)** by a substitution reaction at the β-phosphorus atom of ATP **(38c)** to form 6-hydroxymethyl-7, 8-dihydropterin pyrophosphate **(47a)**, Scheme 4.1.

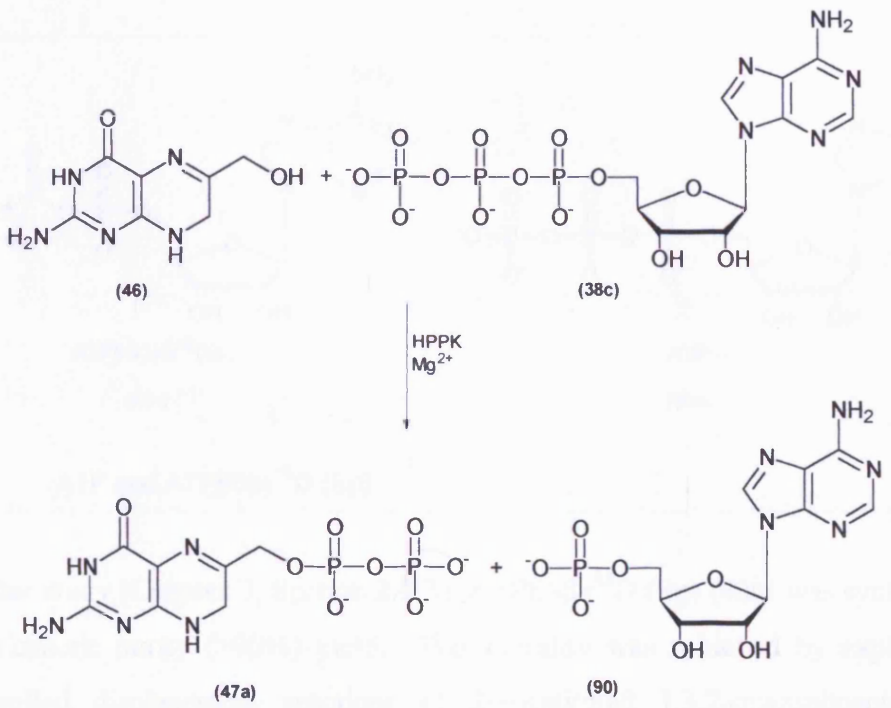

Scheme 4.1 Pyrophosphorylation catalysed by HPPK.

Despite the availability of high-resolution crystal structure of the *E.coli*[69,76,77] and recombinant *Haemophilus influenzae* enzymes,[52] details of the mechanism of the pyrophosphoryl transfer remain to be established. Our aim was to investigate the stereochemical course of the HPPK catalysed reaction by substituting ATP for an analogue that is chiral at the β-phosphoryl centre. The determination of whether the configuration at this centre is inverted or retained as a result of nucleophilic substitution will allow us to distinguish between a single associative in-line pyrophosphoryl transfer and a double displacement (*via* two consecutive inversions of configuration) suggesting that the enzyme utilizes a covalent phosphoenzyme intermediate.

4.3 Strategy.

There is no chirality at the phosphorus centres of naturally occurring ATP **(38c)** (see Chapter 1, Section 1.3), therefore, in order to investigate the stereochemical course of the HPPK catalysed reaction our first objective was to substitute ATP for the isotopically labelled chiral thiophosphate analogue, ATPβSβγ^{18}O (Sp) **(42c)** Figure 4.1.

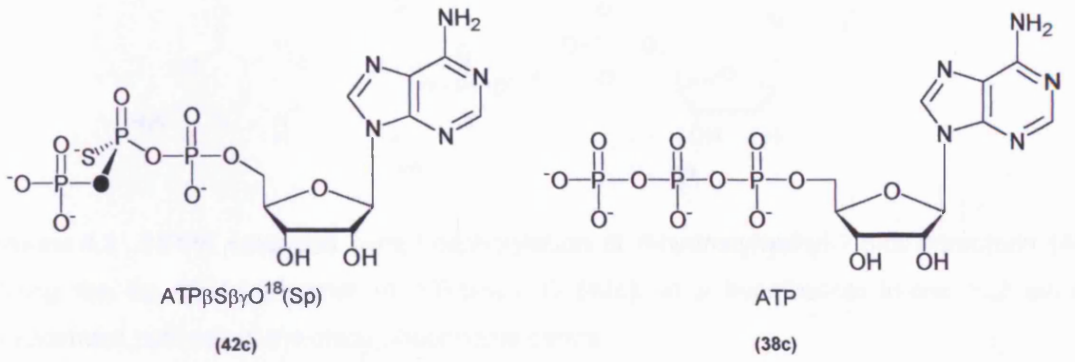

Fig. 4.1 ATP and ATPβSβγ^{18}O (Sp).

In our earlier study (Chapter 2, Section 2.7.3), ATPβSβγ^{18}O (Sp) **(42c)** was synthesised in high enantiomeric purity (>90%) yield. This chirality was achieved by exploiting the stereocontrolled displacement reactions of 2-substituted 1,3,2-oxazaphospholidine-2-thiones which have established precedent.[96] The substitution of ATPβSβγ^{18}O (Sp) **(42c)** for ATP **(38c)** (as the pyrophosphate donor in the HPPK catalysed reaction) has the consequence of introducing an ^{18}O-label into the enantiomeric thiopyrophosphorylated pterin product **(47b)**. The mechanism for this reaction may proceed *via* a direct in-line S_N2 displacement at the chiral phosphorus centre, Scheme 4.2, resulting in inversion of configuration.

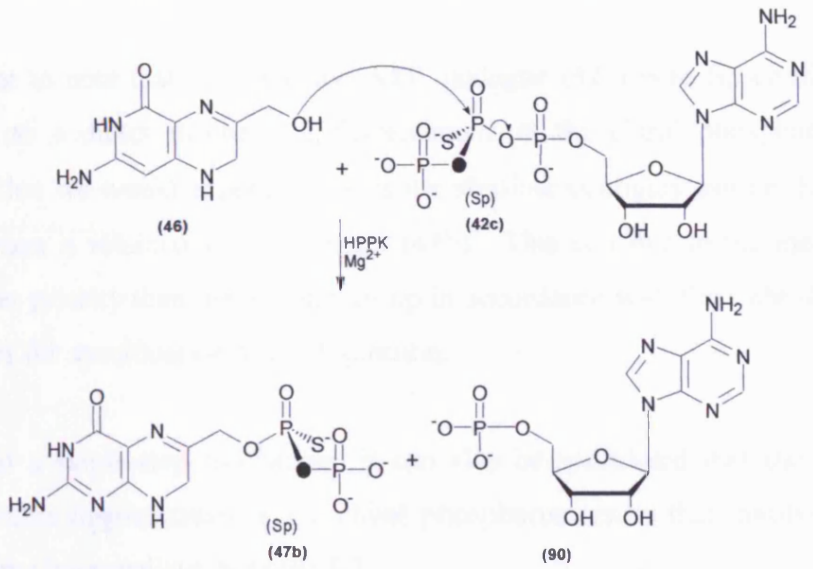

Scheme 4.2 HPPK catalysed pyrophosphorylation of 6-hydroxymethyl-7,8-dihydropterin **(46)** utilising the Sp diastereoisomer of ATPβSβγ^{18}O **(42c)**, in a hypothetical in-line S_N2 single displacement pathway at the chiral phosphorus centre.

The essential feature of this S_N2 mechanism is that the reaction takes place in a single step without intermediates when the hydroxyl group of the pterin attacks the chiral phosphorus centre from a direction directly opposite (180° with respect to) the departing AMP group. This leads to a transition state with a partially formed bond between the pterin hydroxyl group and the β-phosphorus centre and a partially broken bond between the β-phosphorus centre and the departing AMP group, Figure 4.2.

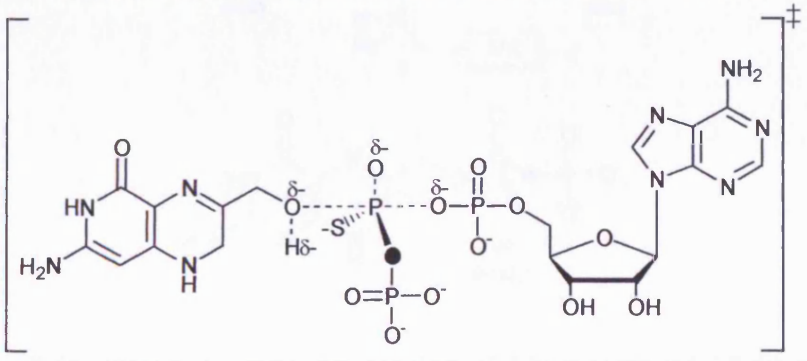

Fig. 4.2 The transition state for an S_N2 displacement reaction at the β-phosphorus centre.

The requirement for back-side attack of the entering pterin hydroxyl group from a direction 180° away from the departing AMP leaving group causes the stereochemistry at the β-phosphorus centre to invert.

It is important to note that although the ATP analogue **(42c)** with Sp configuration has been subject to a direct in-line S_N2 displacement at the chiral phosphorus centre (a mechanisms that we would expect to invert the absolute configuration i.e. Sp → Rp) the Sp configuration is retained in the product **(47b)**. This is a due to the incoming group having a lower priority than the leaving group in accordance with the Cahn-Ingold-Prelog sequence rules for specification of configuration.

In addition to a single-step mechanism it can also be speculated that the enzyme may catalyse a double displacement at the chiral phosphorus centre that involves a covalent phosphoenzyme intermediate, Scheme 4.3.

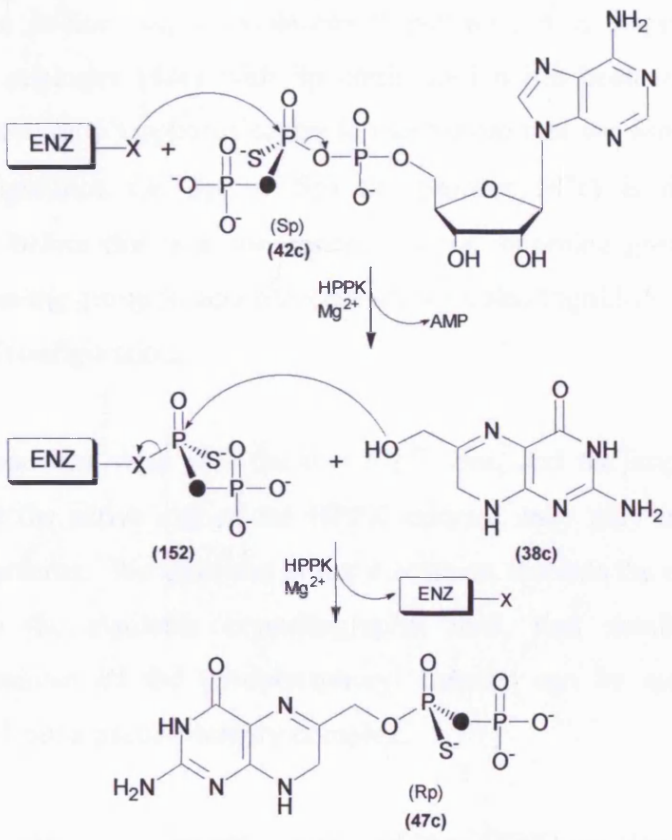

Scheme 4.3 HPPK catalysed pyrophosphorylation of 6-hydroxymethyl-7,8-dihydropterin **(46)** utilising the Sp diastereoisomer of ATPβSβγ^{18}O **(42c)**, in a hypothetical double displacement mechanism (i.e. two consecutive S_N2 displacements at the chiral phosphorus centre) *via* a covalent phosphoenzyme intermediate **(152)**.

The important feature of this mechanism is that there are two in-line S_N2 displacement reactions at the chiral phosphorus centre. The first attack is by a nucleophilic amino acid residue situated at the active site of the enzyme. This forms a covalent phosphoenzyme intermediate in which the absolute configuration at the chiral phosphorus centre is inverted. In a second substitution reaction the hydroxyl group of the pterin attacks the chiral phosphorus centre from a direction directly opposite the departing amino acid residue resulting in a second inversion of configuration at the chiral phosphorus centre. As a result of the two consecutive S_N2 displacement reactions at the chiral phosphorus centre, the configuration is retained in the product **(47c)**. Transition states can be imagined for each of the displacement reactions that, conceptually, are the same as the transition state implied for the single-step reaction; the difference being the identity of the reactants.

Again, as with the in-line single displacement pathway, it is important to note that although the ATP analogue **(42c)** with Sp configuration has been subject to a double displacement at the chiral phosphorus centre (a mechanism that we would expect to retain the absolute configuration i.e. Sp $\rightarrow$ Sp) the product **(47c)** is designated the Rp configuration. As before this is a consequence of the incoming group having a lower priority than the leaving group in accordance with the Cahn-Ingold-Prelog sequence rules for specification of configuration.

It is pertinent to consider what role the two Mg^{2+} ions, and the important amino acid residues located at the active site of the HPPK enzyme, may play in facilitating these hypothetical mechanisms. We shall see in our discussion towards the end of this chapter, with reference to the available crystallographic data, that details concerning the fundamental mechanism of the pyrophosphoryl transfer can be suggested based on observations made from a pseudo-ternary complex.

In order to follow the stereochemical course of the HPPK reaction successfully (and thereby distinguish between the two mechanistic proposals) a configurational analysis is required that can distinguish whether, as a consequence of pyrophosphoryl transfer, we have generated an enantiomer with either the Sp (compound **(47b)**, Scheme 4.2) or Rp (compound **(47c)**, Scheme 4.3) configuration at the chiral phosphorus centre. This

problem was addressed by our earlier configurational analysis of diastereoisomer **(112a)**, Figure 4.3 based on the ^{31}P NMR method (Chapter 3).

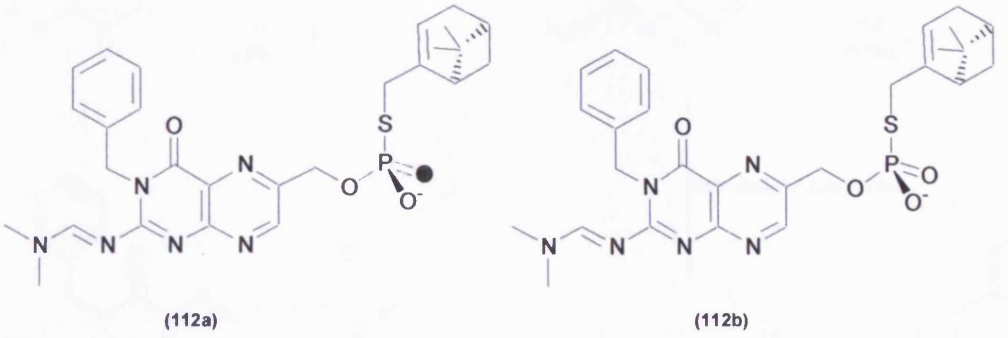

Fig. 4.3

This diastereoisomer **(112a)** was synthesised with an Rp phosphorus centre by exploiting the stereocontrolled displacement reactions of 2-substituted 1,3,2-oxazaphospholidine-2-thione which have established precedent.[96]

A detailed discussion of the synthesis of diastereoisomer **(112a)** is presented in Chapter 2, Section 2.6 and its configurational analysis by O-acetylation is detailed in Chapter 3, Section 3.4. O-Derivatisation of a 3:2 mixture of unlabelled and labelled diastereoisomers of **(112a)** using acetyl chloride in the presence of triethylamine, resulted in the formation of a mixture of phosphotriesters distinguishable on the basis of ^{18}O isotopic shifts seen in the ^{31}P NMR spectrum.

Having assigned the absolute configuration of the diastereoisomers of **(112a)** the unknown configuration of **(47b)** derived from the HPPK catalysed reaction, Scheme 4.2, using the isotopically labelled ATP analogue, ATPβSβγ^{18}O **(42c)** can be determined by the sequence of reactions shown in Scheme 4.4. In subsequent synthetic schemes we shall specify that compound **(47b)** has the Sp absolute configuration in continuation from Scheme 4.2. This makes the assumption that the pyrophosphoryl transfer reaction proceeds *via* a direct in-line displacement mechanism; a proposal that is hypothetical at this point in the discussion. This synthesis was first perfected on unlabelled material, starting from ATPβS (Sp) to give the unlabelled phosphodiester **(112b)**, Figure 4.3.

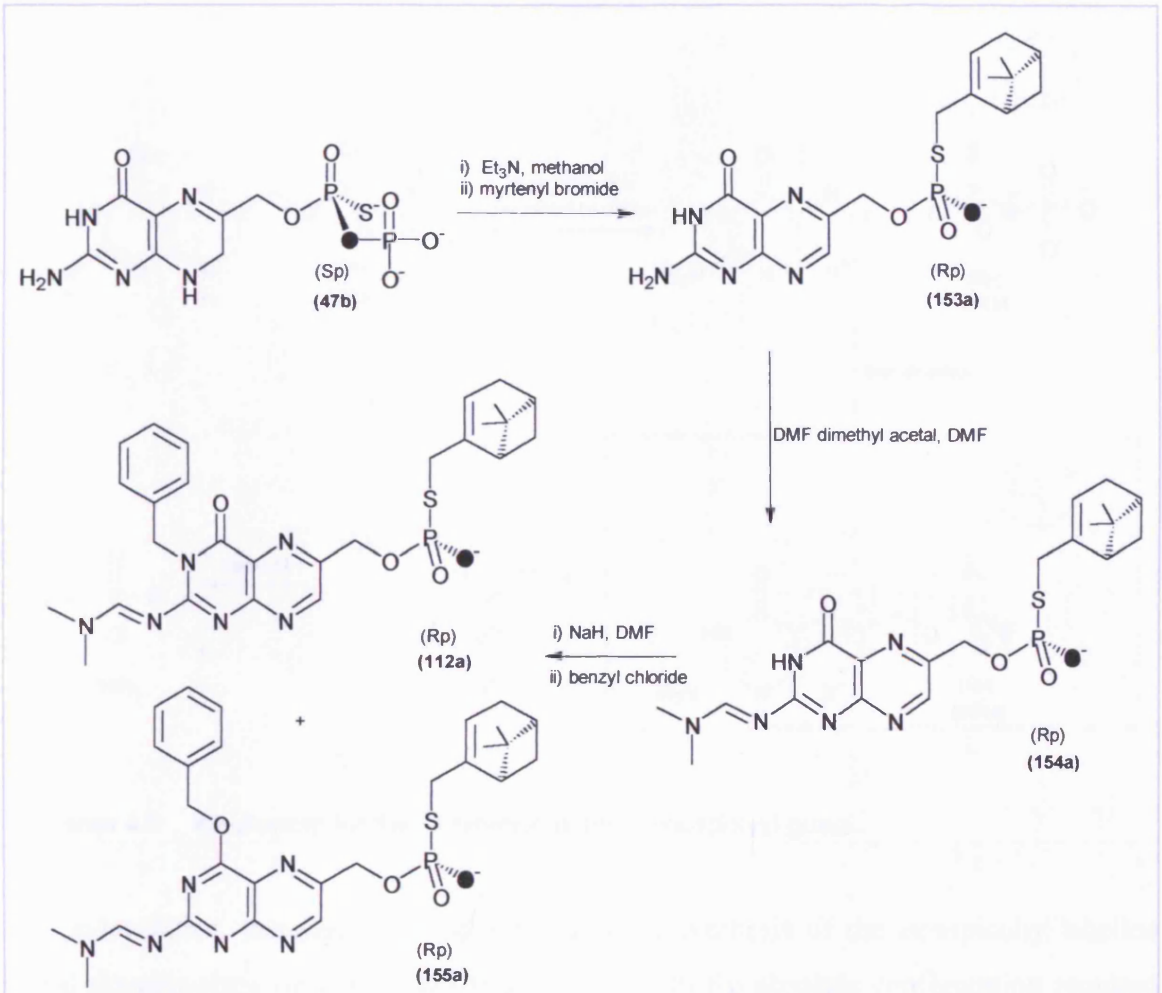

Scheme 4.4 Chemical modification of **(47b)**.

As enantiomers are indistinguishable **(47b)** was made diastereotopic by reaction with the chiral reagent myrtenyl bromide, Scheme 4.4. Derivatisation was found only on the sulphur atom and was accompanied by a large upfield shift in the ^{31}P NMR of the α-phosphorus signal (43.5 → 21.0 p.p.m.) and the spontaneous loss of the β-phosphoryl group. The mechanism for this reaction is believed to involve the elimination of the β-phosphoryl group *via* a dissociative pathway generating monomeric metaphosphate, which is subsequently trapped by the solvent, methanol to form diastereoisomer **(153a)**, Scheme 4.5. This type of reaction has previously been reported and has no effect on the stereochemistry of the α-phosphoryl group, although in accordance with the Cahn-Ingold-Prelog sequence rules for specification of configuration, the α-phosphorus centre is now designated Rp due to the higher priority of ^{18}O over ^{16}O.

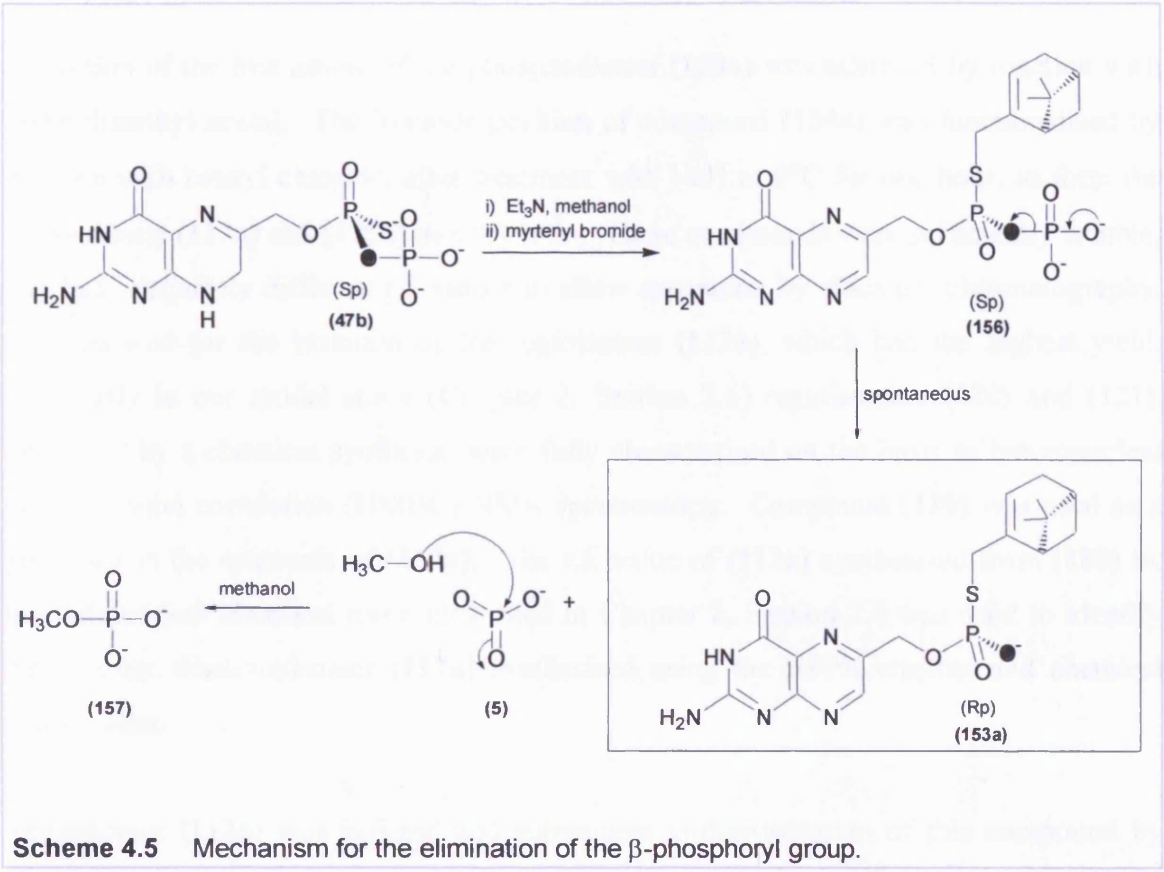

Scheme 4.5 Mechanism for the elimination of the β-phosphoryl group.

The independent, unambiguous and stereospecific synthesis of the isotopically labelled chiral thiophosphate diester **(112a)** (Figure 4.3) with Rp absolute configuration required the use of protecting groups on the pterin substituent. Consequently the diastereoisomer **(112a)** (resulting from the HPPK catalysed reaction and myrtenyl addition) was functionalised with identical protecting groups. Although the ^{31}P NMR configurational analysis method is general for thiophosphate monoesters even a small alteration to the functionality of these compounds can alter the position of the phosphorus resonance. This point was illustrated in Chapter 3, Figures 3.5 and 3.6. It was shown that Rp and Sp diastereoisomers appear as the downfield or upfield resonance depending on the choice of O-derivatising group. O-Derivatisation using an acetyl group gave the Sp diastereoisomer as the downfield resonance whereas when oxygen is functionalised with an isobutyryl group, the Rp diastereoisomer is the downfield resonance. Consequently the compound with unknown absolute configuration was functionalised identically to diastereoisomer **(112a)** synthesised stereospecifically (Figure 4.3) and the configurational analysis was performed with the same O-derivatising group.

Protection of the free amine of the phosphodiester **(153a)** was achieved by reaction with DMF dimethyl acetal. The 3-amide position of compound **(154a)** was functionalised by reaction with benzyl chloride, after treatment with NaH at 0°C for one hour, to form the regioisomers **(112a)** and **(155a)** in a 9:1 ratio. These compounds were sufficiently soluble, and had adequately different r.f. values to allow separation by silica gel chromatography. This allowed for the isolation of the regioisomer **(112a)**, which had the highest yield. Previously in our model study (Chapter 2, Section 2.6) regioisomers **(120)** and **(121)**, generated by a chemical synthesis, were fully characterised on the basis of heteronuclear multiple bond correlation (HMBC) NMR spectroscopy. Compound **(120)** was used as a precursor in the synthesis of **(112a)**. The r.f. value of **(112a)** synthesised from **(120)** by the independent chemical route illustrated in Chapter 2, Section 2.6 was used to identify the required diastereoisomer **(112a)** synthesised using the HPPK enzyme and chemical modification.

Regioisomer **(112a)** was isolated and subsequent O-derivatisation of this compound by acetyl chloride in the presence of triethylamine resulted in the formation of the phosphotriesters **(150a,b,c,d)**, Scheme 4.6.

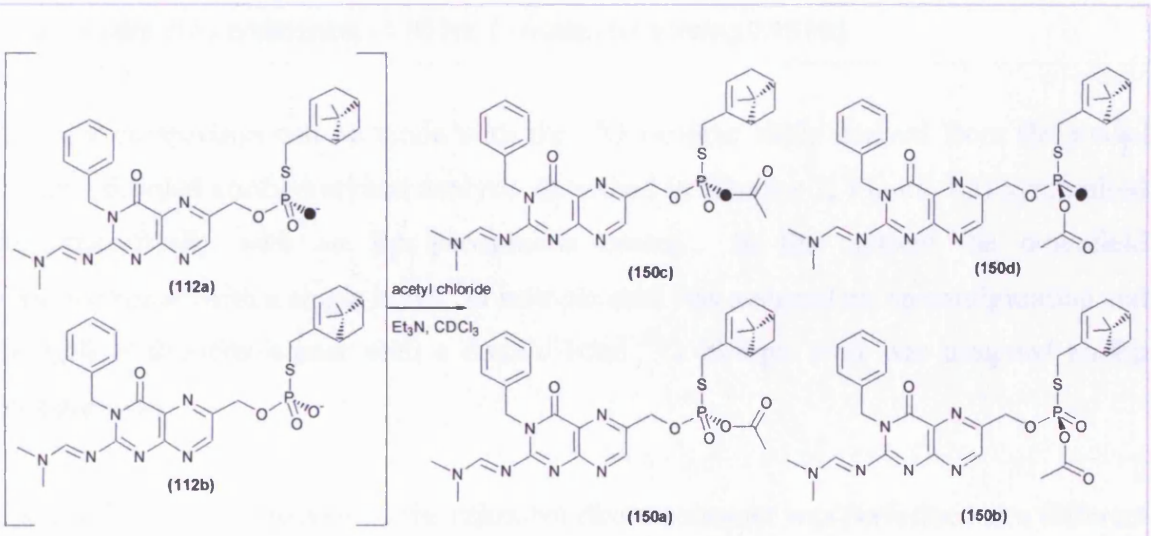

Scheme 4.6 O-Acetylation gave a mixture of four phosphotriesters **(150a,b,c,d)**.

Any attempts to purify the mixture of triesters **(150a,b,c,d)** resulted in their degradation, therefore the reaction was performed in deuterated chloroform to allow *in situ* analysis by ^{31}P NMR. The ^{31}P NMR spectrum of the diastereoisomers of **(112a)** after configurational

analysis, Figure 4.4, shows a single bond ^{18}O isotopic shift on the downfield diastereoisomer and a double bond ^{18}O isotopic shift on the upfield diastereoisomer.

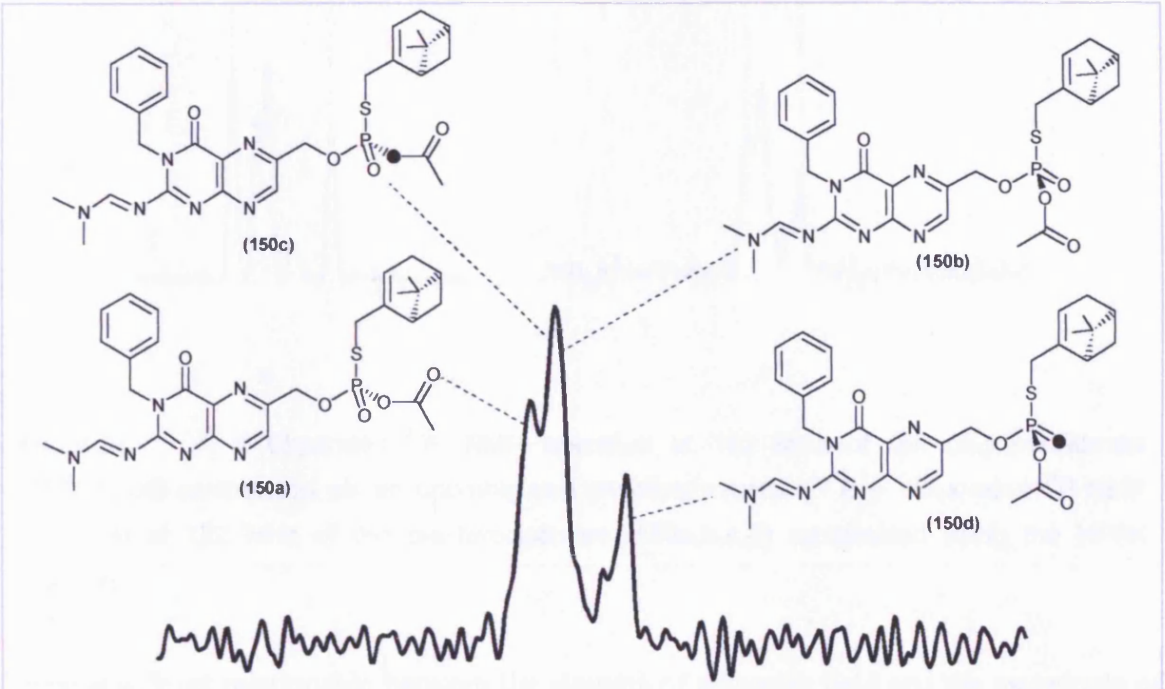

Fig. 4.4 Expanded ^{31}P NMR spectrum (121.9 MHz) of a 3:2 mixture of unlabelled and labelled diastereoisomers of **(150a,b,c,d)**. Spectral parameters: sweep width 366.78 Hz, pulse width 4.5 μsec, acquisition time 2.79 sec, broad-band proton decoupling, Gaussian multiplication (line-broadening –1.80 Hz, Gaussian broadening 0.18 Hz).

A direct comparison can be made with the ^{18}O isotopic shifts derived from the model system (detailed configurational analysis described in Chapter 3, Figure 3.5) synthesised stereospecifically with an Rp phosphorus centre. In this system the downfield diastereoisomer with a single bond ^{18}O isotopic shift was assigned an Sp configuration and the upfield diastereoisomer with a double bond ^{18}O isotopic shift was assigned an Rp configuration.

The configurational analysis of the unknown diastereoisomer was performed at a different magnetic field strength to the model system (121.9 MHz *vs* 162 MHz) resulting in poor signal resolution. The separation between the downfield resonance and the double bond ^{18}O isotopic shift on the upfield diastereoisomer (the only signals resolved clearly enough to measure their separation precisely) was 9 Hz compared with 12 Hz for the model system, Figure 4.5.

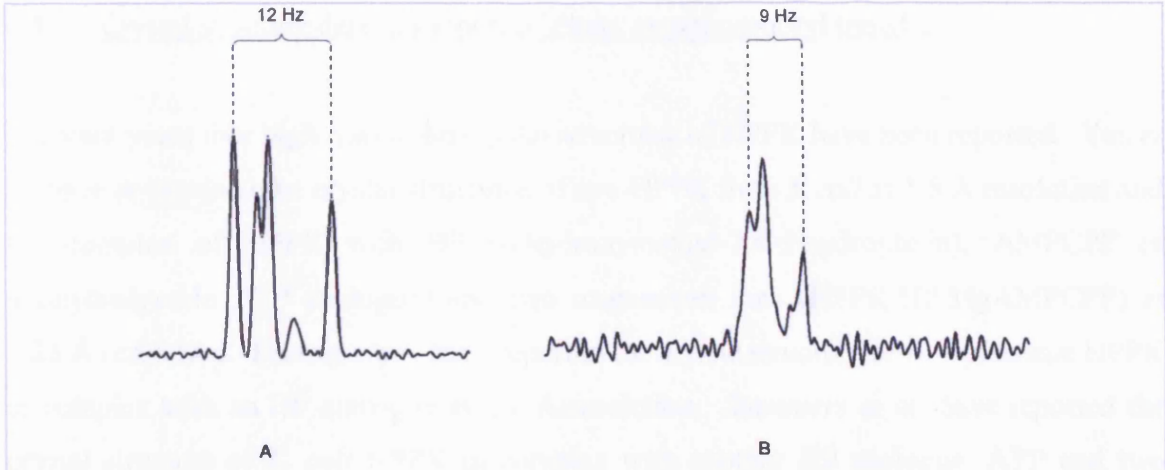

Fig. 4.5 A = Expanded ^{31}P NMR spectrum at 162 MHz of the diastereoisomers **(150a,b,c,d)** synthesised *via* an unambiguous chemically method. B = Expanded ^{31}P NMR spectrum at 122 MHz of the diastereoisomers **(150a,b,c,d)** synthesised using the HPPK enzyme.

There is a direct relationship between the strength of magnetic field and the magnitude of both the separation of diastereoisomers and the ^{18}O isotopic shifts, 9 Hz at 121.9 MHz represents the same magnitude of separation as 12 Hz at 162 MHz. On this basis the configuration at the chiral phosphorus centre of the diastereoisomer **(112a)**, Scheme 4.4, (conditionally assigned Rp in schemes 4.4, 4.5 and 4.6 to illustrate the stereochemical consequences of each chemical transformation) was assigned Rp, which represents the same configuration as the diastereoisomer synthesised *via* the independent, stereospecific and unambiguous route.

Exploitation of these isotopically labelled chiral thiophosphates has shown that the stereochemistry at the original β-phosphoryl centre has been inverted in the product of the enzyme reaction (Sp → Rp). On this basis the mechanism of pyrophosphoryl transfer involves inversion of configuration, suggesting that the reaction proceeds *via* a single in-line S_N2 displacement pathway, (direct pyrophosphoryl transfer).

4.4 Crystal structure data in support of direct pyrophosphoryl transfer.

In recent years four high resolution crystal structures of HPPK have been reported. Yan *et al.* have determined the crystal structures of apo-HPPK from *E.coli* at 1.5 Å resolution and the complex of HPPK with HP (6-hydroxymethyl-7,8-dihydropterin), AMPCPP (a nonhydrolysable ATP analogue) and two magnesium ions (HPPK·HP·MgAMPCPP) at 1.25 Å resolution. Hennig *et al.* have reported the crystal structure of *H. influenzae* HPPK in complex with an HP analogue at 2.1 Å resolution. *Stammers et al.* have reported the crystal structure of *E. coli* HPPK in complex with another HP analogue, ATP and two Mg^{2+} ions at 2.0 Å resolution. Of the three complex structures, HPPK·HP·MgAMPCPP most closely mimics the ternary complex. In our earlier discussion of this complex (Chapter 1, Section 1.4.7) we highlighted details of the secondary structure elements and showed the relative orientations of substrate molecules and the Mg^{2+} ions. We also illustrated the conformational differences between apo-HPPK and the ternary HPPK-HP-MgAMPCPP complex. We now pick up this topic again, with the aim of highlighting the essential role of the Mg^{2+} ions and a number of the highly conserved amino acid residues, in catalysing pyrophosphoryl transfer.

Catalysis by pyrophosphoryl transfer enzymes requires the involvement of two magnesium ions.[76] The HPPK crystal structure data suggests that both Mg^{2+} ions are 5-coordinate square pyramidal. One of the Mg^{2+} ions (Mg1) is coordinated with the α- and β-phosphates and an ordered water molecule. The other Mg^{2+} ion (Mg2) is coordinated with the β- and γ-phosphates of ATP and the hydroxyl oxygen of 6-hydroxymethyl-7,8-dihydropterin. In addition, both magnesium ions are co-ordinated with the carboxyl groups of aspartate-95 and aspartate-97.[76]

In order to support the hypothesis of a single-step pyrophosphoryl transfer *via* a penta-co-ordinate transition state in a concerted $S_N2(P)$ process the enzyme must utilize these Mg^{2+} ions, and a number of essential amino acid, to do four things:

i) Orientate the functional groups of the substituents (the hydroxyl of HP and β-phosphorus of ATP) involved in catalysis at a sufficient proximity to allow

nucleophilic attack in an in-line geometry (nucleophile approaches in-line (180°) with the leaving group).

ii) Improve the leaving group (AMP) by neutralising the charge on the α-phosphate.

iii) Enhance the electrophilicity of the β-phosphoryl centre (neutralising the charge on the oxygen and reducing the electron density on phosphorus).

iv) Increase the nucleophilicity of the hydroxymethylene moiety of the pterin.

Observations made using the crystal structure of the HPPK·HP·MgAMPCPP ternary complex[76] provide evidence in support of each these criteria. This evidence will be reviewed here in a point by point manner.

i) Orientation of substituents.

The relative positions of amino acid residues that are involved in catalysis and substrate binding (i.e. through hydrogen bonding) may be orientated by conformational changes at the active site caused by the presence of the Mg^{2+} ions.

Furthermore, the Mg^{2+} ions orientate the hydroxyl moiety of HP the β-phosphorus and the bridging oxygen between the α- and β-phosphorus atoms of ATP into the arrangement required for the reaction.

It is clear from analysis of the crystal structure that the angle formed by the hydroxyl oxygen of 6-hydroxymethyl-7,8-dihydropterin (HP), the β-phosphorus and the bridging methylene carbon (from the nonhydrolysable ATP analogue α,β-methyleneadenosine triphosphate [AMPCPP]) is 174.5°, only slightly below the ideal value of 180° for an in-line nucleophilic attack, Figure 4.6.

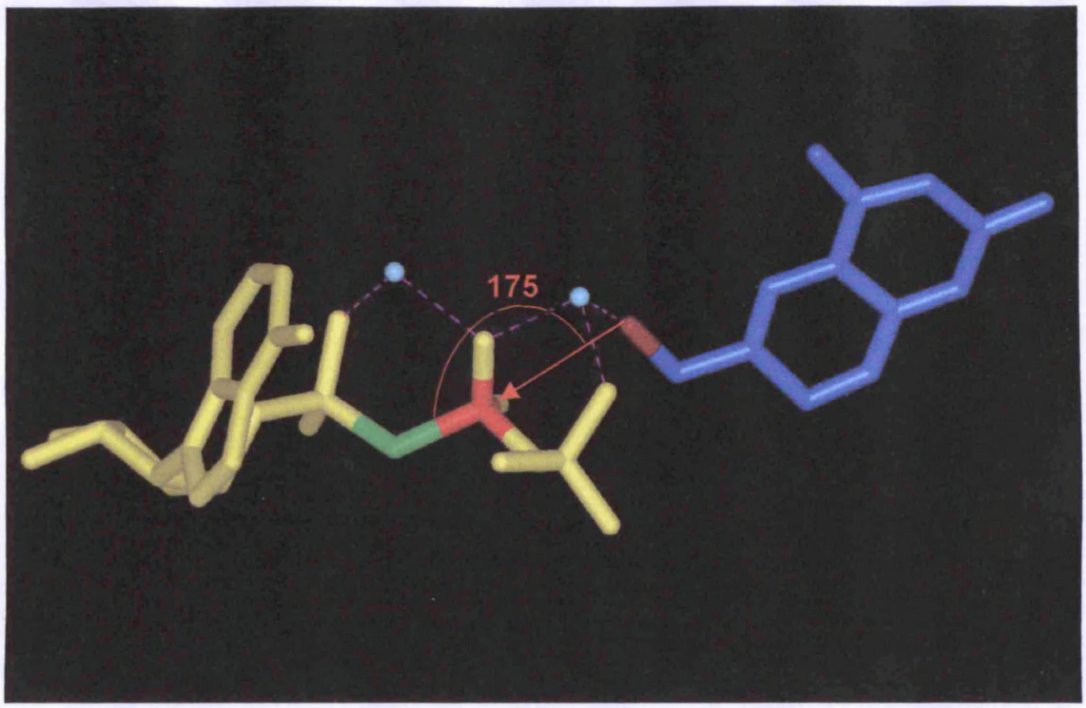

Fig. 4.6 Crystal structure of a ternary complex of *E.coli* HPPK with the substrate analogue AMPCPP (yellow), HP (blue) and two bound Mg^{2+} ions (pale blue). The secondary structure elements have been removed to show the angle formed by the hydroxyl oxygen of HP (brown), the β-phosphorus (red) and the bridging methylene carbon of AMPCPP (green). The distance signified by the red arrow is 3.2Å.

In addition the distance between the hydroxyl oxygen of 6-hydroxymethyl-7,8-dihydropterin and the β-phosphorus is 3.2Å. The reaction coordinate for a completely dissociative mechanism is 4.9Å,[147] suggesting that the reaction has some associative character in the transition state. As this distance is derived from a pseudoternary complex there is the distinct possibility that during catalysis of the natural substrate, ATP, a conformation change occurs that further decreases this distance below 3.2Å.

ii) Improvement of leaving group.

The charge on the α-phosphate of ATP is neutralised by coordination to arginine-84 (bidentate on both arginine and phosphorus), arginine-82 (monodentate on arginine and bidentate on phosphorus) and one of the Mg^{2+} ions (Mg1), Figure 4.7.

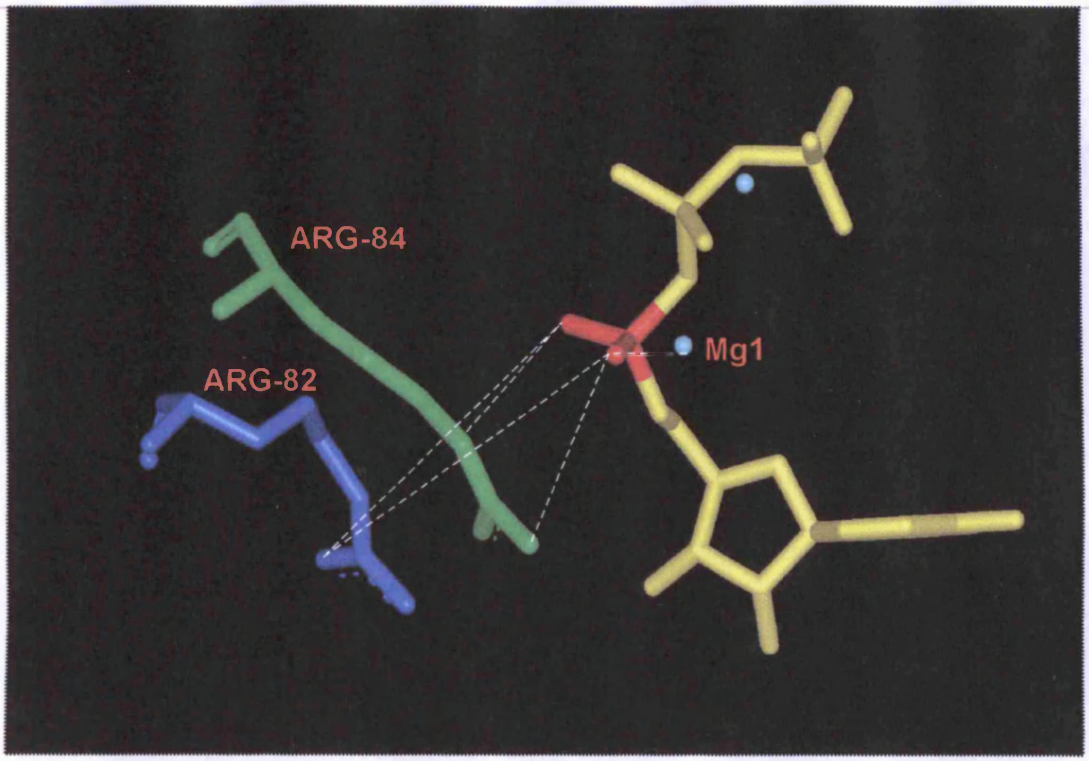

Fig. 4.7 Crystal structure of a ternary complex of *E.coli* HPPK with the substrate analogue AMPCPP (yellow), HP and two bound Mg^{2+} ions (pale blue). The secondary structure elements and HP have been removed and two arginine residues, ARG-82 (blue) and ARG-84 (green) have been highlighted. The coordination of the arginine residues and Mg1 to the α-phosphate (red) is shown.

This coordination will make AMP and excellent leaving group as it can be imagined that the Mg^{2+} acts as a Lewis acid catalyst for AMP elimination.

iii) Enhancement of the electrophilicity of the β-phosphoryl centre.

The charge on the β-phosphorus is neutralised by co-ordination to both magnesium ions (Mg-1 and Mg-2), arginine-82 (monodentate on both arginine and phosphorus) and arginine-92 (bidentate on arginine and monodentate on phosphorus), Figure 4.8.

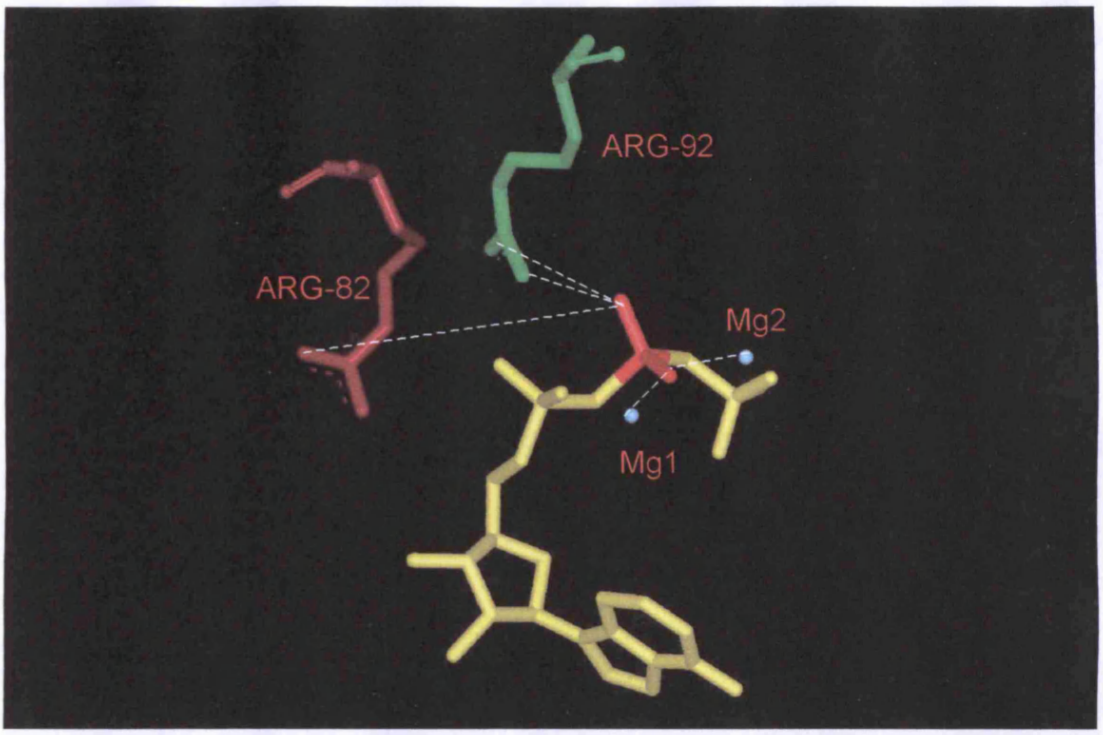

Fig. 4.8 Crystal structure of a ternary complex of *E.coli* HPPK with the substrate analogue AMPCPP (yellow), HP and two bound Mg^{2+} ions (pale blue). The secondary structure elements and HP have been removed and two arginine residues, ARG-82 (brown) and ARG-92 (green) have been highlighted. The coordination of the arginine residues and both Mg^{2+} ions to the β-phosphate (red) is shown.

This Lewis acid catalysis of the electrophilic centre activates the β-phosphorus for nucleophilic attack. Furthermore, the binding of Mg^{2+} *via* the side chains of the conserved residues D97 and H115 could stabilise the negative charge developed in the transition state of the reaction. The participation of an imidazole in magnesium binding in HPPK would require a conformational change of the protein, which is indicated by differential scanning calorimetry and fluorescence stabilization.

iv) Increasing the nucleophilicity of the hydroxymethylene moiety of the pterin.

The co-ordination of Mg-2 with the hydroxyl oxygen of 6-hydroxymethyldihydropterin reduces the pK_a of the hydroxyl group and therefore facilitates the reaction. Such coordination is commonly seen in phosphatases where the nucleophilic water is almost always delivered from one of the metal ions.

Two water molecules and the side chain of the highly conserved acidic residue aspartate 95 are ideally placed to extract a proton from the 6-hydroxymethyl side-chain, leading to the formation of a nucleophilic pterin derivative ready to attack the β-phosphate of bound ATP. Aspartate 95 co-ordinates to both magnesium ions, suggesting that it is unlikely to be the general base that removes the proton from the hydroxyl group. One of the two water molecules, therefore, may act as the general base if necessary, Figure 4.9.[76]

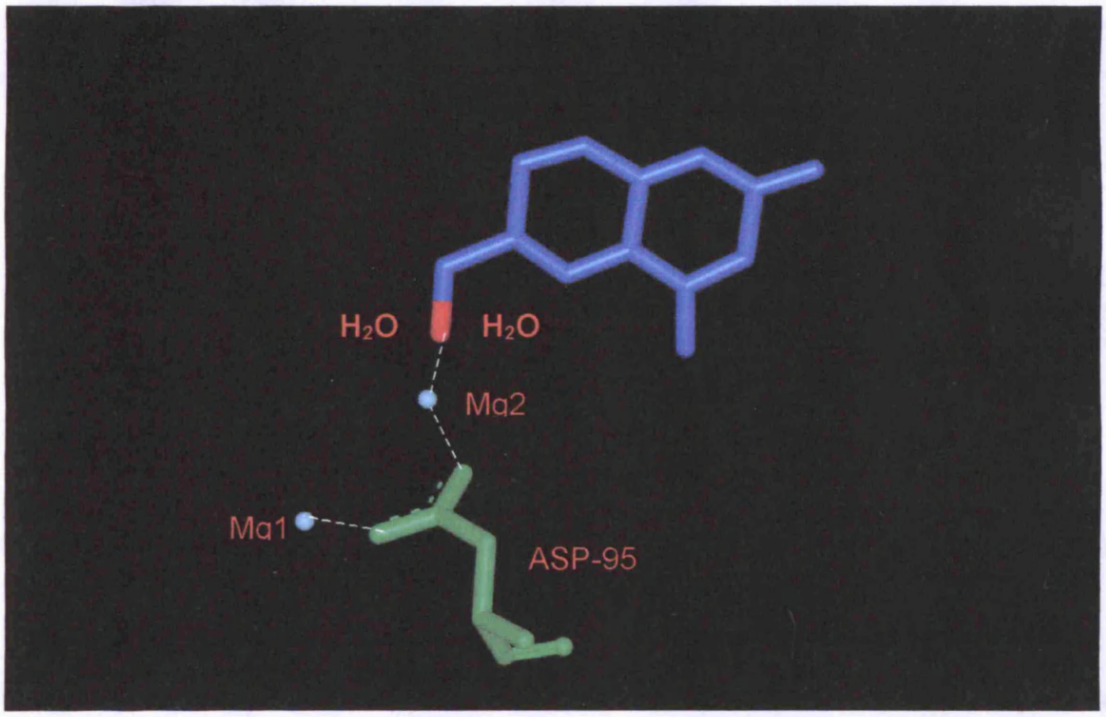

Fig. 4.9 Crystal structure of a ternary complex of *E.coli* HPPK with the substrate analogue AMPCPP, HP (blue) and two bound Mg^{2+} ions (pale blue). The secondary structure elements and AMPCPP have been removed and an aspartate residue, ASP-95 (green) has been highlighted. The coordination of the aspartate residue to both Mg^{2+} ions and of Mg2 to the 6-hydroxyl group (red) of HP (blue) is shown.

A key consideration when examining crystal structure data is that it represents a static structure that may or may not resemble the active species involved in turn over. Furthermore, the nonhydrolysable ATP analogue (AMPCPP) used to obtain the crystal structure may cause the two magnesium ions, and the essential amino acids involved in substrate binding and catalysis of the chemical step, to adopt a conformation that is not representative of the orientation found with ATP.

It can be suggested though, that the HPPK·HP·MgAMPCPP ternary complex is a good representation of the HPPK·HP·MgATP ternary complex, on the basis that mechanistic predictions made from its analysis support the results of our stereochemical study and the available data provided by a kinetic analysis of the enzyme.

4.5 Kinetic data in support of direct pyrophosphoryl transfer.

Kinetic studies can provide evidence for, or against, the existence of covalent intermediates generated during an enzyme-catalysed reaction. Double displacement reactions (*via* a covalent enzyme intermediate) exhibit parallel Lineweaver-Burk plots consistent with a ping-pong mechanism, Scheme 4.7. In principle the first product is released from the enzyme before the second substrate is bound.

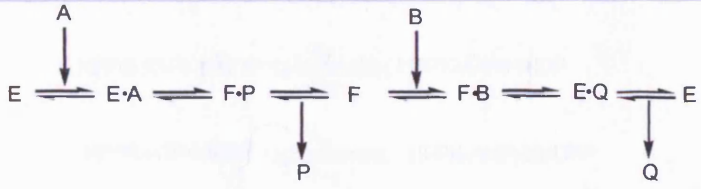

Scheme 4.7 A ping-pong kinetic scheme for a two substrate (A and B) / two product (P and Q) reaction. E represents the free enzyme and F the phosphorylated form of the enzyme.

Alternatively intersecting Lineweaver-Burk plots indicate that a sequential mechanism involving a single displacement step is in action. The reaction must pass through a state (the ternary complex) with both substrates bound simultaneously to the enzyme. The ternary complex can be formed by the binding of substrates in a particular order (a compulsory order mechanism) or the free enzyme can combine with either of the substrates (a random order mechanism). Similar considerations apply to the release of products, Scheme 4.8.

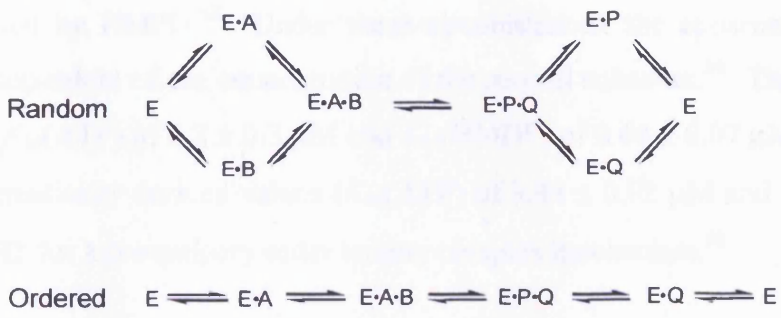

Scheme 4.8 An illustration of a (random) and (ordered) sequential kinetic scheme for a two substrate (A and B) / two product (P and Q) reaction.

The HPPK catalysed reaction has been the subject of several kinetic investigations that support a compulsory order ternary complex mechanism, Scheme 4.9.

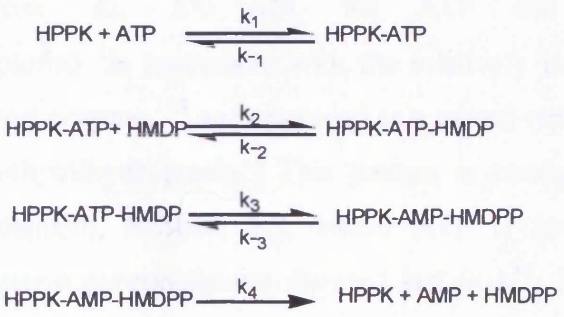

Scheme 4.9 Kinetic mechanism of HPPK.

The pre-steady state kinetic analysis of the binding of substrates to *E. coli* HPPK has been investigated using ATP and the nonhydrolysable ATP analogue α,β-methyleneadenosine triphosphate (AMPCPP).[68] These substrates bind to HPPK with high affinity. The second substrate, HMDP does not bind to the apoenzyme unless AMPCPP is present, suggesting that the enzyme binds ATP first, followed by HMDP. Stopped flow fluorimetry measurements showed that the rate constant for the binding of AMPCPP to HPPK was relatively slow (1.05×10^5 M^{-1} s^{-1}) compared with the on-rate binding of HMDP to the HPPK·AMPCPP binary complex (1.4×10^7 M^{-1} s^{-1}). These results are consistent with a compulsory order ternary complex mechanism, with ATP binding first (k_1) in a relatively slow step, followed by the faster addition of HMDP (k_2).

A steady-state kinetic analysis at multiple concentrations of ATP and HMPD was analysed assuming a compulsory order ternary complex reaction where ATP binds first to the

enzyme followed by HMPD.[68] Under these circumstances, the apparent K_M for each substrate is independent of the concentration of the second substrate.[68] The experimental data obtained (K_M(ATP) of 3.2 ± 0.3 μM and K_M(HMDP) of 0.68 ± 0.07 μM) is consistent with the mathematically derived values (K_M(ATP) of 3.44 ± 0.02 μM and K_M(HMDP) of 0.60 ± 0.01 μM) for a compulsory order ternary complex mechanism.[68]

Additional evidence supporting a single displacement step with an ordered sequential mechanism is provided by an investigation into the product-inhibition pattern (determined for HPPK/DHPS bifunctional protein found in higher-plant mitochondria).[84] Steady state kinetics suggest that 6-hydroxymethyldihydropterin pyrophosphate is a competitive inhibitor of ATP (approx. K_i, 5 μM) and a mixed-type (non-competitive) inhibitor of 6-hydroxymethyl-7,8-dihydropterin (approx. K_i, 10-15 μM).[84] AMP is a poor inhibitor of the reaction,[84] (approx. K_i, 700 μM, for ATP and 400 μM for 6-hydroxymethyldihydropterin) in agreement with the relatively low affinity reported for the monofunctional *E.coli* enzyme,[148] and appeared as a mixed-type inhibitor against both ATP and 6-hydroxymethyldihydropterin. This pattern is compatible with an ordered sequential Bi Bi mechanism, Scheme 4.9, where ATP is bound first (k_1) and 6-hydroxymethyldihydropterin pyrophosphate released last (k_4).[84] In a random sequential mechanism in rapid equilibrium, 6-hydroxymethyldihydropterin pyrophosphate and AMP would have been competitive inhibitors of both substrates.[84]

4.6 Development of antibacterial agents to inhibit HPPK

In Chapter 1, Section 1.4.4 a discussion was given describing how the enzymes of the folic acid biosynthetic pathway have been targets for antimicrobial chemotherapy. HPPK is an attractive potential target for the development of new antibacterial agents. Despite recent high-resolution crystal structure of the *E.coli*[69,76,77] and recombinant *Haemophilus influenzae* enzymes,[52] and detailed kinetic studies[68,149] no compounds with potential therapeutic value have been developed.

The understanding we have gained by determining the reaction mechanism of the HPPK catalysed pyrophosphoryl transfer reaction will be of use in the design of inhibitors with a potential therapeutic value.

The observation that HPPK facilitates a direct in-line attack of 6-hydroxymethyl-7,8-dihydropterin on the Pβ of ATP implies the involvement of the intermediate/transition state shown in Figure 4.10.

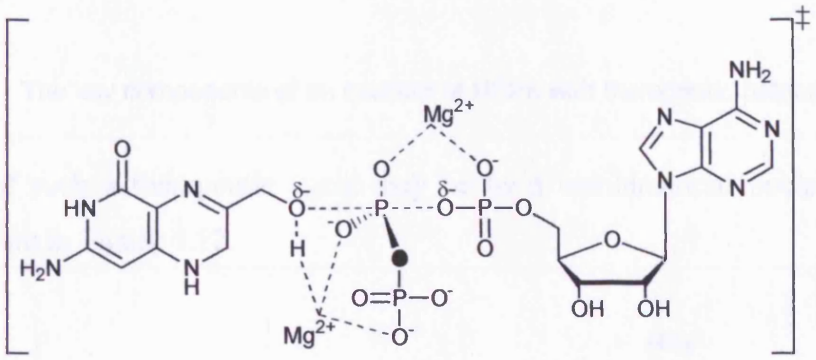

4.10 Intermediate/transition state of the direct in-line attack of 6-hydroxymethyl-7,8-dihydropterin on Pβ of ATP. The metal ion coordination with the phosphate groups is illustrated.

Blaszczyk *et al.* have synthesised bisubstrate analogues that closely mimic this high energy species providing potent inhibitors of HPPK.[78] This topic has been discussed in Chapter 1, Section 1.4.5.

Bisubstrate analogues that incorporate polyphosphates are unlikely to have any therapeutic potential against intracellular enzymes because polyanions cannot cross the cell membrane.

An alternative approach is to seek to design ligands that can access both the adenosine and dihydropterin binding loci and that also incorporate a non-anionic linker that can complex with the magnesium metal ions. Figure 4.11 indicates the key components of such an inhibitor.

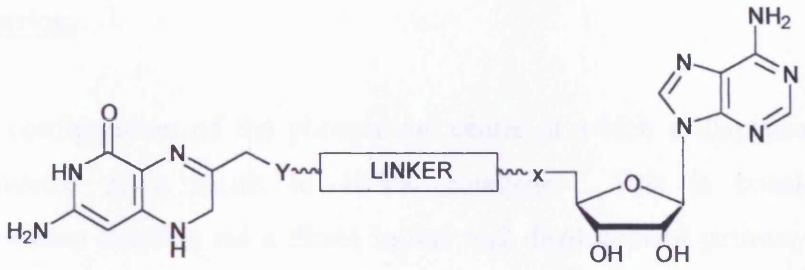

Fig. 4.11 The key components of an inhibitor of HPPK with therapeutic potential.

The design of such a therapeutic agent may be by a combinatorial nucleoside-peptide library as shown in Figure 4.12.

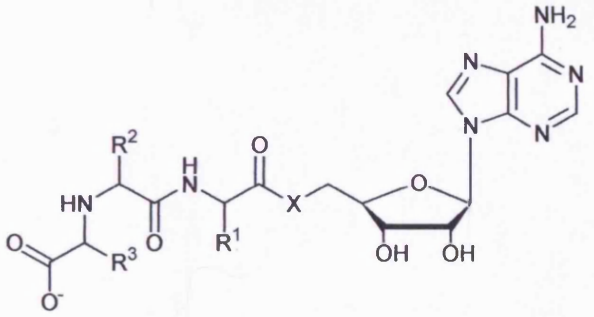

Fig. 4.12 Combinatorial nucleoside-peptide library.

The solid phase synthesis of such a target compound would utilise the common adenosine-loaded polymer and extend this with a randomised tripeptide. The side chain of amino acid 3 (R3) would be chosen to access the pterin binding site, with the terminal carboxyl group replacing Pγ of ATP. Amino acid residues 1 (R1) and 2 (R2) would be selected to provide appropriate metal coordination. The binding of substrates to HPPK is accompanied by a significant change in fluorescence. This fluorescence change could be used to screen the libraries in an off-bead ligand displacement assay. These adenosyl-tripeptides can be viewed as potential ATP analogues and will facilitate wider screening against a range of ATP dependent enzymes.

4.7 Conclusion.

The absolute configuration of the phosphorus centre at which a displacement reaction occurs is inverted as a result of HPPK catalysis. This is consistent with a pyrophosphorylation reaction *via* a direct in-line S_N2 displacement pathway. Although a direct in-line S_N2 displacement pathway has be proposed previously by crystallographic data, we have seen, that in isolation, these proposals are speculative. The stereochemical course of the reaction is one of the most critical mechanistic probes and when this is complemented with crystallographic and kinetic data, provides a definitive answer concerning the involvement of covalent phosphoenzyme intermediates.

CHAPTER 5
Kinetics

5.1 Introduction.

Most ATP-dependent enzymes have a requirement for at least one loosely bound divalent cation (e.g. Mg^{2+} for all phosphokinases) that is coordinated to the oxygens of the triphosphate group. In principle a Mg^{2+} ion(s) can form mono-, bi-, or tridentate chelates with an ATP substrate. In addition, the effect of Mg^{2+} coordination with the α- and β-phosphate groups of ATP (which are both prochiral) is to create chirality at these centres, which leads to the occurrence of various diastereoisomers of ATP. As a consequence it can be imagined that there are many different metal chelated forms of ATP.

This point is significant as an enzyme will have a preference for only one Mg-ATP chelate, with a particular chirality (i.e. Sp or Rp at the chiral phosphorus centre), as a substrate for the reaction that it mediates.

The purpose and nature of ATP coordination with divalent cations (in particular Mg^{2+}), the occurrence of diastereoisomers and the observation that only one metal chelate (Sp or Rp at the chiral phosphorus centre) will be a good substrate for a particular substitution reaction, and the significance of determining the metal·ATP structure, will form the topic of this introductory section.

The initial focus of our attention is to establish what role these metal ions play in catalysing nucleophilic substitution reactions at the phosphoryl centres of ATP. Generally speaking, metal ions can be expected to play several important roles in catalysis. These roles are listed below with examples.

i) The binding of one or more metal ions may induce a conformational change that is necessary to bring many catalytic residues into the active site.

ii) Metal ions can orientate the nucleophile and the phosphoryl centre (at which substitution occurs) into an appropriate angle and distance to allow for a nucleophilic substitution reaction to proceed.

iii) They often function as a Lewis acid catalyst by coordinating to the appropriate phosphate group to provide a more electrophilic centre for attack by the incoming nucleophile. For example, the Mg^{2+} coordination with the α-

phosphoryl centre of ATP in the HPPK mediated pyrophosphoryl transfer reaction makes AMP and excellent leaving group. This observation is explained in Chapter 4, Section 4.4.

iv) The Lewis acid catalysts properties are again used when metal ions coordinate to the appropriate phosphate groups to neutralise charge development during the substitution reaction. For example the metal ion of a phosphokinase co-ordinates with the α- and β-phosphoryl groups of ATP, thereby enhancing the effectiveness of ADP as a leaving group.

v) In many cases metal ions reduce the pK_a of an incoming nucleophile such as a water molecule by coordination with one of the H atoms. This is commonly seen in phosphatases where the nucleophilic water is almost always delivered from one of the metal ions.

A more detailed and specific example of these essential roles in catalysis was given in Chapter 4, Section 4.4 with regard to the HPPK catalysed pyrophosphoryl transfer reaction in which two Mg^{2+} ions are utilised by the enzyme.

We have established that the metal ions present at the active site of ATP-dependent enzymes play an essential catalytic role in the substitution reactions that these enzymes mediate. It is apparent, that for a complete description of the reaction mechanism of any enzyme utilizing ATP, a detailed knowledge of the structure of the metal·ATP substrate, the coordination of the metal to the substrate during the reaction, and finally the metal·product complex is necessary. Furthermore inhibitor design can be based on an understanding of the enzyme mechanism. This topic is discussed in Chapter 4, Section 4.6.

The availability of high resolution crystal structures of many phosphotransfer enzymes has allowed the structure of many metal·ATP complexes's to be proposed. These conclusions though, are based on observations made from inactive complexes, so it can be argued that they do not necessarily describe the structure of the metal·substrate complex in an enzyme actively turning over substrate.

The most frequently used method, to probe the coordination of the metal to the phosphate group in an enzyme actively turning over substrate, is based on the use of chiral phosphorothioate analogues of ATP.

The use of phosphorothioate analogues of ATP rests on the observation made using ^{31}P NMR spectroscopy that Mg^{2+} preferentially coordinates to oxygen, and Cd^{2+} to sulphur. This result is expected because Mg^{2+} is a hard Lewis acid and Cd^{2+} is a soft Lewis acid, while oxygen and sulphur are hard and soft Lewis bases respectively. Other cations such as Co^{2+}, Mn^{2+} and Zn^{2+} are intermediate metal ions.[150]

The stability constants of Mg^{2+} and Cd^{2+} complexes of various phosphorothioate analogues of ATP and ADP have been determined and used to calculate the preference for O and S coordination.[150] The preference for sulphur over oxygen coordination for Cd^{2+} is estimated to be 60 regardless of the position (be it the α-, β- or γ- position of the phosphate chain) of the phosphorothioate group. Preference for oxygen over sulphur coordination for Mg^{2+} is calculated to be 31,000 for MgATPβS, 3,100-3,900 for CaATPβS, and 158-193 for MnATPβS.

At the active sites of phosphoryl transfer enzymes, metal ions can coordinate to either the oxygen or sulphur atom of the chiral thiophosphoryl centre of a phosphorothioate analogue of ATP. As a consequence of the oxophilic/thiophilic nature of the metal ions, only one diastereoisomer of a phosphorothioate analogue will be expected to be a good substrate for a given enzyme reaction, Figure 5.1.[150]

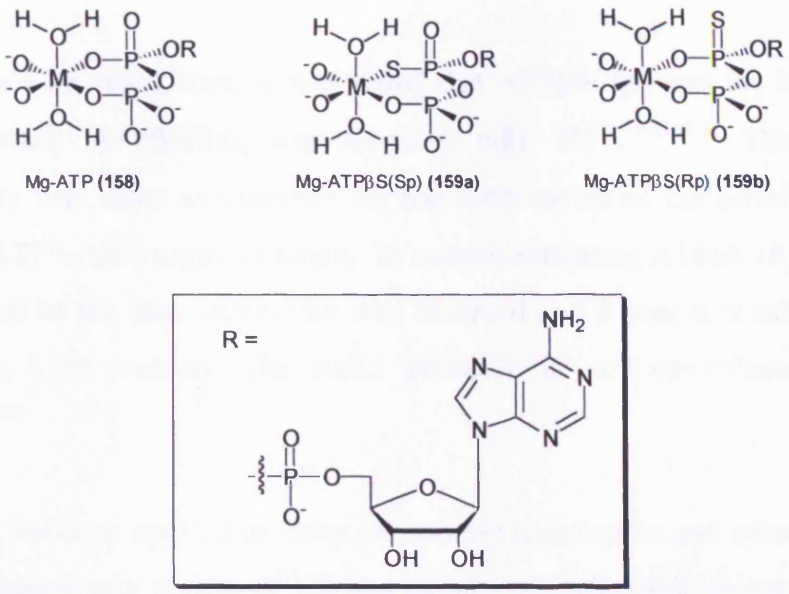

Fig. 5.1 Metal binding stability for ATP, $ATP_{\beta}S(Sp)$ and $ATP_{\beta}S(Rp)$.[150]

In our illustration of the ATP metal ion complex **(158)** there is an interaction between the oxygens on the β- and γ-phosphoryl groups with the metal ion. As a consequence chirality is generated at the β-phosphoryl centre. It can be expected that the enzyme will be sensitive to this chirality, with one configuration (i.e. Sp or Rp) at the β-phosphoryl centre favoured over the other. In addition two strong internal hydrogen bonds between water molecules bound to the metal ion and the phosphate oxygens are formed. In the phosphorothioate analogue metal ion complex with Rp configuration at the β-phosphoryl centre **(159a)**, the substituted sulphur atom does not interact with the metal ion; instead it has a weak interaction with a water proton. In the concomitant metal ion complex using the Sp diastereoisomer **(159b)** the sulphur atom interacts with the metal ion and two strong internal hydrogen bonds between water molecules bound to the metal ion and the phosphate oxygens are formed.

If we imagine, that the metal ion (M) in the above illustration was, in fact a Mg^{2+} ion, as a consequence of the oxophilic/thiophilic nature of the metal, the phosphorothioate ATP analogue with Rp configuration at the chiral thiophosphate centre would be a substrate and the Sp diastereoisomer would be expected to be a significantly worse substrate. Alternatively, if the metal was a Cd^{2+} ion these preferences would be reversed, and the Sp diastereoisomer would be a substrate and the Rp diastereoisomer would be expected to be a significantly worse substrate.

In experiments with hexokinase, it was found that ATPβS(Rp) was the better substrate with Mg^{2+}, while ATPβS(Sp) was favoured with Cd^{2+}.[151,152] This reversal of stereoselectivity was taken as evidence for the coordination of the metal ion to the β-phosphate of ATP in the enzyme reaction. In experiments using ATPαS (Rp) and ATPαS (Sp) no reversal of the stereoselectivity was observed and it was concluded that, in the hexokinase-Mg-ATP complex, the metal probably is not co-ordinated to the α-phosphate.[151,152]

This approach has been applied to many phosphoryl transferases and adenyl transferases and has been extensively reviewed.[61] More recently phosphorothioate substitutions have been used in conjugation with ^{31}P NMR spectroscopy as a probe for metal binding sites in nucleic acids.[153] Generally, reversal of stereoselectivity has been taken as unequivocal evidence for the involvement of the particular phosphate group in metal coordination. When reversal of stereoselectivity is only seen with ATPβS (as was the case with hexokinase above), a β,γ-bidentate metal chelate has been proposed, the involvement of the γ-phosphate being likely due to the greater thermodynamic stability of the six membered β,γ-chelate ring over a β-monodentate complex.

In cases where no metal ion dependent reversal of stereoselectivity is seen the interpretation is ambiguous. One possibility is that the metal ion does not coordinate to this phosphoryl centre. However, another possibility is that constraints imposed by the enzyme active site stabilise an otherwise less favourable metal-ligand interaction (such as Mg-S or Cd-O coordination). One such case is RNA polymerase, where an unfavourable Mg-S interaction was stabilised by an additional interaction of the non-coordinated oxygen with the enzyme.

5.2 Aims.

In our earlier stereochemical study (Chapter 4) the Sp diastereoisomer of ATPβSβγ^{18}O was used as an isotopically labelled chiral substrate to determine the stereochemical course of the HPPK catalysed reaction. The idea that many phosphotransferase enzymes utilize

only one diastereoisomer of a given phosphorothioate analogue of ATP (as a consequence of the oxophilic/thiophilic nature of the metal ions) provided the motivation to determine the selectivity of HPPK toward the diastereoisomers of ATPβS.

On the basis of crystal structure data it was predicted that the Rp diastereoisomer would be a good substrate for HPPK, but the Sp diastereoisomer would be a poor substrate. This conclusion was based on the prediction that the Sp diastereoisomer is subject to a forced magnesium ion-sulphur interaction whereas the orientation of the Rp diastereoisomer is such that the sulphur does not interact with the Mg^{2+} ion. This idea can be explained by analysis of the crystal structure shown in Figure 5.2.

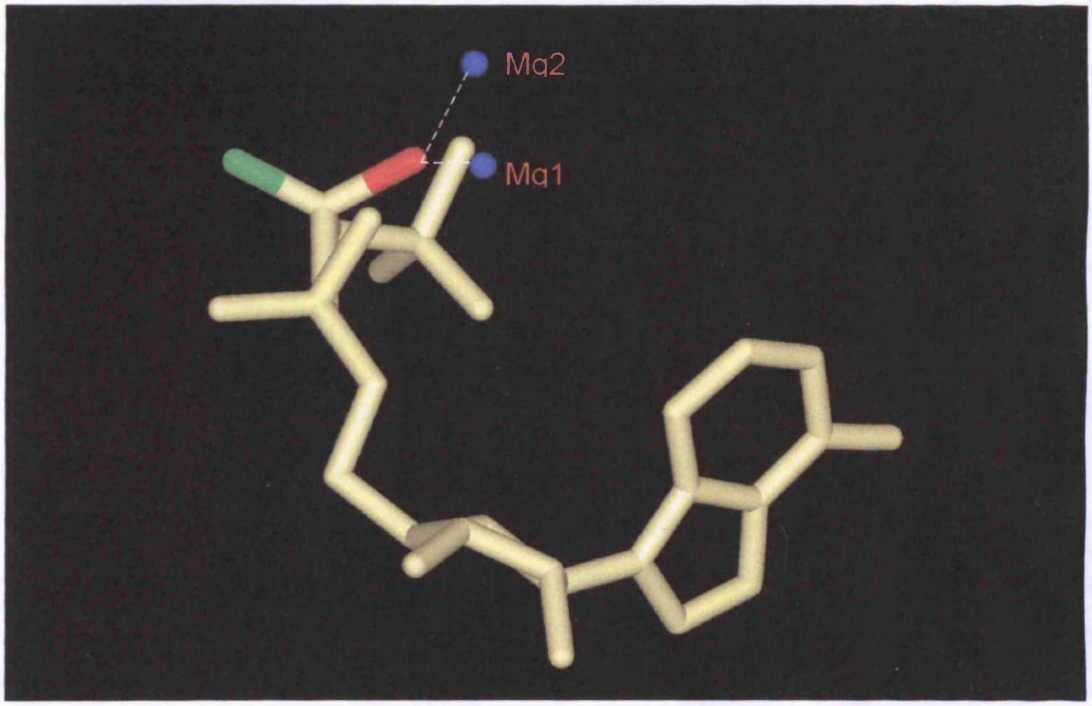

Fig. 5.2 Crystal structure of a ternary complex of *E.coli* HPPK with the substrate analogue AMPCPP (yellow), HP and two bound Mg^{2+} ions (blue). The secondary structure elements and HP have been removed. The orientation of the prochiral oxygens of the AMPCPP analogue with Mg1 (blue) at the active site of HPPK is illustrated.

If the diastereoisomers of ATPβS are superimposed onto the AMPCPP, shown in yellow, we find that when sulphur is placed at the red position the β-phosphorus centre has an Sp configuration and when it is placed at the green position the β-phosphorus centre has an Rp configuration. Consequently in the Sp diastereoisomer of ATPβS the sulphur atom interacts with the two Mg^{2+} ions, but in the Rp diastereoisomer the oxygen atom interacts with the two Mg^{2+} ions.

To test the proposal that Rp diastereoisomer of ATPβS(Sp) would be a better substrate for HPPK than the Sp diastereoisomer the steady-state kinetics of the *E. coli* HPPK catalysed pyrophosphorylation of HMDP using ATP, ATPβS(Rp) and ATPβS(Sp) were to be examined. A number of assays have been developed by previous investigators to determine the kinetic characteristics of the HPPK enzyme. This data is summarized in Table 5.1

Enzyme	Substrate	K_M (μM)	K_d (μM)
E.coli HPPK	ATP	17 ± 3[a]	38 ± 2.7[b]
	HMDP	1.6 ± 0.4[a]	89 ± 14[a]
	MgATP		2.6 ± 0.06[b]
	MgHMDP		0.17 ± 0.01[a]

Table 5.1 Binding properties of HPPK. [a] From Talarico *et al.*[81] [b] From Shi *et al.*[148]

Early steady-state kinetic studies were based on the measurement of radioactive phosphorylated pteridine generated by the substitution of 6-hydroxymethyl-7,8-dihydropterin for a radioactive counterpart.[67] More recently [α-^{32}P] ATP has been used to incorporate radioactivity into the pyrophosphorylated pteridine product.[78,84] In both cases the radioactive compound is isolated by either PEI-cellulose plates[67,78] or HPLC.[84] These techniques are coupled to scintillation counters to measure radioactivity allowing the rate of reaction to be determined.

Although the HPPK catalysed reaction proceeds without a UV absorbance change, Derrick *et al.*[68] has developed a spectrophomeric coupled enzyme assay. The HPPK product, 6-hydroxymethyl-7,8-dihydropterin pyrophosphate, was converted by an excess of dihydropteroate synthase (DHPS), the next enzyme in the folate synthesis pathway, into dihydropteroate and inorganic pyrophosphate. The pyrophosphate is then converted to inorganic phosphate by cleavage with inorganic pyrophosphatase. Inorganic phosphate is used by purine nucleoside phosphorylase to cleave 2-amino-6-mercapto-7-methylpurine ribonucleoside (MESG) into the products ribose-1-phosphate and a purine base. The

cleavage of MESG gives a measurable absorbance change at 360 nm between pH 6.5 and 8.5.[154]

In addition to the catalytic constant (kcat) and the overall dissociation constant (K_M) a fluorometric competitive binding assay has been used to dissect the energetic contributions of the various moieties of MgATP to its binding to *E. coli* HPPK.[148] Binding constants (K_d) were determined by the displacement of the fluorescent ATP analogue, 3'(2)-*o*-anthraniloyladenosine 5'-triphosphate (Ant-ATP) from the ATP binding site with a variety of nucleoside mono-, di- and triphosphates. The results suggest that among the three phosphoryl groups of MgATP, the γ-phosphoryl group is the most critical for binding to HPPK and the α-phosphoryl group contributes little to the binding of the nucleotide.[148]

The design of a novel HPPK assay was required in order to determine the kinetic parameters kcat and K_M for the thiophosphate analogues of ATP as previous assays were unsuitable for the task. For example, the key step in the spectrophomeric coupled enzyme assay developed by Derrick *et al.* is the conversion of 6-hydroxymethyl-7,8-dihydropterin pyrophosphate into dihydropteroate and inorganic pyrophosphate. This reaction is catalysed by an excess of dihydropteroate synthase. The product of the HPPK catalysed reaction, using a thiophosphate analogue of ATP, is 6-hydroxymethyl-7,8-dihydropterin α-thiopyrophosphate. This may be a poor substrate for dihydropteroate synthase and compromise the results obtained using the spectrophomeric coupled enzyme assay.

5.3 Steady-state analysis of the HPPK catalysed pyrophosphorylation of HMDP using ATP, ATPβS(Rp) and ATPβS(Sp).

The HPPK activity was estimated through monitoring the formation of AMP in the presence of ATP, ATPβS (Rp) or ATPβS (Sp), Scheme 5.1.

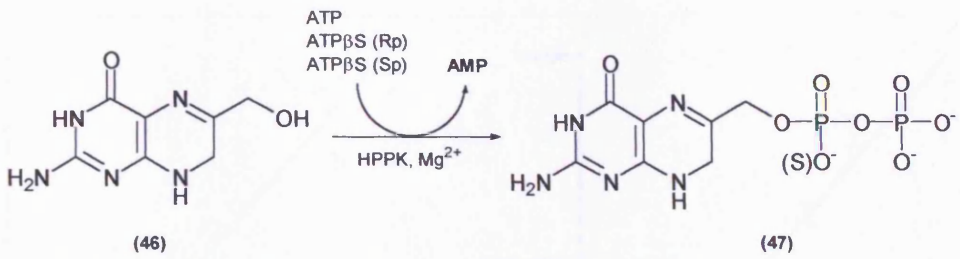

Scheme 5.1 The pyrophosphoryl transfer reaction liberates AMP.

AMP production was monitored by reversed-phase HPLC coupled to a UV detector (256 nm) and an electrospray mass spectrometer. Using ATP, ATPβS (Rp) or ATPβS (Sp), we identified within our HPLC conditions a peak (retention time, 4.65 min) that increased with the time course of the reaction, Figure 5.3.

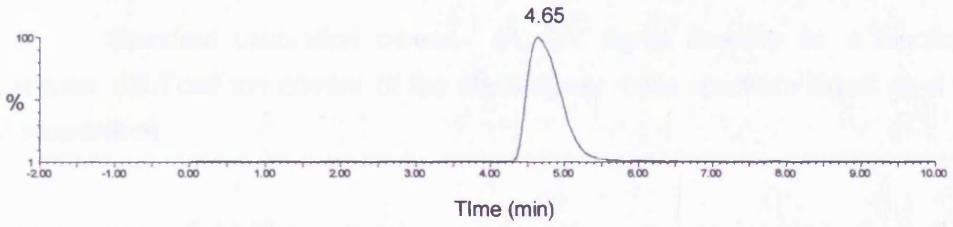

Fig. 5.3 HPLC identification of AMP.

This peak was identified as AMP on the basis of its co-elution with authentic AMP and the determination of its molecular weight (348, MH^+ *c.f.* 348 MH^+ authentic AMP) by the coupled electrospray mass spectrometer.

AMP calibration curves based on a comparison of the total ion current and the UV signal intensity with AMP concentration were generated using AMP standards at a range of concentrations, Figure 5.4.

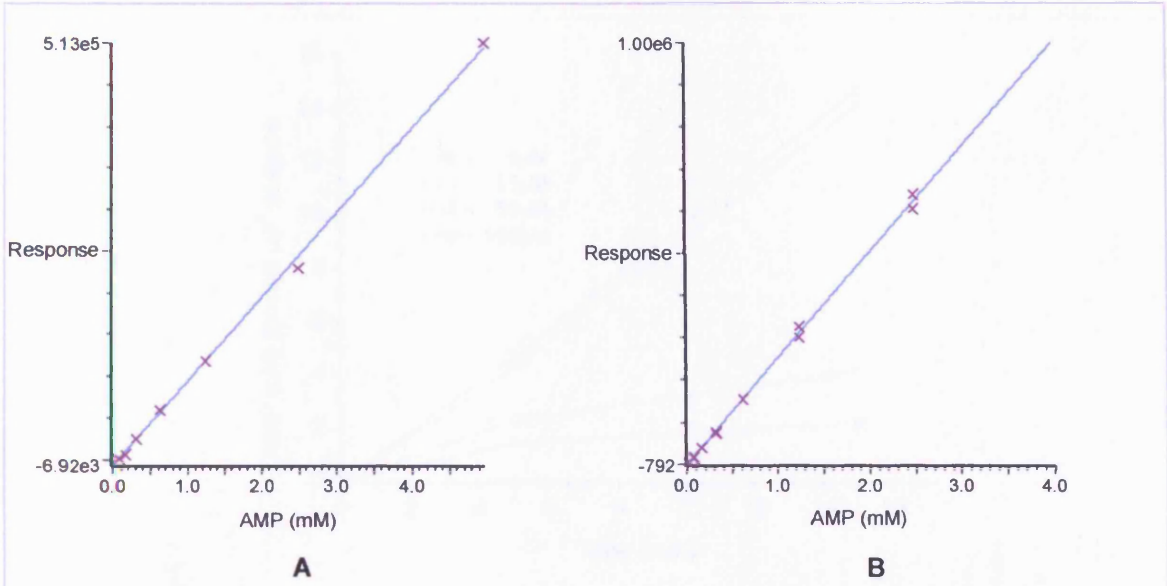

Fig. 5.4 Standard calibration curves. (A) UV signal intensity as a function of AMP concentration. (B) Total ion current of the electrospray mass spectrum signal as a function of AMP concentration.

The concentration of AMP present in samples taken at time intervals from the enzyme assay was estimated by comparison of its UV signal intensity and the total ion current of the mass spectrum signal with the calibration curves, A and B (Figure 5.4) respectively. The amount of AMP calculated at various time intervals (to a maximum of 15 minutes) provided a time course of AMP production for ATP, ATPβS (Rp) and ATPβS (Sp). The time course of AMP production for ATP at a variety of concentrations is presented in Figure 5.5.

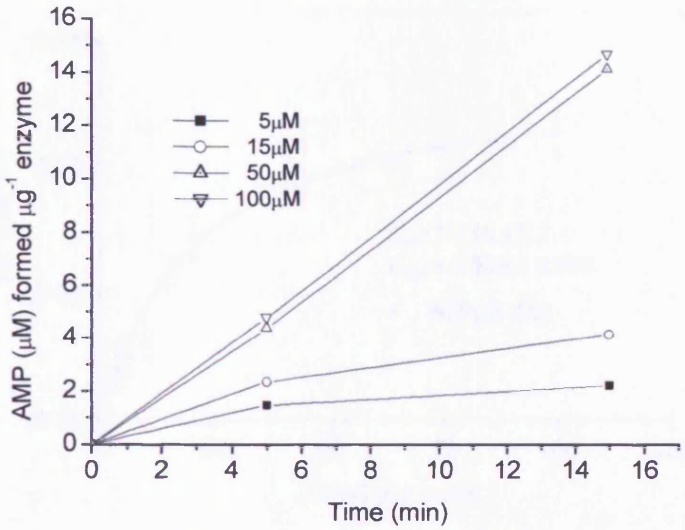

Fig. 5.5 Time course for formation of AMP at 5, 15, 50 and 100 μM ATP concentration. HPPK activity is expressed as μM of product (AMP) formed / μg of enzyme. Each point is a mean of four measurements based on two electrospray mass spectrum and two UV coupled assays.

The rate of AMP formation as a function of ATP, ATPβS (Rp) and ATPβS (Sp) concentration was plotted, Figures 5.6, 5.7 and 5.8. The kinetic parameters were obtained by a nonlinear least-squares fit of the data to the Michaelis-Menten equation using GraphPad Prism software.

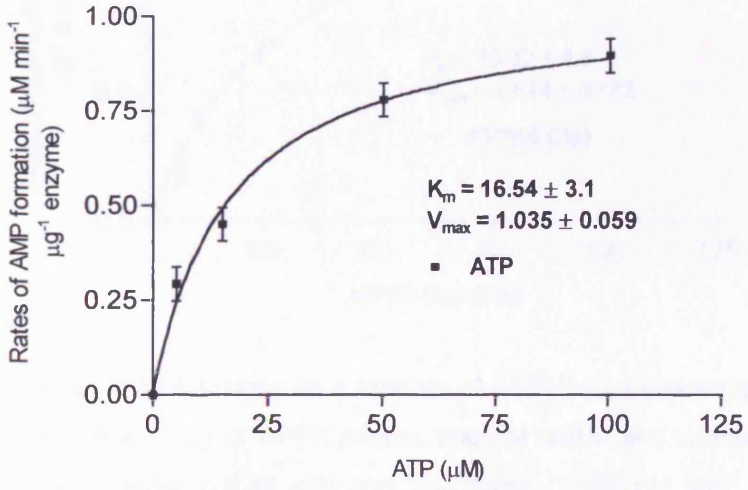

Fig. 5.6 Rate of AMP formation as a function of ATP concentration. The reaction medium (1 cm^3) contained 1 μg of HPPK protein, 200 μM HMDP and various concentrations of ATP. The K_M value (16.54 μM) and V_{max} value (1.035 μM min^{-1} μg^{-1} enzyme) was estimated by direct fitting to the Michaelis-Menten curve using non-linear regression and GraphPad Prism software.

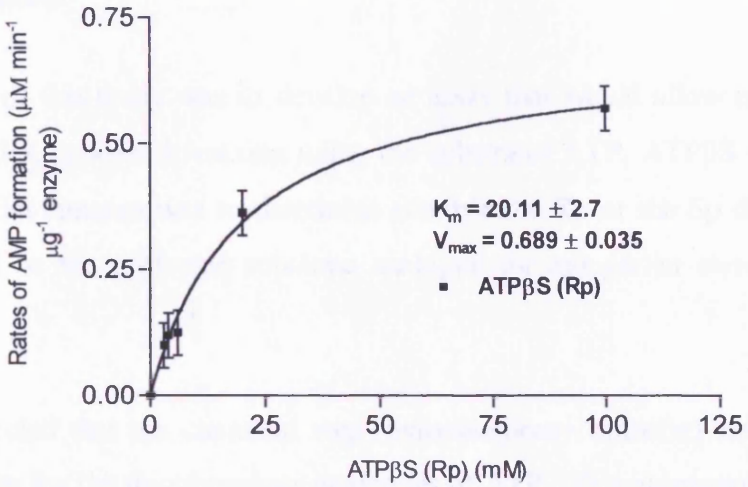

Fig. 5.7 Rate of AMP formation as a function of ATPβS (Rp) concentration. The reaction medium (1 cm^3) contained 1 μg of HPPK protein, 200 μM HMDP and various concentrations of ATPβS (Rp). The K_M value (20.11 μM) and V_{max} value (0.689 μM min^{-1} $μg^{-1}$ enzyme) was estimated by direct fitting to the Michaelis-Menten curve using non-linear regression and GraphPad Prism software.

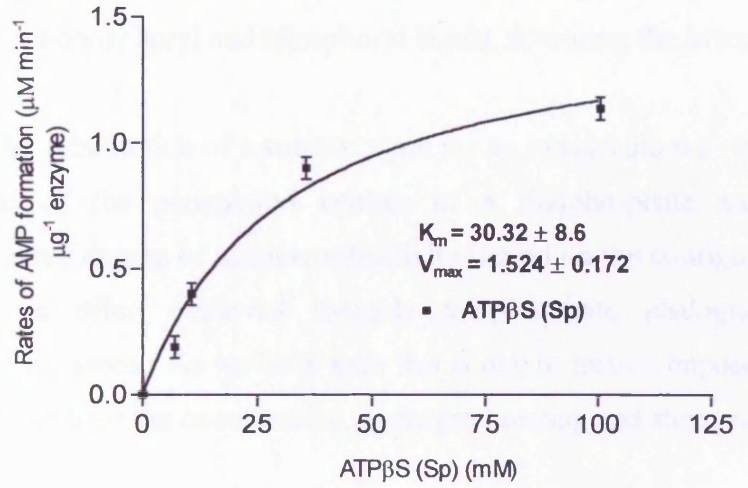

Fig. 5.8 Rate of AMP formation as a function of ATPβS (Sp) concentration. The reaction medium (1 cm^3) contained 1 μg of HPPK protein, 200 μM HMDP and various concentrations of ATPβS (Sp). The K_M value (30.32 μM) and V_{max} value (1.524 μM min^{-1} $μg^{-1}$ enzyme) was estimated by direct fitting to the Michaelis-Menten curve using non-linear regression and GraphPad Prism software.

5.4 Discussion.

The objective of this study was to develop an assay that would allow us to compare the rate of the HPPK catalysed reaction using the substrates ATP, ATPβS (Rp) and ATPβS (Sp). Our initial concern was to determine whether the Rp or the Sp diastereoisomer of ATPβS would be the preferred substrate analogue for our earlier stereochemical study (Chapter 4).

It can be expected that the chemical step (pyrophosphoryl transfer) catalysed by HPPK would be slower for the thiophosphate analogues of ATP. This judgement can be made on the basis that P=O substrates are intrinsically more reactive than their P=S counterparts towards uncatalysed nucleophilic substitution reactions by two or more orders of magnitude.[120] This order of reactivity has been ascribed to one or more of the following: (i) poorer electron-donating ability of the thioanion relative to the oxyanion in expelling the leaving group;[155] (ii) the superior ability of O over S to stabilize the developing positive charge at the P centre;[155] (iii) lower electrophilicity of P in P=S relative to P=O due to electronegativity differences, favouring O over S;[120] (iv) differences in the degree of polarization of thiophosphoryl and phosphoryl bonds, favouring the latter.

As a result of the substitution of a sulphur atom for an oxygen atom a new chiral centre is created at one of the phosphoryl centres of a thiophosphate analogue of ATP. Consequently, some degree of diastereoselectivity (based on the configuration at this new chiral centre) is often observed towards thiophosphate analogues of ATP by phosphotransfer enzymes. As we have seen this is due to factors imposed by the enzyme active site such as metal ion coordination, hydrogen bonding and steric considerations (see Section 5.1).

On this basis an analysis of crystallographic data suggested to us that in order to accommodate Sp ATPβS both Mg^{2+} ions at the active site of HPPK are forced into coordination with sulphur. Alternatively Rp ATPβS retains the two oxygen-Mg^{2+} interactions evident with ATP. As a consequence of the oxophilic/thiophilic nature of

Mg^{2+}, the Rp diastereoisomer of ATPβS should be a substrate but the Sp ATPβS would be expected to be significantly worse substrate.

The results of our steady-state kinetic analysis (Table 5.2) show very little variation between the rate constants (V_{max}) and the binding constants (K_M) for each substrate.

Substrate	K_M (μM)	V_{max} (μM min^{-1} μg^{-1})
ATP	16.5 ± 3.1	1.03 ± 0.06
ATPβS (Rp)	20.1 ± 2.7	0.69 ± 0.04
ATPβS (Sp)	30.3 ± 8.6	1.52 ± 0.17

Table 5.2 Kinetic parameters derived from steady-state analysis.

These results can be rationalised by considering that the rate-limiting step for the reaction is not the chemical step. Although the constraints imposed by the active site that determine diastereoselectivity would still occur, they would only have a nominal affect on the overall rate of reaction resulting in no observable difference in the V_{max} or K_M between ATPβS (Rp) or ATPβS (Sp). Furthermore the presence of a phosphorothioate group that would be expected to decelerate the enzymatic reaction due to the intrinsic differences between nucleophilic substitution at P=O and P=S centres would lead to little or no change in the overall rate.

Our conclusion is consistent with a recent publication that concluded that the chemical transformation step is not rate-limiting in the reaction catalysed by *E.coli* HPPK.[149] This result is significant as the chemical step catalysed by pyrophosphoryl transfer enzymes has been suspected to be the cause of their low k_{cat} values.[147] This is due to greater electron density at the Pβ of ATP which makes nucleophilic substitutions at this centre intrinsically more difficult than at Pα or Pγ.

Their conclusion was based on the fact that the rate constant for the chemical transformation step (k_3 = 16 s^{-1}; measured by pre-steady state kinetics), Scheme 5.2, is >20 times the rate constant of the steady-state phase (k_{cat} = 0.71 s^{-1}; representing the overall

turnover number). Thus, the small k_{cat} of the HPPK is not due to the chemical step but rather due to a slow step or steps after the pyrophosphoryl transfer.

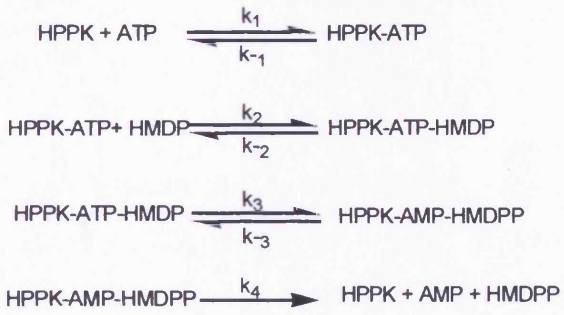

Scheme 5.2 Kinetic mechanism of HPPK.

The rate-limiting step may be due to the slow release of products or a slow step involving a conformational change step after the chemical step. These proposals are consistent with the observations made from a comparison of the crystal structures of the unligated HPPK[77] and its complex with HMDP, AMPCPP (a nonhydrolysable ATP analogue), and two Mg^{2+} ions.[76] These crystal structures suggest that in the ternary complex HPPK·Mg^{2+}·AMPCPP·HMDP the active centre is sealed by the movement of three catalytic loops. Consequently the reactants are buried in the active centre when the chemical step occurs suggesting that a second conformational change would be required to release the products. The opening of the active centre could be rate-limiting if it is slow relative to the chemical step.[149]

5.5 Conclusion.

Our kinetic analysis suggests that either diastereoisomer of ATPβS would be suitable to use as a chiral alternative to ATP in our stereochemical study (Chapter 4). Furthermore our results are consistent with the rate-limiting step of the HPPK catalysed reaction not being the pyrophosphoryl transfer.

CHAPTER 6
Experimental

6.1 General Conditions.

6.1.1 Materials.

Escherichia coli HPPK was supplied by Jeremy Derrick, Department of Biomolecular Sciences, UMIST PO Box 88, Manchester M60 1QD, United Kingdom. All other chemicals and solvents were obtained from Aldrich Chemical Company Ltd, Lancaster Synthesis or Sigma Chemical Company Ltd.

6.1.2 Methods and Instrumentation.

Melting points were determined on a Kofler Hot Stage apparatus and are uncorrected.

Thin Layer Chromatography (TLC) analysis was conducted on standard commercial aluminium sheet pre-coated with a 0.2 mm layer of silica gel F_{254} (Merck 5554) and were visualised by short wave ultraviolet light (UV). Flash chromatography was carried out according to Still's method using sorbisol C-60 silica gel, 40-60 μm.[156]

Infrared spectra (IR) were recorded on a Perkin Elmer 298 IR spectrometer in units of cm^{-1}, the samples prepared as solution cells in CH_2Cl_2 unless otherwise stated. The peaks are referred to as very strong (vs), strong (s), medium (m) or weak (w). Optical rotations were measured using a Perkin Elmer 341 polarimeter, the values given in units of 10^{-1} deg cm^2g^{-1}. Mass spectra were recorded on a Kratos Concept Sector double focusing mass spectrometer using electron impact (EI) at 70eV and 170 °C or fast atom bombardment (FAB) ionisation.

^1H and ^{13}C NMR spectra were recorded on a bruker ARX250 spectrometer (250MHz for ^1H and 62.9MHz for ^{13}C) unless otherwise specified. Spectra were recorded in deuterochloroform ($CDCl_3$) unless otherwise stated, with chemical shift values quoted in p.p.m. relative to tetramethyl silane (TMS) internal standard and $CDCl_3$ (^1H, δ7.27; ^{13}C, δ77.0), and are reported as positive when downfield from the standard. *J* values are given

in hertz (Hz). The following abbreviations are used: (s)-singlet, (d)-doublet, (t)-triplet, (q)-quartet, (quin)-quintet, (m)-multiplet, and (br)-broad. ^{13}C spectra were proton decoupled and multiplicities were determined by performing DEPT experiments at 90° and 135°.

All organic extracts were dried over anhydrous sodium sulphate or anhydrous magnesium sulphate, and solvents were removed *in vacuo* by means of a Buchi rotary evaporator.

6.1.3 Anion-exchange chromatography using DEAE-Sephadex A25 resin.

Diethylaminoethyl (DEAE) Sephadex provides a convenient support for the separation of negatively charged molecules. 1 M TEAB buffer was prepared by bubbling CO_2 (produced from dry ice) through a 1 M solution of freshly distilled triethylamine until the pH was approximately 7.6. The buffer was stored at 4°C for up to three months. Approximately 20 g DEAE-Sephadex A25 (Pharmacia) was activated from powder by treatment overnight with 1 M NH_4HCO_3. The swelled resin was then washed thoroughly with water and stored in a sealed beaker at 4°C in a fridge. A suitably sized glass column was filled with resin that was packed and equilibrated with water. The sample was loaded onto the column *via* a peristaltic pump (LKB) and eluted with approximately 20 column volumes of a linear concentration gradient of TEAB. The elute was monitored spectroscopically at 260 nm and collected in a fraction collector. Used Sephadex was regenerated by treatment with 1 M NH_4HCO_3 followed by water.

6.1.4 High Performance Liquid Chromatography (HPLC).

Reverse phase HPLC was used both analytically and preparatively to separate mixtures of nucleotides. Separations were performed on a Shimadzu LC-4A fitted with a Shimadzu CR2 AX chart recorder. For analytical separations a 5 μm ODS-hypersil 250 mm x 4.6 mm C18 reverse phase column (FSA chromatography) was used while a larger S5ODS2 20 mm x 250 mm reverse phase column was used for preparative purposes. Conditions were based on those reported by Lazewska and Granowski;[157] Marquetant and Goody.[158] The column was equilibrated with 100 mM TEAB (pH 7.6) at a flow rate of 1.5-2.0

cm^3/min. or 8 cm^3/min. for the analytical or preparative column respectively. Between 12 nmoles (analytical column) and 60 μmoles (preparative column) of nucleotide in 24 μl to 2000 μl was injected *via* a Rheodyne loop onto the column and eluted with a linear gradient of acetonitrile. The gradients used varied for different experiments up to 20% acetonitrile. For the separations of the diastereoisomers of $ATP_{\beta}S$ 20 mM $MgCl_2$ was included in the TEAB buffer. It was important not to exceed 20% acetonitrile in the $MgCl_2$ experiments because $MgCl_2$ was insoluble at high acetonitrile concentrations.

6.2 Synthesis of (Racemic at Pα) adenosine 5'-O-(1-thiotriphosphate), (ATPαS) **(41)**.[159] Beilstein Registry Number 1235596, CAS Registry Number 29220-54-0

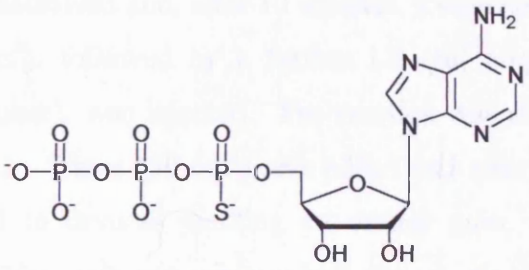

(41)

2',3'-Di-O-acetyl adenosine **(130)** (0.352 g, 1 mmol) was dissolved in dry pyridine (20 cm^3) and evaporated to dryness. The residue was further dried over phosphorus pentoxide under vacuum for 1 hour. Argon was introduced into the reaction flask, which was sealed with a rubber septum. A small positive pressure of argon was maintained in the reaction vessel by connecting an argon-filled balloon. Dry pyridine (1.0 cm^3) was injected through the septum followed by dry dioxane (3.0 cm^3). A freshly prepared 1 M solution of 2-chloro-4H-1,3,2-benzodioxaphophorin-4-one **(131)** (salicyl phosphorochloridite) in dry dioxane (1.1 cm^3, 1.1 μmol), was injected into the stirred solution of the nucleoside and a white precipitate of 2-(2',3'-di-O-acetyladenosyl)-4H-1,3,2-benzodioxaphophorin-4-one **(132)** was formed. After 10 minutes a well-vortexed mixture of a 0.5 M solution of bis(tri-*n*-butylammonium) pyrophosphate in dry pyridine (3.0 cm^3) and tri-*n*-butylamine (1.0 cm^3) was injected.

Bis(tri-*n*-butylammonium) pyrophosphate was prepared according to the procedure of Moffatt[160] as follows. Tetrasodium pyrophosphate decahydrate (2.23 g, 5 mmol) was dissolved in water (50 cm^3). This was passed through a column of Dowex 50WX8-200 in the protonated form. The column was washed with water and the elute dropped directly into a cooled (ice-water) and stirred solution of tri-n-butylamine (2.38 cm^3, 10 mmol) in ethanol (20 cm^3). The column was washed until the pH of the elute increased to 5.0 (approximately 70 cm^3 water). The ethanol/water solution was evaporated to dryness and re-evaporated twice with ethanol and finally with anhydrous DMF (30 cm^3). The residue was dissolved and diluted to 10 cm^3 DMF. The slightly yellow solution was stirred over 4Å molecular sieves.

On addition of bis(tri-*n*-butylammonium) pyrophosphate to the nucleotide, the white precipitate immediately dissolved and, after 10 minutes, a suspension of sulphur (64 mg, 2 mmol) in DMF (2.0 cm^3), followed by a further 1.0 cm^3 aliquot of DMF (to ensure complete transfer of sulphur), was injected. The reaction was stirred for 10 minutes and the septum was removed. Water (50 cm^3) was added and after 30 minutes the reaction mixture was evaporated to dryness yielding an orange gum. This was dissolved in concentrated ammonia (200 cm^3) and ammonolysis was carried out for 5 hours at 25°C. The reaction mixture was evaporated to dryness, and the residue was dissolved in water (50 cm^3) and applied to a DEAE-Sephadex A25 column (2.5 cm x 60 cm) which was eluted with a linear gradient of TEAB (0.2 M-1.0 M; 1.5 L + 1.5 L). The fraction eluting at 650 mM TEAB was co-evaporated with methanol several times to give **(41)** (361 mg, 69%); $\lambda_{max}(H_2O)$/nm 260 (ε/dm^3 mol^{-1} cm^{-1} 14 900); δ_H(300 MHz; D_2O; Me_4Si) 3.98 (1 H, m, C*H*CH_2), 4.01 (2 H, m, CHC*H*$_2$), 4.20 (1 H, m, C*H*OH), 4.60 (1 H, t, *J* 5.2 Hz, C*H*OH), 5.96 (1 H, d, *J* 5.6 Hz, N-CH), 8.22 (1 H, s, N=C-H), 8.43 (1 H, s, N=C-H); δ_C(75.8 MHz; D_2O; Me_4Si) 65.5 (CH_2, d, *J* 5.1 Hz), 70.8 (CH), 73.9 (CH), 83.6 (CH, d, *J* 8.4 Hz), 87.4 (CH), 119.2 (C), 140.1 (CH), 149.6 (C), 151.6 (CH), 155.2 (C); δ_P(101.3 MHz; D_2O, 0.1 M Tris buffer, EDTA (10mM), pH 9.3) 44.9 (d, *J* 34 Hz, P_α), -23.4 (overlapping t, *J* 20 Hz P_β), -9.0 (d, *J* 20 Hz, P_γ); HRMS (FAB) 521.96524 (M^- $C_{10}H_{15}N_5O_{12}P_3S$ requires 521.96509); *m/z* (ES) 522 (M^-, 40%), 442 (100, ADPαS) 362 (45, AMPαS), 95 (70), 79 (100).

6.2.1 Synthesis of the pure diastereoisomers of ATPαS: ATPαS (Rp) **(41a).** Beilstein Registry Number 1235596, CAS Registry Number 58976-48-0 and ATPαS (Sp) **(41b).** Beilstein Registry Number 1235596, CAS Registry Number 58976-49-1

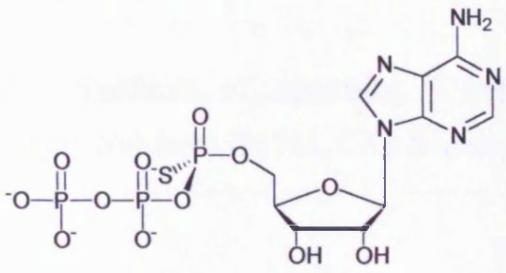

(41a)

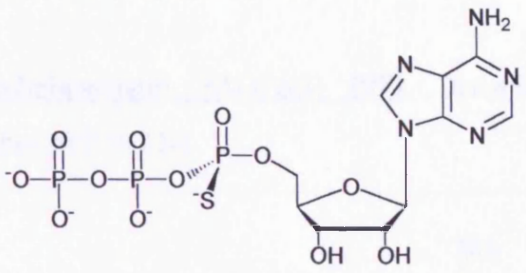

(41b)

The Rp **(41a)** and Sp **(41b)** epimers of ATPαS were prepared from a racemic mixture by preparative reverse phase HPLC. A maximum of 60 μmoles of ATPαS was loaded onto the column which was eluted with a linear gradient of acetonitrile with the Sp epimer eluting before the Rp diastereoisomer. Fractions corresponding to single peaks on the chromatogram were pooled. These were then concentrated on a rotary evaporator, treated with methanol to remove TEAB, and stored at -20°C as an aqueous solution. The isomeric purity of the samples was confirmed by analytical reverse phase HPLC; ATPαS(Rp) **(41a)** (194 mg, 37%); $\lambda_{max}(H_2O)$/nm 260 (ε/dm^3 mol^{-1} cm^{-1} 14 900); δ_H(300 MHz; D_2O; Me_4Si) 3.98 (1 H, m, C*H*CH_2), 4.01 (2 H, m, CHCH_2), 4.20 (1 H, m, C*H*OH), 4.60 (1 H, t, *J* 5.2 Hz, C*H*OH), 5.96 (1 H, d, *J* 5.6 Hz, N-CH), 8.22 (1 H, s, N=C-H), 8.43 (1 H, s, N=C-H); δ_C(75.8 MHz; D_2O; Me_4Si) 65.5 (CH_2, d, *J* 5.1 Hz), 70.8 (CH), 73.9 (CH), 83.6 (CH, d, *J* 8.4 Hz), 87.4 (CH), 119.2 (C), 140.1 (CH), 149.6 (C), 151.6 (CH), 155.2 (C); δ_P(101.3 MHz; D_2O, 0.1 M Tris buffer, EDTA (10mM), pH 9.3) 42.44 (d, *J* 28 Hz, P_α), -23.13 (m, P_β), -6.19 (d, *J* 20 Hz, P_γ); HRMS (FAB) 521.96524 (M^- $C_{10}H_{15}N_5O_{12}P_3S$ requires 521.96509); *m/z* (ES) 522 (M^-, 40%), 442 (100, ADPαS) 362 (45, AMPαS), 95 (70), 79 (100). ATPαS(Sp) **(41b)** (189 mg, 36%); $\lambda_{max}(H_2O)$/nm 260 (ε/dm^3 mol^{-1} cm^{-1} 14 900); δ_H(300 MHz; D_2O; Me_4Si) 3.98 (1 H, m, C*H*CH_2), 4.01 (2 H, m, CHCH_2), 4.20 (1 H, m, C*H*OH), 4.60 (1 H, t, *J* 5.2 Hz, C*H*OH), 5.96 (1 H, d, *J* 5.6 Hz, N-CH), 8.22 (1 H, s, N=C-H), 8.43 (1 H, s, N=C-H); δ_C(75.8 MHz; D_2O; Me_4Si) 65.5 (CH_2, d, *J* 5.1 Hz), 70.8 (CH), 73.9 (CH), 83.6 (CH, d, *J* 8.4 Hz), 87.4 (CH), 119.2 (C), 140.1 (CH), 149.6 (C), 151.6

(CH), 155.2 (C); δ_P(101.3 MHz; D_2O, 0.1 M Tris buffer, EDTA (10mM), pH 9.3) 42.75 (d, *J* 28 Hz, P_α), -23.11 (m, P_β), -6.20 (d, *J* 20 Hz, P_γ); HRMS (FAB) 521.96524 (M^- $C_{10}H_{15}N_5O_{12}P_3S$ requires 521.96509); *m/z* (ES) 522 (M^-, 40%), 442 (100, ADPαS) 362 (45, AMPαS), 95 (70), 79 (100).

6.3 Synthesis of adenosine 5`-O-(-1-thiodiphosphate), (ADPαS) **(97).** Beilstein Registry Number 1193312, CAS Registry Number 51777-22-1

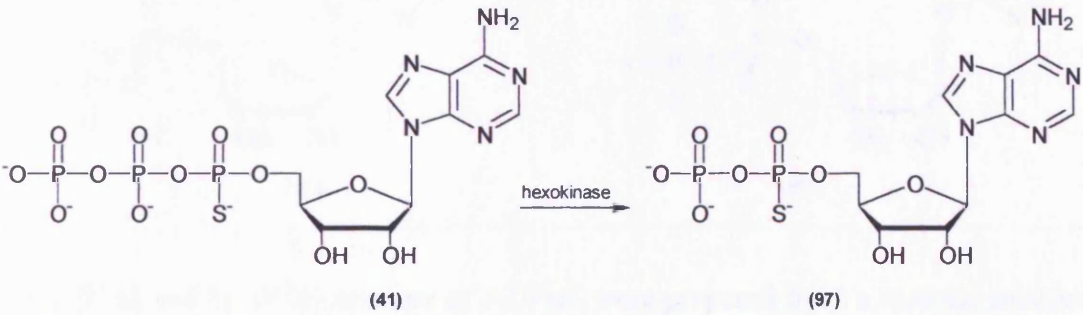

(41) (97)

Hexokinase was used to degrade a racemic mixture of ATPαS **(141)** to racemic ADPαS (97). The reaction conditions for the hexokinase catalysed reaction were as follows: 50 mM Tris.HCl (pH 8.0), 100 mM KCl, 1 mM DTT, 4 mM $MgCl_2$, 1 mM ATPαS **(41)** (racemic), 1 mM glucose, hexokinase (400 µl, 250 units), water to a final volume of 25 cm^3. The reaction was incubated at 25°C for 4 hours. The reaction was monitored by removing aliquots at various times and extracting with an equal volume of chloroform/isoamyl alcohol followed by HPLC analysis.

After 4 hours the reaction was stopped by passage through Chelex 100 and the ADPαS **(97)** was purified by anion-exchange chromatography. After removal of triethylammonium bicarbonate, an aqueous solution of the triethylammonium salt of ADPαS **(97)** was stored at -20°C; (24 mg, 56%) $\lambda_{max}(H_2O)$/nm 260 (ε/dm^3 mol^{-1} cm^{-1} 14 900); δ_H(300 MHz; D_2O; Me_4Si) 3.98 (1 H, m, C*H*CH_2), 4.01 (2 H, m, CHC*H*$_2$), 4.20 (1 H, m, C*H*OH), 4.60 (1 H, t, *J* 5.2 Hz, C*H*OH), 5.96 (1 H, d, *J* 5.6 Hz, N-CH), 8.22 (1 H, s, N=C-H), 8.43 (1 H, s, N=C-H); δ_C(75.8 MHz; D_2O; Me_4Si) 65.5 (CH_2, d, *J* 5.1 Hz), 70.8 (CH), 73.9 (CH), 83.6 (CH, d, *J* 8.4 Hz), 87.4 (CH), 119.2 (C), 140.1 (CH), 149.6 (C), 151.6 (CH), 155.2 (C); δ_P(101.3 MHz; D_2O) 41.50 (d, *J* 31 Hz, P_α), -7.50 (d, *J* 31 Hz, P_β); HRMS (FAB) 441.99877 (M^-

$C_{10}H_{14}N_5O_9P_2S$ requires 441.99875); *m/z* (ES) 442 (M^-, 40%), 362 (45, AMPαS), 95 (70), 79 (100).

6.3.1 Preparation of the pure diastereoisomers of ADPαS: ADPαS (Rp) **(97a)**. Beilstein Registry Number 1193312, CAS Registry Number 59286-20-3 and ADPαS (Sp) **(97b)**. Beilstein Registry Number 1193312, CAS Registry Number 59331-71-4

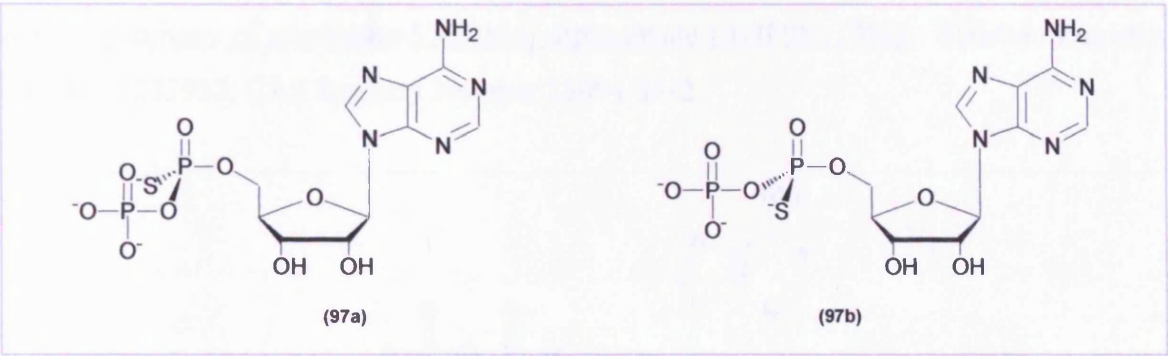

The Rp **(97a)** and Sp **(97b)** epimers of ADPαS were prepared from a racemic mixture by preparative reverse phase HPLC. A maximum of 60 μmoles of ADPαS was loaded onto the column which was eluted with a linear gradient of acetonitrile with the Sp epimer eluting before the Rp. Fractions (1 cm^3) were collected and the A260 of each was verified on a spectrophotometer before fractions corresponding to single peaks on the chromatogram were pooled. These were then concentrated on a rotary evaporator, treated with methanol to remove TEAB, and stored at -20°C as an aqueous solution. The isomeric purity of the samples was confirmed by analytical reverse phase HPLC; ADPαS(Rp) **(97a)** (9 mg, 38%) $\lambda_{max}(H_2O)$/nm 260 (ε/dm^3 mol^{-1} cm^{-1} 14 900); δ_H(300 MHz; D_2O; Me_4Si) 3.98 (1 H, m, C*H*CH_2), 4.01 (2 H, m, CHC*H*$_2$), 4.20 (1 H, m, C*H*OH), 4.60 (1 H, t, *J* 5.2 Hz, C*H*OH), 5.96 (1 H, d, *J* 5.6 Hz, N-CH), 8.22 (1 H, s, N=C-H), 8.43 (1 H, s, N=C-H); δ_C(75.8 MHz; D_2O; Me_4Si) 65.5 (CH_2, d, *J* 5.1 Hz), 70.8 (CH), 73.9 (CH), 83.6 (CH, d, *J* 8.4 Hz), 87.4 (CH), 119.2 (C), 140.1 (CH), 149.6 (C), 151.6 (CH), 155.2 (C); δ_P(101.3 MHz; D_2O) 41.50 (d, *J* 31 Hz, P_α), -7.50 (d, *J* 31 Hz, P_β); HRMS (FAB) 441.99877 (M^- $C_{10}H_{14}N_5O_9P_2S$ requires 441.99875); *m/z* (ES) 442 (M^-, 40%), 362 (45, AMPαS), 95 (70), 79 (100). ADPαS(Sp) **(97b)**(10 mg, 41%) $\lambda_{max}(H_2O)$/nm 260 (ε/dm^3 mol^{-1} cm^{-1} 14 900); δ_H(300 MHz; D_2O; Me_4Si) 3.98 (1 H, m, C*H*CH_2), 4.01 (2 H, m, CHC*H*$_2$), 4.20 (1 H, m, C*H*OH), 4.60 (1 H, t, *J* 5.2 Hz, C*H*OH), 5.96 (1 H, d, *J* 5.6 Hz, N-CH), 8.22 (1 H, s, N=C-

H), 8.43 (1 H, s, N=C-H); δ_C(75.8 MHz; D_2O; Me_4Si) 65.5 (CH_2, d, *J* 5.1 Hz), 70.8 (CH), 73.9 (CH), 83.6 (CH, d, *J* 8.4 Hz), 87.4 (CH), 119.2 (C), 140.1 (CH), 149.6 (C), 151.6 (CH), 155.2 (C); δ_P(101.3 MHz; D_2O) 41.50 (d, *J* 31 Hz, P_α), -7.50 (d, *J* 31 Hz, P_β); HRMS (FAB) 441.99877 (M^- $C_{10}H_{14}N_5O_9P_2S$ requires 441.99875); *m/z* (ES) 442 (M^-, 40%), 362 (45, AMPαS), 95 (70), 79 (100).

6.4 Synthesis of adenosine-5'[β-thio] diphosphate (ADPβS) **(96c).** Beilstein Registry Number 1233937, CAS Registry Number 35094-45-2

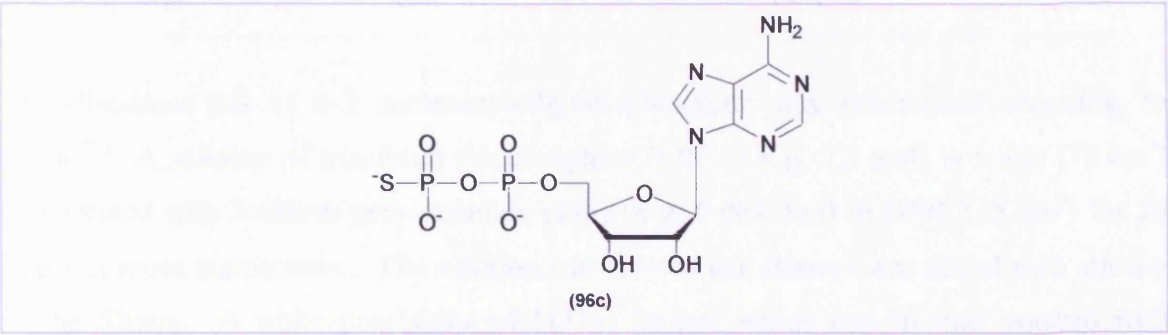

(96c)

6.4.1 Synthesis of trisodium thiophosphate **(135).** CAS Registry Number 10101-88-9

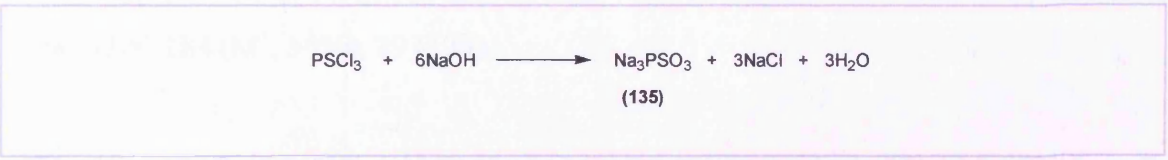

(135)

The trisodium salt of inorganic thiophosphate was synthesised based on the methods of Arnold.[161] Sodium hydroxide pellets (54 g, 1.35 mol) were dissolved in 250 cm^3 water and thiophosphoryl chloride (17.5 cm^3, 0.17 mol), freshly distilled under nitrogen at reduced pressure (20 mmHg), was added. The mixture was stirred at 80°C for 30 minutes, following the reaction by ^{31}P NMR. The clear solution was kept in a fridge at 4°C overnight during which time a white precipitate formed. This was collected by filtration and washed with 100 cm^3 water/ethanol (1:1 ($^v/_v$)).

The precipitate was dissolved in 200 cm^3 water at 50°C and reprecipitated by slow addition of methanol (100 cm^3) under constant rapid stirring. The solution was cooled under tap water, filtered, and the resulting white crystals were washed with ethanol (50

cm^3). The product was made anhydrous by stirring in methanol (200 cm^3) for 90 minutes, filtering and extensive drying *in vacuo* at 80°C to leave the product, trisodium thiophosphate **(135)** as a white powder (8.65 g, 29%); δ_P(101.3 MHz; D_2O) 32.21 (1 P, s); *m/z* (ES) 181 (M^+, 20 %), 139 (100), 107 (80), 105 (90).

6.4.2 Preparation of S-2 carbamoylethylthiophosphate **(137a).** CAS Registry Number 82305-17-7

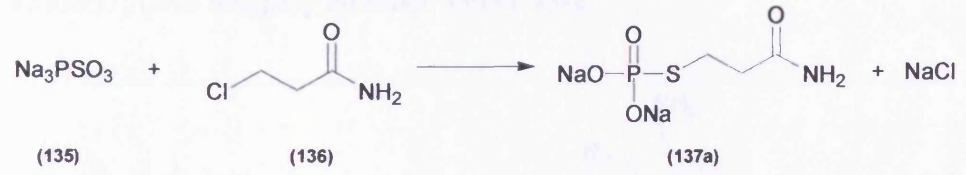

(135) (136) (137a)

The disodium salt of S-2 carbamoylethylthiophosphate was synthesised according to Cook.[162] A solution of trisodium thiophosphate **(135)** (8.8 g, 0.5 mol) in water (75 cm^3) was treated with 3-chloro-propionamide **(136)** (8 g, 0.084 mol) in DMF (15 cm^3) for 24 hours at room temperature. The solution was filtered and ethanol was added with stirring to the filtrate. A white precipitate of **(137a)** formed which was filtered, washed with ethanol, dried in a desiccator and stored at -20°C; (7.33 g, 64%); δ_H(250 MHz; D_2O; Me_4Si) 2.62 (2 H, t, *J* 7.6 Hz, SCH_2CH_2), 2.91 (2 H, m, SCH_2CH_2); δ_C(62.9; D_2O; Me_4Si) 25.9 (CH_2, d, *J* 3 Hz), 37.1 (CH_2, d, *J* 4.7 Hz), 178.6 (CO); δ_P(101.3 MHz; D_2O) 16.5 (1 P, s); *m/z* (ES) 184 (M^+, 50%), 79 (100).

6.4.3 Synthesis of S-2-carbamoylethylthiophosphate (tri-n-butyl ammonium salt) **(137b).** CAS Registry Number 82305-17-7

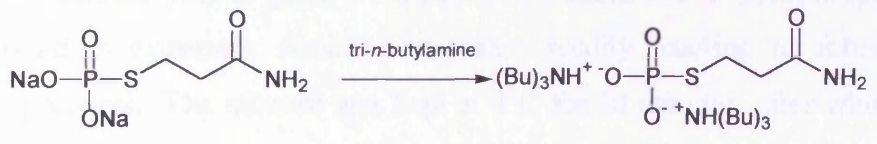

(137a) (137b)

The sodium salt of S-2 carbamoylethylthiophosphate **(137a)** (0.916 g, 4 mmol) was dissolved in water and added to approximately 50 cm^3 Dowex-50 in the pyridinium form. The reaction was done on ice to limit thermal decomposition. The solution was filtered and water was removed by freeze drying. The residue was dissolved in cold methanol

containing tri-*n*-butylamine (950 µl, 4 mmol) and stirred for approximately 30 minutes on ice. After removal of the methanol the slightly yellow oil product **(137b)** was dried by three successive evaporations of 5 cm^3 aliquots of dry pyridine on a cold finger rotary evaporator at low temperature, < 30°C; δ_P(101.3 MHz; D_2O) 16.67 (1 P, s).

6.4.4 Synthesis of adenosine-5'[β-thio] diphosphate (ADPβS) **(96c).** Beilstein Registry Number 1233937, CAS Registry Number 35094-45-2

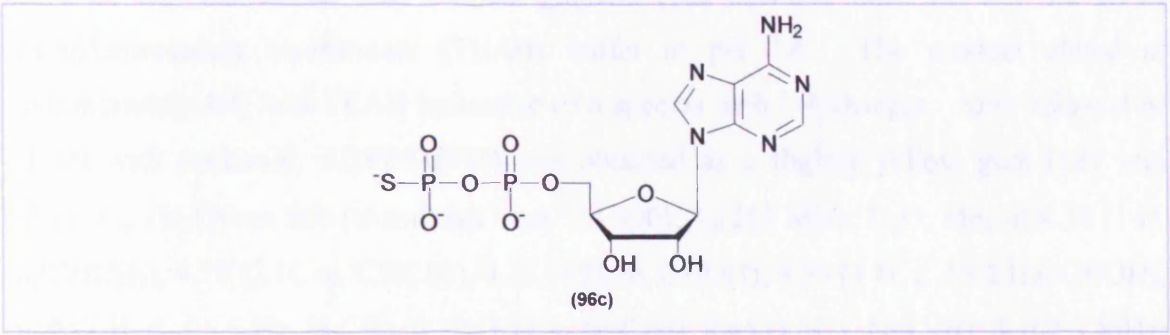

(96c)

The triethylammonium salt of 5'-O-(2-thiodiphosphate) **(96c)** was synthesised following the procedure of Goody and Eckstein.[93] Adenosine 5'-phosphate (free acid, 174 mg, 0.5 mmol) was added to dry methanol (2.5 cm^3) and tri-*n*-octylamine (220 µl, 0.5 mmol) and the mixture was gently warmed until a solution was obtained. The solvent was removed by extensive evaporation on a cold finger rotary evaporator with dry DMF (4x3 cm^3). Dry dioxane (4 cm^3) was added to the residue, followed by dry DMF (600 µl). Diphenylphosphorochloridate (150 µl, 0.72 mmol) and tri-n-butylamine (150 µl) were then added. A white precipitate was formed which redissolved on stirring. After 3 hours at room temperature the solvent was removed by evaporation and dry ether (25 cm^3) was added to the residual yellow gum, P1-diphenyl P2-adenosine 5'-pyrophosphate **(138)**. This compound is extremely sensitive to water, readily reacting to form unwanted dissociation products. The mixture was kept at 4°C for 30 minutes, after which time the ether was removed by decantation. The remaining solid was freed of volatile by evaporation of dry dioxane (3 cm^3) to yield a yellow gum **(138)**, which was used rapidly for subsequent synthetic steps without characterization.

A solution of the tri-n-butylammonium salt of S-2-carbamoylethylthiophosphate **(137b)** (1 mmol) in dry pyridine (3 cm^3) was added to the activated adenosine 5'-phosphate species

(138). The solution was left with stirring at room temperature for 3 hours for a precipitate to form. Activated adenosine 5'-phosphate was only partially soluble in dry pyridine, making precipitate identification difficult. Pyridine was removed on a cold finger rotary evaporator to give P^1-S2-carmaboylethyl P^2-adenosine 5'-pyrophosphate **(139)**. Sodium hydroxide (0.2 M, 40 cm^3) was added to compound **(139)**. The cloudy suspension was heated at 100°C for 10 minutes. After cooling, the mixture was neutralised by passage through Dowex-50 (pyridinium form) and treated with 2-mercaptoethanol (200 μl). The solution was filtered and the filtrate was applied to a DEAE-Sephadex A25 column (1.5 cm x 80 cm) and eluted with a linear gradient (100 mM-600 mM; 1.5 L + 1.5 L) of triethylammonium bicarbonate (TEAB) buffer at pH 7.6. The product eluted at approximately 460 mM TEAB indicative of a species with 2-4 charges. After removal of TEAB with methanol, ADPβS **(96c)** was obtained as a slightly yellow gum (137 mg, 62%); $\lambda_{max}(H_2O)$/nm 260 (ε/dm^3 mol^{-1} cm^{-1} 14 900); δ_H(250 MHz; D_2O; Me_4Si) 4.14 (1 H, m, C*H*CH_2), 4.19 (2 H, m, CHC*H*$_2$), 4.21 (1 H, m, C*H*OH), 4.30 (1 H, t, *J* 5.2 Hz, C*H*OH), 6.00 (1 H, d, *J* 5.6 Hz, N-CH), 8.10 (1 H, s, N=C-H), 8.46 (1 H, s, N=C-H); δ_C(62.3 MHz; D_2O; Me_4Si) 65.1 (CH_2, d, *J* 5.1 Hz), 70.6 (CH), 74.7 (CH), 84.4 (CH, d, *J* 8.4 Hz), 87.2 (CH), 119.2 (C), 140.1 (CH), 149.2 (C), 152.9 (CH), 155.6 (C); δ_P(101.3 MHz; D_2O) 32.85 (d, *J* 34.5 Hz, P_β), -11.7 (d, *J* 34.5 Hz, P_α); HRMS (FAB) 441.99877 (M^- $C_{10}H_{14}N_5O_9P_2S$ requires 441.99875); *m/z* (ES) 442 (M^-, 40%), 346 (45, AMP), 95 (70), 79 (100).

6.5 Stereospecific enzymatic phosphorylation of ADPβS (96c).

The pure Rp **(42a)** and Sp **(42b)** epimers of ATPβS were prepared from ADPβS **(96c)** by exploiting the stereospecificity of kinase action at prochiral centres using high-energy phosphorylating agents. Procedures were based on those reported by Eckstein and Goody.[104]

6.5.1 Synthesis of the Rp epimer of adenosine 5`-O-(2-thiotriphosphate), ATPβS (Rp) **(42a)**. Beilstein Registry Number 1235599, CAS Registry Number 59261-35-7

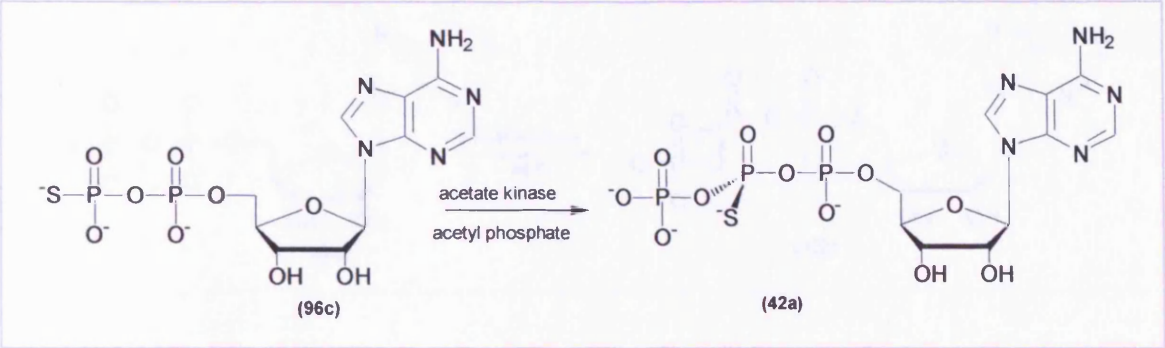

Acetate kinase was used to give entirely the Rp epimer. The reaction conditions for the acetate kinase catalysed reaction were: 50 mM Tris. HCl (pH 8.0), 7.2 mM $MgCl_2$, 1 mM DTT, 3.6 mM ADPβS **(96c)**, 30 mM acetyl phosphate, acetate kinase (400 units). The reaction was incubated at 25°C for 4 hours monitoring the reaction by t.l.c. The reaction was stopped by extracting with an equal volume of chloroform/isoamyl alcohol. Rp ATPβS **(42a)** was purified by ion-exchange chromatography as described for the Sp epimer. A small amount of the reaction mixture was analysed by HPLC as also previously described. After removal of the triethylammonium bicarbonate, an aqueous solution of the triethylammonium salt of the ATPβS(Rp) **(42a)** was stored at -20°C (10 mg, 77%); $\lambda_{max}(H_2O)$/nm 260 (ε/dm^3 mol^{-1} cm^{-1} 14 900); δ_H(250 MHz; D_2O; Me_4Si) 4.14 (1 H, m, C*H*CH_2), 4.19 (2 H, m, CHC*H*$_2$), 4.21 (1 H, m, C*H*OH), 4.30 (1 H, t, *J* 5.2 Hz, C*H*OH), 6.00 (1 H, d, *J* 5.6 Hz, N-CH), 8.10 (1 H, s, N=C-H), 8.46 (1 H, s, N=C-H); δ_C(62.3 MHz; D_2O; Me_4Si) 65.1 (CH_2, d, *J* 5.1 Hz), 70.6 (CH), 74.7 (CH), 84.4 (CH, d, *J* 8.4 Hz), 87.2 (CH), 119.2 (C), 140.1 (CH), 149.2 (C), 152.9 (CH), 155.6 (C); δ_P(101.3 MHz; D_2O, 0.1 M Tris buffer, EDTA (10 mM), pH 9.3) 29.8 (t, *J* 26.4 Hz, P_β), -10.1 (d, *J* 26.4 Hz, P_γ) – 11.8 (d, *J* 26.4 Hz P_α); HRMS (FAB) 521.96524 (M^- $C_{10}H_{15}N_5O_{12}P_3S$ requires 521.96509); *m/z* (ES) 522 (M^-, 40%), 442 (ADPβS), 346 (45, AMP), 95 (70), 79 (100).

6.5.2 Synthesis of the Sp epimer of adenosine 5`-O-(2-thiotriphosphate), ATPβS (Sp) **(42b)**. Beilstein Registry Number 1235599, CAS Registry Number 59261-36-8.

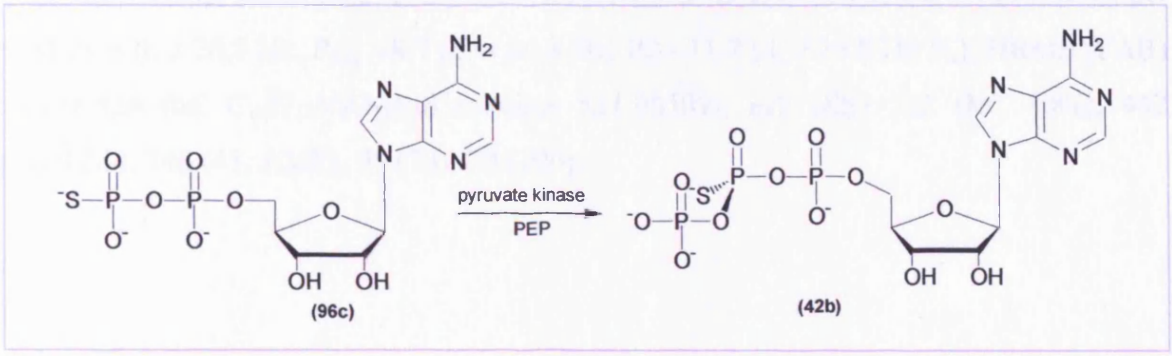

Pyruvate kinase was used to give predominantly the Sp epimer of ATPβS while hexokinase was used to degrade contaminating amounts of the Rp epimer.

The reaction conditions for the pyruvate kinase catalysed reaction were as follows: 50 mM Tris.HCl (pH 8.0), 200 mM KCl, 1 mM DTT, 4 mM $MgCl_2$, 2 mM ADPβS, 2.2 mM PEP, 0.7 mg pyruvate kinase (350 units), water to a final volume of 27 cm^3. The reaction was incubated at 25°C for 4 hours and the progress was monitored by t.l.c. After 4 hours the reaction was stopped by extraction with an equal volume of chloroform/isoamyl alcohol. The aqueous layer was loaded onto a DEAE-Sephadex column and eluted with TEAB in the usual way. A small amount of the reaction mixture was retained for analysis by HPLC.

The isolated Sp ATPβS **(42b)** contained significant amounts of the Rp epimer. This was degraded to ADPβS **(96c)** using the following conditions: 50 mM Tris.HCl (pH 8.0), 100 mM KCl, 1 mM DTT, 4 mM $MgCl_2$, 1 mM ATPβS(Sp) **(42b)**, 1 mM glucose, hexokinase (400 µl, 250 units), water to a final volume of 25 cm^3. Aliquots were removed at various times and extracted with an equal volume of chloroform/isoamyl alcohol before analysis by HPLC to monitor the reaction. The reaction was stopped by passage through Chelex 100 (Sigma) and the pure ATPβS(Sp) **(42b)** was purified by ion-exchange. After removal of triethylammonium bicarbonate, an aqueous solution of the triethylammonium salt of ATPβS(Sp) **(42b)** was stored at -20°C (10 mg, 77%); $\lambda_{max}(H_2O)$/nm 260 (ε/dm^3 mol^{-1} cm^{-1} 14 900); δ_H(250 MHz; D_2O; Me_4Si) 4.14 (1 H, m, C*H*CH_2), 4.19 (2 H, m, CHC*H*$_2$), 4.21 (1 H, m, C*H*OH), 4.30 (1 H, t, *J* 5.2 Hz, C*H*OH), 6.00 (1 H, d, *J* 5.6 Hz, N-CH), 8.10 (1 H,

s, N=C-H), 8.46 (1 H, s, N=C-H); δ_C(62.3 MHz; D_2O; Me_4Si) 65.1 (CH_2, d, *J* 5.1 Hz), 70.6 (CH), 74.7 (CH), 84.4 (CH, d, *J* 8.4 Hz), 87.2 (CH), 119.2 (C), 140.1 (CH), 149.2 (C), 152.9 (CH), 155.6 (C); δ_P(101.3 MHz; D_2O, 0.1 M Tris buffer, EDTA (10 mM), pH 9.3) 29.6 (t, *J* 26.8 Hz, P_β), -8.7 (d, *J* 26.8 Hz, P_γ) –11.7 (d, *J* 26.8 Hz P_α); HRMS (FAB) 521.96524 (M^- $C_{10}H_{15}N_5O_{12}P_3S$ requires 521.96509); *m/z* (ES) 522 (M^-, 40%), 442 (ADPβS), 346 (45, AMP), 95 (70), 79 (100).

6.6 Synthesis of (Sp)-adenosine-5'-[β-thio] triphosphate (ATPβS) **(42b)** *via* the ephedrine route.[36] Beilstein Registry Number 1235599, CAS Registry Number 59261-36-8

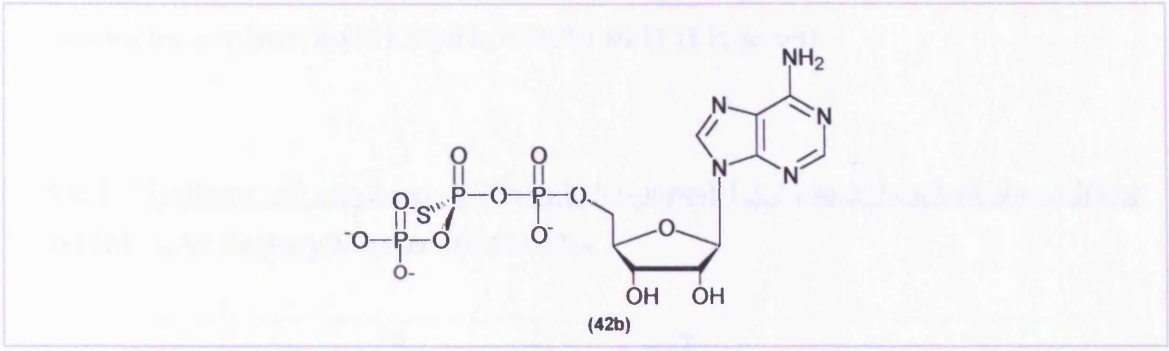

(42b)

6.6.1 Synthesis of cis (4S,5R)-2-chloro-3,4-dimethyl-5-phenyl-1,3,2 oxazaphospholidine-2-thione **(107a).**[36] Beilstein Registry Number 1075999, CAS Registry Number 57651-34-0

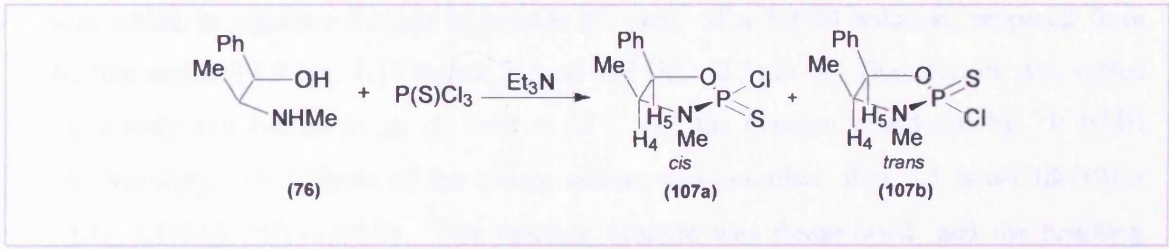

(76) (107a) (107b)

A solution of thiophosphoryl chloride (4.1 cm^3, 41 mmol) in benzene (25 cm^3) was slowly added to a suspension of (-)-ephedrine hydrochloride **(76)** (8.2 g, 50 mmol) in triethylamine (34.5 cm^3, 247 mmol) and benzene (150 cm^3). The white suspension was stirred under nitrogen for 15 hours at room temperature and then poured into an excess of water. The organic layer was isolated and the aqueous layer extracted with more benzene (3 x 50 cm^3), the combined organic extracts were dried (Na_2SO_4), filtered and the solvent was removed in vacuo. The resulting light brown oil was purified by silica flash chromatography [light petroleum - chloroform (3:1), R.f. = 0.42]. The fractions containing product were collected and the solvent was removed in vacuo. The resulting off-white solid was recrystallised from di-isopropyl ether to give the cis epimer **(107a)** as shiny white crystals (5.7 g, 53%), m.p. 125-127 °C (Lit.,[96] 125-128 °C); δ_H(300 MHz; $CDCl_3$; Me_4Si) 1.01 (3 H, d, *J* 6.90 Hz, CH_3), 3.04 (3 H, d, $^3J_{PH}$ 14.69 Hz, NCH_3), 3.96 (1 H, dquin, *J* 6.65 Hz, $^3J_{PH}$ 28.7 Hz, H-4), 5.96 (1 H, br d, *J* 6.43 Hz, H-5), 7.48 (5 H, m, Ph);

δ_C(62.9 MHz; $CDCl_3$; Me_4Si) 12.5 (CH_3), 29.7 (CH_3, d, *J* 6.6 Hz), 61.1 (CH, d, *J* 9.6 Hz), 84.4 (CH, d, *J* 3.0 Hz), 126.4 (CH), 128.7 (2 CH), 128.9 (2 CH), 135.1 (C, d, *J* 7.7 Hz); δ_P(101.3 MHz; $CDCl_3$) 75.12 (1 P, sextet); HRMS (FAB) 262.02226 (M^+ $C_{10}H_{14}NO^{35}ClPS$ requires 262.02223); *m/z* (FAB) 262 (M^+, 40%), 148 (100). Selected data for trans epimer; δ_P(101.3 MHz; $CDCl_3$) 80.11 (1 P, sextet).

6.6.2 Synthesis of cis 2-oxy-3,4-dimethyl-5-phenyl-1,3,2-oxazaphospholidine-2-thione **(110b)**. CAS Registry Number 105229-43-4

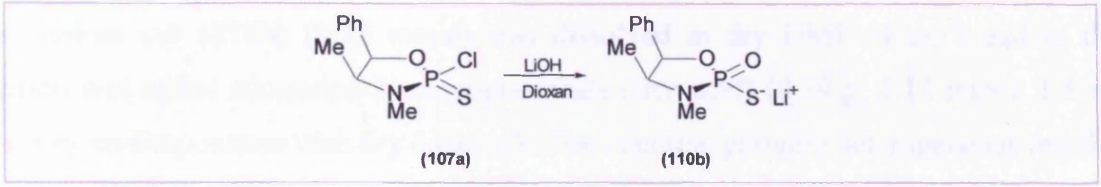

(107a) (110b)

Purified cis 2-chloro-3,4-dimethyl-5-phenyl-1,3,2-oxazaphospholidine-2-thione **(107a)** (0.2 g, 0.075 mmol) was dissolved in dry dioxane (1.5 cm^3) and this colourless solution was added to aqueous lithium hydroxide [0.5 cm^3 of a 3.4 M solution; prepared from lithium metal (11.9 mg, 1.17 mmol, 2.2 eq) and H_2O (0.5 cm^3)]. This mixture was stirred vigorously and heated in an oil bath at 35°C and the reaction monitored by ^{31}P NMR spectroscopy. Hydrolysis of the chloro adduct was complete after 5.5 hours (δ_P(101.3 MHz; $CDCl_3$) 75.2→ 70.9). The reaction mixture was freeze-dried, and the resulting white solid was then redissolved in dry dioxane (2 cm^3) and freeze-dried twice to give the hydrolysed product, cis 2-oxy-3,4-dimethyl-5-phenyl-1,3,2-oxazaphospholidine-2-thione **(110b)** as the lithium salt in essentially a quantitative yield.

6.6.3 P—N bond cleavage of cis 2-oxy-3,4-dimethyl-5-phenyl-1,3,2-oxazaphospholidine-2-thione **(110b).**

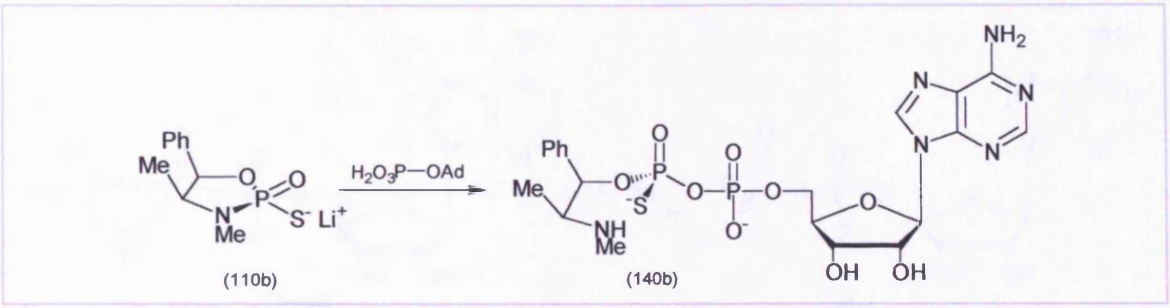

(110b) (140b)

The lithium salt **(110b)** (0.75 mmol) was dissolved in dry DMF (4 cm^3) and to this solution was added adenosine-5'-monophosphate (free acid) (0.39 g, 1.12 mmol, 1.5 eq) (dried by co-evaporation with dry dioxane). The resulting partially heterogeneous reaction mixture was vigorously stirred at 60°C in an oil bath and the reaction monitored by ^{31}P NMR spectroscopy. After 8 hours, the ^{31}P NMR spectrum of the mixture showed no starting material. The reaction mixture was quenched with triethylamine (0.25 cm^3) and water (100 cm^3) and then applied to an ion-exchange column (1.5 x 30 cm) eluting with a linear gradient of 50-200 mM-TEAB, pH = 7.6 (vol. = 2000 cm^3). The flow rate of the buffer through the column was set at 70 cm^3 per hour and the elute monitored at λ = 260 nm.

The P—N bond cleaved product **(140b)** was eluted at a buffer concentration of 60 mM. The appropriate fractions were combined and concentrated under a high vacuum and the residual TEAB was removed as before to leave the product **(140b)** (mono-triethylammonium salt) as a colourless gum [0.54 mmol, 70% (based on UV absorbency at 260 nm]; $\lambda_{max}(H_2O)$/nm 260 (ε/dm^3 mol^{-1} cm^{-1} 14 900); δ_H(250 MHz; CD_3OD; Me_4Si) 1.21 (3 H, d, *J* 6.6 Hz, CHC*H*$_3$), 2.28 (3 H, s, N-CH_3) 3.84 (1 H, m, H-4), 4.41 (1 H, m, C*H*CH_2), 4.44 (2 H, m, CHC*H*$_2$), 4.73 (1 H, m, C*H*OH), 4.90 (1 H, t, *J* 5.2 Hz, C*H*OH), 6.05 (1 H, br s, H-5) 6.25 (1 H, d, *J* 5.6 Hz, N-CH), 7.35-7.70 (5 H, m, Ph), 8.30 (1 H, s, N=C-H), 8.70 (1 H, s, N=C-H); δ_P (101.3 MHz; CD_3OD; Me_4Si) 46.11 (d, *J* 35.6 Hz, Pβ), -10.81 (d, *J* 35.6 Hz, Pα); *m/z* (ES) 589 (M^-, 100%), 346 (10, AMP).

6.6.4 C—O bond cleavage of **(140b)** using Na/liq. NH_3 to give [ADPβS] **(96c).**

Beilstein Registry Number 1233937, CAS Registry Number 35094-45-2

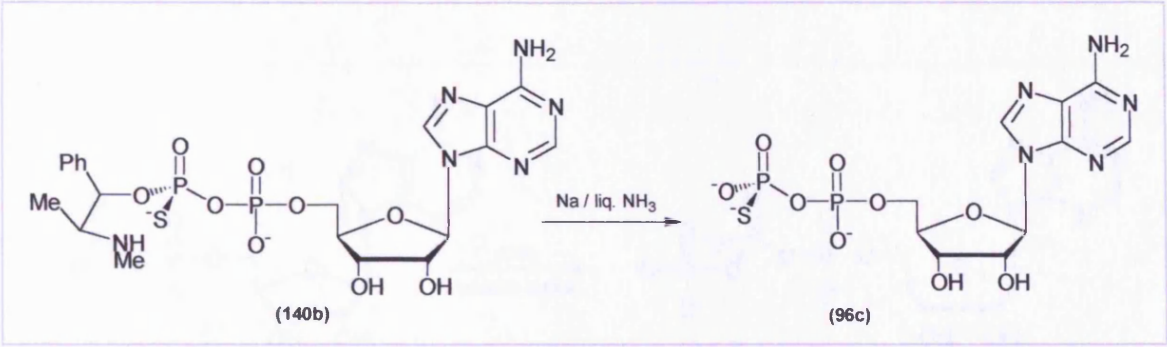

Compound **(140b)** (118 mg, 0.2 mmol) was dissolved in methanol and transferred to a 3-neck round-bottom flask. The methanol was then removed under reduced pressure.

Ammonia (50 cm^3) was condensed at -78°C under dry nitrogen and dried by distillation from sodium. Sodium (69 mg, 3 mmol) was added to the freshly distilled ammonia. When the sodium had dissolved, the resulting dark blue solution was quickly syphoned into the vessel containing **(140b)** *via* a glass tube. The reaction mixture was stirred at -78°C for 4 minutes and then quenched with ammonium chloride (0.6 g). The reaction vessel was removed from the cooling bath and the ammonia allowed to evaporate. The resulting pale yellow residue was dissolved in water (80 cm^3) an applied to an ion-exchange column (1.5 x 20 cm). The column was with 50-900mM-TEAB buffer (vol. = 2000 cm^3, pH = 7.7) at 70 cm^3 per hour. The combined fractions containing the product (eluted at 390 mM buffer concentration) were evaporated under a high vacuum; the residual TEAB was removed as before to leave the product, ADPβS **(96c)** as a yellow gum (49 mg, 0.11 mmol, 55%); $\lambda_{max}(H_2O)$/nm 260 (ε/dm^3 mol^{-1} cm^{-1} 14 900); δ_H(250 MHz; D_2O; Me_4Si) 4.14 (1 H, m, C*H*CH_2), 4.19 (2 H, m, CHC*H*$_2$), 4.21 (1 H, m, C*H*OH), 4.30 (1 H, t, *J* 5.2 Hz, C*H*OH), 6.00 (1 H, d, *J* 5.6 Hz, N-CH), 8.10 (1 H, s, N=C-H), 8.46 (1 H, s, N=C-H); δ_C(62.3 MHz; D_2O; Me_4Si) 65.1 (CH_2, d, *J* 5.1 Hz), 70.6 (CH), 74.7 (CH), 84.4 (CH, d, *J* 8.4 Hz), 87.2 (CH), 119.2 (C), 140.1 (CH), 149.2 (C), 152.9 (CH), 155.6 (C); δ_P(101.3 MHz; D_2O) 32.85 (d, *J* 34.5 Hz, P_β), -11.60 (d, *J* 34.5 Hz, P_α); HRMS (FAB) 441.99877 (M^- $C_{10}H_{14}N_5O_9P_2S$ requires 441.99875); *m/z* (ES) 442 (M^-, 40%), 346 (45, AMP), 95 (70), 79 (100).

6.6.5 Stereospecific enzymatic phosphorylation of ADPβS **(96c)** to give ATPβS (Sp) **(42b)**. Beilstein Registry Number 1235599, CAS Registry Number 59261-36-8

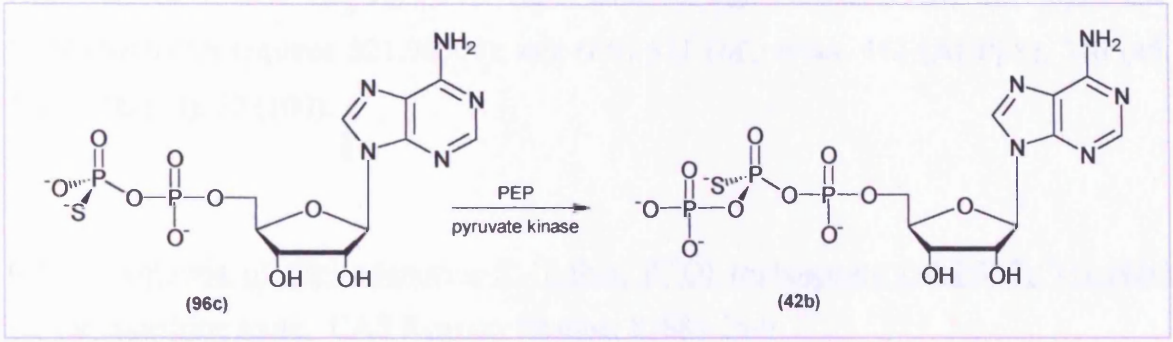

Pyruvate kinase was used to give predominantly the Sp epimer of ATPβS **(42b)** while hexokinase was used to degrade contaminating amounts of the Rp epimer.

The reaction conditions for the pyruvate kinase catalysed reaction were as follows: 50 mM Tris.HCl (pH 8.0), 200 mM KCl, 1 mM DTT, 4 mM $MgCl_2$, 2 mM ADPβS, 2.2 mM PEP, 0.7 mg pyruvate kinase (350 units), water to a final volume of 27 cm^3. The reaction was incubated at 25°C for 4 hours and the progress was monitored by t.l.c. After 4 hours the reaction was stopped by extraction with an equal volume of chloroform/isoamyl alcohol. The aqueous layer was loaded onto a DEAE-Sephadex column and eluted with TEAB in the usual way. A small amount of the reaction mixture was retained for analysis by HPLC.

The isolated Sp ATPβS **(42b)** contained significant amounts of the Rp epimer. This was degraded to ADPβS **(96c)** using the following conditions: 50 mM Tris.HCl (pH 8.0), 100 mM KCl, 1 mM DTT, 4 mM $MgCl_2$, 1 mM ATPβS(Sp) **(42b)**, 1 mM glucose, hexokinase (400 µl, 250 units), water to a final volume of 25 cm^3. Aliquots were removed at various times and extracted with an equal volume of chloroform/isoamyl alcohol before analysis by HPLC to monitor the reaction. The reaction was stopped by passage through Chelex 100 (Sigma) and the pure ATPβS(Sp) **(42b)** was purified by ion-exchange. Removal of triethylammonium bicarbonate, gave the triethylammonium salt of ATPβS (Sp) **(42b)** (15.7 mg, 30 mmol, 54%); $\lambda_{max}(H_2O)$/nm 260 (ε/dm^3 mol^{-1} cm^{-1} 14 900); δ_H(250 MHz; D_2O; Me_4Si) 4.14 (1 H, m, C*H*CH_2), 4.19 (2 H, m, CHC*H*$_2$), 4.21 (1 H, m, C*H*OH), 4.30 (1 H, t, *J* 5.2 Hz, C*H*OH), 6.00 (1 H, d, *J* 5.6 Hz, N-CH), 8.10 (1 H, s, N=C-H), 8.46 (1 H,

s, N=C-H); δ_C(62.3 MHz; D_2O; Me_4Si) 65.1 (CH_2, d, *J* 5.1 Hz), 70.6 (CH), 74.7 (CH), 84.4 (CH, d, *J* 8.4 Hz), 87.2 (CH), 119.2 (C), 140.1 (CH), 149.2 (C), 152.9 (CH), 155.6 (C); δ_P(101.3 MHz; D_2O, 0.1 M Tris buffer, EDTA (10 mM), pH 9.3) 29.6 (t, *J* 26.8 Hz, P_β), -8.7 (d, *J* 26.8 Hz, P_γ) –11.7 (d, *J* 26.8 Hz P_α); HRMS (FAB) 521.96524 (M^- $C_{10}H_{15}N_5O_{12}P_3S$ requires 521.96509); *m/z* (ES) 522 (M^-, 40%), 442 (ADPβS), 346 (45, AMP), 95 (70), 79 (100).

6.7 Synthesis of (Sp)-adenosine-5'-[β-thio, $\beta^{18}O$] triphosphate (ATPβSβγ^{18}O) **(42c)** *via* the ephedrine route. CAS Registry Number 87883-26-9

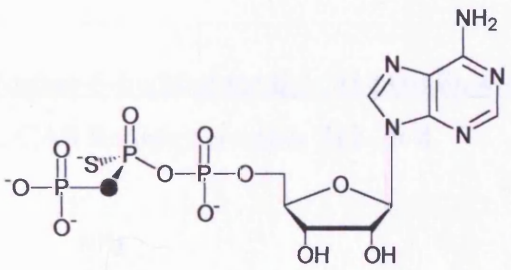

(42c)

This was prepared in the same way as the unlabelled ATPβS (Sp) **(42b)** described above, starting with cis 2-chloro-3,4-dimethyl-5-phenyl-1,3,2-oxazaphospholidine-2-thione **(107a)** (0.2 g, 0.75 mmol) and aqueous Li^{18}OH [0.5 cm^3 of a 3.4 M solution; prepared from lithium metal (11.9 mg, 1.17 mol) and $H_2{}^{18}O$ (0.5 cm^3 of 98% atom excess)]. Subsequent reactions gave ATPβSβγ^{18}O **(42c)** (53 μmol, 74% from ADPβSβ^{18}O); $\lambda_{max}(H_2O)$/nm 260 (ε/dm^3 mol^{-1} cm^{-1} 14 900); δ_H(250 MHz; D_2O; Me_4Si) 4.14 (1 H, m, C*H*CH_2), 4.19 (2 H, m, CHC*H*$_2$), 4.21 (1 H, m, C*H*OH), 4.30 (1 H, t, *J* 5.2 Hz, C*H*OH), 6.00 (1 H, d, *J* 5.6 Hz, N-CH), 8.10 (1 H, s, N=C-H), 8.46 (1 H, s, N=C-H); δ_C(62.3 MHz; D_2O; Me_4Si) 65.1 (CH_2, d, *J* 5.1 Hz), 70.6 (CH), 74.7 (CH), 84.4 (CH, d, *J* 8.4 Hz), 87.2 (CH), 119.2 (C), 140.1 (CH), 149.2 (C), 152.9 (CH), 155.6 (C); δ_P(121.9 MHz; D_2O, 0.1 M Tris buffer, EDTA (10 mM), pH 9.3, mixed with authentic ATPβB [ca. 1:1]) –12.5 (d, $J_{P\alpha OP\beta}$ 27.6 Hz, P_α), 27.74 (dd, ^{18}O isotopomer, ^{18}O isotopic shift = 2.7 Hz, $P_\beta[\beta\gamma^{18}O]$) 27.76 (dd, $J_{P\beta OP\alpha}$ 27.6 Hz, $J_{P\beta OP\gamma}$ 28.9 Hz, $P_\beta[\beta\gamma^{16}O]$), -7.02 (d, $J_{P\gamma OP\beta}$ 28.9 Hz, $P_\gamma[\beta\gamma^{18}O]$), -7.04 (d, ^{18}O isotopomer, ^{18}O isotopic shift = 2.7 Hz, $P_\gamma[\beta\gamma^{18}O]$); 524 ($M^-$, 20%), 444 (55, ADPβSβ^{18}O).

6.8 Synthesis of thiophosphoric acid O-[3-benzyl-2-(dimethylamino-methinimino)-4-oxo-3,4-dihydro-pteridin-6-ylmethyl] ester S-(6,6-dimethyl-bicyclo[3.1.1]hept-2-en-2-ylmethyl) ester **(112b).**

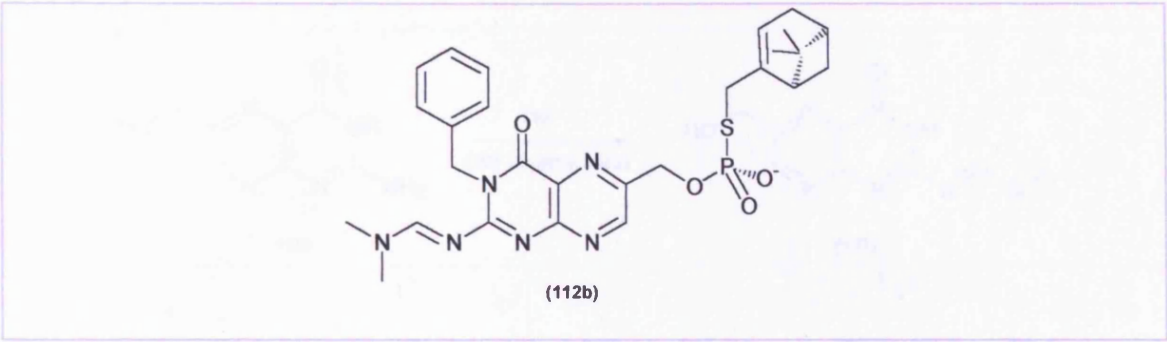

(112b)

6.8.1 Synthesis of 2-Amino-6-hydroxymethyl-3H-pteridin-4-one **(113).**[126] Beilstein Registry Number 183333, CAS Registry Number 712-29-8

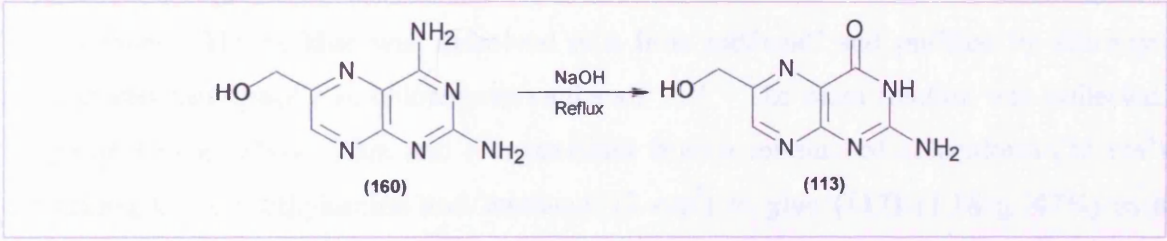

(160) (113)

Compound **(160)** (966 mg, 5 mmol) was heated under reflux in 0.1 M NaOH (200 cm^3) for 2.5 hours. The solution was treated with charcoal, filtered and the warm filtrate acidified by acetic acid. On cooling and standing for several hours the precipitate was collected, washed and dried to give 70-90% yield of pterin **(113)**. Purification was achieved by dissolving the crude material in hot H_2O (75 cm^3) and addition of ammonia. If a red solution was obtained another charcoal treatment was carried out. The hot solution was added dropwise into a hot solution of acetic acid (5%, 150 cm^3) with stirring. The resulting precipitate was collected after cooling overnight (4 °C) to give **(113)** as a yellow crystal powder (676 mg, 70%); m.p. >350°; purity determined by analytical reverse phase HPLC to be 85 % at 254 nm; λ_{max}(0.1 M NaOH)/nm 254 (ε/dm^3 mol^{-1} cm^{-1} 20 867), 364 (7 427); δ_H(250 MHz; 0.1 M NaOD; Me_4Si) 4.58 (2 H, s C(6) H), 4.99 (2 H, s, NH_2), 8.37 (1 H, s, C(7)H); δ_C(62.9 MHz; 0.1 M NaOD; Me_4Si) 63.6 (CH_2), 127.7 (C), 147.9 (CH),

152.1 (C), 155.1 (C), 163. 8 (CO), 173.2 (C); *m/z* (ES) 194 (M^+, 40%), 176 (100), 134 (55), 108 (40), 106 (65).

6.8.2 Synthesis of 2-(N,N-Dimethylaminomethinimino)-6-hydroxymethyl-pteridin-4(3H)-one **(117).**[125,126] CAS Registry Number 222612-05-7

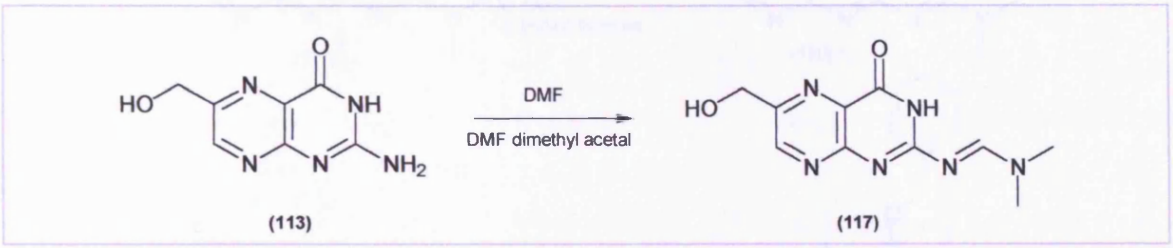

A suspension of 2-amino-6-hydroxymethyl-3H-pteridin-4-one **(113)** (2.0 g, 10,2 mmole) in DMF (200 cm^3) was treated with N,N-dimethylformamide-dimethylacetal (10 cm^3, 75 mmol) at room temperature for 2 hours with stirring. The red-coloured solution was evaporated in high vacuum and co-evaporated with chloroform several times to give a brown foam. The residue was dissolved in a little methanol and purified by silica-gel column chromatography in chloroform/methanol 10:1. The main fraction was collected, evaporated to a yellow foam and recrystallised from a mixture of chloroform (28 cm^3) containing 0.1% triethylamine and methanol (2 cm^3) to give **(117)** (1.18 g, 47%) as a yellow powder of m.p. >350 °C; λ_{max}(0.1 M NaOH)/nm 258 (ε/dm^3 mol^{-1} cm^{-1} 15 883), 364 (6 627); ν_{max}/cm^{-1} (CH_2Cl_2) 3053s, 2985m, 2684w, 2520w, 2409w, 2358w, 2305m, 2126w, 2054w, 1684w, 1631w, 1525w, 1421m, 1259vs, 1155w, 895m, 736vs; δ_H(300 MHz; D_6-DMSO; Me_4Si) 3.08 (3 H, s, N-CH_3), 3.21 (3 H, s, N-CH_3), 4.64 (2 H, d, *J* 4.1 Hz, C(6)H), 5.61 (1 H, t, *J* 4.1 Hz, OH), 8.79 (2 H, s, C(7)H, N=C-H); δ_C(75.8 MHz; D_6-DMSO; Me_4Si) 37.8 (CH_3), 43.1 (CH_3), 65.5 (CH_2, d, *J* 5.1 Hz), 132.1 (C), 151.1 (CH), 154.8 (C), 158.2 (C), 160.8 (CO), 161.9 (CH), 165.1 (C); *m/z* (FAB) 249 (M^+, 100%); HRMS (FAB) 249.11003 (M^+ $C_{10}H_{13}N_6O_2$ requires 249.1100).

6.8.3 Synthesis of N'-(3-Benzyl-6-hydroxymethyl-4-oxo-3,4-dihydro-pteridin-2-yl)-N,N-dimethyl-formamidine **(120).**

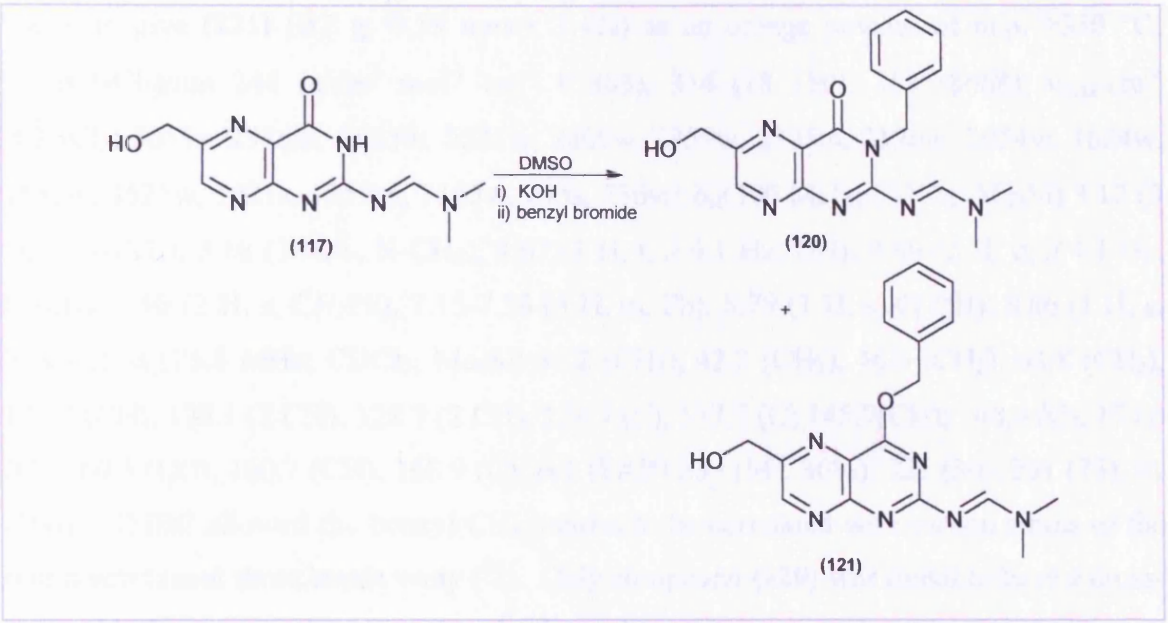

2-(N,N-Dimethylaminomethinimino)-6-hydroxymethyl-pteridin-4(3H)-one **(117)** (2 g, 8 mmol) was dissolved in DMSO (100 cm^3). Benzyl chloride (1.3 g, 0.934 cm^3, 8 mmol) and potassium hydroxide (0.561 g, 10 mmol) were added to this solution and the resulting mixture was stirred at 20°C for 5 hours. The DMSO was removed in vacuo and the resulting residue was suspended with water (400 cm^3) and extracted with dichloromethane (3 x 200 cm^3). The combined organic extracts were dried (Na_2SO_4), filtered and the solvent was removed in vacuo. The resulting yellow oil was purified by silica flash chromatography [dichloromethane - methanol (10:1), R.f. = 0.46]. The fractions containing product were collected and the solvent was removed in vacuo to give **(120)** (1.86 g, 5.48 mol, 69%) as an orange powder of m.p. >350 °C; $\lambda_{max}(CHCl_3)$/nm 244 ($\varepsilon/dm^3\ mol^{-1}\ cm^{-1}$ 9 557), 314 (17 650), 358 (8165); ν_{max}/cm^{-1} (CH_2Cl_2) 3053s, 2986m, 2685w, 2521w, 2409w, 2359w, 2305m, 2126w, 2054w, 1684w, 1631w, 1525w, 1421s, 1259vs, 1155w, 895s, 736vs; δ_H(300 MHz; $CDCl_3$; Me_4Si) 3.12 (3 H, s, N-CH_3), 3.16 (3 H, s, N-CH_3), 3.67 (1 H, t, *J* 4.1 Hz, OH), 4.89 (2 H, d, *J* 4.1 Hz, C(6)H), 5.50 (2 H, s, CH_2Ph), 7.10-7.40 (5 H, m, Ph), 8.79 (1 H, s, C(7)H), 8.82 (1 H, s, N=C-H); δ_C(75.8 MHz; $CDCl_3$; Me_4Si) 36.0 (CH_3), 42.0 (CH_3), 46.6 (CH_2), 63.8 (CH_2), 127.6 (CH), 128.6 (2 CH), 128.7 (2 CH), 129.0 (C), 137.8 (C) 149.2 (CH), 152.7 (C), 154.1 (C), 158.0 (CO), 159.6 (CH), 162.9 (C); *m/z* (FAB) 339 (M^+, 30%), 321 (30), 231 (75), 91 (100); HRMS (FAB) 339.15700 (M^+ $C_{17}H_{19}N_6O_2$ requires 339.15695). The corresponding regioisomer **(121)**

was isolated by silica flash chromatography [dichloromethane - methanol (10:1), R.f. = 0.56]. The fractions containing product were collected and the solvent was removed in vacuo to give **(121)** (0.2 g, 0.59 mmol, 7.4%) as an orange powder of m.p. >350 °C; $\lambda_{max}(CHCl_3)$/nm 244 (ε/dm^3 mol^{-1} cm^{-1} 9 803), 314 (18 350), 358 (8668); ν_{max}/cm^{-1} (CH_2Cl_2) 3053s, 2986m, 2685w, 2521w, 2409w, 2359w, 2305m, 2126w, 2054w, 1684w, 1631w, 1525w, 1421s, 1259vs, 1155w, 895s, 736vs; δ_H(300 MHz; $CDCl_3$; Me_4Si) 3.12 (3 H, s, N-CH_3), 3.16 (3 H, s, N-CH_3), 3.67 (1 H, t, *J* 4.1 Hz, OH), 4.89 (2 H, d, *J* 4.1 Hz, C(6)H), 5.50 (2 H, s, C*H*$_2$Ph), 7.15-7.38 (5 H, m, Ph), 8.79 (1 H, s, C(7)H), 8.86 (1 H, s, N=C-H); δ_C(75.8 MHz; $CDCl_3$; Me_4Si) 36.2 (CH_3), 42.2 (CH_3), 46.6 (CH_2), 63.8 (CH_2), 127.7 (CH), 128.1 (2 CH), 128.7 (2 CH), 129.7 (C), 137.7 (C) 145.7(CH), 148.0 (C), 153.8 (C), 160.3 (CO), 160.7 (CH), 168.9 (C); *m/z* (FAB) 339 (M^+, 30%), 321 (30), 231 (75), 91 (100). HMBC allowed the benzyl CH_2 protons to be correlated with carbon atoms of the pterin substituent three bonds away (^{3}J). Only compound **(120)** was found to have a cross-peak with the pterin carbon bound to the three nitrogen's.

6.8.4 Synthesis of N'-[3-Benzyl-6-(3,4-dimethyl-5-phenyl-2-thioxo-2λ^5 [1,3,2] oxaza-phospholidin-2-yloxymethyl)-4-oxo-3,4-dihydro-pteridin-2-yl]-N,N-dimethyl-formamidine **(123).**

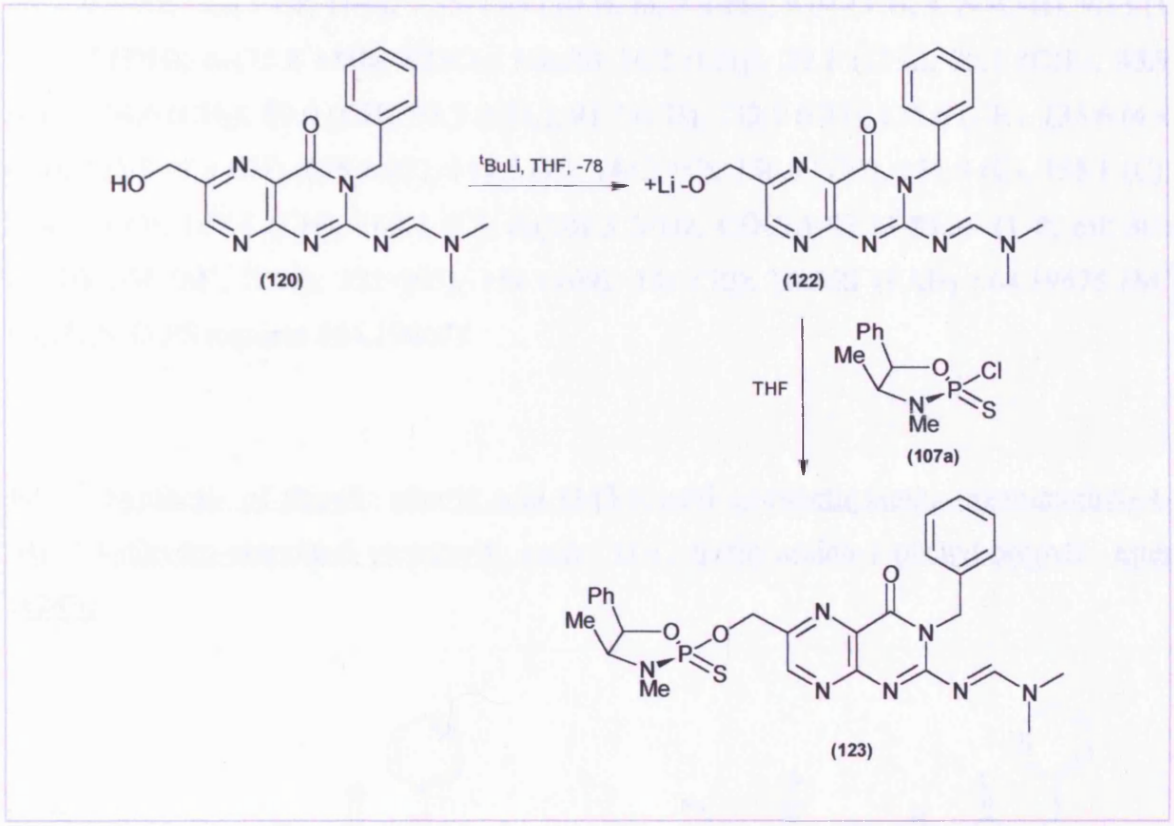

A suspension of N'-(3-benzyl-6-hydroxymethyl-4-oxo-3,4-dihydro-pteridin-2-yl)-N,N-dimethyl-formamidine **(120)** (2.0 g, 5.9 mmol) in dry THF (50 cm^3) was treated with ^{t}butylithium 1.6 M in hexane (5.53 cm^3, 8.85 mmol, 1.5 eq.) at O°C for 1 hour with stirring under nitrogen. The chloro derivative **(107a)** (1.54 g, 5.9 mmol) in dry THF (20 cm^3) was added to the alkoxide **(122)** over a period of 5 minutes at O°C under nitrogen. The mixture was then refluxed for 10 hours after which time it was allowed to cool to 20°C. The THF was diluted with water (400 cm^3) and extracted with dichloromethane (3 x 200 cm^3). The combined organic extracts were dried (Na_2SO_4), filtered and the solvent was removed in vacuo. The resulting dark yellow oil was purified by silica flash chromatography [dichloromethane - methanol (15:1), R.f. = 0.48]. The fractions containing product were collected and the solvent was removed in vacuo to give **(123)** (1.52 g, 46%) as a yellow powder of m.p. >350 °C; $\lambda_{max}(CHCl_3)$/nm 244 (ε/dm^3 mol^{-1} cm^{-1} 9957), 314 (18 388), 358 (8 502); ν_{max}/cm^{-1} (CH_2Cl_2) 3686w 3053s, 2986w, 2685w, 2357w, 1684w, 1631w, 1606w, 1525w, 1495w, 1421m, 1392w, 1271vs, 1258vs, 1050w,

895m, 767s; δ_H(250 MHz; $CDCl_3$; Me_4Si) 0.98 (3 H, d, *J* 6.6 Hz, CHC*H*$_3$), 2.93 (3 H, d, $^3J_{PH}$ 12.2 Hz, N-CH_3), 3.33 (3 H, s, N-CH_3), 3.37 (3 H, s, N-CH_3), 3.84 (1 H, $^3J_{PH}$ 18 Hz, dquin *J* 6.7 Hz, H-4) 5.65 (2 H, d, $^3J_{PH}$ 12.2 Hz, C(6)H), 5.73 (2 H, s, CH_2Ph), 5.82 (1 H, dd, *J* 6.3 Hz, $^3J_{PH}$ 3 Hz, H-5), 7.35-7.65 (10 H, m, 2 x Ph), 9.08 (1 H, s, N=C-H), 9.13 (1 H, s, C(7)H); δ_C(75.8 MHz; $CDCl_3$; Me_4Si) 16.2 (CH_3), 29.1 (CH_3), 39.4 (CH_3), 43.9 (CH_3), 54.6 (CH_2), 69.0 (CH), 73.7 (CH_2), 83.7 (CH), 132.9 (CH), 135.6 (CH), 135.6 (4 x CH), 135.8 (4 x CH), 136.1 (C), 143.5 (C), 144.2 (C), 156.8 (CH), 157.9 (C), 158.1 (C), 164.2 (CO), 167.4 (CH), 169.1 (C); δ_P(101.3 MHz; $CDCl_3$) 82.93-83.36 (1 P, m); *m/z* (FAB) 564 (M^+, 25%), 321 (65), 154 (100), 136 (70); HRMS (FAB) 564.19475 (M^+ $C_{27}H_{30}N_7O_3PS$ requires 564.19467).

6.8.5 Synthesis of thiophosphoric acid O-[3-benzyl-2-(dimethylamino-methinimino)-4-oxo-3,4-dihydro-pteridin-6-ylmethyl] ester O'-(2-methylamino-1-phenyl-propyl) ester **(124b)**.

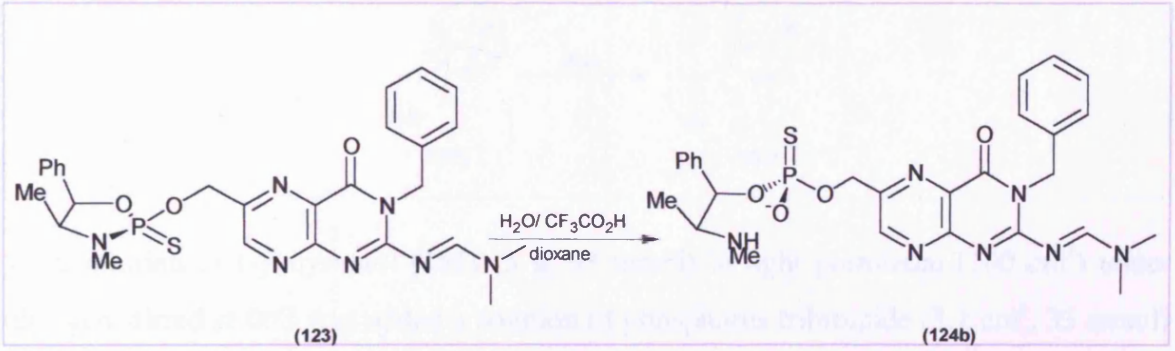

To a solution of **(123)** (563 mg, 1 mmol) in dry dioxane (0.8 cm^3) was added a solution of trifluoroacetic acid (0.23 cm^3, 3 mmol, 3 eq.) in water (0.3 cm^3) and the mixture was stirred at 20°C. After 1 hour, the ^{31}P NMR spectrum of the mixture showed no starting material remained (δ_P 83.1 → 66.7). Removal of the solvent by evaporation under reduced pressure was followed by co-evaporation of the residue from dry dioxane (6 x 3 cm^3) to give the P-N bond cleavage product **(124b)** as its zwitterion (581 mg, 1 mmol, 100%) as an orange powder of m.p. >350 °C; λ_{max}($CHCl_3$)/nm 244 (ε/dm^3 mol^{-1} cm^{-1} 9657), 314 (18 588), 358 (8 702); ν_{max}/cm^{-1} (CH_2Cl_2) 3696w 3043s, 2986w, 2685w, 2357w, 1684w, 1631w, 1606w, 1526w, 1495w, 1421m, 1392w, 1278vs, 1258vs, 1060w, 885m, 766s; δ_H(250 MHz; $CDCl_3$; Me_4Si) 1.12 (3 H, d, *J* 6.6 Hz, CHC*H*$_3$), 2.86 (3 H, s, N-

CH_3), 3.33 (3 H, s, N-CH_3), 3.37 (3 H, s, N-CH_3), 3.84 (1 H, m, H-4) 5.65 (2 H, m, C(6)H), 5.73 (2 H, s, CH_2Ph), 5.82 (1 H, d, *J* 6.3 Hz, H-5), 7.05-7.45 (10 H, m, 2 x Ph), 8.68 (1 H, s, N=C-H), 8.90 (1 H, s, C(7)H); δ_C(75.8 MHz; $CDCl_3$; Me_4Si) 14.2 (CH_3), 24.1 (CH_3), 38.9 (CH_3), 43.7 (CH_3), 54.6 (CH_2), 64.9 (CH), 71.7 (CH_2), 81.7 (CH), 131.9 (CH), 135.2 (CH), 135.7 (4 x CH), 135.6 (4 x CH), 136.7 (C), 143.3 (C), 144.4 (C), 154.5 (CH), 157.6 (C), 158.0 (C), 164.3 (CO), 167.7 (CH), 169.4 (C); δ_P(101.3 MHz; $CDCl_3$) 60.77 (1 P, q, *J* 12.4 Hz); *m/z* (ES) 582 (M^+, 100%), 226 (25). Selected data for the compound that results from ^{18}O incorporation using $H_2{}^{18}O$. HRMS (FAB) 584.20942 (M^+ $C_{27}H_{33}N_7O_3O^{18}PS$ requires 584.20949).

6.8.6 Synthesis of 2-Bromomethyl-6,6-dimethyl-bicyclo[3.1.1]hept-2-ene (1R-Myrtenyl bromide) **(162)**.[163] Beilstein Registry Number 2081677, CAS Registry Number 55527-89-4

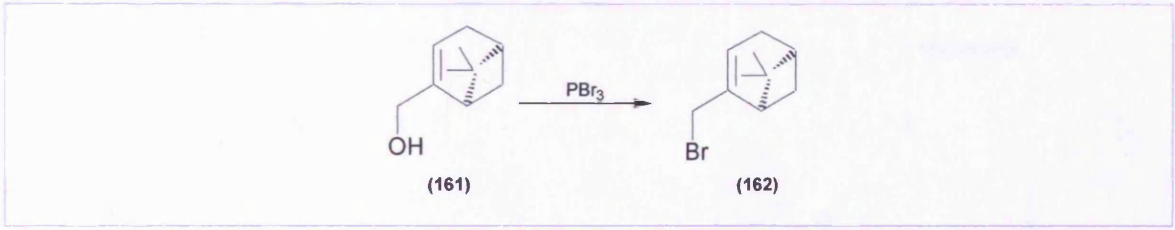

To a solution of (-)-myrtenol **(161)** (5 g, 33 mmol) in light petroleum (100 cm^3) under nitrogen stirred at 0°C was added a solution of phosphorus tribromide (3.1 cm^3, 33 mmol) in light petroleum (100 cm^3) over a period of 30 minutes. After allowing the reaction mixture to warm to room temperature over a 3 hour period, the colourless solution was washed with ice cold 0.8 M potassium carbonate solution (3 x 40 cm^3). The organic layer was separated, dried ($MgSO_4$), filtered and evaporated under reduced pressure. The resulting light orange oil was Kugelröhr distilled to give the isocyclic compound **(162)** as a colourless oil (4.7 g, 67%); b.p. 109-111°C (2 mmHg); $[\alpha]_D$ –42.4 (*c* 1.02 in chloroform at 22°C); ν_{max}/cm^{-1} ($CHCl_3$) 242 ($\varepsilon/dm^3\ mol^{-1}\ cm^{-1}$ 47 009); δ_H(300 MHz; $CDCl_3$; Me_4Si) 0.62 (3 H, s, CCH_3), 1.35 (1 H, d, *J* 8 Hz), 1.4 (3H, s, CCH_3), 2.1-2.6 (5H, m), 4.05 (2 H, s, CH_2Br), 5.81 (1H, br s, R_2C=C*H*); δ_C(75.8 MHz; $CDCl_3$; Me_4Si) 21.6 (CH_3), 26.4 (CH_3), 31.7 (CH_2), 31.9 (CH_2), 38.3 (CH_2, d, *J* 8.8 Hz), 40.7 (CH), 45.2 (CH), 88.0 (C),

123.6 (CH), 144.6 (C); HRMS (EI) 214.03586 (M^+ $C_{10}H_{15}Br^{79}$ requires 214.03571); *m/z* (ES) 214/216 (M^+, 20%), 171/173 (65).

6.8.7 Synthesis of thiophosphoric acid O-[3-benzyl-2-(dimethylamino-methinimino)-4-oxo-3,4-dihydro-pteridin-6-ylmethyl] ester S-(6,6-dimethyl-bicyclo[3.1.1]hept-2-en-2-ylmethyl) ester **(112b)**.

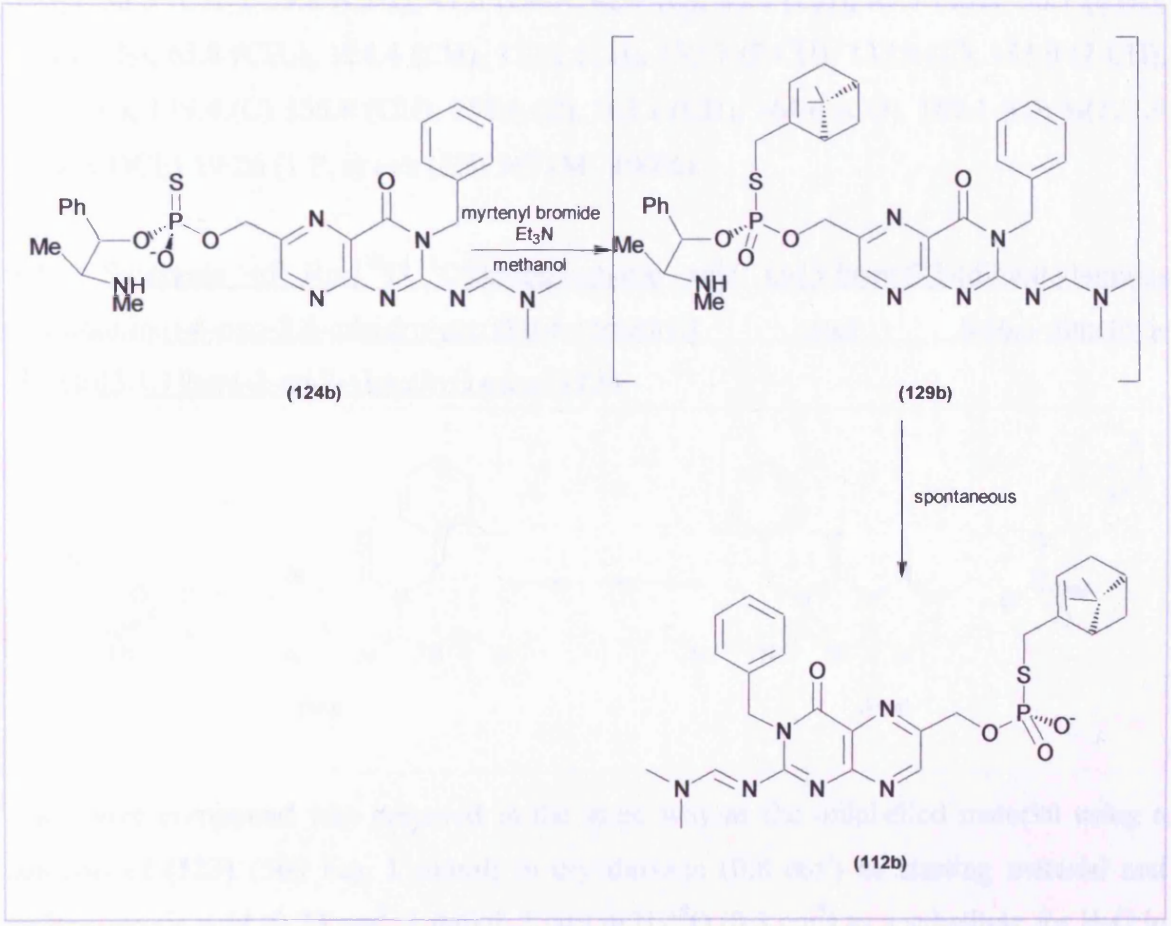

Thiophosphoric acid O-[3-benzyl-2-(dimethylamino-methinimino)-4-oxo-3,4-dihydro-pteridin-6-ylmethyl] ester O'-(2-methylamino-1-phenyl-propyl) ester **(124b)** (100 mg, 0.17 mmol) was dissolved in methanol (1 cm^3). 1R-Myrtenyl bromide **(162)** (36.7 mg, 30.6 µl, 0.17 mmol) and triethylamine (50 µl) were added and the solution was stirred at 20°C for 2 hours. The solvent was removed in vacuo and the resulting yellow oil was purified by silica flash chromatography [dichloromethane - methanol (10:1), R.f. = 0.53]. The fractions containing product were collected and the solvent was removed in vacuo to give **(112b)** (75 mg, 78%) as a yellow powder of m.p. >350 °C; $\lambda_{max}(CHCl_3)$/nm 244 (ε/dm^3 mol^{-1} cm^{-1} 9 727), 314 (17 950), 358 (8305); ν_{max}/cm^{-1} (CH_2Cl_2) 3053s, 2986m, 2685w,

2521w, 2409w, 2359w, 2305m, 2126w, 2054w, 1684w, 1631w, 1525w, 1421s, 1259vs, 1155w, 895s, 736vs; δ_H(300 MHz; CD_3OD; Me_4Si) 0.62 (3 H, s, CCH_3), 0.92 (1 H, d, *J* 8.5 Hz), 1.07 (3 H, s, CCH_3), 1.92 (3 H, m), 2.10 (1 H, br s), 2.21 (1 H, m), 3.04 (3 H, s, N-CH_3), 3.14 (3 H, s, N-CH_3), 3.21 (2 H, m, S-CH_2) 4.98 (2 H, d, $^3J_{PH}$ 10.5 Hz, C(6)H), 5.23 (1 H, br s, CH_2CH=C) 5.39 (2 H, s, CH_2Ph), 7.05-7.25 (5 H, m, Ph), 8.70 (1 H, s, C(7)H), 8.73 (1 H, s, N=C-H); δ_C(75.8 MHz; $CDCl_3$; Me_4Si) 25.5 (CH_3), 30.3 (CH_3), 35.9 (CH_2), 36.3 (CH_2), 39.8 (CH_3), 41.6 (CH_2), 42.7 (C), 45.5 (CH), 45.7 (CH), 50.1 (CH_3), 51.4 (CH_2), 63.8 (CH_2), 124.4 (CH), 132.1 (CH), 132.7 (2 CH), 132.9 (C), 133.0 (2 CH), 142.1 (C), 149.4 (C) 155.8 (CH), 158.8 (C), 163.1 (CH), 164.6 (CO), 169.1 (C); δ_P(121.9 MHz; $CDCl_3$) 19.26 (1 P, s) *m/z* (ES) 567 (M^-, 100%).

6.9 Synthesis of Rp-[^{16}O,^{18}O]thiophosphoric acid O-[3-benzyl-2-(dimethylamino-methinimino)-4-oxo-3,4-dihydro-pteridin-6-ylmethyl] ester S-(6,6-dimethyl-bicyclo[3.1.1]hept-2-en-2-ylmethyl) ester **(112a**

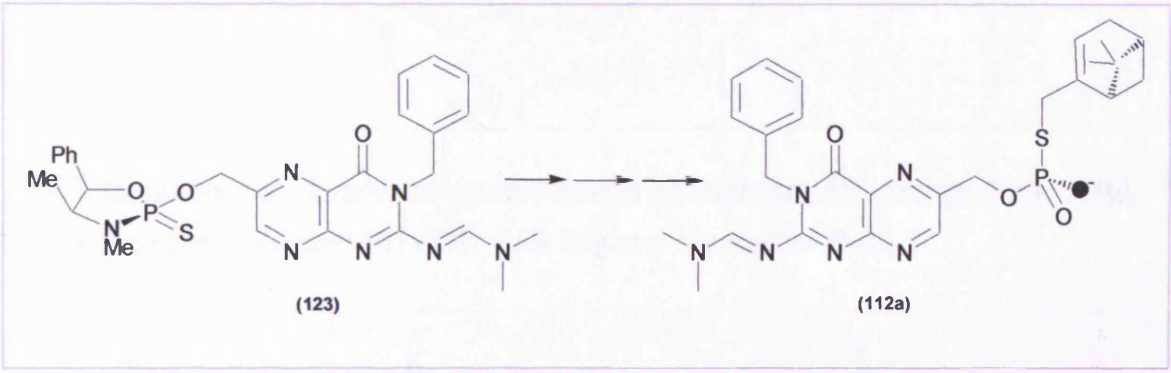

The above compound was prepared in the same way as the unlabelled material using a solution of **(123)** (563 mg, 1 mmol) in dry dioxane (0.8 cm^3) as starting material and trifluoroacetic acid (0.23 cm^3, 3 mmol, 3 eq.) in $H_2{}^{18}O$ (0.3 cm^3) as a substitute for H_2O in the P-N cleavage step. This gave the labelled thiophosphate **(112a)** (75 mg, 78%) as the triethylammonium salt of m.p. >350 °C; λ_{max}($CHCl_3$)/nm 244 (ε/dm^3 mol^{-1} cm^{-1} 9 727), 314 (17 950), 358 (8305); ν_{max}/cm^{-1} (CH_2Cl_2) 3053s, 2986m, 2685w, 2521w, 2409w, 2359w, 2305m, 2126w, 2054w, 1684w, 1631w, 1525w, 1421s, 1259vs, 1155w, 895s, 736vs; δ_H(300 MHz; CD_3OD; Me_4Si) 0.62 (3 H, s, CCH_3), 0.92 (1 H, d, *J* 8.5 Hz), 1.07 (3 H, s, CCH_3), 1.92 (3 H, m), 2.10 (1 H, br s), 2.21 (1 H, m), 3.04 (3 H, s, N-CH_3), 3.14 (3 H, s, N-CH_3), 3.21 (2 H, m, S-CH_2) 4.98 (2 H, d, $^3J_{PH}$ 10.5 Hz, C(6)H), 5.23 (1 H, br s, CH_2CH=C) 5.39 (2 H, s, CH_2Ph), 7.05-7.25 (5 H, m, Ph), 8.70 (1 H, s, C(7)H), 8.73 (1 H, s, N=C-H); δ_C(75.8 MHz; $CDCl_3$; Me_4Si) 25.5 (CH_3), 30.3 (CH_3), 35.9 (CH_2), 36.3 (CH_2)

39.8 (CH_3), 41.6 (CH_2), 42.7 (C), 45.5 (CH), 45.7 (CH), 50.1 (CH_3), 51.4 (CH_2), 63.8 (CH_2), 124.4 (CH) 132.1 (CH), 132.7 (2 CH), 132.9 (C), 133.0 (2 CH), 142.1 (C), 149.4 (C) 155.8 (CH), 158.8 (C), 163.1 (CH), 164.6 (CO), 169.1 (C); δ_P(121.9 MHz; $CDCl_3$) 19.26 (1 P, s) *m/z* (ES) 567 (M^-, 100%); HRMS (FAB) 569.19879 (M^+ $C_{27}H_{32}N_6O_3{}^{18}OPS$ requires 569.19859).

6.10 Synthesis of thiophosphoric acid O-[3-benzyl-2-(dimethylamino-methinimino)-4-oxo-3,4-dihydro-pteridin-6-ylmethyl] ester S-(6,6-dimethyl-bicyclo[3.1.1]hept-2-en-2-ylmethyl) ester **(112b)** *via* the HPPK route.

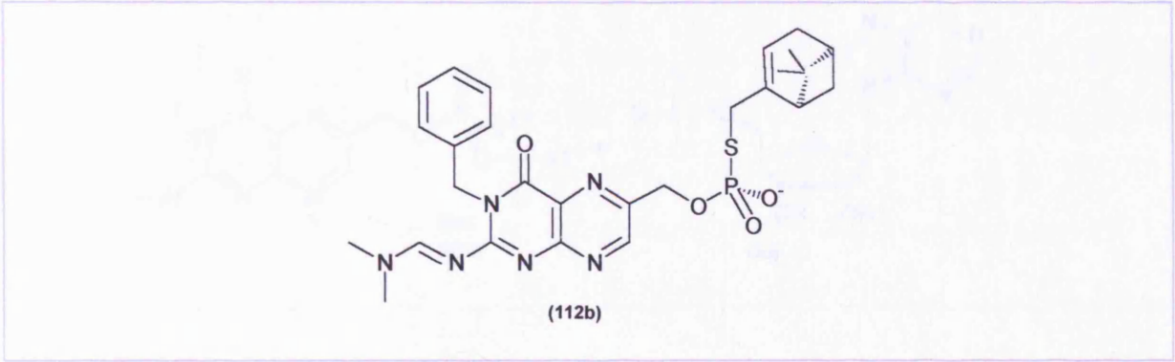

(112b)

6.10.1 Synthesis of 2-Amino-6-hydroxymethyl-7,8-dihydro-3H-pteridin-4-one **(46).**[164]
Beilstein Registry Number 5018822, CAS Registry Number 3672-03-5

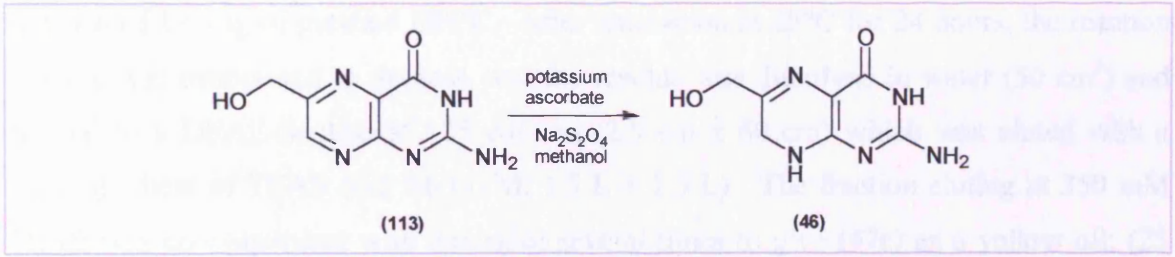

(113) (46)

2-Amino-6-hydroxymethyl-7,8-dihydro-3H-pteridin-4-one **(46)** was prepared by reducing 2-amino-6-hydroxymethyl-3H-pteridin-4-one **(113)** with dithionite. Specifically, Compound **(113)** (20 mg, 0.1 mmol) was suspended in water (2 cm^3) and dissolved by the dropwise addition of NaOH (1 M). A solution of sodium ascorbate (5 cm^3, pH 6.0, 100 mg, 0.5 mmol of ascorbic acid per cm^3) and $Na_2S_2O_4$ (200 mg, 1.15 mmol) were added. The mixture was held for 15 minutes at room temperature before use.

6.10.2 Synthesis of α-thiopyrophosphoric acid O-(2-amino-4-oxo-3,4-dihydro-pteridin-6-ylmethyl) ester **(47c)**.

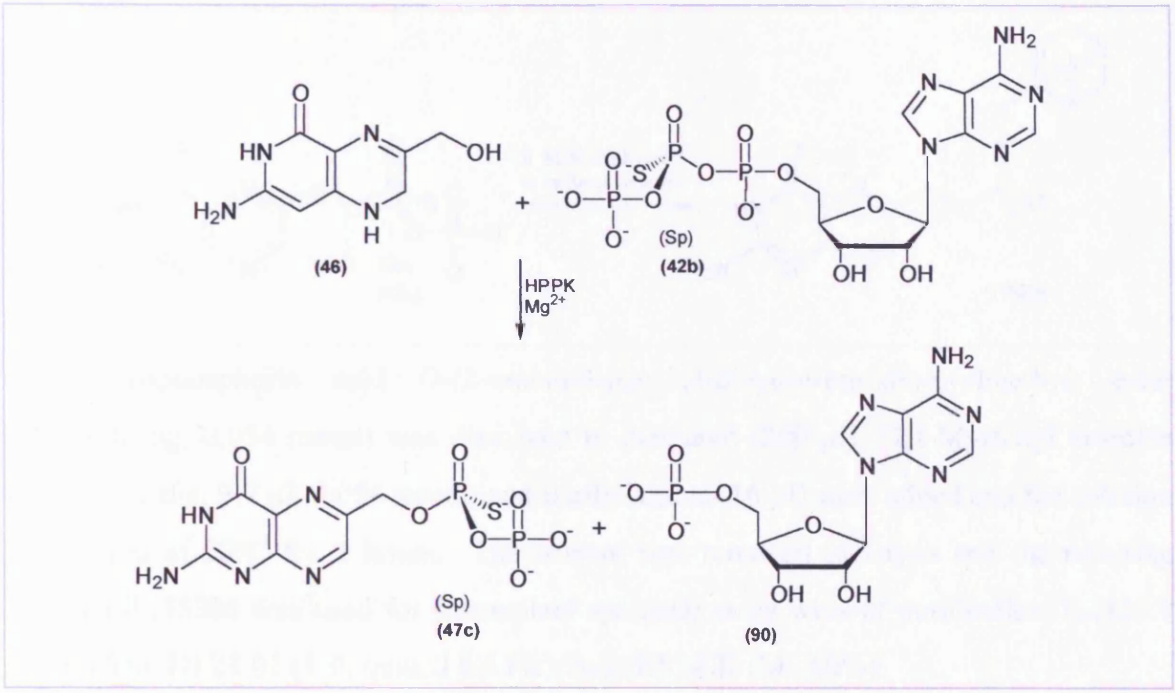

The HPPK catalysed reaction was conducted in 800 cm^3 of 50 mM Hepes/NaOH buffer (pH 7.6) containing 10 mM $MgCl_2$, 0.2 mM ATPβS (Sp) **(42b)**, 0.2 mM 2-amino-6-hydroxymethyl-7,8-dihydro-3H-pteridin-4-one **(46)**. The reaction was initiated by the addition of 1.4 mg of purified HPPK. After incubation at 25°C for 24 hours, the reaction mixture was evaporated to dryness, and the residue was dissolved in water (50 cm^3) and applied to a DEAE-Sephadex A25 column (2.5 cm x 60 cm) which was eluted with a linear gradient of TEAB (0.2 M-1.0 M; 1.5 L + 1.5 L). The fraction eluting at 350 mM TEAB was co-evaporated with methanol several times to give **(47c)** as a yellow oil; (25 mg, 30%); $[\alpha]_D$ (10^{-1} deg cm^2 g^{-1}) –7.9 (*c* 0.18 in MeOH); $\lambda_{max}(CHCl_3)$/nm 254 (ε/dm^3 mol^{-1} cm^{-1} 21 327), 346 (14 123); ν_{max}/cm^{-1} (MeOH) 3053s, 2986m, 2685w, 2521w, 2409w, 2359w, 2305m, 2126w, 2054w, 1684w, 1631w, 1525w, 1421s, 1259vs, 1155w, 895s, 736vs; δ_H(300 MHz; D_2O; Me_4Si) 5.19 (2 H, d, J 8.2 Hz, CH_2O), 8.86 (1 H, s, N=CH); δ_P(121.9 MHz; D_2O) 45.89 (1 P, d, J 30.6 Hz, P_α), -9.67 (1 P, d, J 30.6 Hz, P_β); *m/z* (ES) 368 (M^-, 10%), 253 (20), 236 (30), 113 (60), 69 (100).

6.10.3 Synthesis of thiophosphoric acid O-(2-amino-4-oxo-3,4-dihydro-pteridin-6 ylmethyl) ester S-(6,6-dimethyl-bicyclo[3.1.1]hept-2-en-2-ylmethyl) ester **(153b).**

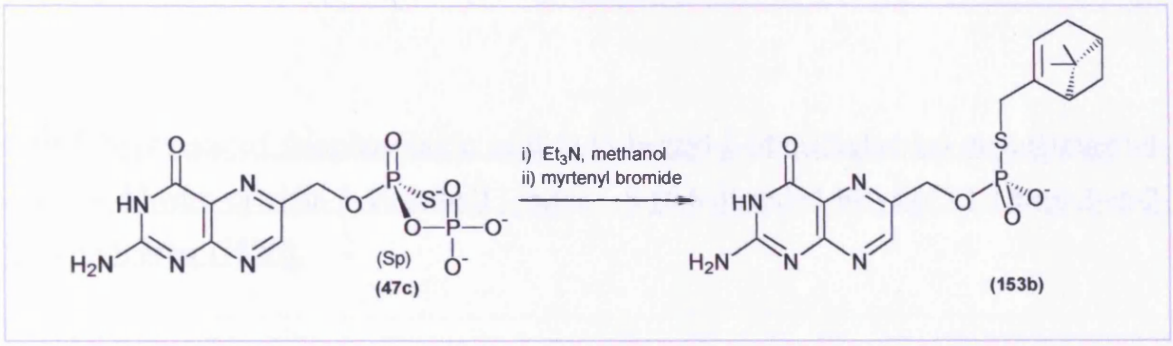

α-Thiopyrophosphoric acid O-(2-amino-4-oxo-3,4-dihydro-pteridin-6-ylmethyl) ester **(47c)** (20 mg, 0.054 mmol) was dissolved in methanol (200 µl). 1R-Myrtenyl bromide **(162)** (11.7 mg, 9.7 µl, 0.054 mmol) and triethylamine (16 µl) were added and the solution was stirred at 20°C for 2 hours. The solvent was removed in vacuo and the resulting yellow oil **(153b)** was used for subsequent synthetic steps without purification; δ_P(121.9 MHz; CD_3OD) 21.01 (1 P, quin, *J* 8.6 Hz); m/z (ES) 422 (M^-, 60%)

6.10.4 Synthesis of thiophosphoric acid O-[2-(dimethylamino-methinimino)-4-oxo-3,4-dihydro-pteridin-6-ylmethyl] ester S-(6,6-dimethyl-bicyclo[3.1.1]hept-2-en-2-ylmethyl) ester **(154b).**

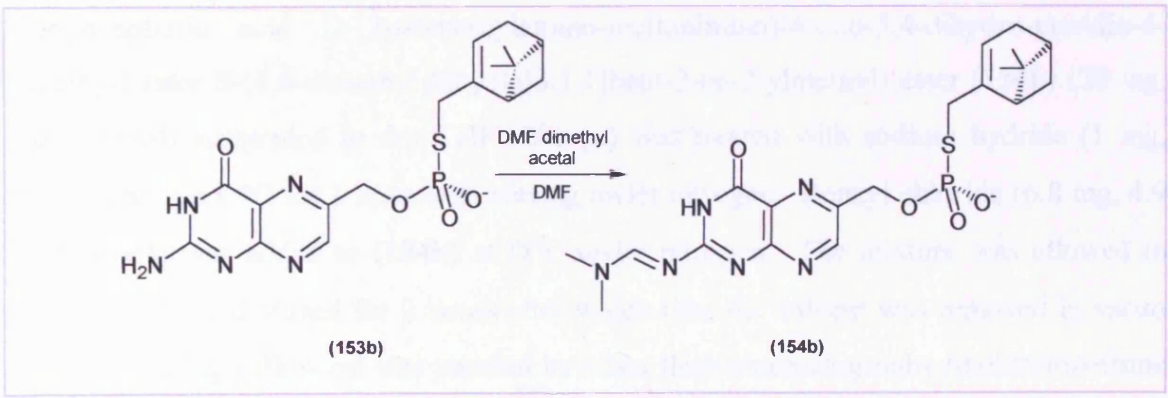

A suspension of thiophosphoric acid O-(2-amino-4-oxo-3,4-dihydro-pteridin-6 ylmethyl) ester S-(6,6-dimethyl-bicyclo[3.1.1]hept-2-en-2-ylmethyl) ester **(153b)** (20 mg, 0.048 mmole) in DMF (100 µ) was treated with N,N-dimethylformamide-dimethylacetal (6.4 µl, 0.048 mmol) at room temperature for 2 hours with stirring. The yellow-coloured solution

was evaporated in high vacuum and co-evaporated with chloroform several times to give a yellow foam. The residue **(154b)** was used for subsequent synthetic steps without purification; δ_P(121.9 MHz; CD_3OD) 21.43 (1 P, m).

6.10.5 Synthesis of thiophosphoric acid O-[3-benzyl-2-(dimethylamino-methinimino)-4-oxo-3,4-dihydro-pteridin-6-ylmethyl] ester S-(6,6-dimethyl-bicyclo[3.1.1]hept-2-en-2-ylmethyl) ester **(112b).**

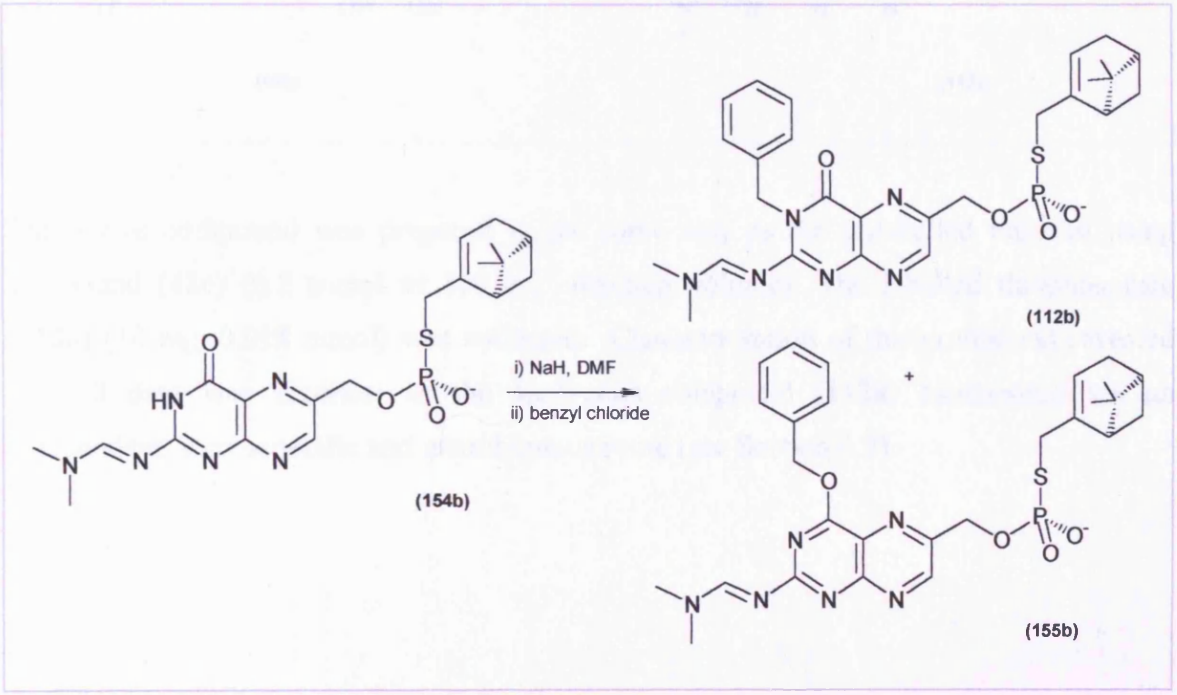

Thiophosphoric acid O-[2-(dimethylamino-methinimino)-4-oxo-3,4-dihydro-pteridin-6-ylmethyl] ester S-(6,6-dimethyl-bicyclo[3.1.1]hept-2-en-2-ylmethyl) ester **(154b)** (20 mg, 0.042 mmol) suspended in dry THF (200 µl) was treated with sodium hydride (1 mg, 0.042 mmol) at O°C for 1 hour with stirring under nitrogen. Benzyl chloride (6.8 mg, 4.9 µl, 8 mmol) was added to **(154b)** at O°C under nitrogen. The mixture was allowed to warm to 20°C and stirred for 2 hours after which time the solvent was removed in vacuo and the resulting yellow oil was purified by silica flash chromatography [dichloromethane - methanol (10:1), R.f. = 0.53]. The fractions containing product were collected and the solvent was removed in vacuo to give **(112b)** (15 mg, 0.026 mmol) as a yellow powder of m.p. >350 °C. Characterisation of this compound revealed that all data was identical to the analogous compound **(112b)** synthesised via an independent, stereospecific and unambiguous route (see Section 6.8.7).

6.11 Synthesis of Rp-[^{16}O,^{18}O]thiophosphoric acid O-[3-benzyl-2-(dimethylamino-methinimino)-4-oxo-3,4-dihydro-pteridin-6-ylmethyl] ester S-(6,6-dimethyl-bicyclo[3.1.1]hept-2-en-2-ylmethyl) ester **(112a)**.

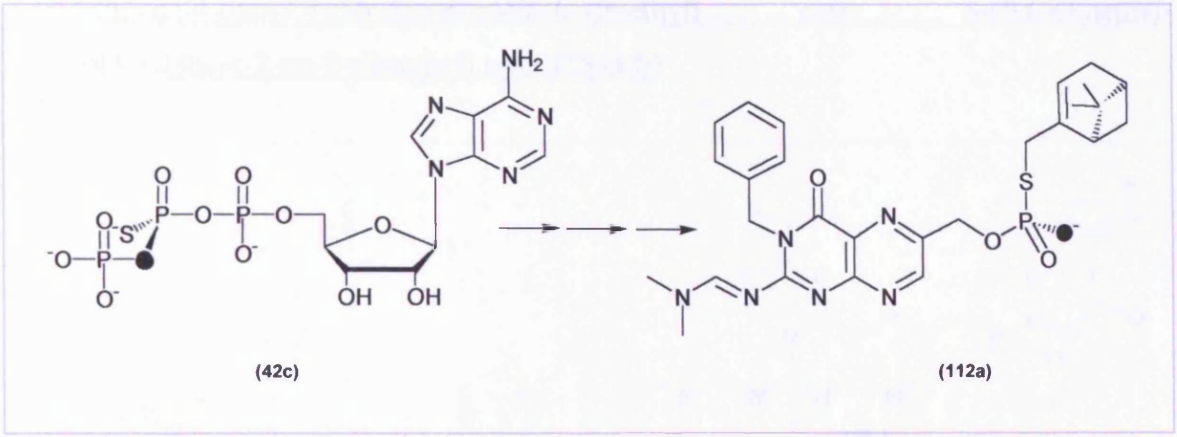

(42c) (112a)

The above compound was prepared in the same way as the unlabelled material using compound **(42c)** (0.2 mmol in 800 cm^3 reaction volume). The labelled thiophosphate **(112a)** (10 mg, 0.018 mmol) was collected. Characterisation of this compound revealed that all data was identical to the analogous compound **(112a)** synthesised via an independent, stereospecific and unambiguous route (see Section 6.9).

6.12 O-Derivatisation of S-alkylated thiophosphate diesters.

6.12.1 Synthesis of thiophosphoric acid O-acetyl O-[3-benzyl-2-(dimethylamino-methinimino)-4-oxo-3,4-dihydro-pteridin-6-ylmethyl] ester S-(6,6-dimethyl-bicyclo[3.1.1]hept-2-en-2-ylmethyl) ester **(150a,b)**

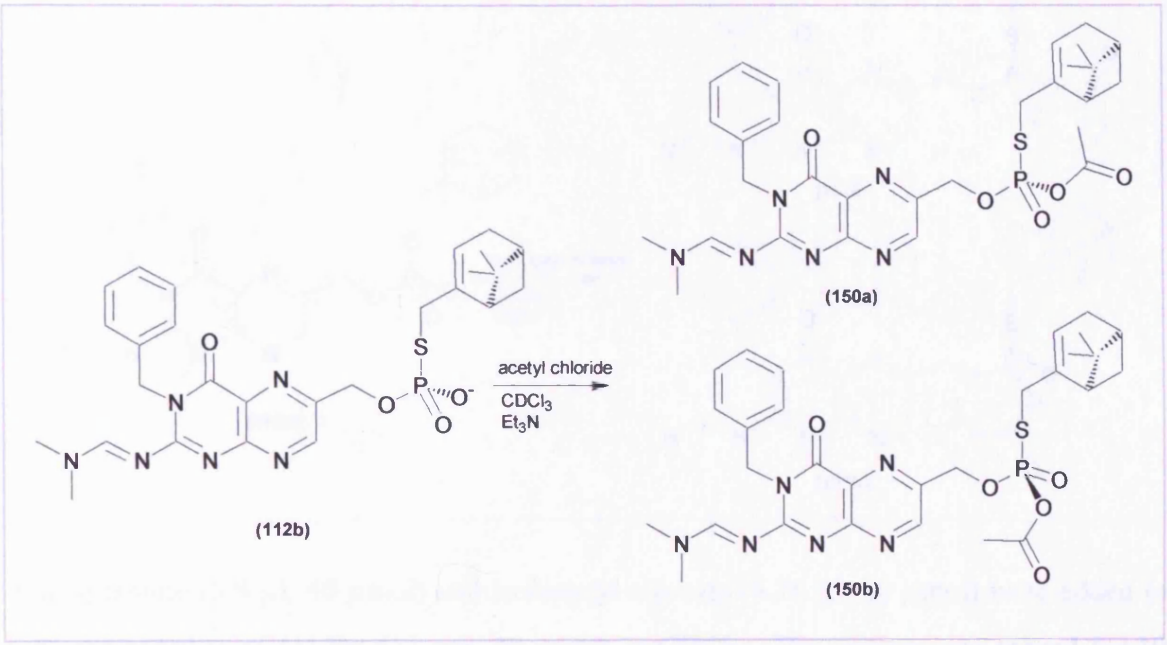

Triethylamine (5.8 µl, 40 µmol) and acetyl chloride (3.14 µl, 40 µmol) were added to a stirred solution of **(112b)** (11 mg, 20 µmol) in $CDCl_3$. The mixture was stirred for 10 minutes, and taken directly for analysis by ^{31}P NMR; δ_P(162.0 MHz; $CDCl_3$) 24.85 [1 P **(150a)**, s], 24.83 [1 P **(150b)**, s], diastereoisomeric separation = 4.3 Hz.

6.12.2 Synthesis of thiophosphoric acid O-isobutyryl O-[3-benzyl-2-(dimethylamino-methinimino)-4-oxo-3,4-dihydro-pteridin-6-ylmethyl] ester S-(6,6-dimethyl-bicyclo[3.1.1]hept-2-en-2-ylmethyl) ester **(151a,b)**

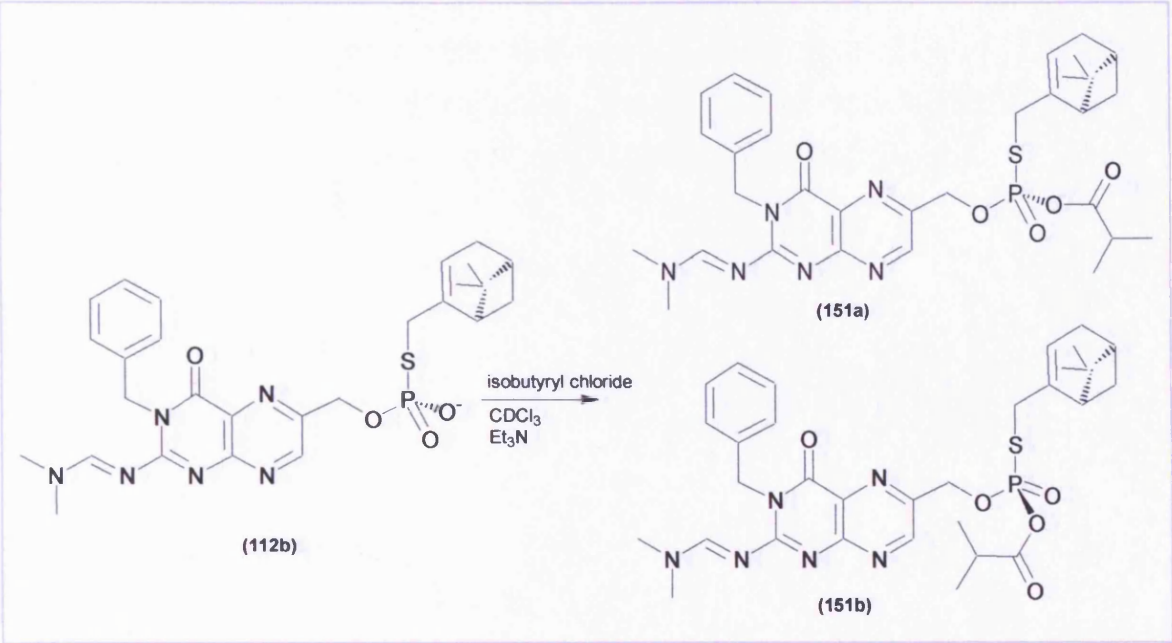

Triethylamine (5.8 µl, 40 µmol) and isobutyryl chloride (4.26 µl, 40 µmol) were added to a stirred solution of **(112b)** (11 mg, 20 µmol) in $CDCl_3$. The mixture was stirred for 10 minutes, and taken directly for analysis by ^{31}P NMR; δ_P(162.0 MHz; $CDCl_3$) 25.74 [1 P **(151b)**, s], 25.70 [1 P **(150a)**, s], diastereoisomeric separation = 6.1 Hz.

6.12.3 Synthesis of the diastereoisomers of Rp-[^{16}O,^{18}O]thiophosphoric acid O-acetyl O-[3-benzyl-2-(dimethylamino-methinimino)-4-oxo-3,4-dihydro-pteridin-6-ylmethyl] ester S-(6,6-dimethyl-bicyclo[3.1.1]hept-2-en-2-ylmethyl) ester **(150a,b,c,d)**

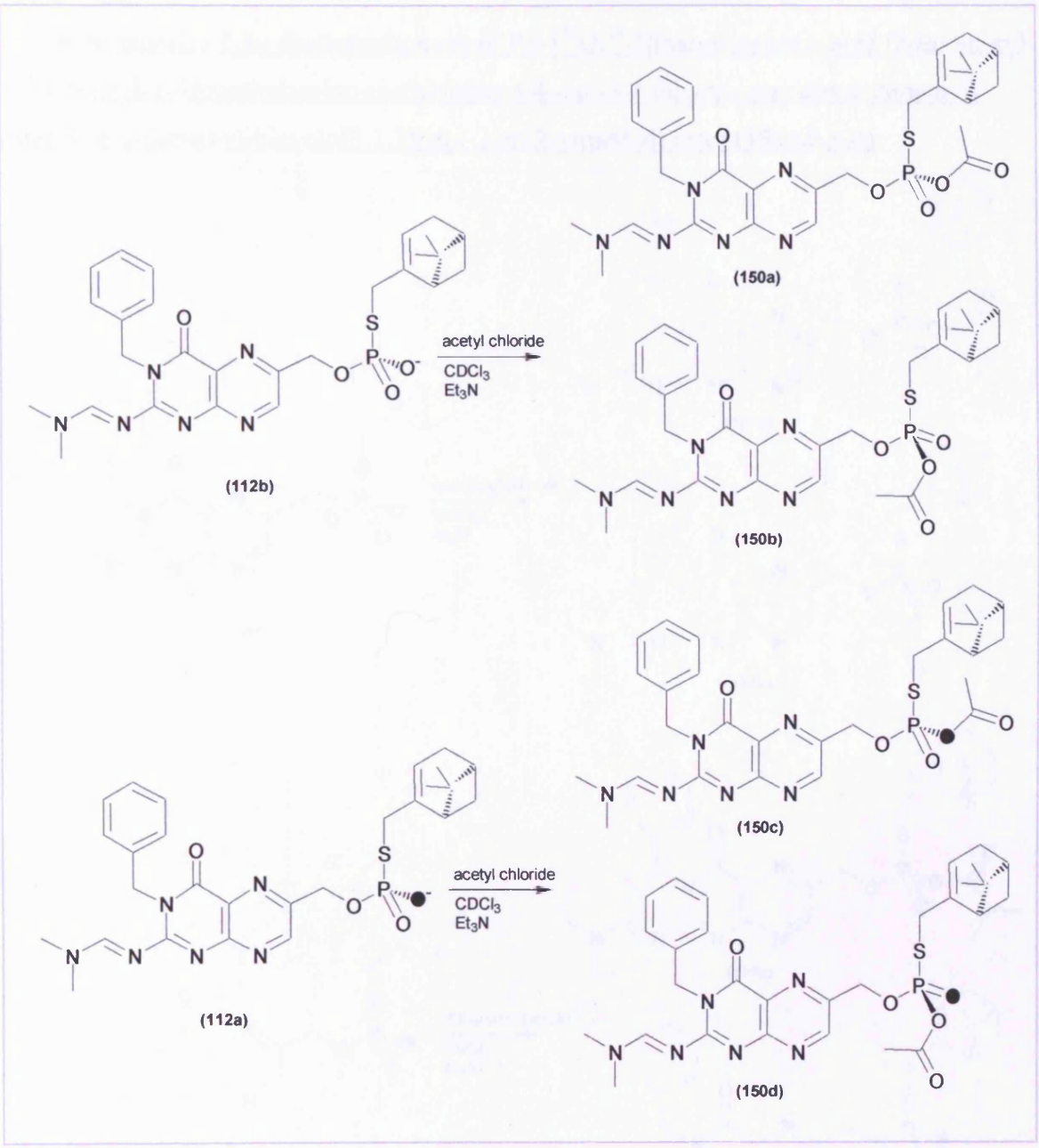

Triethylamine (5.8 µl, 40 µmol) and acetyl chloride (3.14 µl, 40 µmol) were added to a stirred solution of **(112b)** and **(112a)** (3:2 mixture) (11 mg, 20 µmol) in $CDCl_3$. The mixture was stirred for 10 minutes, and taken directly for analysis by ^{31}P NMR; δ_P(162.0 MHz; $CDCl_3$) 24.85 [1 P **(150a)**, s], 24.84 [1 P **(150c)**, s] (^{18}O isotopic shift = 2.8 Hz),

24.83 [1 P **(150b)**, s], 24.78 [1 P **(150d)**, s] (^{18}O isotopic shift = 4.7 Hz), (see Figure 3.5, Chapter 3).

6.12.4 Synthesis of the diastereoisomers of Rp-[^{16}O,^{18}O]thiophosphoric acid O-isobutyryl O-[3-benzyl-2-(dimethylamino-methinimino)-4-oxo-3,4-dihydro-pteridin-6-ylmethyl] ester S-(6,6-dimethyl-bicyclo[3.1.1]hept-2-en-2-ylmethyl) ester **(151a,b,c,d)**

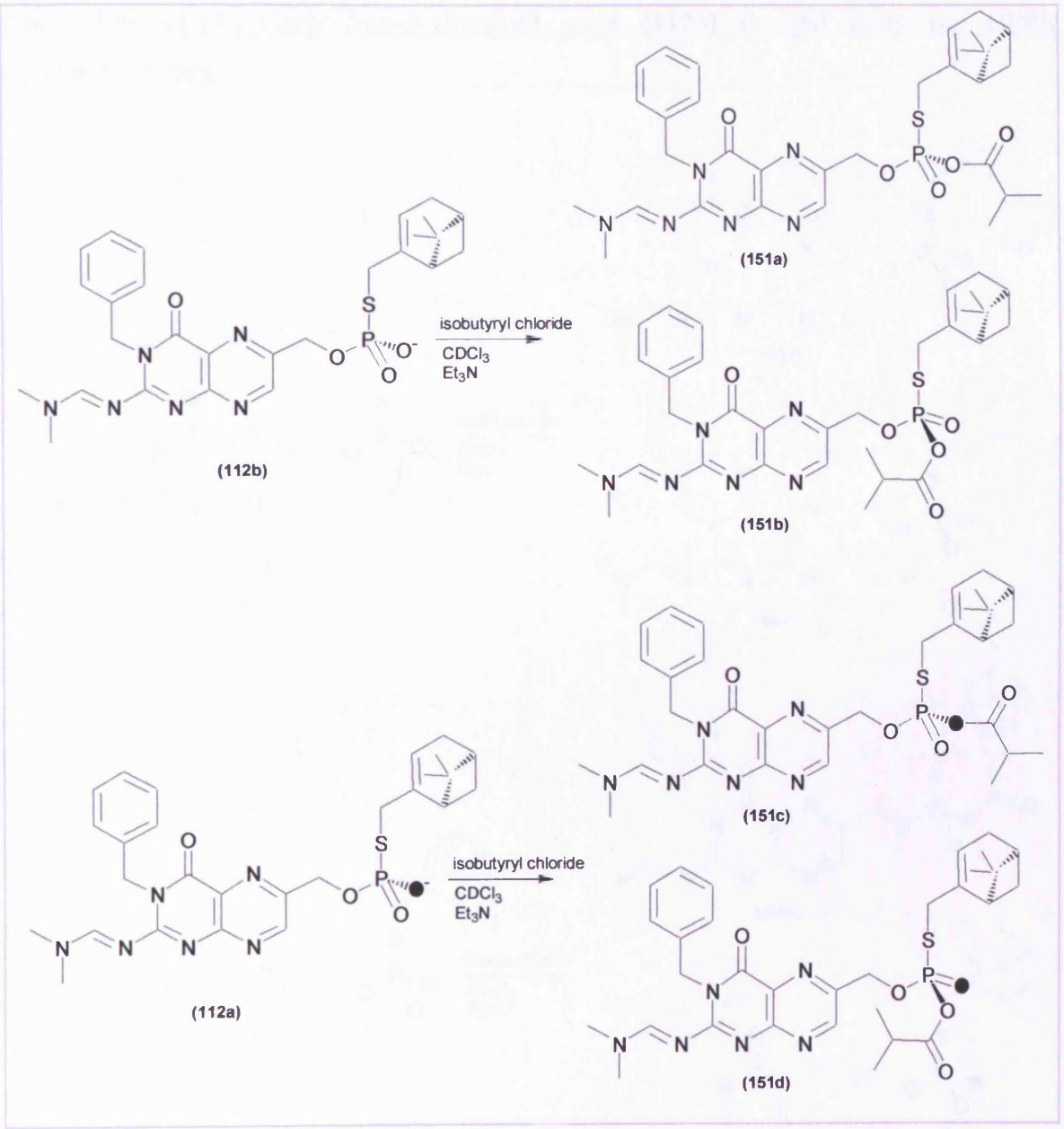

Triethylamine (5.8 µl, 40 µmol) and isobutyryl chloride (4.26 µl, 40 µmol) were added to a stirred solution of **(112b)** and **(112a)** (3:2 mixture) (11 mg, 20 µmol) in $CDCl_3$. The mixture was stirred for 10 minutes, and taken directly for analysis by ^{31}P NMR; δ_P(162.0

MHz; $CDCl_3$) 25.74 [1 P **(151b)**, s], 25.69 [1 P **(151d)**, s] (^{18}O isotopic shift = 8.1 Hz), 25.70 [1 P **(151a)**, s], 25.68 [1 P **(151c)**, s] (^{18}O isotopic shift = 3.2 Hz), (see Figure 3.6, Chapter 3).

6.12.5 Configurational analysis of Rp-[^{16}O,^{18}O]thiophosphoric acid O-[3-benzyl-2-(dimethylamino-methinimino)-4-oxo-3,4-dihydro-pteridin-6-ylmethyl] ester S-(6,6-dimethyl-bicyclo[3.1.1]hept-2-en-2-ylmethyl) ester **(112a)** derived from the HPPK catalysed reaction.

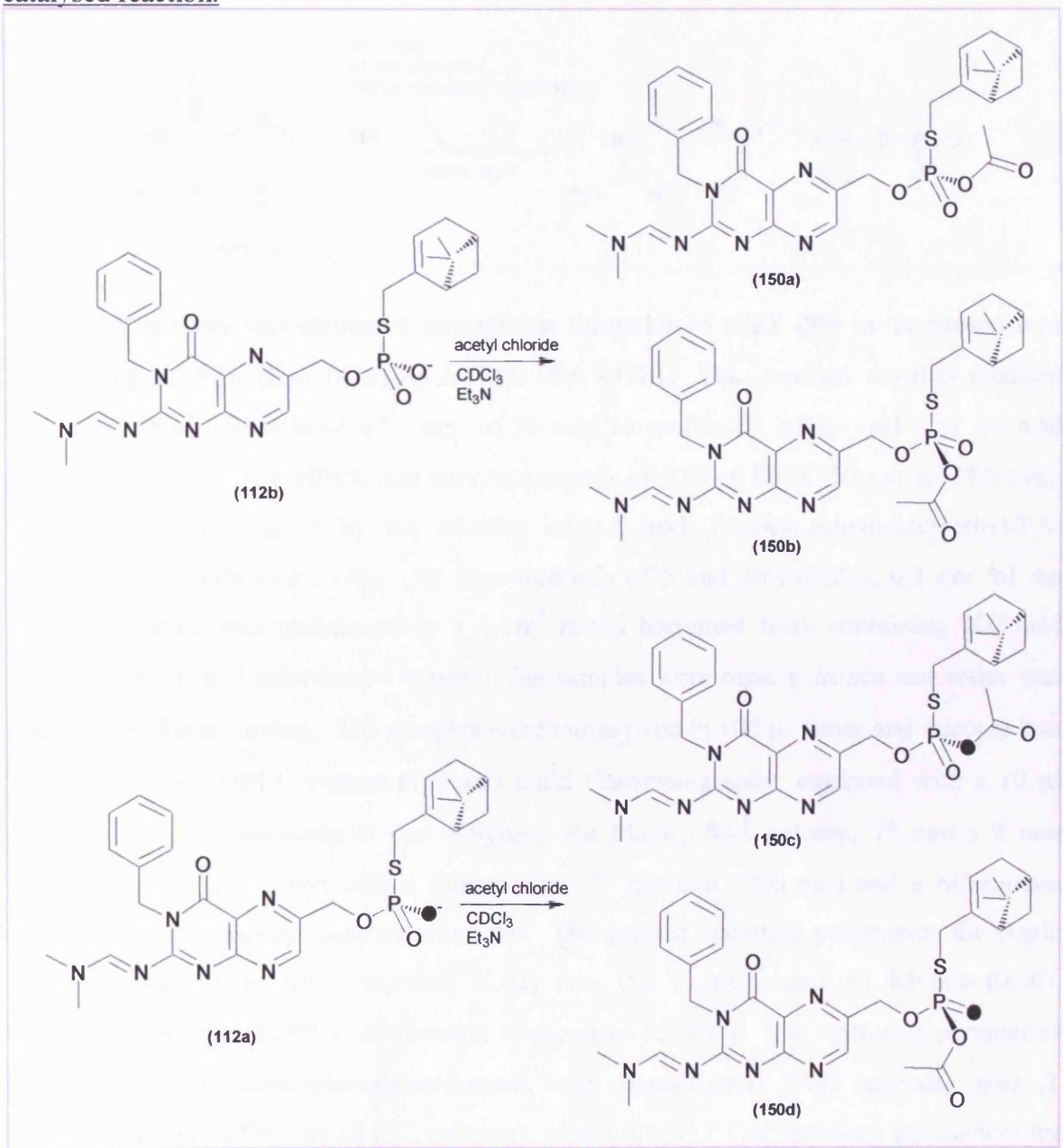

Triethylamine (5.8 μl, 40 μmol) and acetyl chloride (3.14 μl, 40 μmol) were added to a stirred solution of **(112b)** and **(112a)** (3:2 mixture) (11 mg, 20 μmol) in $CDCl_3$. The mixture was stirred for 10 minutes, and taken directly for analysis by ^{31}P NMR; δ_P(121.0 MHz; $CDCl_3$) 25.90 [1 P, **(150a)** s], 25.89 [2 P **(150b)** and **(150c)**, s], 25.83 [1 P **(150d)**, s], (see Figure 4.4, Chapter 4).

6.13 Steady-State HPPK Kinetics.

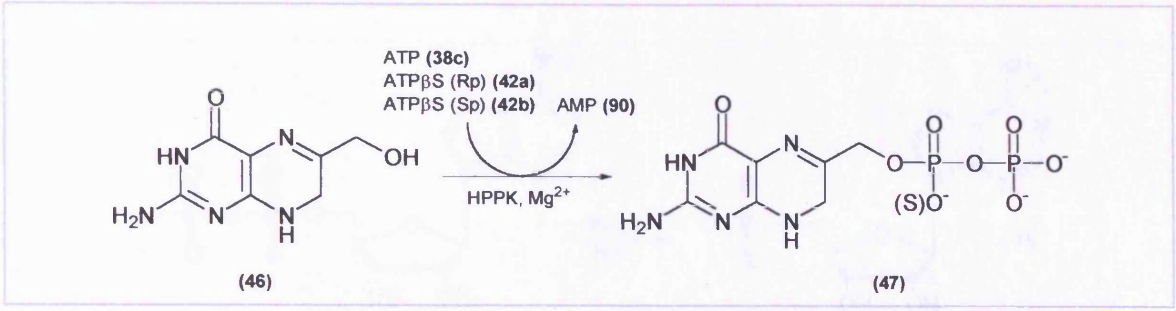

The HPPK activity was estimated through the formation of AMP **(90)** in the presence of ATP **(38c)**, ATPβS (Rp) **(42a)** or ATPβS (Sp) **(42b)**. The standard reaction medium contained, in a total volume of 1 cm^3 of 50 mM Hepes/NaOH buffer (pH 7.6): 10 mM $MgCl_2$, 1 μg of purified HPPK and various amounts of ATP, ATPβS (Rp) or ATPβS (Sp). The reaction was started by the addition of 0.2 mM 2-amino-6-hydroxymethyl-7,8-dihydro-3H-pteridin-4-one **(46)**. At time intervals of 5 and 30 minutes, 0.5 cm^3 of the reaction mixture was transferred to a 5 cm^3 round bottomed flask containing 200 mM EDTA (100 μl) and mixed on a vortex. The samples were rapidly frozen and water was removed by freeze-drying. The samples were redissolved in 100 μl water and injected into a reversed-phase HPLC system (Gilson Liquid Chromatography, equipped with a 10 μl injection, 231 XL autosampler and a Synergi 4μ MaxRp 80Å column, 75 mm x 2 mm internal diameter) coupled with a Gilson 118 UV detector (256 nm) and a Micromass Quattro LC electrospray mass spectrometer. The general operating parameters for single ion mass spectrometry were: capillary (4.02), cone (50 V), extractor (10), RF lens (0.50), source temperature (125°C), desolvation temperature (200°C). The operating parameters for the single ion mass spectrometry were: inter channel delay (0.03 seconds), span (1 dalton), mass (348 Da), dwell (0.2 seconds), cone (100 V). The operating parameters for MS/MS mass spectrometry were: inter channel delay (0.03 seconds), span (1 dalton),

parent mass (348 Da), daughter mass (136 Da), dwell (0.2 seconds), coil energy (12 eV), cone (100 V). The solvent system used for the HPLC system was 10 mM ammonium acetate, pH 5 at a flow rate of 200 $\mu l \cdot min^{-1}$. Within these experimental conditions, AMP was eluted after 5 minutes of chromatography. In separate control experiments it was verified that non-enzymatic formation of AMP was negligible during the course of the experiment.

6.14 Snake venom phosphodiesterase hydrolysis of a racemic mixture of ADPαS (97).

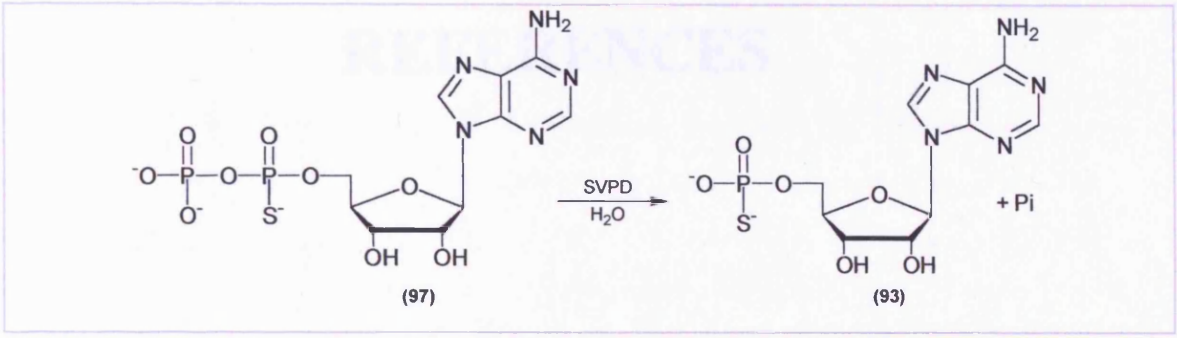

The diastereoisomers of ADPαS **(97)** were hydrolysed with snake venom phosphodiesterase. The reaction conditions for the snake venom catalysed reaction were as follows: ADPαS **(97)** (10 μmol of a 1:1 synthetic mixture of diastereoisomers), $MgCl_2$ solution (100 mM, 80 μl), TrisHCl buffer pH 10 (1 M, 160 μl) and snake venom phosphodiesterase (0.1 unit, 100 μl) and water to a final volume of 850 μl. The reaction was incubated at 37°C for 15 hours. After various incubation periods, 20 μl of the assay medium were injected into a reversed-phase HPLC system (Shimadzu LC-4A fitted with a 5 μm ODS-hypersil 25 mm x 4.6 mm c18 reverse phase column and Shimadzu CR2 AX chart recorder *via* a rheodyne. The HPLC conditions were: solvent A, 100 mM TEAB buffer, pH 7.6; solvent B, acetonitrile; solvent B increased linearly by 0.8%/min at a flow rate of 1 $cm^3 \cdot min^{-1}$. The UV wavelength used to monitor the elution of compound was 260 nm. Within these experimental conditions, AMPS, ADPαS (Sp) and ADPαS (Rp) were eluted after 12, 14 and 15 minutes of chromatography, respectively. In separate control experiments it was verified that non-enzymatic hydrolysis of the diastereoisomers of ADPαS was negligible during the course of the experiment.

REFERENCES

(1) Thatcher, G. R. J.; Kluger, R. *Adv. Phys. Org. Chem.* **1989**, *25*, 99-265.

(2) Stryer, L. *Biochemistry*; 4 ed.; W. H. Freeman and Company: New York, 1995.

(3) Weiner, D. P., University of Leicester, PhD thesis, 1992.

(4) Adams, J. A. *Chem. Rev.***2001**, *101*, 2271-2290.

(5) Gillespie, P.; Hoffman, P.; Klusacek, H.; Marquarding, D.; Pfohl, S.; Ramirez, F.; Tsolis, E. A.; Ugi, I. *Angew. Chem. Int. Ed. Engl.* **1971**, *10*, 687-715.

(6) Berry, R. S. *J. Chem. Phys.* **1960**, *32*, 933-8.

(7) Denney, D. B.; Relles, H. M. *J. Am. Chem. Soc.* **1964**, *86*, 3897-8.

(8) Westheimer, F. H. *Acc. Chem. Res.* **1968**, *1*, 70-78.

(9) Kumamoto, J.; Cox, J. R., Jr.; Westheimer, F. H. *J. Am. Chem. Soc.* **1956**, *78*, 4858-60.

(10) Covitz, F.; Westheimer, F. H. *J. Am. Chem. Soc.* **1963**, *85*, 1773-7.

(11) Khorana, H. G.; Tener, G. M.; Wright, R. S.; Moffatt, J. G. *J. Am. Chem. Soc.* **1957**, *79*, 430-6.

(12) Haake, P. C.; Westheimer, F. H. *J. Am. Chem. Soc.* **1961**, *83*, 1102-9.

(13) Dennis, E. A.; Westheimer, F. H. *J. Am. Chem. Soc.* **1966**, *88*, 3432-3.

(14) Gorenstein, D. G.; Westheimer, F. H. *J. Am. Chem. Soc.* **1967**, *89*, 2762-4.

(15) Hall, C. R.; Inch, T. D. *Tetrahedron* **1980**, *36*, 2059-2095.

(16) Trippett, S. *Phosphorus Sulfur* **1976**, *1*, 89-98.

(17) Cleland, W. W.; Hengge, A. C. *FASEB Journal* **1995**, *9*, 1585-1594.

(18) Florian, J.; Aaqvist, J.; Warshel, A. *J. Am. Chem. Soc.* **1998**, *120*, 11524-11525.

(19) Benkovic, S. J.; Schray, K. J. *Enzymes, 3rd Ed.* **1973**, *8*, 201-38.

(20) Aqvist, J.; Kolmodin, K.; Florian, J.; Warshel, A. *Chemistry & Biology* **1999**, *6*, R71-R80.

(21) Kirby, A. J.; Jencks, W. P. *J. Am. Chem. Soc.* **1965**, *87*, 3209-16.

(22) Kirby, A. J.; Jencks, W. P. *J. Am. Chem. Soc.* **1965**, *87*, 3217-24.

(23) Skoog, M. T.; Jencks, W. P. *J. Am. Chem. Soc.* **1984**, *106*, 7597-7606.

(24) Herschlag, D.; Jencks, W. P. *J. Am. Chem. Soc.* **1989**, *111*, 7579-86.

(25) Hengge, A. C. *FEBS Lett.* **2001**, *501*, 99-102.

(26) Friedman, J. M.; Freeman, S.; Knowles, J. R. *J. Am. Chem. Soc.* **1988**, *110*, 1268-75.

(27) Thompson, P. R.; Cole, P. A. *Proc. Natl. Acad. Sci. USA* **2001**, *98*, 8170-8171.

(28) Knowles, J. R. *Annu. Rev. Biochem.***1980**, 877-919.

(29) Hengge, A. C.; Cleland, W. W. *J. Am. Chem. Soc.* **1991**, *113*, 5835-41.

(30) Caldwell, S. R.; Raushel, F. M.; Weiss, P. M.; Cleland, W. W. *Biochemistry* **1991**, *30*, 7444-7450.

(31) Weiss, P. M.; Cleland, W. W. *J. Am. Chem. Soc.* **1989**, *111*, 1928-1929.

(32) Hollfelder, F.; Herschlag, D. *Biochemistry* **1995**, *34*, 12255-12264.

(33) Admiraal, S. J.; Herschlag, D. *Chem. Biol.* **1995**, *2*, 729-739.

(34) Hengge, A. C.; Edens, W. A.; Elsing, H. *J. Am. Chem. Soc.* **1994**, *116*, 5045-5049.

(35) Hassett, A.; Blattler, W.; Knowles, J. R. *Biochemistry* **1982**, *21*, 6335-6340.

(36) Misra, R., University of Leicester, PhD thesis, 1991.

(37) Fersht, A. *Enzyme structure and mechanism*; W. H. Freeman and Company, 1997.

(38) Kim, K.; Cole, P. A. *J. Am. Chem. Soc.* **1997**, *119*, 11096-11097.

(39) Hengge, A. C.; Sowa, G. A.; Wu, L.; Zhang, Z. Y. *Biochemistry* **1995**, *34*, 13982-7.

(40) Johnson, L. N.; Noble, M. E.; Owen, D. J. *Cell* **1996**, *85*, 149-58.

(41) Jackson, M. D.; Denu, J. M. *Chem. Rev.* **2001**, *101*, 2313-2340.

(42) Hoff, R. H.; Hengge, A. C.; Wu, L.; Keng, Y. F.; Zhang, Z. Y. *Biochemistry* **2000**, *39*, 46-54.

(43) Midelfort, C. F.; Rose, I. A. *J. Biol. Chem.* **1976**, *251*, 5881-5887.

(44) Lowe, G.; Sproat, B. S. *J. Biol. Chem.* **1980**, *255*, 3944-3951.

(45) Rose, I. A. *Biochem. Biophys. Res. Commun.* **1980**, *94*, 573-578.

(46) Gerratana, B.; Frey, P. A.; Cleland, W. W. *Biochemistry* **2001**, *40*, 2972-2977.

(47) Gerratana, B.; Sowa, G. A.; Cleland, W. W. *J. Am. Chem. Soc.* **2000**, *122*, 12615-12621.

(48) Cohn, M. *J Cell Comp Physiol.* **1959**, *54*, 17-31.

(49) Mildvan, A. S. *The Enzymes*; 3rd Edn. ed.; Boyer, P. D., Ed.; Academic press: New York, 1970, p 445-536.

(50) Eriksen, T. A.; Kadziola, A.; Bentsen, A. K.; Harlow, K. W.; Larsen, S. *Nature Structural Biology* **2000**, *7*, 303-308.

(51) Baker, L. J.; Dorocke, J. A.; Harris, R. A.; Timm, D. E. *Structure* **2001**, *9*, 539-546.

(52) Hennig, M.; Dale, G. E.; D'Arcy, A.; Danel, F.; Fischer, S.; Gray, C. P.; Jolidon, S.; Muller, F.; Page, M. G. P.; Pattison, P.; Oefner, C. *J. Mol. Biol.* **1999**, *287*, 211-219.

(53) Hutchins, A. M.; Holden, J. F.; Adams, M. W. W. *Journal of Bacteriology* **2001**, *183*, 709-715.

(54) Cook, A. F.; Knowles, J. R. *Biochemistry* **1985**, *24*, 51-58.

(55) Vetter, I. R.; Wittinghofer, A. *Quarterly Reviews of Biophysics* **1999**, *32*, 1-56.

(56) Bodley, A. L.; Jencks, W. P. *J. Biol. Chem.* **1987**, *262*, 13997-14004.

(57) Cho, H.; Wang, W. R.; Kim, R.; Yokota, H.; Damo, S.; Kim, S. H.; Wemmer, D.; Kustu, S.; Yan, D. L. *Proc. Natl. Acad. Sci. USA* **2001**, *98*, 8525-8530.

(58) Barford, D.; Das, A. K.; Egloff, M. P. *Annual Review of Biophysics and Biomolecular Structure* **1998**, *27*, 133-164.

(59) Denu, J. M.; Stuckey, J. A.; Saper, M. A.; Dixon, J. E. *Cell* **1996**, *87*, 361-364.

(60) Cohn, M. *Acc. Chem. Res.* **1982**, *15*, 326-332.

(61) Eckstein, F. *Annu. Rev. Biochem.* **1985**, *54*, 367-402.

(62) Frey, P. A. *Adv. Enzymol. Relat. Areas Mol. Biol.* **1989**, *62*, 119-201.

(63) Eckstein, F. *Antisense & Nucleic Acid Drug Development* **2000**, *10*, 117-121.

(64) Buchwald, S. L.; Hansen, D. E.; Hassett, A.; Knowles, J. R. *Methods In Enzymology* **1982**, *87*, 279-301.

(65) Liang, C.; Allen, L. C. *J. Am. Chem. Soc* **1987**, *109*, 6449-6453.

(66) Frey, P. A.; Sammons, R. D. *Science* **1985**, *228*, 541-545.

(67) Richey, D. P.; Brown, G. M. *J. Biol. Chem.* **1969**, *244*, 1582-1592.

(68) Bermingham, A.; Bottomley, J. R.; Primrose, W. U.; Derrick, J. P. *J. Biol. Chem.* **2000**, *275*, 17962-17967.

(69) Yan, H. G.; Blaszczyk, J.; Xiao, B.; Shi, G. B.; Ji, X. H. *Journal of Molecular Graphics & Modelling* **2001**, *19*, 70-77.

(70) Huovinen, P.; Sundstrom, L.; Swedberg, G.; Skold, O. *Antimicrobial Agents and Chemotherapy* **1995**, *39*, 279-289.

(71) Williams, R. A. D.; Kruk, Z. L. *The Biochemistry and Pharmacology of Antibacterial Agents*; Croom Helm London: London, 1981.

(72) Swedberg, G.; Fermer, C.; Skold, O. In *Chemistry and biology of pteridines and folates*; Ayling, J. E. ed.; Plenum Press: New York, 1993, p 555-558.

(73) Flensburg, J.; Skold, O. *Eur. J. Biochem.* **1987**, *162*, 473-476.

(74) Vinnicombe, H. G.; Derrick, J. P. *Biochem. Biophys. Res. Commun.* **1999**, *258*, 752-757.

(75) Baca, A. M.; Sirawaraporn, R.; Turley, S.; Sirawaraporn, W.; Hol, W. G. J. *J. Mol. Biol.* **2000**, *302*, 1193-1212.

(76) Blaszczyk, J.; Shi, G.; Yan, H.; Ji, X. *Structure* **2000**, *8*, 1049-1058.

(77) Xiao, B.; Shi, G. B.; Chen, X.; Yan, H. G.; Ji, X. H. *Structure with Folding & Design* **1999**, *7*, 489-496.

(78) Shi, G. B.; Blaszczyk, J.; Ji, X. H.; Yan, H. G. *J. Med. Chem.* **2001**, *44*, 1364-1371.

(79) Weisman, R. A.; Brown, G. M. *J. Biol. Chem.* **1964**, *239*, 326-331.

(80) Lopez, P.; Greenberg, B.; Lacks, S. A. *Journal of Bacteriology* **1990**, *172*, 4766-4774.

(81) Talarico, T. L.; Dev, I. K.; Dallas, W. S.; Ferone, R.; Ray, P. H. *Journal of Bacteriology* **1991**, *173*, 7029-7032.

(82) Talarico, T. L.; Ray, P. H.; Dev, I. K.; Merrill, B. M.; Dallas, W. S. *Journal of Bacteriology* **1992**, *174*, 5971-5977.

(83) Rebeille, F.; Macherel, D.; Mouillon, J. M.; Garin, J.; Douce, R. *Embo Journal* **1997**, *16*, 947-957.

(84) Mouillon, J. M.; Ravanel, S.; Douce, R.; Rebeille, F. *Biochem. J.* **2002**, *363*, 313-319.

(85) Schmincke-Ott, E.; Bisswanger, H. In *Multifunctional proteins*; Wiley: New York, 1980, p 1-29.

(86) Ballantine, S. P.; Volpe, F.; Delves, C. J. *Protein Expression and Purification* **1994**, *5*, 371-378.

(87) Xiao, B.; Shi, G. B.; Gao, J. H.; Blaszczyk, J.; Liu, Q.; Ji, X. H.; Yan, H. G. *J. Biol. Chem.* **2001**, *276*, 40274-40281.

(88) Stammers, D. K.; Achari, A.; Somers, D. O.; Bryant, P. K.; Rosemond, J.; Scott, D. L.; Champness, J. N. *FEBS Lett.* **1999**, *456*, 49-53.

(89) Yan, H. **2002**; http://www.bch.msu.edu/labs/yan/hppk.htm

(90) Abbott, S. J.; Jones, S. R.; Weinman, S. A.; Knowles, J. R. *J. Am. Chem. Soc.* **1978**, *100*, 2558-2560.

(91) Abend, A.; Garrison, P. N.; Barnes, L. D.; Frey, P. A. *Biochemistry* **1999**, *38*, 3668-3676.

(92) Fauroux, C. M. J.; Lee, M.; Cullis, P. M.; Douglas, K. T.; Freeman, S.; Gore, M. G. *J. Am. Chem. Soc.* **1999**, *121*, 8385-8386.

(93) Goody, R. S.; Eckstein, F. *J. Am. Chem. Soc.* **1971**, *93*, 6252-6257.

(94) Jaffe, E. K.; Cohn, M. *Biochemistry* **1978**, *17*, 652-657.

(95) Lagrossi, A., University of Leicester, PhD Thesis, **1988**.

(96) Cooper, D. B.; Hall, C. R.; Harrison, J. M.; Inch, T. D. *J. Chem. Soc., Perkin Trans. 1* **1977**, 1969-80.

(97) Herriott, A. W. *J. Amer. Chem. Soc.* **1971**, *93*, 3304-5.

(98) Cullis, P. M.; Lowe, G. *J. Chem. Soc., Chem. Commun.* **1978**, *12*, 512-514.

(99) Blattler, W. A.; Knowles, J. R. *Biochemistry* **1979**, *18*, 3927-3933.

(100) Jones, S. R.; Kindman, L. A.; Knowles, J. R. *Nature* **1978**, *275*, 564-565.

(101) Eckstein, F.; Gindl, H. *Chem. Ber.* **1968**, *101*, 1670-1673.

(102) Usher, D. A.; Richardson, D. I. J.; Eckstein, F. *Nature* **1970**, *228*, 663-665.

(103) Richard, J. P.; Frey, P. A. *J. Am. Chem. Soc.* **1982**, *104*, 3476-3481.

(104) Eckstein, F.; Goody, R. S. *Biochemistry* **1976**, *15*, 1685-1691.

(105) Sheu, K.-F.; Frey, P. A. *Biol. Chem.* **1977**, *252*, 4445-4448.

(106) Guga, P.; Domanski, K.; Stec, W. J. *Angew. Chem. Int. Ed.* **2001**, *40*, 610-613.

(107) Iyer, R. P.; Guo, M. J.; Yu, D.; Agrawal, S. *Tetrahedron Lett.* **1998**, *39*, 2491-2494.

(108) Iyer, R. P.; Yu, D.; Devlin, T.; Ho, N. H.; Agrawal, S. *J. Org. Chem.* **1995**, *60*, 5388-5389.

(109) Iyer, R. P.; Yu, D.; Ho, N. H.; Tan, W. T.; Agrawal, S. *Tetrahedron-Asymmetry* **1995**, *6*, 1051-1054.

(110) Wilk, A.; Grajkowski, A.; Phillips, L. R.; Beaucage, S. L. *J. Am. Chem. Soc.* **2000**, *122*, 2149-2156.

(111) Brautigam, C. A.; Steitz, T. A. *J. Mol. Biol.* **1998**, *277*, 363-377.

(112) Koziolkiewicz, M.; Krakowiak, A.; Kwinkowski, M.; Boczkowska, M.; Stec, W. J. *Nucleic Acids Research* **1995**, *23*, 5000-5005.

(113) Kennedy, A. K.; Haniford, D. B.; Mizuuchi, K. *Cell* **2000**, *101*, 295-305.

(114) Mizuuchi, K.; Nobbs, T. J.; Halford, S. E.; Adzuma, K.; Qin, J. *Biochemistry* **1999**, *38*, 4640-4648.

(115) Connolly, B. A.; Potter, B. V. L.; Eckstein, F.; Pingoud, A.; Grotjahn, L. *Biochemistry* **1984**, *23*, 3443-3453.

(116) Jarvest, R. L.; Lowe, G. *J. Chem. Soc., Chem. Commun.* **1979**, *8*, 364-366.

(117) Cullis, P. M.; Iagrossi, A. *J. Am. Chem. Soc.* **1986**, *108*, 7870-7871.

(118) Cullis, P. M.; Iagrossi, A.; Rous, A. J. *J. Am. Chem. Soc.* **1986**, *108*, 7869-7870.

(119) Abbott, S. J.; Jones, S. R.; Weinman, S. A.; Bockhoff, F. M.; McLafferty, F. W. *J. Am. Chem. Soc.* **1979**, *101*, 4323-4332.

(120) Ketelaar, J. A. A.; Gersmann, H. R.; Koopmans, K. *Rec. Trav. Chim.* **1952**, *71*, 1253-1258.

(121) Degraw, J. I.; Colwell, W. T.; Piper, J. R.; Sirotnak, F. M. *J. Med. Chem.* **1993**, *36*, 2228-2231.

(122) Taylor, E. C.; Harrington, P. J.; Fletcher, S. R.; Beardsley, G. P.; Moran, R. G. *J. Med. Chem.* **1985**, *28*, 914-921.

(123) Molina, S.; Cabo, J.; Melguizo, M.; Noguerao, A.; Sanchez, A. In *Chemistry and biology of pterins and folates*; W. Pfleiderer and H. Rokos, Blackwell Science, Berlin ed. 1997, p 57.

(124) Russell, J. R.; Garner, C. D.; Joule, J. A. *Tetrahedron Lett.* **1992**, *33*, 3371-3374.

(125) Gibson, C. L.; Lang, A.; Ohta, K.; Suckling, C. J. *J. Chem. Soc., Perkin Trans.1* **1999**, 163-169.

(126) Traub, H.; Pfleiderer, W. *Pteridines* **1999**, *10*, 79-90.

(127) Harger, M. J. P. *J. Chem. Soc., Chem. Commun.* **1976**, *13*, 520-522.

(128) Eckstein, F. *Angew. Chem. Int. Ed. Engl.* **1983**, *22*, 423-439.

(129) Frey, P. A. *Tetrahedron* **1982**, *38*, 1541-1567.

(130) Lowe, G.; Sproat, B. S. *J. Chem. Soc., Chem. Commun.* **1978**, *13*, 565-566.

(131) Cohn, M.; Hu, A. *Proc. Natl. Acad. Sci. USA* **1978**, *75*, 200-203.

(132) Lutz, O.; Nolle, A.; Staschewski, D. *Z. Naturforsch* **1978**, *33A*, 380-382.

(133) Lowe, G.; Potter, B. V. L.; Sproat, B. S.; Hull, W. E. *J. Chem. Soc., Chem. Commun.* **1979**, *17*, 733-735.

(134) Webb, M. R.; Trentham, D. R. *J. Biol. Chem.* **1981**, *256*, 4884-4887.

(135) Jarvest, R. L.; Lowe, G.; Potter, B. V. L. *J. Chem. Soc., Chem. Commun.* **1980**, 1142-5.

(136) Buchwald, S. L.; Knowles, J. R. *J. Am. Chem. Soc.* **1980**, *102*, 6601-2.

(137) Burgers, P. M. J.; Eckstein, F. *Proc. Natl. Acad. Sci. USA* **1978**, *75*, 4798-4800.

(138) Cullis, P. M.; Iagrossi, A.; Rous, A. J.; Schilling, M. B. *J. Chem. Soc., Chem. Commun.* **1987**, 996-8.

(139) Cullis, P. M.; Misra, R.; Wilkins, D. J. *Tetrahedron Lett.* **1987**, *28*, 4211-14.

(140) Cummins, J. H.; Potter, B. V. L. *Eur. J. Biochem.* **1987**, *162*, 123-128.

(141) Culp, J. S.; Butler, L. G. *Arch. Biochem. Biophys.* **1986**, *246*, 245-9.

(142) Garciadiaz, M.; Avalos, M.; Cameselle, J. C. *Eur. J. Biochem.* **1993**, *213*, 1139-1148.

(143) Vergeles, J. M.; Garciadiaz, M.; Cameselle, J. C. *Eur. J. Biochem.* **1995**, *233*, 442-447.

(144) Garciadiaz, M.; Avalos, M.; Cameselle, J. C. *Eur. J. Biochem.* **1991**, *196*, 451-457.

(145) Gerlt, J. A.; Coderre, J. A.; Mehdi, S. *Adv. Enzymol. Relat. Areas Mol. Biol.* **1983**, *55*, 291-380.

(146) Pliura, D. H.; Schomburg, D.; Richard, J. P.; Frey, P. A.; Knowles, J. R. *Biochemistry* **1980**, *19*, 325-329.

(147) Mildvan, A. S.; Weber, D. J.; Abeygunawardana, C. In *Advances in Enzymology, Vol 73*; John Wiley & Sons Inc: New York, **1999**; Vol. 73, p 183-207.

(148) Shi, G. B.; Gong, Y. C.; Savchenko, A.; Zeikus, J. G.; Xiao, B.; Ji, X. H.; Yan, H. G. *Biochimica Et Biophysica Acta-Protein Structure and Molecular Enzymology* **2000**, *1478*, 289-299.

(149) Li, Y.; Gong, Y. C.; Shi, G.; Blaszczyk, J.; Ji, X.; Yan, H. *Biochemistry* **2002**, *41*, 8777-8783.

(150) Pecoraro, V. L.; Hermes, J. D.; Cleland, W. W. *Biochemistry* **1984**, *23*, 5262-5271.

(151) Jaffe, E. K.; Cohn, M. *J. Biol. Chem.* **1978**, *253*, 4823-4825.

(152) Jaffe, E. K.; Cohn, M. *J. Biol. Chem.* **1979**, *254*, 10839-10845.

(153) Maderia, M.; Hunsicker, L. M.; DeRose, V. J. *Biochemistry* **2000**, *39*, 12113-12120.

(154) Webb, M. R. *Proc. Natl. Acad. Sci. USA* **1992**, *89*, 4884-4887.

(155) Williams, A.; Douglas, K. T.; Loran, J. S. *J. Chem. Soc., Perkin Trans. 2* **1975**, 1010-16.

(156) Still, W. C.; Kahn, M.; Mitra, A. *J. Org. Chem.* **1978**, *43*, 2923-5.

(157) Lazewska, D.; Guranowski, A. *Nucleic Acids Res.* **1990**, *18*, 6083-6088.

(158) Marquetant, R.; Goody, R. S. *J. Chromatogr.* **1983**, *280*, 386-389.

(159) Ludwig, J.; Eckstein, F. *J. Org. Chem.* **1989**, *54*, 631-635.

(160) Moffatt, J. G. *Can. J. Chem.* **1964**, *42*, 599-604.

(161) Arnold, J. PhD, Oxford, 1986.

(162) Cook, A. F. *J. Amer. Chem. Soc.* **1970**, *92*, 190-199.

(163) Kay, P. B.; Trippett, S. *J. Chem. Soc., Perkin Trans. 1* **1987**, 1813-15.

(164) Futterman, S. *J. Biol. Chem* **1957**, *228*, 1031-8.